Magnetic Nanoparticles as a Versatile Platform for Catalytic Applications

PhD Thesis presented by:

Sara Ranjbar

Developed under the supervision of:

Prof. Miquel A. Pericàs, Prof. Oliver Reiser
and
Dr. Carles Rodríguez-Escrich

Department of Analytical and Organic Chemistry (URV),
Chemistry Department (UR) and
Institute of Chemical Research of Catalonia (ICIQ)

UNIVERSITAT ROVIRA i VIRGILI

Tarragona 2016

UNIVERSITAT ROVIRA I VIRGILI

Universität Regensburg

Prof. Dr. OLIVER REISER, Prof. Dr. MIQUEL A. PERICÀS BRONDO AND Dr. CARLES RODRÍGUEZ-ESCRICH

STATE, that the present Doctoral Thesis entitled: **" Magnetic Nanoparticles as a Versatile Platform for Catalytic Applications"**, presented by Sara Ranjbar Rizi to recieve the degree of Doctor, has been carried out under their supervision between the University of Regensburg (UR) and the Institute of Chemical Research of Catalonia (ICIQ).

PhD Thesis Supervisor	PhD Thesis Supervisor	PhD Thesis Supervisor
Prof. Dr. Oliver Reiser	Prof. Dr. Miquel Àngel Pericàs Brondo	Dr. Carles Rodríguez-Escrich

Acknowledgements

During my PhD journey, many people have made my time unforgettable.

I would like to thank my PhD advisors, Prof. Miquel A. Pericàs and Prof. Oliver Reiser to believe in me and giving me the opportunity to work in European union project ¨Mag(net)icFun¨ and starting my research in an international team which has given me a lot of adventure and experience.

I would like to give special thanks to Dr. Carles Rodríguez-Escrich for his support and his kind advices (during my research and writing part). I am really thankful for his patience and advices.

Also I would like to give my special thanks to Dr. Paola Riente to give me advices in my research during the time in ICIQ.

Just countless thanks to my family, especially my parents, for their support in each part of my life and encouraging me in the PhD part. I would like to express my special thanks to my sister and brothers for all of their support throughout this time.

I am also grateful to the thesis committee for their time and consideration.

I would also like to express special thanks to the past and present group members; Patricia, Laura Osorio, Laura Buglioni, Lidia, Marta, Lluis, Pablo, Ada, Andrea, Santiago, Toni, Evgeny, Shoulei, Marco, Esther, Sonia, Alba, Jagjit, Soumi, Carles Ayats, Carles Lizandara, Erhan, Pinar, Irina and Carmen, Xinyuan, Luca, Javi. I am sincerely grateful for the time we spent together, all the experience and truthful and illuminating views which we have shared together.

I would like to thank my friends, Christian Kaiser and Saerom Park for our joys and difficulties we shared during my secondment stay in Regensburg.

Also I would like to thank technical support and administrative staff in ICIQ and express special thanks to Sara Garcia and Marta Moya for the bureaucratic part.

During the adventure in PhD journey, there also have been unexpected joyful and enchanting moments which I really feel gratful for.

Probably, it is impossible to count how many times I have been grateful to everybody for the PhD period that I've spent here in Tarragona. Thank you very much to all of you.

The work developed in the present doctoral thesis has been possible thanks to the EU-ITN network Mag(net)icFun (PITN-GA-2012-290248) and Institute of Chemical Research of Catalonia (ICIQ) Foundation.

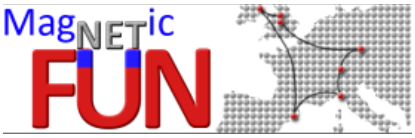

To my Family

تقدیم به خانواده ام

List of Abbreviations

MNP	magnetic nanoparticle
NP	nanoparticle
QD	quantum dot
Co/C NB	carbon-coated cobalt nanobead
MRImagnetic	resonance imaging
PVP	polyvinyl pyrrolidone
CTAB	cetyltrimethyl ammonium bromide
w/o	water-in-oil
Brij30	non-ionic polyoxyethylated lauryl ether surfactant
Igepal CO-520	polyoxyethylene nonylphenylether
Tritron-X	polyethylene glycol *tert*-octylphenyl ether
TEOS	tetraethyl orthosilicate
PEG	poly(ethyleneglycol)
PVA	poly(vinyl alcohol)
PLA	poly(lactic acid)
PMMA	polymethylmethacrylate
SOMO	singly occupied molecular orbital
HOMO	highest occupied molecular orbital
LUMO	lowest unoccupied molecular orbital
CuAAC	copper-catalyzed azide-alkyne cycloaddition
DVS	divinyl sulfone
AOT	sodium bis(2-ethylhexyl) sulfosuccinate
TMS	trimethylsilyl
TES	triethylsilyl
TBS	tert-butyldimethylsilyl
TIPS	triisopropylsilyl
TEM	transmission electron microscopy
MCF	siliceous mesocellular foam
TON	turnover number
Pd NP	palladium nanoparticle
PVP	poly(N-vinyl-2-pyrrolidone
DA	dopamine

MWCNT	multiwall carbon nanotubes
MOP	microporous organic polymers
PAFs	porous aromatic frameworks
CTFs	covalent triazine-based frameworks
PIMs	polymers of intrinsic microporosity

List of publications

- Hybrid magnetic materials (Fe_3O_4–κ-carrageenan) as catalysts for the Michael addition of aldehydes to nitroalkenes. Sara Ranjbar, Carmen A. Mak, Paola Riente, Carles Rodríguez-Escrich, Miquel A. Pericàs. *Tetrahedron* **2014**, *70*, 6169.

- Polystyrene or Magnetic Nanoparticles as Support in Enantioselective Organocatalysis? A Case Study in Friedel-Crafts Chemistry. Sara Ranjbar, Paola Riente, Carles Rodríguez-Escrich, Jagjit Yadav, Kishore Ramineni, Miquel A. Pericàs. *Org. Lett*. **2016**, *18*, 1602.

Furthermore one manuscript is under preparation concerning ¨preparation of microporous polymeric nanoreactors encapsulated with palladium nanoparticles and Co/C nanobeads¨ the authors including Prof. Oliver Reiser, Dr. Jian Zhi, Sara Ranjbar, Lisa Stadler and Andreas Hartl.

Abstract

This thesis focuses on the application of magnetic nanoparticles (MNPs) in different catalytic reactions. In this research the main goal is to develop different catalysts based on MNPs and study the advantages and disadvantages of these catalytic materials.

In the first part of the research, two new hybrid materials based on carrageenan and MNPs were developed and tested in the Michael addition of aldehydes to nitroalkenes. The first one, a combination of carrageenan and MNPs, showed good results in this reaction while the individual components were inactive. The second catalyst, which included an analogue of the Jørgensen-Hayashi catalyst also showed good activity and excellent enantioselectivity.

In the second project, an analogue of the second generation MacMillan catalyst was immobilized onto Fe_3O_4 NPs and polystyrene. The resulting catalysts were applied to the asymmetric Friedel-Crafts alkylation of indoles with α,β-unsaturated aldehydes. In this study, the polystyrene-based catalyst showed higher stability and provided better stereoselectivity.

In the last project, another kind of hybrid material was synthesized based on microporous organic polymers (MOPs) encapsulated with Pd nanoparticle and Co/C nanobeads. To build up the polymer, different substrates such as toluene, aniline and phenol were used. After synthesising Pd nanoparticle inside of the pores of polymer, these catalysts were applied to the hydrogenation and Suzuki cross-coupling reactions. Despite moderate to good yields that were obtained, these catalysts suffer from leaching of Pd, so further research for optimizing this catalyst system is required.

Resumen

Esta tesis se ha centrado en el uso de nanopartículas magnéticas (MNPs) en catálisis. Éstas permiten una fácil recuperación del catalizador después de la reacción, lo que las convierte en una herramienta interesante para ser utilizada en procesos a gran escala. Además, la modificación de la superficie de las nanopartículas con diferentes linkers nos dio la oportunidad de anclar una variedad de organocatalizadores, dando lugar a materiales catalíticos basados en MNPs.

En el primer proyecto, dos nuevos materiales híbridos basados en carragenano y MNPs fueron desarrollados y probados en la adición de Michael de aldehídos a nitroalquenos. La primera, una combinación de carragenano y MNPs mostró buenos resultados en esta reacción pese a que los componentes individuales eran inactivos. El segundo catalizador, que incluye un análogo del catalizador de Jørgensen-Hayashi, también mostró buena actividad y dio excelentes ee's.

En el segundo proyecto, un análogo del catalizador de MacMillan de segunda generación fue inmovilizado sobre NPs de Fe_3O_4 y poliestireno. Los catalizadores resultantes se aplicaron a la alquilación asimétrica de Friedel-Crafts de indoles con aldehídos α,β-insaturados. En este estudio, el catalizador basado en poliestireno mostró una mayor estabilidad, proporcionando mejores estereoselectividades.

El último proyecto se ha centrado en el uso de nanopartículas magnéticas de cobalto revestidas de carbono (Co/CNP) en la catálisis. Por lo tanto, otro material híbrido fue desarrollado a base de polímeros orgánicos microporosos (MOPs) encapsulados con nanopartículas de Pd y Co/CNP. Para construir el polímero, se utilizaron diferentes sustratos tales como tolueno, anilina y fenol. Después de sintetizar nanopartículas de Pd dentro de los poros del polímero, estos catalizadores se aplicaron a reacciones de hidrogenación y acoplamiento cruzado de Suzuki. A pesar de dar rendimientos de buenos a moderados, estos catalizadores sufren de lixiviación de Pd, por lo que se requiere más investigación.

Zusammenfassung

Das Hauptthema dieser Doktorarbeit ist die Anwendung von magnetischen Nanopartikeln (MNP) in verschiedenen katalytischen Reaktionen. Das Hauptziel ist die Entwicklung neuer Katalysatoren auf Basis von MNP und die Bestimmung der Vor- und Nachteile dieser katalytischen Materialien.

Im ersten Teil der Arbeit wurden zwei neue Hybridmaterialien auf Basis von Carrageenan und MNP entwickelt und in der Michael-Addition von Aldehyden an Nitroalkenen getestet. Der erste Katalysator, der aus Carrageenan und MNP entsteht, liefert gute Ausbeuten in dieser Reaktion, obwohl die einzelnen Komponenten nicht katalytisch aktiv sind. Das zweite Material auf der Basis des Jørgensen-Hayashi Katalysators zeigt ebenfalls sehr gute Aktivität und eine ausgezeichnete Enantioselektivität.

Im zweiten Projekt wurde der MacMillan Katalysator der zweiten Generation auf Fe_3O_4-Nanopartikeln und Polystyrol immobilisiert. Die entstehende Katalysatoren wurden für die asymmetrische Friedel-Crafts-Alkylierung von Indolen mit α,β-ungesättigten Aldehyden angewandt. Der auf Polystyrol basierende Katalysator liefert dabei eine höhere Stabilität und eine bessere Stereoselektivität.

Im letzten Projekt wurde eine andere Art von Hybridmaterial synthetisiert, nämlich mikroporöse organische Polymere (MOPS) eingekapselt mit Pd-Nanopartikeln und Co/C Nanobeads. Verschiedene Substrate wie z. B. Toluol, Anilin und Phenol wurden für die Herstellung der Polymeren verwendet. Nachdem Pd-Nanopartikel im Inneren des porösen Polymers synthetisiert wurden, sind diese Materialen für die Hydrierung und Suzuki-Kreuzkupplungsreaktionen verwendet. Obwohl die Katalysatoren mäßige bis gute Ausbeuten liefern, ist das Ausbluten von Pd ein wesentlicher Nachteil, weitere Forschung zur Optimierung dieses Katalysatorsystems erforderlich ist.

Thesis Overview

Chapter I

This chapter is a general introduction that deals with the application of MNPs in catalysis. It starts introducing the different kinds of nanoparticles and then a variety methods for synthesizing MNPs and how to protect and stabilize them are described. Afterward, the concept of organocatalyst and aminocatalyst is explained. At the end, some examples are mentioned based on the functionalization of NPs with copper catalyzed azide alkyne cycloaddition.

Chapter II

In chapter II the concept of hybrid material is defined and examples of their applications are given. Due to the importance of carrageenan in this chapter, some applications of this kind of sugar are also mentioned. Afterwards, a brief summary of enamine catalysis is outlined. Then some examples concerning heterogeneous catalysis are mentioned to make more comprehensible the advantages of this field of chemistry. At the end of chapter II can be found an article where two carrageenan-MNPs based hybrid materials are prepared and applied for Michael addition reaction.

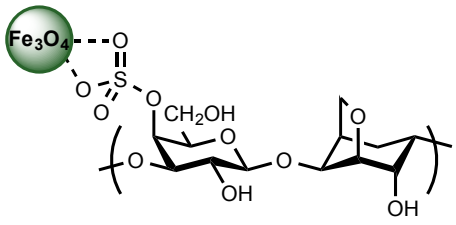

Chapter III

Iminium catalysis is explained in more detail. In this chapter, first and second generation of MacMillan catalysts are described and examples of immobilized imidazolidinone organocatalysts are given. In the attached paper, an analogue of second generation MacMillan catalyst was immobilized into Fe_3O_4 NPs and polystyrene. The resulting catalysts were applied to the asymmetric Friedel-Crafts alkylation of indoles with α,β-unsaturated aldehydes. In this project, the polystyrene-based catalyst showed higher stability and provided better stereoselectivities.

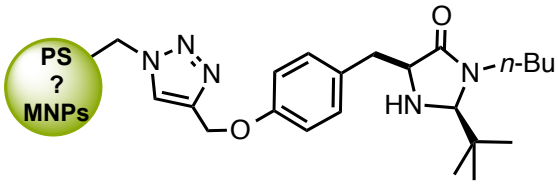

Chapter IV

In the last chapter, another kind of hybrid material was synthesized based on microporous organic polymers (MOPs) encapsulated with Pd nanoparticles and Co/C nanobeads. To build up the polymer, different substrates such as toluene, aniline and phenol were used. Afterwards, these catalysts were applied to the hydrogenation and Suzuki cross-coupling reactions. Despite giving from good to moderate yields, these catalysts suffer from leaching of Pd, so further research is required.

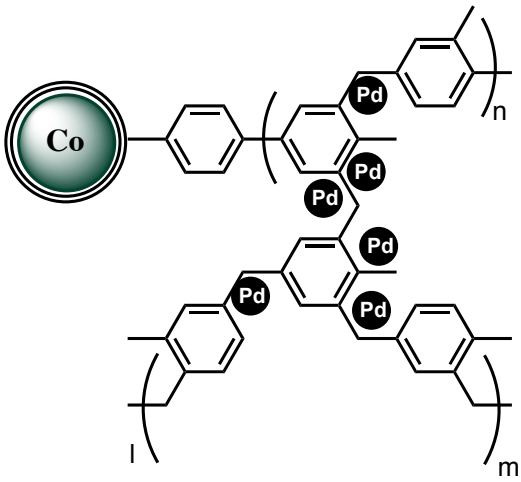

Table of contents

Chapter I

General Introduction

Table of Contents

General Introduction

1. Introduction

The present manuscript deals with the use of magnetic nanoparticles (MNPs) as a platform to support catalytic entities. Thus, the introduction will be divided in two main parts covering the multidisciplinar nature of the projects presented herein: the first section will introduce the field of nanoparticles whereas the second will focus on catalysis, with special emphasis on enantioselective organocatalysis.

1.1. Introduction to Nanoparticles

The term nanostructured material refers to every object which in at least one dimension has a length scale between 1 and 100 nm.[1] Nanomaterials usually present properties different from their bulk solid or molecules, their size being ultimately responsible for their physical and chemical behavior.[2]

For instance, optical properties like refractive index and absorbance of a bulk material are related to its mass or volume; however, in nanoparticles optical properties depend on the size and shape of that specific nanoparticle. This significant size dependent feature allows them to be used in a variety of applications such as information storage,[3] magnetic refrigeration,[4] as ferrofluids,[5] toxic chemical adsorbents,[6] gas storage[7] or in drug delivery.[8]

The high surface area to volume ratio in nanoparticles generates a fast diffusion even at lower temperature. Indeed, high surface area improves chemical and physical interactions of nanoparticles with solids, liquids or polymer matrixes as surrounding environments. Thanks to this property, nanoparticles can be used as nanocarriers in the human body.[9]

For all these reasons nanoparticles hold enough potential to revolutionize the life of human beings.

---

[1] a) Leslie-Pelecky, D. L.; Rieke, R. D. *Chem. Mater.* **1996**, *8*, 1770; b) Murray, C. B.; Kagan, C. R.; Bawendi, M. G. *Annu. Rev. Mater. Sci.* **2000**, *30*, 545.
[2] Rao, C. N. R.; Kulkarni, G. U.; Thomas, P. J.; Edwards, P. P. *Chem. Eur. J.* **2002**, *8*, 29.
[3] Sun, S. H.; Murray, C. B.; Weller, D.; Folks, L.; Moser, A. *Science* **2000**, *287*, 1989.
[4] Shull, R. D. *IEEE Trans. Magn.* **1993**, *29*, 2614.
[5] a) Ziolo, R. F.; Giannelis, E. P.; Weinstein, B. A.; Ohoro, M. P.; Ganguly, B. N.; Mehrotra, V.; Russell, M. W.; Huffman, D. R. *Science **1992**, 257*, 219; b) Anton, I.; Desabata, I.; Vekas, L. *J. Magn. Magn. Mater.* **1990**, *85*, 219; c) Odenbach, S. *Adv. Colloid Interface Sci*. **1993**, *46*, 263.
[6] Koper, O.; Lagadic, I.; Klabunde, K. J. *Chem. Mater.* **1997**, *9*, 838.
[7] Zandonella, C. *Nature* **2001**,*410*, 734.
[8] Santini, J. T.; Cima, M. J.; Langer, R. *Nature* **1999**, *397*, 335.
[9] Kuchibhatla, S. V. N. T.; Karakoti, A. S.; Bera, D.; Seal, S. *Prog. Mater. Sci.* **2007**, 52, 699.

1.1.1. Types of Metal Based Nanoparticles

Nanoparticles can be divided in several categories. Herein we will try to summarize the ones which are most relevant to our work and introduce their main features.

1.1.1.1. Plasmonic Nanoparticles

Plasmonic nanoparticles are a class of nanoparticles which are highly efficient at absorbing and scattering light and typically contain gold and silver particles with diameters ranging from 10-150 nm. In these particles the electron in the nanometal has interaction with the wavelength of light,[10] which depends on the size, shape and surface coating, and is responsible for the change in color of the nanoparticles. It is interesting to know that people already started to use this feature in art before understanding the fundamental and physical properties behind these particles. One example is the Lycurgus cup, which remains from roman smithery. Made from ruby glass, this cup looks green in daylight but when it is illuminated from inside it turns red because of the small gold and silver nanoparticles in the glass with a size of 50-100 nm.[11]

Figure 1. The Lycurgus cup illuminated with ambient lighting (left) and illuminated from inside (right) (British Museum; AD fourth century). Picture taken from reference 11.

Plasmonic nanoparticles have plenty of applications in Raman spectroscopy, sensing, catalysis and also biology.[12]

[10] Shuwen, Z.; Xia, Y.; Wing-Cheung, L.; Yating. Z.; Rui, H.; Xuan-Quyen, D.; Ho-Pui, H.; Ken-Tye, Y. *Sens. Actuator B-Chem.* **2013**, *176*, 1128.
[11] Leonhardt, U. *Nat. Photonics* **2007**, *1*, 207.
[12] a) Al-Akraa, I.; Mohammad, A.; El-Deab, M.; El-Anadouli, B. *Int. J. Electrochem. Sci.* **2013**, *8*, 458; b) Dreaden, E. C.; Alkilany, A. M.; Huang, X.; Murphy, C. J.; El-Sayed, M. A. *Chem. Soc. Rev.* **2012,** 41, 2740; c) Eustis, S.; El-Sayed, M. A. *Chem. Soc. Rev.* **2006**, *35*, 209.

1.1.1.2. Quantum Dots

Highly fluorescent semiconductor nanocrystals or quantum dots (QDs) are another relevant class of inorganic nanomaterials with dimensions between 1 and 10 nm. Quantum dots had been theorized in the 70's but were not made until the 80's.[13]

Most of the QDs typically contain core/shell structures where the core part is covered with another semiconductor material to protect and enhance their optical properties.

Early QDs involved a CdSe core with ZnS shell but afterwards they were developed using other alloy compositions because of the cytotoxicity of the cadmium ion. Thus, for making QDs more biocompatible, the synthetic pathway was changed to cadmium-free quantum dots (CFQDs). For instance silicon QDs (Si QDs), carbon dots (C-dots), graphene QDs (GQDs), Ag_2Se, Ag_2S, InP or $CuInS_2$ /ZnS.[14]

QDs have a lot of applications in biological imaging, and especially in drug delivery.[15] Also in the industry they have found applications in LEDs, solid state lighting, displays and photovoltaic.[16]

1.1.1.3. Magnetic Nanomaterials

Magnetic nanoparticles are one class of nanomaterial which contains at least one magnetic element. They can be composed of a series of metals like cobalt and nickel, alloys like iron/platinum and metal oxides like iron oxides[17] and ferrites.[18]

These materials have applications in different forms, for example in solution as ferrofluids for audio speakers,[19] as surface functionalized particles for biosensing applications,[20] as particle arrays in magnetic storage media,[3] or as contrasting agents in magnetic resonance imaging.[21] Such disparate applications are testimony to their unique properties. For instance, magnetic nanoparticles are able to remotely heat when exposed to an alternating magnetic field due to the absorption of energy from the magnetic field and conversion into heat, mainly Brownian

[13] a) Resch-Genger, U.; Grabolle, M.; Cavaliere-Jaricot, S.; Nitschke, R.; Nann, T. *Nat. Methods* **2008**, 5, 763; b) Jamieson, T.; Bakhshi, R.; Petrova, D.; Pocock, R.; Imani, M.; Seifalian, A. M. *Biomaterials* **2007**, *2*8, 4717.

[14] Zhu**,** J.-J.; Li**,** J.-J.; Huang, H.-P.; Cheng, F.-F. Quantum Dots for DNA Biosensing, Springer Science & Business Media, **2013**, 91.

[15] Qi, L.; Gao, X. *Expert Opin. Drug Deliv*. **2008**, *5*, 263.

[16] a) Vahala, K. J. *Nature* **2003**, *424*, 839; b) Yoffe, A. D. *Adv. Phys.* **2001**, *50*, 1; c) Nirmal, M.; Brus, L. *Acc. Chem. Res.* **1999**, *32*, 407; d) Sargent, E. H. *Nature Photon*. **2012**, *6*, 133.

[17] Laurent, S.; Forge, D.; Port, M.; Roch, A.; Robic, C.; Vander Elst, L.; Muller, R. N. *Chem. Rev*. **2008**, *108*, 2064.

[18] Kodama, R. H. *J. Magn. Magn. Mater*. **1999**, *200*, 359.

[19] Willard, M. A.; Kurihara, L. K.; Carpenter, E. E.; Calvin, S.; Harris, V. G. *Int. Mater. Rev.* **2004**, *49*, 125.

[20] a) Blanc-Beguin, F.; Nabily, S.; Gieraltowski, J.; Turzo, A.; Querellou, S.; Salaun, P. Y. *J. Magn. Magn. Mater.* **2009**, *321*, 192; b) Cavalli, G.; Banu, S.; Ranasinghe, T.; Broder, G. R.; Martins, H. F. P.; Neylon, C.; Morgan, H.; Bradley, M.; Roach, P. L. *J. Comb. Chem.* **2007**, *9*, 462; c) Togawa, K.; Sanbonsugi, H.; Sandhu, A.; Abe, M.; Narimatsu, H.; Nishio, K.; Handa, H. *Jpn. J. Appl. Phys*. **2005**, *44*, 1494.

[21] a) Kooi, M. E.; Cappendijk, V. C.; Cleutjens, K.; Kessels, A. G. H.; Kitslaar, P.; Borgers, M.; Frederik, P. M.; Daemen, M.; van Engelshoven, J. M. A. *Circulation* **2003**, *107*, 2453; b) Trivedi, R. A.; U-King-Im, J. M.; Graves, M. J.; Cross, J. J.; Horsley, J.; Goddard, M. J.; Skepper, J. N.; Quartey, G.; Warburton, E.; Joubert, I.; Wang, L. Q.; Kirkpatrick, P. J.; Brown, J.; Gillard, J. H. *Stroke* **2004**, 35, 1631.

relaxation and Neel relaxation.[22]

1.1.2. Application of Magnetic Nanoparticles

There is a growing interest to find new properties and applications for magnetic nanoparticles, with a very promising future for their use in life sciences.

However, a common solution is not feasible, since each application of the magnetic nanoparticles requires different properties. For example, for biomedical applications, they should display a superparamagnetic behavior at room temperature. Also in therapeutical, biological and medical diagnosis applications, magnetic particles need to be stable in water at pH 7 and in a physiological environment.[23] In data storage industry, it is required to have particles with stable and switchable magnetic moments to have bits of information that are not affected by temperature.[24] Magnetic nanoparticles are also used in waste water treatment as a practical sorbent to separate contaminants from water. At the end, they are separated from water by an applied magnetic field.[25] They can also be utilized as surface functionalized particles for biosensing applications[26] or as particle arrays in magnetic storage media.[3]

Indeed, in industry hematite and magnetite were utilized as catalysts for a number of important reactions, such as the desulfurization of natural gas, the synthesis of NH_3, and the high-temperature water-gas shift reaction. Some other reactions like the Fisher-Tropsch synthesis of hydrocarbons, the dehydrogenation of ethylbenzene to styrene, the oxidation of alcohols, and the large-scale synthesis of butadiene involve processing with magnetic nanoparticles.[27] They also have applications in magnetic inks and magnetic memory devices.[28]

In the case of biomedical applications of magnetic nanoparticles, they are classified as in vivo (inside the body) or in vitro (outside the body). The latter include diagnostic separation, selection, and magnetorelaxometry, whereas in vivo applications involve therapeutic applications such as

[22] Kittel, C. Introduction to solid state physics. 8th ed. Hoboken, NJ: John Wiley & Sons; **2005**.
[23] a) Garcell, L.; Morales, M. P.; Andres-Verges, M.; Tartaj, P.; Serna, C. J. *J. Colloid Interface Sci*. **1998**, *205*, 470; b) Ersoy, H.; Rybicki, F. J. *J. Magn. Reson. Imaging* **2007**, *26*, 1190.
[24] Akbarzadeh, A.; Samiei, M.; Davaran, S. *Nanoscale Res. Lett.* **2012**, *7*,144.
[25] Girginova, P. I.; Daniel-da-Silva, A. L.; Lopes, C. B.; Figueira, P.; Otero, M.; Amaral, V. S.; Pereira, E.; Trindade, T. *J. Colloid Interface Sci.* **2010**, *345*, 234.
[26] Miller, M. M.; Prinz, G. A.; Cheng, S. F.; Bounnak, S. *Appl. Phys. Lett*. **2002**, *81*, 2211.
[27] a) Park, S. J.; Kim, S.; Lee S.; Khim Z. G.; Char K.; Hyeon, T. *J. Am. Chem. Soc*, **2000**, 122, 8581; b) Dumestre F.; Chaudret B.; Amiens C.; Fromen M. C.; Casanove M. J, Renaud, P.; Zurcher, P. *Angew. Chem. Int. Ed*. **2002**, *41*, 4286; c) Dumestre, F.; Chaudret, B.; Amiens, C.; Renaud, P.; Fejes, P. *Science* **2004**, 303, 821.
[28] a) Prozorov, T.; Mallapragada, S. K.; Narasimhan, B.; Wang, L.; Palo, P.; Nilsen-Hamilton, M.; Williams, T. J.; Bazylinski, D. A.; Prozorov, R.; Canfield, P. C. *Adv. Funct. Mater*. **2007**, *17*, 951; b) Jun, Y. W.; Choi, J. S.; Cheon, J. *Angew. Chem. Int. Ed*. **2006**, 45, 3414; c) Nunez, N. O.; Tartaj, P.; Morales, M. P.; Pozas, R.; Ocana, M.; Serna, J. C. *Chem. Mater*. **2003**, 15, 3558.

hyperthermia or drug-targeting and diagnostic applications such as nuclear magnetic resonance imaging (MRI).[29]

This thesis will focus on the application of magnetic nanoparticles as a versatile support that can be used as a practical platform to anchor and magnetically recover catalysts. In the absence of an external magnetic field, the magnetic nanoparticles are dispersed in the reaction media like any other nanoparticle. When a magnetic field is applied, the magnetic nanoparticles are attracted towards the magnet, so they can be removed from reaction media through convenient magnetic separation and reused. [30]

1.1.3. Synthesis of Magnetic Nanostructures

The synthesis of nanoparticles can be done with two approaches: top-down and bottom-up. In top-down pathway, the synthesis begins from a bulk starting material, which is converted to the nanoparticles by means of physical or chemical synthesis. Top-down approach has some advantages such as low cost and high volume manufacturing capability. However it involves some issues making difficult the constant of size and shape.

In contrast, in the bottom-up approach, the synthesis starts from atoms, then molecules and nanoparticles are formed by self-assembly.

Several methods can be used to synthesize magnetic nanoparticles such as microemulsions,[31] sol-gel synthesis,[32] sonochemical reactions,[33] hydrothermal reactions,[34] hydrolysis and thermolysis of precursors, [35]flow injection syntheses [36]and electrospray synthesis.[37]

With such a wide choice, there are two main keys to find the best approach: the first one is to select a process that leads to monodispersed magnetic nanoparticles, whereas the second important point is to develop a reproducible method that can be industrialized without any complex purification procedure. Figure 2 summarizes the three most important pathways for the preparation of magnetic nanoparticles, chemical synthesis being the most common way. Some of these methods will be explained in more detail hereafter.

[29] a) Piao, Y.; Kim, J.; Bin, N. H.; Kim, D.; Baek, J. S.; Ko, M. K.; Lee, J. H.; Shokouhimehr, M.; Hyeon, T. *Nature Materials* **2008**, *7*, 242; b) Liu, C.; Wu, X. W.; Klemmer, T.; Shukla, N.; Weller, D. *Chem. Mater*. **2005**, *17*, 620; c) Park, J. I.; Cheon, J. *J. Am. Chem. Soc*. **2001**, *123*, 5743.
[30] Baig, R. B. N.; Varma, R. S. *Chem. Commun*. **2013**, *49*, 752.
[31] Chin, A. B.; Yaacob, I. I. *J. Mater. Proc. Technol*. **2007**, *191*, 235.
[32] Albornoz, C.; Jacobo, S. E. *J. Magn. Magn. Mater*. **2006**, *305*, 12.
[33] Kim, E. H.; Lee, H. S.; Kwak, B. K.; Kim, B. K. *J, Magn. Magn. Mater*. **2005**, *289*, 328.
[34] Wan, J.; Chen, X.; Wang, Z.; Yang, X.; Qian, Y. *J. Cryst. Growth*. **2005**, *276*, 571.
[35] Kimata, M.; Nakagawa, D.; Hasegawa, M. *Powder Technol*. **2003**, *132*, 112.
[36] Alvarez, G. S.; Muhammed, M.; Zagorodni, A. A. *Chem. Eng. Sci*. **2006**, *61*, 4625.
[37] Basak, S.; Chen, D.-R.; Biswas, P. *Chem. Eng. Sci*. **2007**, *62*, 1263.

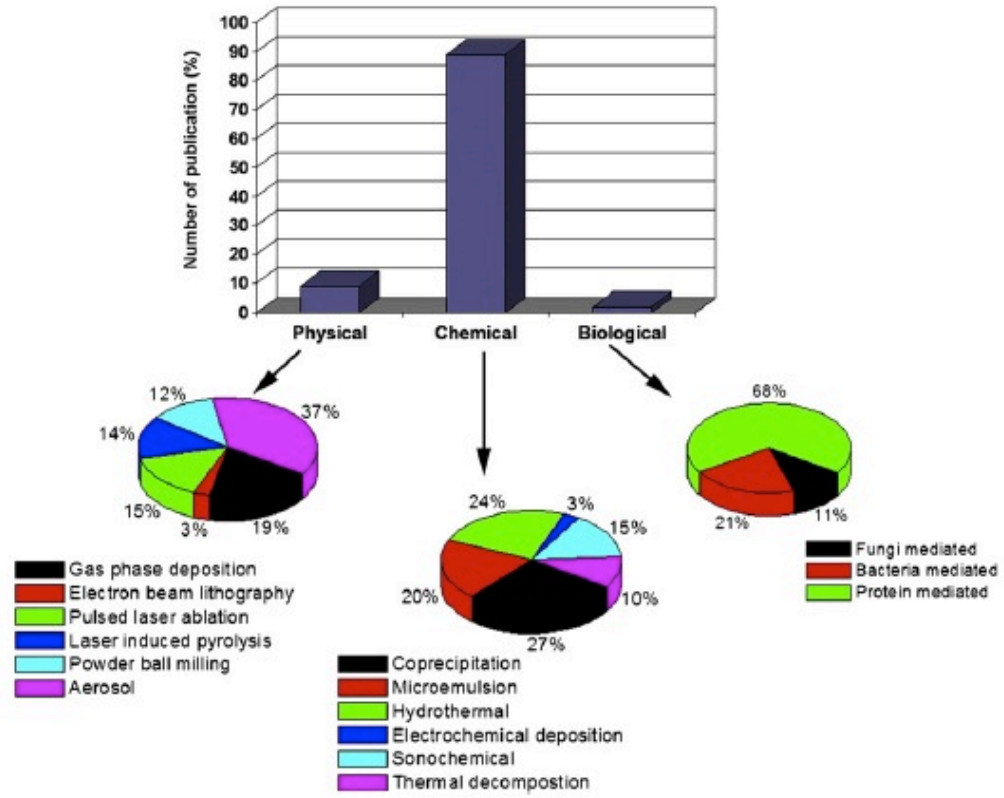

Figure 2. A comparison of published work on the synthesis of magnetic nanoparticles by three different routes.[38]

1.1.3.1. Chemical Synthesis Method

When trying to find the proper method for synthesizing magnetic nanoparticles, some parameters should be considered. There are some factors like phase purity and morphology of the particles that allow controlling the particle size, decreasing the aggregation of particles and achieving regular size distribution. For reliable reproducibility, it is essential to have enough knowledge about the most important factors for the formation of particles of the desired phase.

In this part, the focus is on the chemical methods because of cost effectiveness of the bulk quantity production, control of the particle size and size distribution, morphology and agglomeration level.

La Mer and Dinegar[39] showed that the metal salt is reduced to zero valent metal atoms. These atoms collide in reaction media to produce stable 'seed' nucleus in an irreversible step. In order to start nucleation, the concentration of metal atoms in solution should be high enough to achieve a specific concentration called 'supersaturation'.[40]

[38] Mahmoudi, M.; Sant, S.; Wang, B.; Laurent, S.; Sen, T. *Adv. Drug Deliv. Rev*. **2011**, *63*, 24.
[39] La Mer, V. K, Dinegar, R. H. *J. Am. Chem. Soc.* **1950**, *72*, 4847.
[40] Peng, X.; Manna, L.; Yang, W.; Wickham, J.; Scher, E.; Kadavanich, A.; Alivisatos, A. P. *Nature* **2000**, *404*, 59.

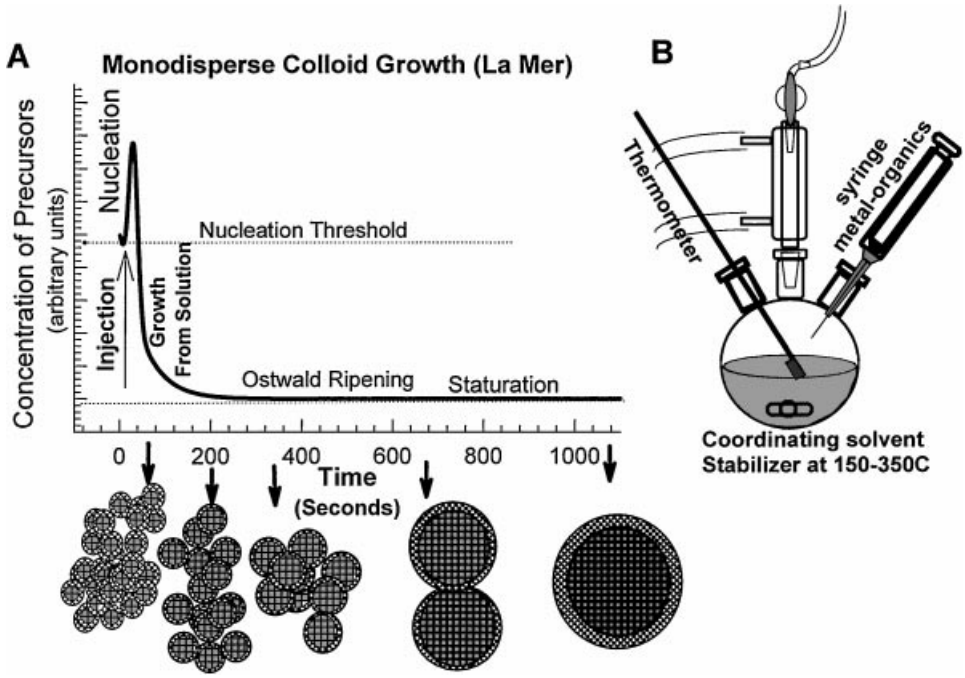

Figure 3. (a) Description of the La Mer model: separate nucleation and growth for the synthesis of monodisperse nanoparticles; (b) a typical ''hot-injection'' set-up to achieve the burst nucleation in (a). Picture taken from reference 1b.

The main methods of chemical synthesis of magnetic nanoparticles are the following:

Coprecipitation

The coprecipitation method is a simple and productive procedure. Iron oxide nanoparticles are produced by an ageing stoichiometric mixture of ferrous and ferric salts in aqueous media. The shape, size and composition of nanoparticles are determined by the Fe^{3+} and Fe^{2+} ratio, the pH of the solution, the temperature, and the ionic strength of the media. The special properties of coprecipitation method such as ease of implementation and lack of hazardous materials and procedures make it appropriate for biomedical applications.[41]

Thermal Decomposition

This method involves the chemical decomposition of the substance at the appropriate temperature. During this step, the breaking of the chemical bond will take place. This thermal decomposition pathway involves organometallic compounds such as iron (III) acetylacetonate in organic solvents (ethylenediamine or benzyl ether) with surfactants such as oleic acid, oleylamine, polyvinyl pyrrolidone (PVP), cetyltrimethyl ammonium bromide (CTAB) and

[41] a) Massart, R. *IEEE Trans. Magn*. **1981**, *17*, 1247; b) Zhao, Y.; Qiu, Z.; Huang, J. *Chin. J. Chem. Eng.* **2008**, *16*, 451; c) Indira, T. K.; Lakshmi, P. K. *Int. J. Pharm. Sci. Nanotech.* **2010**, *3*, 1035; d) Massart, R.; Cabuil, V. *J. Chem. Phys*. **1987**, *84*, 967; e) Sjogren, C. E.; Briley-Saebo, K.; Hanson, M.; Johansson, C. *Magn. Reson. Med.* **1994**, *31*, 268.

hexadecylamine. This approach has been used to control size distribution (4-45 nm) and morphology (spherical particles, cubes).[42] Sun, Zeng *et al.* presented the fabrication of monodisperse magnetite nanoparticles with size ranges of 2-20 nm by decomposition of iron (III) acetylacetonate at 260 °C in the presence of benzyl ether, oleic acid and oleylamine.[43]

The thermal decomposition method was also used by Nogués *et al*. to prepare highly mono disperse cubic and spherical maghemite (Fe_2O_3) nanocrystals.[44] They observed formation of monocrystals whose size and morphology could be controlled by the ratio of precursors and the decomposition time. Spherical nanoparticles resulted from short times (2-4 h) while particles with cubic morphology could be obtained in longer times (10-12 h).

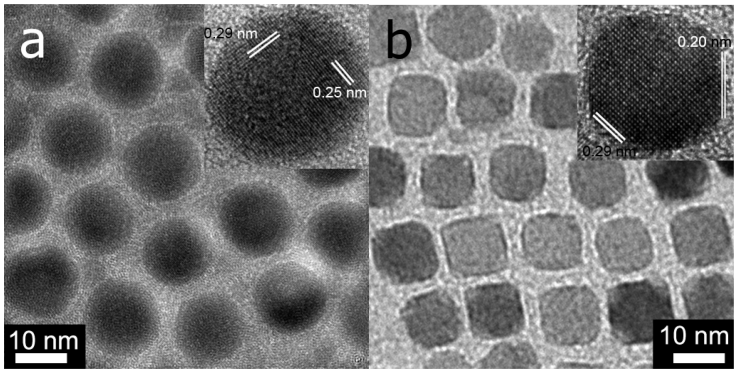

Figure 4. High resolution TEM images showing the mono disperse (a) nanosphere and (b) nanocubes achieved by the thermal decomposition method. Picture taken from reference 44.

Hydrothermal Synthesis

In this method, formation of particles is performed in aqueous media in reactors or autoclaves where the pressure can be more than 2000 psi and temperature can be above 200 °C. There are two main pathways for the formation of ferrites through hydrothermal conditions: hydrolysis and oxidation or neutralization of mixed metal hydroxides.[45] Results showed that the size of Fe_3O_4 particles increased with longer reaction times and higher water content caused the precipitation of larger Fe_3O_4 particles.[46] Also, when the temperature is increased, the nucleation process gets faster than crystal growth, which gives rise to nanoparticles with the smallest size. On the other hand, longer reaction times lead to larger nanoparticles because crystal growth overcomes the

[42] a) Jana, N. R.; Chen, Y.; Peng, X. *Chem. Mater.* **2004**. *16*. 3931; b) Rockenberger, J.; Scher, E. C.; Alivisatos, A. P. *J. Am. Chem. Soc.* **1999**. *121*, 11595.
[43] a) Sun, S.; Zeng, H. *J. Am. Chem. Soc.* **2002**, *124*, 8204; b) Sun, S.; Zeng, H.; Robinson, D. B.; Raoux, S.; Rice, P. M.; Wang, S. X.; Li, G. *J. Am. Chem. Soc.* **2004**, 126, 273.
[44] Salazar-Alvarez, G.; Qin, J.; Šepelák, V.; Bergmann, I.; Vasilakaki, M.; Trohidou, K. N.; Ardisson, J. D.; Macedo, W. A. A.; Mikhaylova, M.; Muhammed, M.; Baró, M. D.; Nogués, J. *J. Am. Chem. Soc.* **2008**, *130*, 13234.
[45] Willard, M. A.; Kurihara, L. K.; Carpenter, E. E.; Calvin, S.; Harris, V. G. Encyclopedia of Nanoscience and Nanotechnology. Nalwa, H. S, Ed. American Scientific Publishers: Valencia, CA, **2004***, 1,* 815.
[46] a) Lu, A.-H.; Salabas, E.; Schüth, F. *Angew. Chem. Int. Ed*. **2007**, *46*, 1222; b) Faraji, M.; Yamini, Y.; Rezaee, M. *J. Iran Chem. Soc.* **2010**, *7*, 1.

nucleation process.[47]

Synthesis of Magnetic Nanoparticles by Water-In-Oil Methods

The microemulsion technique is another important procedure to synthesize MNPs. First water-in-oil (w/o) microemulsions are formed by amphoteric surfactants. Normally, water creates a microdroplet surrounded by a monolayer of surfactant molecules organized with their polar heads toward the aqueous core, known as the water-pool, and the hydrophobic tails in contact with the bulk nonpolar solvent. With suitable surfactants, chemical composition and appropriate concentration of reactants, micellar cores can play a role as nanoreactors to form nanoparticles.[48] Different forms of nanoparticles can be generated in microemulsion systems. The water-in-oil microemulsion technique was used to synthesize iron nanoparticles, polymer coated magnetite nanoparticles and other nanoparticles such as gold, platinum or copper.[49]

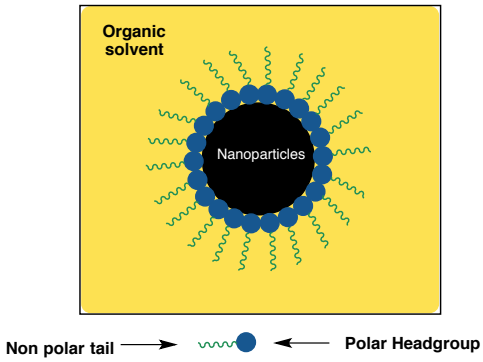

Figure 5. A reverse micelle (water in oil micelle) that encapsulates a nanoparticle within the aqueous core.

Decomposition of Metal-Containing Compounds on Ultrasonic Treatment

In this process metal carbonyls and their derivatives are used as precursors, albeit other organometallic compounds have also been used successfully. For example, Co nanoparticles were synthesized from solution of $Co_2(CO)_8$ in toluene by ultrasound-induced decomposition.[50]

1.1.4. Coatings and Stabilization (Core-Shell)

Surface modification plays an important role in the successful application of nanoparticles by improving stability, preventing agglomeration or improving biocompatibility. Moreover it provides additional functionalities, which allow anchoring a given catalyst, functionalization with different linkers or drug release strategies. In summary, core-shell strategy gives the chance to

[47] Zheng, Y. H.; Cheng, Y.; Bao, F.; Wang, Y. S. *Mater. Res. Bull.* **2006**, *41*, 525.
[48] a) Das, D.; Das, P. K. *Langmuir* **2003**, *19*, 9114; b) Deng, Y.; Wang, L.; Yang, W.; Fu, S.; Elaissari, A. *J. Magn. Magn. Mater*. **2003**, *257*, 69.
[49] Atkins, P.; Jones, L. *Chemical Principles: The Quest for Insight, 2nd Ed*. W. H. Freeman: **2001**, 1024.
[50] Yin, J. S.; Wang, Z. L. *Nanostruct. Mater.* **1999**, *10*, 845.

merge multiple functionalities on a single nanoparticle.

MNPs tend to aggregate because of the Brownian motion of bare nanoparticles putting them in close contact in combination through attractive Van der Waals and magnetic dipole-dipole interactions. As outcome, magnetic and nanoscale properties might be lost. If these particles are utilized in catalysis, agglomeration affects the catalytic activity because of the decreasing number of accessible reactive groups and diminished specific surface area.[51] In addition, nanoparticles of some metals are known to be pyrophoric, so finding an appropriate route to protect them is an important task.[52]

When it comes to in vivo application of MNPs one should take into account possible biodegradation when exposed to the biological system, as well as the formation of large aggregates. In this case, MNPs must be encapsulated with a biocompatible material.[53]

In addition to coating magnetic nanoparticles with a material to improve colloidal stability and biocompatibility, an additional concern is preventing further oxidation of the magnetic core which would alter its physical properties. In terms of drug delivery, magnetic nanoparticles are potential candidates for drug tracking with magnetic resonance imaging and the thermal delivery of a therapeutic agent.[54]

Surface coating provides magnetic nanomaterials with an outer shell, which can be of inorganic nature like silica, noble metals like gold or a biocompatible polymer. On the other hand, the choice of coating on NPs is based on the envisaged application. Organic molecules such as hydroxyl, carboxyl, amino or aldehyde introduce a functional group that allows for further functionalization. Polymers are interesting due to their biocompatibility and biodegradability. Coating by metals or metal oxides, in some cases, could increase the magnetic properties of NPs.[55]

1.1.4.1. Silica Coating

One of the most promising and important approaches in the development of core shell nanoparticles is the amorphous silica layer. The properties of silica are unique since it is nontoxic, biocompatible, optically transparent, chemically inert, thermally stable, allows regulation of the coating process, gives controlled porosity and has a well-known surface

[51] Majewski, P.; Thierry, B. *Crit. Rev. Solid State Mater. Sci.* **2007**, *32*, 203.
[52] Kitahara, H.; Oku, T.; Hirano, T.; Suganuma, K. *Diamond Relat. Mater*. **2001**, *10*, 1210.
[53] a) Muldoon, L. L.; Sandor, M.; Pinkston, K. E.; Neuwelt, E. A. *Neurosurgery* **2005**, *57*, 785; b) Moghimi, S. M.; Hunter, A. C.; Murray, J. C. *Pharmacol. Rev*. **2001**, 53, 283; c) Sosnovik, D. E.; Nahrendorf, M.; Weissleder, R. *Circulation* **2007**, *115*, 2076.
[54] a) Sun, Y.; Duan, L.; Guo, Z.; DuanMu, Y.; Ma, M.; Xu, L.; Zhang, Y.; Gu, N. *J. Magn. Magn. Mater.* **2005**, *285*, 65; b) Gupta, A. K.; Gupta, M. *Biomaterials* **2005**, *26*, 3995.
[55] Wu, W.; He, Q.; Jiang, C. *Nanoscale Res. Lett*. **2008**, *3*, 397.

chemistry.[56]

Indeed, surface modifications are easy because of the existence of plenty silanol groups on the silica layer. These silanol groups can be modified with different linkers or coupling agents to anchor ligands. Moreover, silica layers afford magnetic nanoparticles which are more compatible with biological systems.[57]

Several methods have been reported for the preparation of silica coated magnetic core shell nanoparticles; the most common reported pathways consist in reverse microemulsion synthesis and the Stöber sol-gel process.[58]

In reverse microemulsion method, non-ionic surfactants like Brij30 (non-ionic polyoxyethylated lauryl ether surfactant), Igepal CO-520 or Tritron-X are used in the formation of micelles. The micelles are used to control the extent of silica shell around the particles by hydrolysis and condensation of tetraethyl orthosilicate (TEOS).[59] The thickness of silica shell can be controlled by the amount of TEOS or nanoparticles.

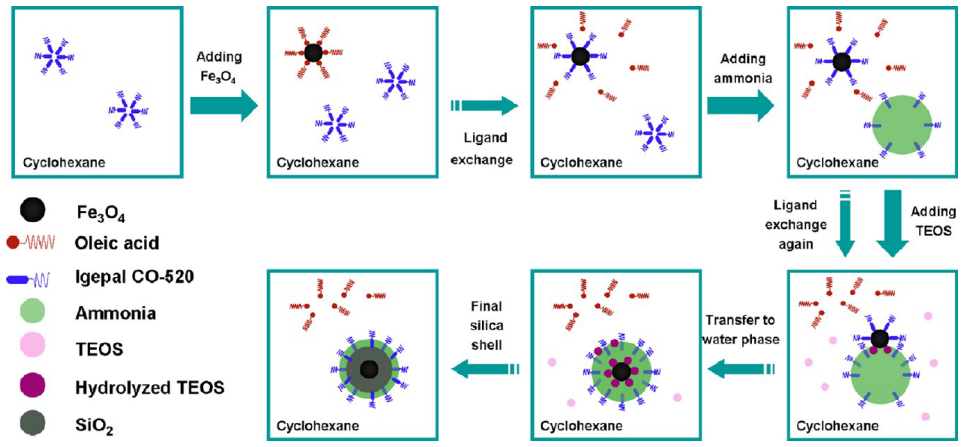

Figure 6. Procedure for coating of SiO_2 on the surface of Fe_3O_4 NPs with reverse microemulsion method. Picture taken from reference 59d.

The so-called Stöber method is the fastest and simplest method for synthesizing monodispersed spherical silica particles with the size between 20 nm and 2000 nm. In this pathway, a silica precursor such as TEOS is hydrolyzed and condensed in an ethanolic medium in the presence of

[56] a) Noh, M. S.; Jun, B. H.; Kim, S.; Kang, H.; Woo, M. A.; Minai-Tehrani A.; Kim, J. E.; Kim, J.; Park, J.; Lim, H.T. *Biomaterials* **2009**, *30*, 3915; b) Zhao, W.; Gu, J.; Zhang, L.; Chen, H.; Shi, J. *J. Am. Chem. Soc*. **2005**, *127,* 8916; c) Nooney, R. I.; Dhanasekaran, T.; Chen, Y.; Josephs, R.; Ostafin, A. E. *Adv. Mater*. **2002**, *14*, 529.

[57] a) Philipse, A. P.; van Bruggen, M. P. B.; Pathmamanoharan, C. *Langmuir* **1994**, *10*, 92; b) Liu, Q.; Xu, Z.; Finch, J. A.; Egerton, R. *Chem. Mater*. **1998**, *10*, 3936; c) Liu, X. Q.; Ma, Z. Y.; Xing, J. M.; Liu, H. Z.; *J. Magn. Magn. Mater*. **2004**, *270*, 1.

[58] Melancon, M. P.; Li, C. Core–shell magnetic nanomaterials for medical diagnosis and therapy. In: Kumar, C. Ed. Magnetic Nanomaterials. Weinheim, Wiley-VCH, **2009**, 259.

[59] a) Santra, S.; Tapec, R.; Theodoropoulou, N.; Dobson, J.; Hebard, A.; Tan, W. *Langmuir* **2001**. *17*, 2900; b) Yan, S.; Yin, J.; Zhou, E. *Colloids Surf. A*. **2006**, *287*, 153; c) Zhang, M.; Cushing, B. L.; O'Connor, C. J. *Nanotechnology* **2008**, 19, 1; d) Ding, H. L.; Zhang, Y. X.; Wang, S.; Xu, J. M.; Xu, S. C.; Li, G. H. *Chem. Mater*. **2012**, *24*, 4572.

ammonia at room temperature.[60]

In the case of preparing silica shell nanoparticles based on the Stöber method, silica shell is formed by the hydrolysis and condensation of tetraethoxysilane on the surface of nanoparticles in an aqueous solution containing ethanol and ammonia.[61]

1.1.4.2. Gold Coating

Another inorganic coating commonly used as a shell around particles is gold, which improves their stability in aqueous dispersions. Also, gold-coated core shell nanoparticles have plenty of applications in sensors, drug delivery and biodetection technologies.[62]

The main advantages of the gold shell are its high chemical stability, biocompatibility and the affinity for binding to amine and thiol terminal groups in organic molecules.[63]

Despite these advantages one must bear in mind that gold nanoshells should be thin enough in order to keep the magnetic properties of the magnetite core.

Dumbbell-like Fe_3O_4@Au nanoparticles were synthesized by decomposing iron pentacarbonyl, $Fe(CO)_5$, in the presence of oleic acid and oleylamine on the surface of gold nanoparticles.[64] The size of nanoparticles could be modulated by some factors like the temperature of injection of $HAuCl_4$ (as precursor for synthesis of Au NPs), or the $HAuCl_4$/oleylamine ratio.

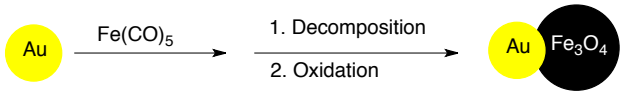

Scheme 1. Dumbbell-like Fe_3O_4@Au nanoparticles.

1.1.4.3. Polymers

Biocompatibility, or the ability of an engineered system to fulfill its intended application while minimizing undesirable interactions within the body, is a critical issue when using NPs in vivo.

In the case of polymer functionalized nanoparticles, the biocompatibility will be increased since the polymer layer helps shielding them from unintended biological interactions.[65]

---

[60] Stöber, W.; Fink, A.; Bohn, E. *J. Colloid. Interface Sci.* **1968**, *26*, 62.

[61] a) Almeida, M.P.S.; Caiado, K.L.; Sartoratto, P.P.C.; Cintra e Silva, D. O.; Pereira, A. R.; Morais, P. C. *J. Alloys Compd.* **2010**, *500*, 149; b) Digigow, R. G.; Dechézelles, J. F.; Dietsch, H.; Geissbühler, I.; Vanhecke, D.; Geers, C.; Hirt, A. M.; Rothen-Rutishauser, B. *J. Magn. Magn. Mater.* **2014**, *362*, 72.

[62] A) Ahmad, T.; Bae, H.; Rhee, I.; Chang, Y.; Jin, S. U.; Hong, S. *J. Nanosci. Nanotechnol*. **2012**, *12*, 5132; b) Kumagai, M.; Sarma, T. K.; Cabral, H.; Kaida, S.; Sekino, M.; Herlambang, N.; Osada, K.; Kano, M. R.; Nishiyama, N.; Kataoka, K.; *Macromol. Rapid Commun*. **2010**, *31*, 1521; c) Kayal, S.; Ramanujan, R. V. *J. Nanosci. Nanotechnol.* **2010**, *10*, 5527.

[63] Robinson, I.; Tung, L. D.; Maenosono; S.; Wälti, C.; Thanh, N. T. K. Nanoscale **2010**, *2*, 2624.

[64] Yu, H.; Chen, M.; Rice, P. M.; Wang, S. X.; White, R. L.; Sun, S. *Nano Lett.* **2005**, *5*, 379.

[65] Lewinski, N.; Colvin, V.; Drezek, R. *Small* **2008**, *4*, 26.

The polymeric coating of nanoparticles can be divided in two groups: synthetic polymers like poly(ethyleneglycol) (PEG),[66] poly(vinyl alcohol) (PVA),[67] poly(lactic acid) (PLA),[68] alginate,[69] polymethylmethacrylate (PMMA),[70] and natural polymers such as chitosan,[33] gelatin, [71] starch[72] and dextran.[73]

1.1.4.4. Functionalization with Silanes

Bifunctional silanes are a class of molecules with a general chemical formula $Y\text{-}(CH_2)_n\text{-}SiR_3$. Y is the headgroup functionality that can be anchored to other molecules such as organocatalysts, antibodies or immunoglobulins. On the other hand, $(CH_2)_n$ is an alkyl chain acting as a spacer of tunable length and SiR_3 the anchor group by which the silane will be grafted to the metal oxide surface. Silanes bind to the metal oxide surface through adsorptive bond or covalent bond. Their deposition on the surface of metal oxide nanoparticles takes place in two steps: (i) trimethoxysilane condenses to silane polymers in the presence of acid; (ii) the polymer forms a covalent bond with a hydroxy group on the surface of metal nanoparticles through a dehydration reaction, which leads to the formation of Si-O bonds.[17]

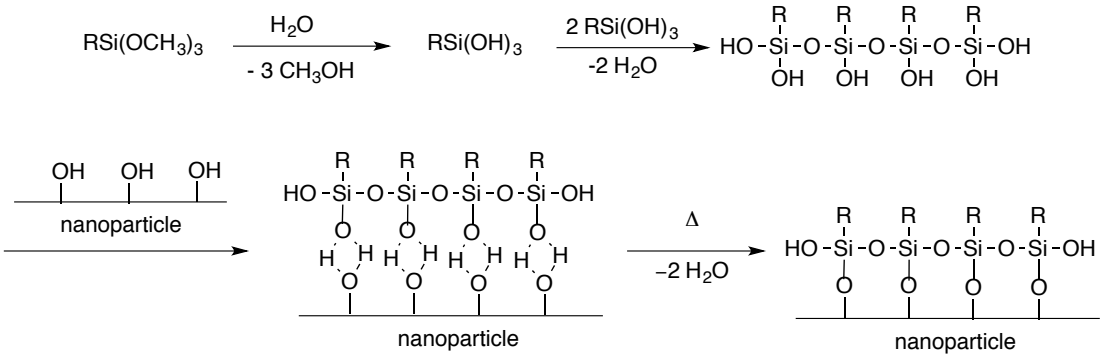

Scheme 2. Chemical reactions of silane-coupling agents on magnetic particles.

Perhaps one of their main advantages is the wide variety of commercially available choices, which include silanes with different functionalities such as amino, cyano, carboxylic acid, azide,

[66] Mondini, S.; Cenedese, S.; Marinoni, G.; Molteni, G.; Santo, N.; Bianchi, C. L.; Ponti, A. *J. Colloid. Interface Sci.* **2008**, *322*, 173.
[67] a) Pardoe, H.; Chua-anusorn, W.; Pierre, T. G.; Dobson, J. *J. Magn. Magn. Mater*. **2001**, *225*, 41; b) D'Souza, A. J. M.; Schowen, R. L.; Topp, E. M. *J. Control. Release* **2004**, *94*, 91.
[68] Chen, F.; Gao, Q.; Hong, G.; Ni, J. *J. Magn. Magn. Mater.* **2008**, *320*, 1921.
[69] Morales, M. A.; Finotelli, P. V.; Coaquira, J. A. H.; Rocha-Leão, M. H. M.; Diaz-Aguila C.; Baggio-Saitovitch, E. M.; Rossi, A. M. *Mater. Sci. Eng. C*. **2007**, *28*. 253.
[70] Zhu, D. M.; Wang, F.; Han, M.; Li, H. B.; Xu, Z.; Chin. J. *Inorg. Chem*. **2007**, *23*, 2128.
[71] Gaihre, B.; Aryal, S.; Khil, M. S.; Kim, H. Y. *J. Microencapsul.* **2008**, *25*, 21.
[72] Wang, W.; Zhang Z. K.; *J. Dispersion Sci. Technol*. **2007**, *28*, 557.
[73] Bautista, M. C.; Bomati-Miguel, O.; Morales, M. P.; Serna, C. J.; Veintemillas-Verdaguer S. *J. Magn. Magn. Mater.* **2005**, *293*, 20.

etc.[74] Some of these bifunctional silanes are shown in Figure 7.

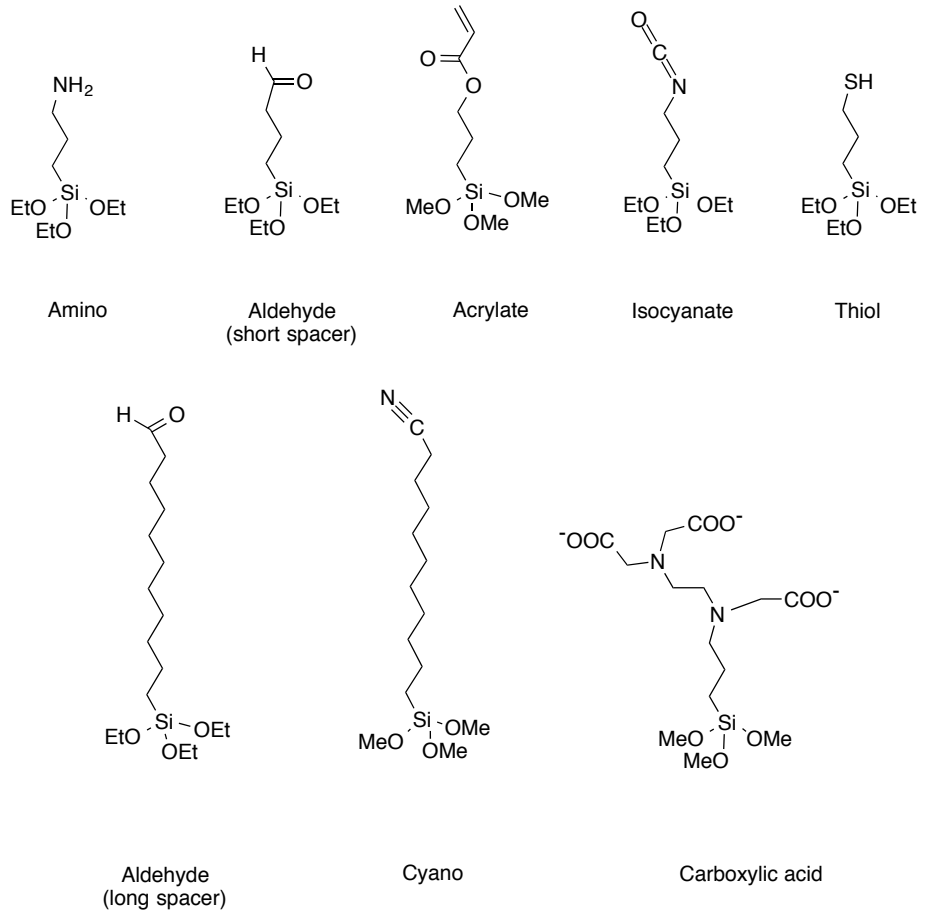

Figure 7. Bifunctional silanes.

1.1.4.5. Carbon

Another alternative way for protecting magnetic nanoparticles is using carbon which prevents them from corrosion and oxidation. A wide variety of methodologies have been used for the synthesis of carbon coating: for instance, electric arc discharge, catalytic pyrolysis of organic compounds, and the hydrothermal methods most of which are in small scale.[75] Stark *et al.*[76] developed a method to synthesize carbon-coated ferromagnetic cobalt nanoparticles (Co/C) in large scale.

[74] Palma, R. D.; Peeters, S.; Van Bael, M. J.; Van den Rul, H.; Bonroy, K.; Laureyn, W.; Mullens, J.; Borghs, G.; M. Guido. *Chem. Mater*. **2007**, *19*, 1821.
[75] a) Saito, Y. *Carbon* **1995**, *33*, 979; b) Junichi, N.; Chie, O.; Osamu, O.; Nobuyuki, N. *Carbon* **2006**, *44*, 2943; c) Taylor, A.; Krupskaya, Y.; Costa, S.; Oswald, S.; Krämer, K.; Füssel, S.; Klingeler, R.; Büchner, B.; Borowiak-Palen, E.; Wirth, M. P. *J. Nanopart. Res*. **2010**, *12*, 513; d) Bonanni, A.; Ambrosi, A.; Pumera, M. *Chem. Eur. J.* **2012**, *18*, 4541.
[76] Grass, R. N.; Athanassiou, E. K.; Stark, W. J. *Angew. Chem. Int. Ed.* **2007**, *46*, 4909.

1.2. Catalysis

A catalyst is a substance that can accelerate the rate of a chemical reaction by reducing its activation energy without being consumed itself during the reaction. They play an important role in our daily life, from producing wine or vinegar, to the revolutionary processes of Haber-Bosch and Ostwald to produce ammonia or nitric acid. Indeed nowadays more than 90% of produced chemical compounds, such as pharmaceuticals, basic materials and chemicals, processed food, etc. are obtained by the effects of catalysts, mainly in heterogeneous catalytic processes (multiphase catalysis).[77]

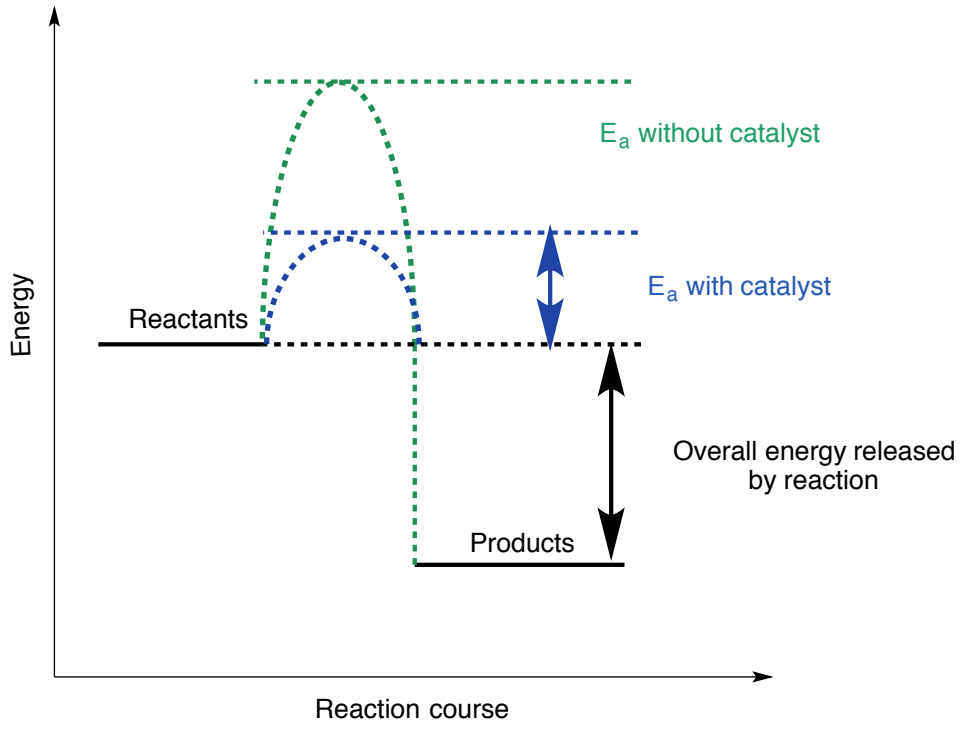

Figure 8. Potential energy diagram of a catalytic reaction.

1.2.1. Heterogeneous or Homogeneous

There are two main types of catalysis: heterogeneous or homogeneous. In the former, the catalyst is in a different phase than the reactants, while in the homogeneous, they are in the same phase.[78] Both processes have their own benefits and drawbacks. The reactions with homogeneous catalysts tend to be fast and have good conversion rate per molecule of the catalyst. However, separating them from the reaction media or reusing the catalyst is a challenging task.[79] In the heterogeneous case separation of catalyst from reaction media is simplified although the reaction

[77] a) Schüth, F. *Chem. Unserer Zeit*. **2006**, *40*, 92; b) Thomas, J. M.; Thomas, W. J. Principles and Practice of Heterogeneous Catalysis, Vol. 1, Wiley-VCH, Weinheim, 1996.
[78] Philipse, A. P. *J. Chem. Educ*. **2011**, *88*, 59.
[79] a) Cole-Hamilton, D. J. *Science* **2003**, *299*, 1702; b) Cornils, B.; Herrmann, W. A. *J. Catal*. **2003**, *216*, 23.

rate is usually limited due to their lower surface area. In addition the reaction can be performed in both gas and liquid phase.[80]

1.2.2. Asymmetric Catalysis

Chirality of molecules is an important parameter in nature. Many compounds related to living entities such as DNA, enzymes and hormones are chiral. Nature is able to select one enantiomer from its energetically identical enantiomer to build up life. This selection could give scientists a message about the importance of preparation of enantiomerically enriched products.[81] These compounds have a lot of applications in pharmaceutical, agricultural, organic synthesis, and natural product chemistry.

Indeed, both enantiomers of the same biologically active compounds such as drugs and agrochemicals have different bioactivity depending on their absolute configuration.[82]

Many natural products present interesting biological properties. However, it is not always easy to isolate them in practical amounts. Thus, the synthesis of natural products[83] is still an active area of research that allows to have access to the target compounds, as well as to derivatives with improved biological profiles.

Finding efficient methods to prepare enantiomerically pure compounds has been a challenge during years. In 2001, Knowles,[84] Noyori,[85] and Sharpless[86] received the Nobel prize for developing asymmetric catalytic oxidation and hydrogenation reactions.

In this approach, complexes involving a variety of metals such as Rh, Ru, Ir, etc. and many different ligands have been used to transform a prochiral substrate into a chiral molecule in a stereodirected manner.

More recently, asymmetric catalysis was expanded to include small organic molecules as catalysts in what is known as organocatalysis. This approach overcomes some issues of transition metals such as their toxicity and high cost.[87]

[80] Sheldon, R. A.; Downing, R. S. *Appl. Catal. A* **1999**, *189*, 163.
[81] a) Eschenmoser, A. *Tetrahedron* **2007**, *63*, 12821; b) Hein, J. E.; Blackmond, D. G. *Acc. Chem. Res.* **2012**, *45*, 2045.
[82] Ando, Y.; Fuse, E.; Figg, W. D. *Clin. Cancer Res*. **2002** , *8*, 1964.
[83] a) Najera, C.; Sansano, J. M. *Chem. Rev*. **2007**, *107*, 4584; b) Dounay, A. B.; Overman, L. E. *Chem. Rev*. **2003**, *103*, 2945; c) Gaunt, M. J.; Johansson, C. C. C. *Chem. Rev*. **2007**, *107*, 5596.
[84] Knowles, W. S. *Angew. Chem., Int. Ed.* **2002**, *41*, 1998.
[85] Noyori, R. *Angew. Chem., Int. Ed.* **2002**, *41*, 2008.
[86] Sharpless, K. B. *Angew. Chem., Int. Ed.* **2002**, *41*, 2024.
[87] Erkkila, A.; Majander, I.; Pihko, P. M. *Chem. Rev*. **2007**, *107*, 5416.

1.2.2.1. Asymmetric Organocatalysis

The first report for an asymmetric organocatalyzed reaction dates back to the 1970s by Hajos, Parrish, Eder, Sauer and Wiechert, when a simple amino acid (proline) was used as an enantioselective catalyst for the intramolecular aldol cyclization of a triketone.[88] Afterwards, in 2000 with two outstanding reports on chiral secondary amine catalysis (one by List, Lerner and Barbas and the other by MacMillan and co-workers,[89] dealing respectively with enamine and iminium ion catalysis) the underlying principles were rationalized and organocatalysis as a field started.

The enormous advantages of the metal-free organocatalysts were obvious: they are non-toxic and usually less expensive than organometallic catalysts. Also, organocatalysts are generally insensitive to oxygen and moisture in the atmosphere because of their purely organic nature. Therefore, the use of special conditions like dry solvents and reagents, using particular reaction vessels or storage containers is avoided. The main benefit of organocatalysis is its high reproducibility and operational simplicity. If bulk use is considered, organocatalysts offer the advantages of low cost and easy preparation in large quantities. After the two initial reports in 2000, a worldwide development in this field took place. Nowadays, organocatalysis plays a significant role in the field of enantioselective catalysis due to its potential for saving cost, time and energy, the simplicity of experimental procedures involved and the reduction in chemical waste.[90]

1.2.3. Two Typical Groups of Organocatalysts

Given their structural diversity, organocatalysts admit multiple classifications. One of the most important is made on the basis of the catalyst-substrate interaction. According to this, organocatalysts can be divided between those that estabilish a covalent bond with the substrate and those that do not, which mainly act by hydrogen bonding or ion pairing. In this thesis we willl deal with organocatalysts that bond covalently with substrates, in particular aminocatalysts.[91]

1.2.3.1. Aminocatalysts

Once the field of organocatalysts was opened, the development of new organocatalysts and

[88] a) Hajos, Z. G.; Parrish, D. R. German Patent DE 2102623, 29 July, 1971; b) Eder. U.; Sauer, G.; Wiechert, R.; German Patent DE 2014757, 7 October, 1971; c) Eder, U.; Sauer, G.; Wiechert, R. *Angew. Chem*. **1971**, *83*, 492; d) Hajos, Z. G.; Parrish, D. R. *J. Org. Chem.* **1974**, *39,* 1615.
[89] a) List, B.; Lerner, R. A.; Barbas, C. F.*J. Am. Chem. Soc*. **2000**, *122*, 2395; b) Ahrendt, K. A.; Borths, C. J.; MacMillan, D. W. C.; *J. Am. Chem. Soc*. **2000**, *122*, 4243.
[90] MacMillan, D. W. C. *Nature* **2008**, *455*, 304.
[91] Dalko, P. I.; Moisan, L. *Angew. Chem. Int. Ed*. **2004**, *43*, 5138.

activation modes became a very atractive area. One of the subgroup of organocatalysts is aminocatalysts that can be defined as secondary or primary chiral amines acting through the activation of carbonyl compounds such as aldehydes and ketones to construct chiral carbonyl compounds.

Chiral imidazolines, pyrrolidines and their derivatives and α-amino acids, to name a few, are known as efficient aminocatalysts.[92, 90, 87] In Figure 9 several aminocatalysts are shown.[93]

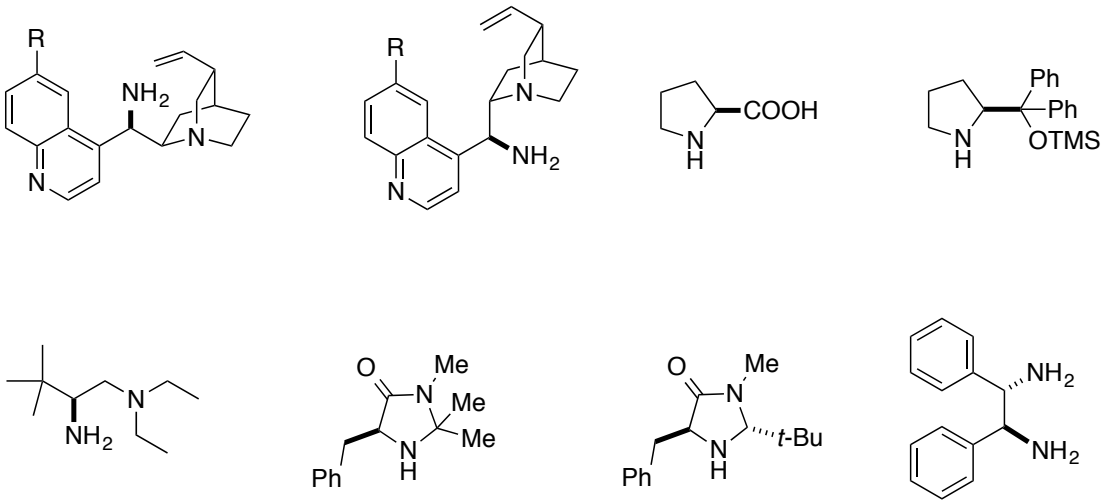

Figure 9. selected examples of aminocatalysts.

Given the broad functional group compatibility, the use of organocatalysts has been merged with photoredox catalysis[94] or metal catalysts,[95] allowing the synthesis of very complex molecules in straightforward manner.

This section will breifly adress the different activation modes of aminocatalysts: enamine catalysis, dienamine catalysis, iminium catalysis and SOMO catalysis.

Enamine Catalysis

Enamines are nucleophilic intermediates formed upon condensation between an amine and an enolizable carbonyl compound. Enamines have the ability to react with electrophiles to provide

[92] Mukherjee, S.; Yang, J. W.; Hoffmann, S.; List, B. *Chem. Rev.* **2007**, *107*, 5471;

[93] a) Rogozińska-Szymczak, M.; Jacek Mlynarski, *J. Eur. J. Org. Chem*. **2015**, 6047; b) Zhang, L.; Fu, N.; Luo, S. *Acc. Chem. Res*. **2015**, *48*, 986; c) Reddy, G. M.; Ko, C-T.; Hsieh, K-H.; Lee, C-J.; Das, U.; Lin, W. *J. Org. Chem.* **2016**, *81*, 2420; d) Wende, R. C.; Schreiner, P. R. *Green Chem.* **2012**, *14*, 1821; e) Bertelsen, S.; Marigo, M.; Brandes, S.; Dinér, P.; Jørgensen, K. A. *J. Am. Chem. Soc*. **2006**, *128*, 12973; f) Srivastava, V. *Asymmetric Catal.* **2014**, *1*, 8.

[94] a) Hopkinson, M. N.; Sahoo, B.; Li, J. L.; Glorius, F. *Chem. Eur. J.* **2014**, *20*, 3874; b) Lang, X.; Zhao, J.; Chen, X. *Chem. Soc. Rev.* **2016**, *45*, 3026.

[95] a) Deng, Y.; Kumar, S.; Wang, H. *Chem. Commun.* **2014**, *50*, 4272; b) Du, Z.; Shao, Z. *Chem. Soc. Rev.* **2013**, *42*, 1337.

the corresponding α-functionalized products.[96, 92]

Scheme 3. Enamine catalyst.

Actually, an intermolecular aldol addition catalyzed by proline had been reported in the early seventies and is known as the Hajos-Parrish-Eder-Sauer-Wiechert reaction.

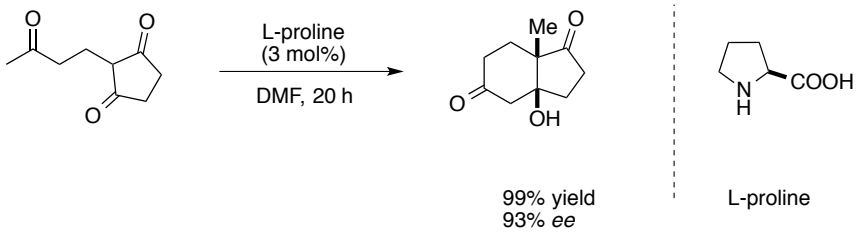

Scheme 4. The Hajos-Parrish-Eder-Sauer-Wiechert reaction.

Despite these early successes, it took a long time for synthetic organic chemists to identify and appreciate the importance of asymmetric organocatalysis.

As mentioned before, the breakthrough discovery of organocatalysis happened in 2000 with two papers which introduced two new modes of activation of carbonyl compounds.

The first one was reported by List, Lerner and Barbas who used proline as an organocatalyst for the asymmetric intermolecular aldol reaction between ketones and unmodified aldehydes (Scheme 5).

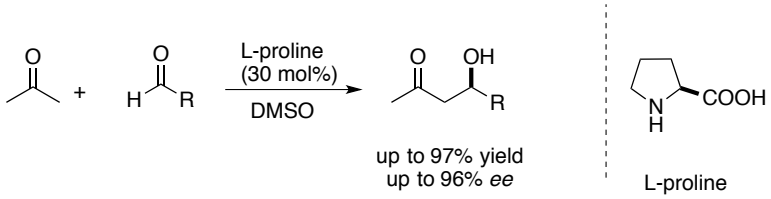

Scheme 5. Proline-catalyzed intermolecular aldol reaction.

Afterwards, proline and its derivatives presented significant potential to catalyse different reactions such as Mannich reactions, Michael addition reactions, α-aminations, α-aminoxylations,

[96] a) List, B. *Acc. Chem. Res*. **2004**, *37*, 548; b) Pihko, P. M.; Majander, I.; Erkkilä, A. *Top. Curr. Chem*. **2010**, *291*, 29.

alkylations and chlorination reactions among many others. Enamine catalysis will be explained in more detail in Chapter 2.

Dienamine Catalysis

This concept was found by Jørgensen and co-workers unexpectedly when they studied the iminium ion intermediate A from the reaction between 2-pentenal and a chiral amine-based catalyst (Scheme 6).[93e] They found that around 50% of intermediate is in the form of electron-rich dienamine B. This discovery inspired them to study the nucleophilicity of the γ-position instead of the β-position. In this manner, they developed the first enantioselective organocatalytic strategy that targets the γ-position of an α,β-unsaturated aldehyde.

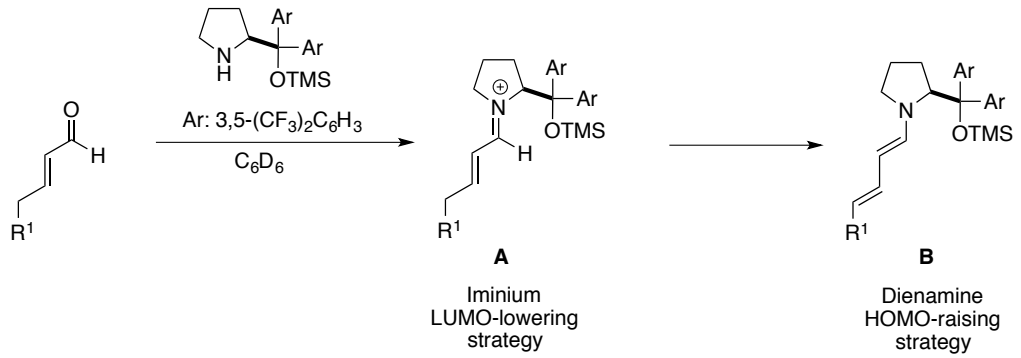

Scheme 6. Dienamine catalysis.

Iminium Ion Catalysis

In iminium ion catalysis the addition of an aminocatalyst to an α,β-unsaturated carbonyl structure generates an iminium ion. This is more electrophilic than its carbonyl precursor, and thus the carbonyl component is activated towards nucleophilic attack (Scheme 7, A). As mentioned before MacMillan and co-workers developed chiral imidazolidinones as catalysts for iminium ion activation for the enantioselective Diels-Alder reaction for α,β-unsaturated aldehydes with dienes in a pioneering work published in 2000 (Scheme 7, B).

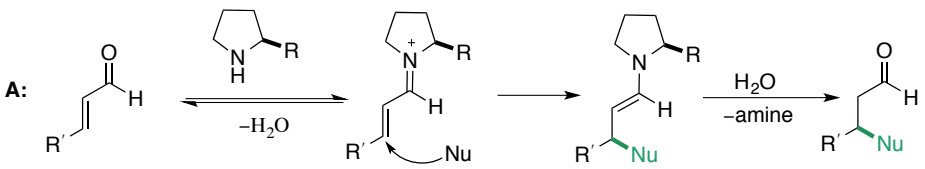

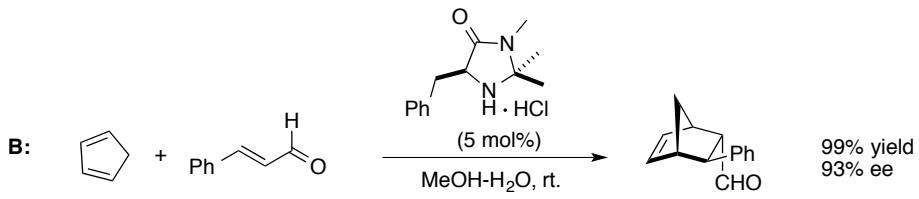

Scheme 7. (A) Iminium catalyst, (B) MacMillan organocatalytic Diels-Alder reaction.

In this example, the condensation of the catalyst with an enal leads to the formation of an iminium ion, which reacts as a dienophile with the diene leading to a Diels-Alder adduct. Iminium ion catalysis will be explained in more detail in Chapter 3.

SOMO Catalysis

In 2000, MacMillan *et al*. introduced another kind of organocatalytic activation mode, SOMO (singly occupied molecular orbital) catalysis, by generating a three-π-electron radical cation from an electron-rich enamine by one-electron oxidation step.[97] The high activity of the single occupied molecular orbital (SOMO) of this intermediate allows it to react with different nucleophiles at the α-carbon of the enamine (Scheme 8).

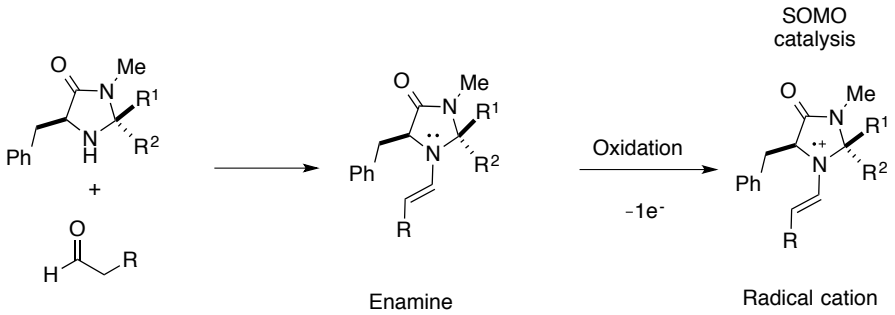

Scheme 8. The principle of SOMO catalysis.

SOMO-catalysis has been applied to asymmetric α-enolation, α-allylation and α-arylation of aldehydes.[98]

1.3. Magnetic Nanoparticle as Supports for Asymmetric Catalysts

The role of magnetite nanoparticles in science and technology is getting more and more significant because of their unique properties such as ease of availability, chemical inertness, high

[97] MacMillan, D. W. C. *Nature* **2008**, *455*, 304.
[98] a) Beeson, T. D.; Mastracchio, A.; Hong, J.-B.; Ashton, K.; MacMillan, D. W. C. *Science* **2007**, *316*, 582; b) Jang, H.-Y.; Hong, J.-B.; MacMillan, D. W. C. *J. Am. Chem. Soc*. **2007**, *129*, 7004; c) Sibi, M. P.; Hasegawa, M. *J. Am. Chem. Soc*. **2007**, *129*, 4124; d) Mukherjee, S.; List, B. *Nature* **2007**, 447, 152; e) Bertelsen, S.; Nielsen, M.; Jørgensen, K. A. *Angew. Chem. Int. Ed.* **2007**, *46*, 7356.

surface area-to-volume ratio and excellent thermal stability. Also, magnetic nanoparticles (MNPs) are easy to separate from the reaction mixture with an external magnet, which means there is no need to use filtration and centrifugation, which helps to save energy and also reduce catalyst loss.[99]

1.3.1. Common Techniques for Immobilization of Homogeneous Asymmetric Catalysts

The immobilization of catalytic species onto a variety supports is strategy that aims at facilitating their separation from the reaction media with the ultimate goal of being able to reuse these catalytic materials as many times as possible. Several methods are used to anchor chiral catalysts to an insoluble support, each of them having their own advantages and drawbacks.

The adsorption approach is a very facile method that relies in non-covalent interactions. However, catalysts anchored via adsorption tend to be unstable in the case only weak van der Waals interactions are in play. This causes catalyst leaching due to competing interactions with solvents and/or substrates (Figure 10a).

Electrostatic interactions are another simple method, which can be applied to ionic catalytic species. In this case, the solid support can be either anionic or cationic, whatever is required for the catalyst to have ion-pairing interaction with support. Different supports like organic or inorganic ion-exchange resins, inorganic clays and zeolites can be used with this technique. However, there is a competition with other ionic species (either present in or produced during the reaction) in solution which eventually leads to catalyst instability and leaching. (Figure 10b)

A third technique involves an entrapped catalytic complex inside of the pores of a solid support. In this case, the size of the metal complex is related to that of the window or tunnel of the porous solid. However this methodology is more complex than the two other ones (Figure 10c)

Finally, we have covalent linkage strategy (Figure 10d), which is the strongest binding between linker or catalyst and a support. However, for covalent linkage, a complementary functionalization of the catalyst and the surface of support is required. On the other hand this modification gives rise to materials that are more stable than with any other technique.[100]

[99] a) Shylesh, S.; Schnemann, V.; Thiel, W. R. *Angew. Chem. Int. Ed*. **2010**, *49*, 3428; b) Polshettiwar, V.; Baruwati, B.; Varma, R. S. *Chem. Commun*. **2009**, 1837; c) Polshettiwar, V.; Varma, R. S. *Org. Biomol. Chem.* **2009**, *7*, 37; d) Gawande, M. B.; Branco, P. S.; Varma, R. S. *Chem. Soc. Rev.* **2013**, *42*, 3371.

[100] Wang, Z.; Ding, K.; Uozumi, Y. *Handbook of Asymmetric Heterogeneous Catalysis.* Ding, K.; Y. Uozumi, Eds. WILEY-VCH Verlag GmbH & Co. KGaA, Weinheim, **2008**.

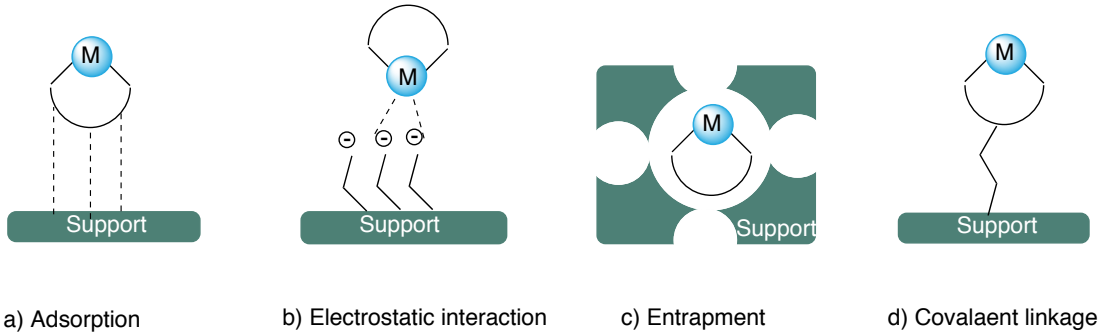

Figure 10. Strategies for immobilizing homogeneous chiral catalysts onto solid supports.

1.3.1.1. The "Click Chemistry"

To take inspiration on how to synthesize huge molecules one can turn to nature, which is able to make nucleic acids, proteins and polysaccharides based on carbon-heteroatom linkages. Following nature's guidance, the term "click chemistry" was highlighted by Sharpless *et al.* [101] and it refers to the development of powerful methods to build up organic molecules using blocks such as azides or alkynes. In addition, other reactions such as nucleophilic ring opening of aziridines and epoxides, carbonyl chemistry, additions to carbon–carbon multiple bonds such as Michael additions and cycloaddition reactions such as Diels–Alder reaction could be mentioned in this area.[102] However, among them the copper-catalyzed azide-alkyne cycloaddition (CuAAC) has attracted a lot of attention because of being very general, experimentally convenient, efficient and high-yielding.

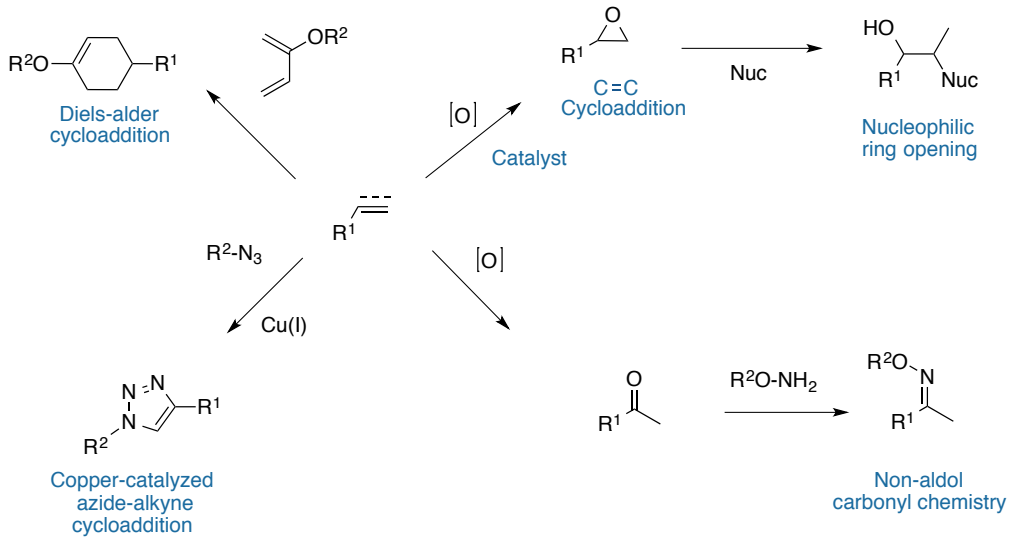

Scheme 9. Some examples of reactions based on the click chemistry concept.

[101] Kolb, H. C.; Finn, M. G.; Sharpless, K. B. *Angew. Chem., Int. Ed.* **2001**, *40*, 2004.
[102] Moses, J. E.; Moorhouse, A. D. *Chem. Soc. Rev.* **2007**, *36*, 1249.

1.3.1.2. Azide-alkyne cycloaddition as "click reaction"

The first examples of click chemistry, can be found in nature with numerous example of carbon-heteroatom linkages, including nucleic acids, proteins, lipids and polysaccharides, which represent a simple way to generate large, diverse oligomers.

In the lab, perhaps the most typical example of click chemistry is the copper(I)-catalyzed azide-alkyne cycloaddition (CuAAC) developed independently by Meldal and Sharpless. CuAAC is a regioselective reaction through which an azide and a terminal alkyne form a 1,4-disubstituted-1,2,3-triazole in the presence of a copper(I) catalyst and copper(I)-binding ligand, as shown in Scheme 10.[103]

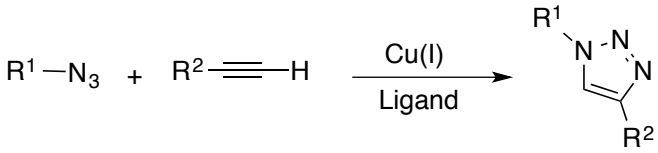

Scheme 10. CuAAC reaction.

The 1,2,3-triazole heterocycle is useful in medicine and pharmaceutical applications due to its high chemical stability, strong dipole moment, aromatic character and hydrogen bond accepting capabilities.[104]

Regarding to numerous drug compounds containing 1,2,3-triazoles, it can be said that click chemistry has sped up the process of drug discovery**.** Examples of such drugs include tazobactam **a**,[105] a penicillin derivative, resveratrol analogue **b**,[106] and histone deacetylase inhibitor **c** (Figure 11).[107]

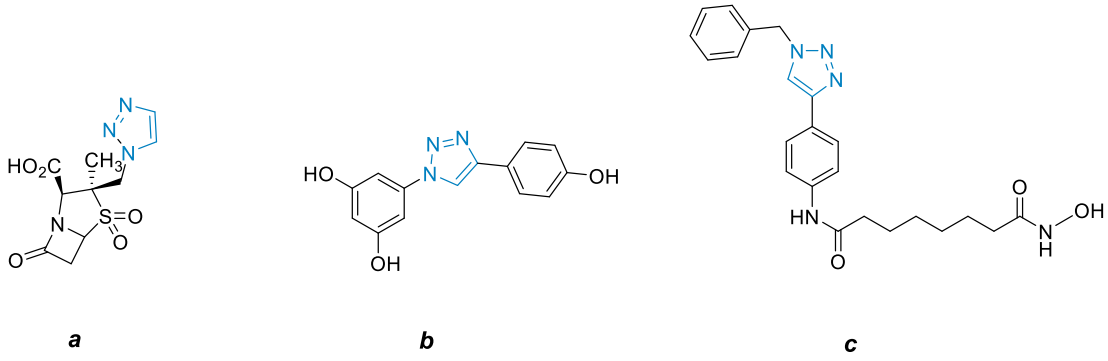

a ***b*** ***c***

Figure 11. Some examples of drugs that contain 1,2,3-triazoles.

[103] a) Tornøe, C. W.; Christensen, C.; Meldal, M. *J. Org. Chem*. **2002**, *67*, 3057; b) Rostovtsev, V. V.; Green, L. G.; Fokin, V. V.; Sharpless, K. B. *Angew. Chem. Int. Ed.* **2002**, 41, 2596.
[104] Finn, M. G.; Fokin, V. V. *Catal. Precious Met*. **2010**, 235.
[105] Bennett, I.; Broom, N. J.; Bruton, G.; Calvert, S.; Clarke, B. P.; Coleman, K.; Edmondson, R.; Edwards, P.; Jones, D.; Osborne, N. F. *J. Antibiot*. **1991**, *44*, 331.
[106] Pagliai, F.; Pirali, T.; Del Grosso, E.; Di Brisco, R.; Tron, G. C.; Sorba, G.; Genazzani, A. A. *J. Med. Chem.* **2006**, *49*, 467.
[107] Chen, Y.; Lopez-Sanchez, M.; Savoy, D. N.; Billadeau, D. D.; Dow, G. S.; Kozikowski, A. P. *J. Med. Chem*. **2008**, *51*, 3437.

With a quick search one can realize that CuAAC has a very broad application in science including live cell labeling,[108] peptide synthesis,[109] bioconjugation,[110] radiolabeling,[111] synthesis and cross-linking of polymers, dendrimers, hydrogels and microgels.[112]

1.3.1.3. Functionalization of NPs and MNPs with CuAAC

The CuAAC reaction has been successfully applied to a variety of scientific areas. Indeed its advantages have allowed application in materials chemistry, [113] dendrimer build-up, [114] polymers,[115] nanoparticle synthesis[116] and interlocked molecules.[117]

Due to its high efficiency, mild reaction condition and versatile binding, the CuAAC has been used for modification of NPs surface and preparing active catalysts with high success. In this regard, some examples for modification of nanoparticles surface will be briefly mentioned.

Au and Ag nanoparticles have been used in biology, medicine, and catalysis. Therefore. It would be interesting to functionalize them, and among all the methods to do so, CuAAC has proven very useful. In 2006, Fleming *et al.* described a method to functionalize the surface of Au NPs: first, the methyl-terminated chains in the surface of NPs were partially replaced with bromo-functionalized thiol and afterwards the bromide was substituted by an azide. Then, several alkynes were anchored to the Au NPs via click chemistry. However for anchoring ethynyl compounds, the reaction requires longer times (24-96 h) and the yields reported for 1,2,3-triazoles are between 5-54%.[118]

[108] Hong, V.; Steinmetz, N. F.; Manchester, M.; Finn, M. G. *Bioconjugate Chem*. **2010**, *21*, 1912.
[109] Lutz, J.-F.; Zarafshani, Z. *Adv. Drug Deliv. Rev. 60*, **2008**, *60*, 958.
[110] a) Weckhuysen, B. M. *Chem. Soc. Rev.* **2010**, *39*, 4557; b) Trache, A.; Meininger, G. A. Total Internal Reflection Fluorescence (TIRF) Microscopy, in Curr. Protoc. Microbiol. 2A.2.1-2A.2.22 (John Wiley & Sons, Inc., 2008).
[111] Sirion, U.; Kim, H. J.; Lee, J, H.; Seo, J, W.; Lee, B, S.; Lee, S. J.; Oh, S. J.; Chi, D. Y. *Tetrahedron Lett.* **2007**, *48*, 3953.
[112] Liang, L.; Astruc, D. *Coord. Chem. Rev*. **2011**, *255*, 2933.
[113] Iha, R. K.; Wooley, K. L.; Nystrom, A. M.; Burke, D. J.; Kade, M. J.; Hawker, C. J. *Chem. Rev*. **2009**, 109, 5620.
[114] Franc, G.; Kakkar, A. *Chem. Commun.* **2008**, *42*, 5267.
[115] a) Dichtel, W. R.; Miljanic, O. S.; Spruell, J. M.; Heath, J. R.; Stoddart, J. F. *J. Am. Chem. Soc*. **2006**, *128*, 10388; b) Meldal, M. *Macromol. Rapid Commun*. **2008**, *29*, 1016.
[116] Boisselier, E.; Diallo, A. K.; Salmon, L.; Ruiz, J.; Astruc, D. *Chem. Commun*. **2008**, *39*, 4819.
[117] a) Megiatto, J. D., Jr.; Schuster, D. I. *J. Am. Chem. Soc*. **2008**, *130*, 12872; b) Megiatto, J. D., Jr.; Schuster, D. I. *Chem. Eur. J.* **2009**, *15*, 5444.
[118] Fleming, D. A.; Thode, C. J.; Williams. M. E. *Chem. Mater*. **2006**, *18*, 2327.

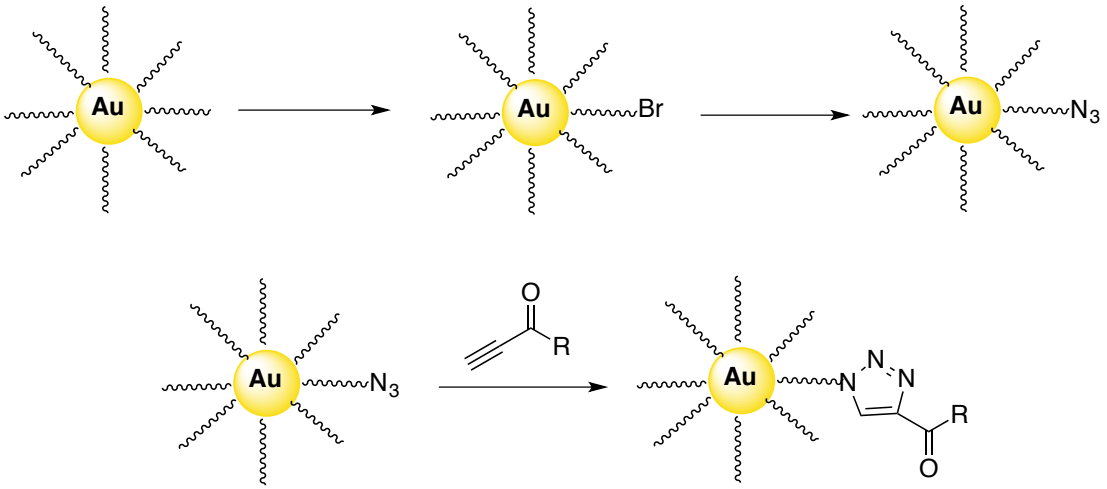

Scheme 11. "Click" functionalization of Au nanoparticle surfaces.

In another report, Williams and coworkers first prepared 11-azidoundecane-1-thiol and then mixed alkyl thiol-protected gold nanoparticle with this linker to achieve azide-functionalized NPs.

The CuAAC-based anchoring of the alkyne moiety was performed under microwave heating, which helped to keep reaction time under 10 minutes. The reported yield was between 78-100%, which is a big improvement for synthesizing modified Au NPs.[119]

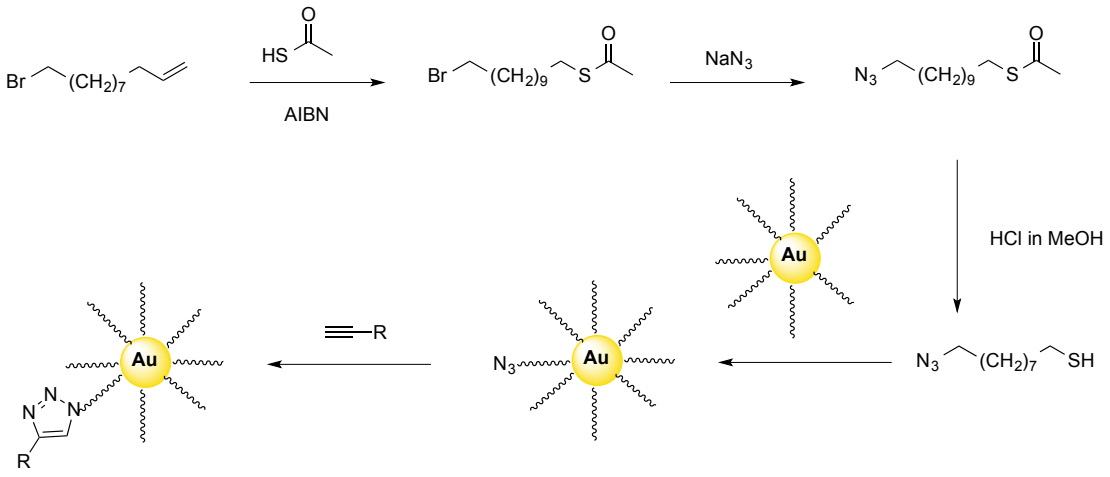

Scheme 12. Synthesis of the azide-functionalized gold nanoparticles.

In another approach, alkyne-functionalized Ag NPs were obtained by reaction between silver nitrate and sodium borohydride in the presence of 4-(prop-2-ynyloxy)pyridine solution at room temperature. Then, azide-functionalized small molecules or polymers were added to the above

[119] Sommer, W. J.; Weck, M. *Langmuir* **2007**, 23, 11991.

alkyne-functionalized Ag NPs suspension for surface modification based on CuAAC reaction.[120]

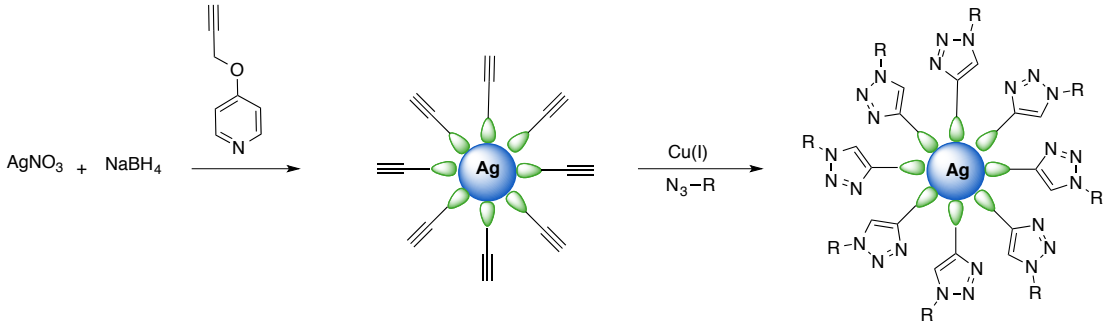

Scheme 13. Synthesis of alkyne-functionalized Ag NPs using in situ reduction of $AgNO_3$.

Surface modification of magnetic nanoparticles is also a big challenge due to their numerous applications in different fields such as biotechnology, medicine[121] and catalysis.[122]

Oleic-acid functionalized MNPs can undergo ligand exchange with phosphoric acid or carboxylic acid-containing ligands that introduce an azide group for further functionalization. Turro *et al.* reported that oleic acid on the surface of MNPs was replaced with phosphoric acid or a 5-hexynoic acid ligand. TEM images did not show any aggregation. Afterwards, a CuAAC reaction was performed in the presence of $CuSO_4$-sodium ascorbate to attach various functionalized molecules or polymers.[123]

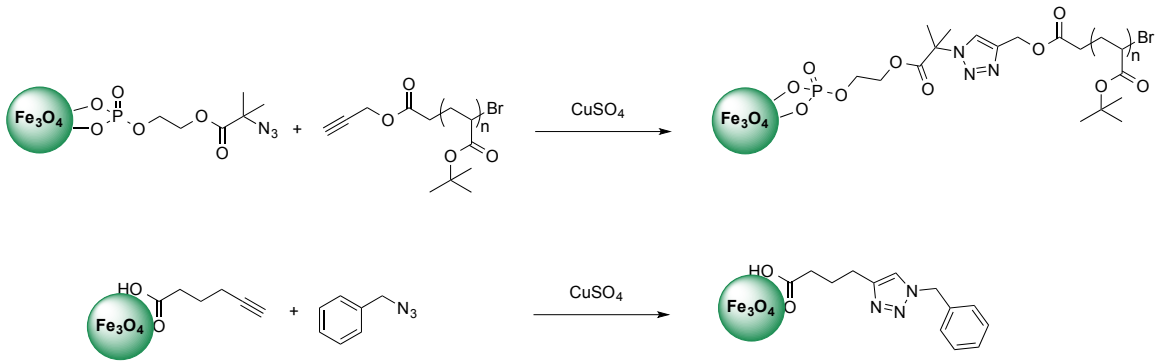

Scheme 14. Click reaction of magnetic nanoparticles.

Click chemistry based on CuAAC was further extended and developed to control the assembly

[120] Li, H.; Yao, Y.; Han, C.; Zhan, J. *Chem. Commun*. **2009**, 4812.
[121] a) Gao, J.; Gu, H.; Xu, B. *Acc. Chem. Res.* **2009**, *42*, 1097;b) Fang, C.; Zhang, M. *J. Mater. Chem*. **2009**, *19*, 6258; c) Ali, I.; Uddin, R.; Salim, K.; Rajora, A. K.; Rather, M. A.; Wani, W. A.; Haque, A. *Curr. Cancer Drug Targets* **2011**, *11*, 135; d) Oh, J. K.; Park, J. M. *Prog. Polym. Sci*. 2011, 36, 168–189.
[122] a) Tucker-Schwartz, A. K.; Garrell, R. L. *Chem. Eur. J.* **2010**, *16*, 12718; b) Gleeson, O.; Davies, G. L.; Peschiulli, A.; Tekoriute, R.; Gun'ko, Y. K.; Connon, S. J. *Org. Biomol. Chem*. **2011**, *9*, 7929; c) Yiu, H. H. P.; Keane, M. A. *J. Chem. Technol. Biotechnol*. **2012**, *87*, 583.
[123] White, M. A.; Johnson, J. A.; Koberstein, J, T.; Turro, N. J. *J. Am. Chem. Soc.* **2006**, *128*, 11356.

and organization of NPs into various multidimensional compounds. To this end, clickable MNPs were first prepared using alkyne and azide linkers and then they were assembled into stable magnetic colloidosomes by crosslinking NPs at water–oil interface using the CuAAC reaction under ambient conditions.

This system is suitable for encapsulating and protecting sensitive molecules such as drugs and biomolecules. Unreacted azide and alkyne sites on the particles also provided attachment sites for further functionality.[124]

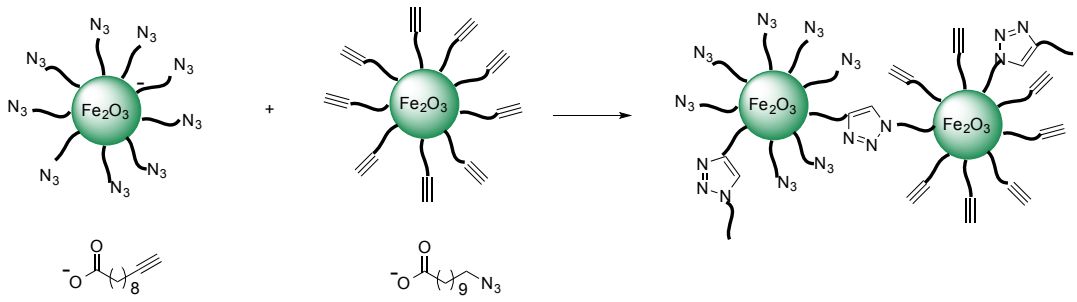

Scheme 15. Formation of magnetic colloidosomes through self-assembly at water–oil interface followed by interfacial crosslinking of NPs via CuAAC reaction.

In another field of chemistry, CuAAC was applied to the construction of dendrimers and also to the functionalization and introduction of multiple functionalities on their structure.[125]

In summary, CuAAC is a remarkable reaction because of its mild conditions, which allows to run the reaction with low amounts of a cheap catalyst and affording the product in excellent yield and without byproducts. [126]

In our group and Prof. Reiser's group, the copper-catalyzed alkyne-azide cycloaddition has been successfully used for covalently anchoring plenty of organocatalysts onto different solid supports. These were tested in a variety of reactions such as aldol,[127] Michael addition,[128] α-aminoxylation of aldehydes and ketones, [129] Mannich,[130] Friedel–Crafts alkylation[131] or oxidation of alcohols[132] (Figure 12).

[124] Samanta, B.; Patra, D.; Subramani, C.; Ofir, Y.; Yesilbag, G.; Sanyal, A.; Rotello, V. M. *Small* **2009**, *5*, 685.
[125] a) Joralemon, M. J.; O'Reilly, R. K.; Matson, J. B.; Nugent, A. K.; Hawker, C. J.; Wooley, K. L. *Macromolecules* **2005**, *38*, 5436; b) Ornelas, C.; Ruiz Aranzaes J.; Cloutet, E.; Alves, S.; Astruc, D. *Angew. Chem. Int. Ed.* **2007**, *46*, 872; c) Goyal, P.; Yoon, K.; Weck, M. *Chem. Eur. J.* **2007**, *13*, 8801; d) Malkoch, M.; Schleicher, K.; Drockenmuller, E.; Hawker, C.J.; Russell, T.P.; Wu, P.; Fokin, V. V. *Macromolecules* **2005**, *38*, 3663.
[126] Zamboulis, A.; Moitra, N.; Moreau, J. J. E.; Cattoën, X.; Wong Chi Man, M. *J. Mater. Chem.* **2010**, *20,* 9322.
[127] Font, D.; Jimeno, C.; Pericàs, M. A. *Org. Lett.* **2006**, *8*, 4653.
[128] a) Alza, E.; Cambeiro, X. C.; Jimeno, C.; Pericàs, M. A. *Org. Lett.* **2007**, *9*, 3717; b) Keller, M.; Perrier, A.; Linhardt, R.; Travers, L.; Wittmann, S.; Caminade, A. M.; Majoral, J. P.; Reiser, O.; Ouali, A. *Adv. Synth. Catal.* **2013**, *355*, 1748; c) Riente, P.; Mendoza, C.; Pericás, M. A. *J. Mater. Chem.* **2011**, *21*, 7350.
[129] Font, D.; Bastero, A.; Sayalero, S.; Jimeno, C.; Pericàs, M. A. *Org. Lett.* **2007**, 9, 1943.
[130] Sayalero, S.; Bastero, A.; Pericàs, M. A. *Chem. Eur. J.* **2009**, *15*, 10167.
[131] Riente, P.; Yadav, J.; Pericàs, M. A. *Org. Lett.* **2012**, *14*, 3668.
[132] Schätz, A.; Grass, R. N.; Stark, W. J.; Reiser, O. *Chem. Eur. J.* **2008**, *14*, 8262.

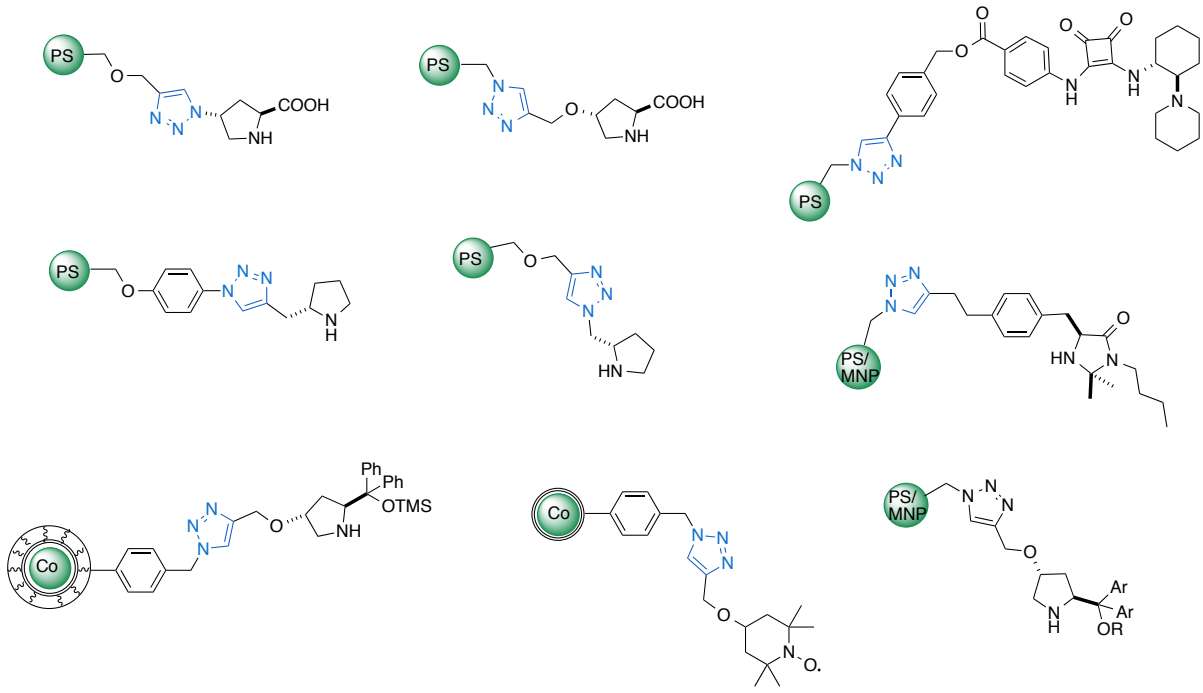

Figure 12. Supported organocatalysts with a triazole linker.

1.4. Aims and objectives

In the present thesis we aim to develop new functional materials based on magnetic nanoparticles and apply them in catalytic reactions. To that aim we will:

1. Prepare hybrid materials based on magnetic nanoparticles, κ-carrageenan and Jørgensen-Hayashi catalysts. Then we will evaluate the activity of these catalysts for Michael addition of aldehydes to nitroalkenes (Chapter 2).
2. Prepare an analogue of the second generation MacMillan catalyst and immobilize it onto Fe_3O_4 NPs and polystyrene. The result heterogeneous catalysts will be tested in the asymmetric Friedel-Crafts alkylation of indoles with α,β-unsaturated aldehydes (Chapter 3).
3. Prepare another hybrid material based on microporous organic polymers (MOPs) encapsulated with Pd nanoparticle and Co/C nanobeads. The activity of these catalysts will be evaluated in the hydrogenation and Suzuki cross-coupling reactions (Chapter 4).

Hybrid magnetic materials (Fe_3O_4-k-carrageenan) as catalysts for the Michael addition of aldehydes to nitroalkenes

Table of Contents

2.1. Hybrid Materials

Hybrid materials are a type of composites made of two substances or more combined in the molecular scale to give rise to a new material.[1] This approach allows the preparation of materials with different properties with an increasing economical interest. Remarkably, even before humans started to use synthetic hybrid materials, a lot of examples could be found in nature such as carved structures found in radiolaria or diatoms, mollusc shells, bone or teeth tissues in vertebrates.[2] And now, in the 21st century, there are broad applications such as photoactive coatings,[3] hybrid organic–inorganic materials containing organic chromophores,[4] biomaterials,[5] dental applications,[6] bone tissue engineering,[7] solar cells applications,[8] or as sorbent for arsenic removal.[9] Nowadays, hybrid materials constitute a research field on their own with a lot of potential for developing new materials. The number of publications from 1980s until 2013 confirms the importance of this field and shows its fast-growing development (Figure 1).

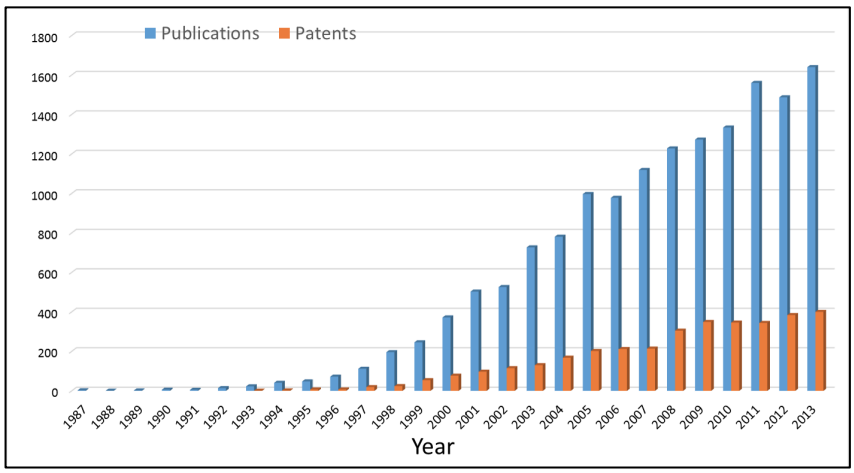

Figure 1. Diagram showing number of publications and patents in the field of inorganic-organic hybrid materials in the last decades. Source: SciFinder Scholar, Keywords: inorganic organic hybrid materials.[10]

[1] a) Sanchez, C.; Ribot, F. *New J. Chem*. **1994**, *18*, 1007; b) Nicole, L.; Rozes, L.; Sanchez, C. *Adv. Mater.* **2010**, *22*, 3208.
[2] Sanchez, C.; Arribart, H.; Giraud-Guille, M. M. *Nature Mater*. **2005**, *4*, 277; b) Mann, S. in Biomimetic Materials Chemistry, ed. S. Mann, Wiley-VCH, Weinheim, 1997, p. 1.
[3] a) Boilot, J. P.; Chaput, F.; Gacoin, T.; Malier, L.; Canva, M.; Brun, A.; Lévy, Y.; Galaup, J. P. *C. R. Acad. Sci.* **1996**, *322*, 27; b) Faloss, M.; Canva, M.; Georges, P.; Brun, A.; Chaput, F.; Boilot, J. P. *Appl. Opt*. **1997**, *36*, 6760.
[4] Sanchez, C.; Lebeau, B.; Chaput, F.; Boilot, J. P. *Adv. Mater*. **2003**, 15, 1969.
[5] Shin, H.; Jo, S.; Mikos, A. G, *Biomaterials* **2003**, *24*, 4353.
[6] a) Wolter, H.; W. Storch, *J. Sol–Gel Sci. Technol*. **1994**, *2*, 93; b) Wolter, H.; Storch, W.; Ott, H, *Mater. Res. Soc. Symp. Proc.* **1994**, *346*, 143.
[7] Fragal, E. H.; Cellet, T. S. P.; Fragal, V. H.; Companhoni, M. V. P.; Ueda-Nakamura, T.; Muniz, E. C.; Silva. R.; Rubira, A. F. *Carbohydr. Polym*. **2016**, *152*, 734.
[8] Ginger, D. S.; Greenham, N. C. *J. Appl. Phys.* **2000**, *87*, 1361.
[9] Martínez-Cabanas, M.; López-García, M.; Barriada, J. L.; Herrero, R.; Sastre de Vicente, M. E. *Chem. Eng. J*. **2016**, *301*, 83.
[10] Kickelbick, G. *Hybrid Mater*. **2014**, *1*, 39.

The fast development of technological applications increases the demand for greener materials which have to fulfil certain conditions in terms of energy consumption and sustainability profile. Thus, one of the biggest aims is to develop organic-inorganic hybrid materials to solve some of the issues posed by this situation. From the beginning of the industrial era, it was a big challenge to combine properties of organic and inorganic compounds to prepare new materials with improved features, characteristics and promising applications.

2.2. Interactions in Hybrid Materials

Organic-inorganic hybrid materials can be classified based on the interactions that hold together the organic and inorganic components. Several types of interaction can be considered such as hydrogen bond, van der Waals or ionic bonds (Figure 2). This kind of interactions can be found in a variety of hybrid materials like organic dyes, organic monomers inserted in sol-gel matrices or inorganic polymers fixed in a polymer.[11] Another category involves inorganic and organic materials linked together by chemical bonds such as covalent or iono-covalent bonds.

This group includes materials which starting building blocks have chloro- or alkoxy groups that can be hydrolyzed in the presence of water, forming a covalent bond.[12]

[11] C. Sanchez, in Functional Hybrid Materials, Ed P. Gomez Romero, C. Sanchez, Wiley Interscience, **2003**. b) Sanchez, C.; Julián, B.; Bellevile, P.; Poppall, M. *J. Mater. Chem*. **2005**, *15*, 3559.

[12] a) Zamboulis, A.; N. Moitra, N.; Moreau, J. J. E.; Cattoën, X.; Chi Man, M. W. *J. Mater. Chem*. **2010**, *20*, 9322; b) P. Judeinstein.; C. Sanchez. *J. Mater. Chem*. **1996**, *6*, 511.

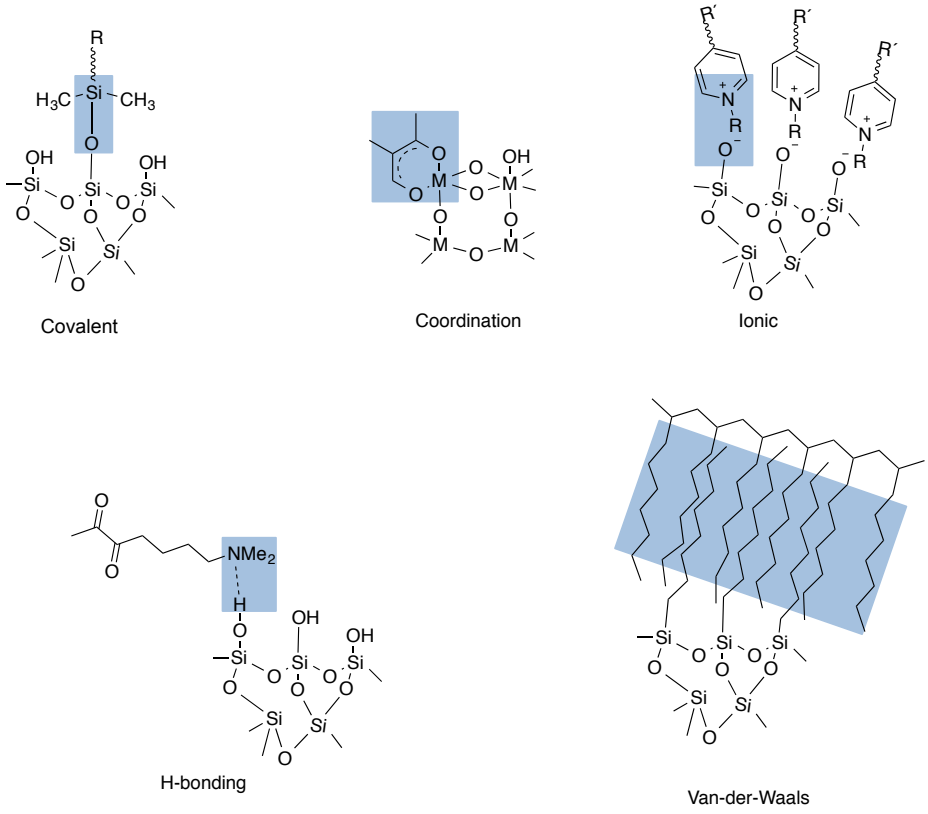

Figure 2. Selected interactions typically present in hybrid materials.

In this regard, Table 1 provides some information about chemical interactions within hybrid materials.[13]

Table 1. Different chemical interactions and their respective strength.

Type of interaction	Strength (kJ mol^{-1})	Range	Character
Van der waals	ca. 50	short	nonselective, nondirectional
H-bonding	5-65	short	selective, directional
coordination bonding	50-200	short	directional
ionic	50-250	long	nonselective
covalent	350	short	predominantly irreversible

[13] a) Kickelbick, G. Hybrid Materials. Synthesis, Characterization, and Applications.; Wiley-VCH: Weinheim, 2007.

2.3. Advantages of Hybrid Organic-Inorganic Materials

The main advantage of hybrid materials, is having one single material with the combined properties of the parent organic and inorganic precursors. This idea includes taking advantage of benefits of each material and even improve them.[14] Indeed, mild reaction conditions can be used to prepare hybrid materials such as solution-based processing or low synthesis temperatures.[15]

In this chapter, two new hybrid materials based on κ-carrageenan, magnetic nanoparticles and an organocatalyst are described. The first one involves only the polysaccharide and the magnetic nanobeads whereas the second one also incorporates an analogue of the Jørgensen-Hayashi organocatalyst. Here, carrageenan is used as a sustainable platform for anchoring the catalyst while magnetic nanoparticles allow to recover and reuse the catalytic material from the reaction media through magnetic decantation. Interestingly, the first hybrid material showed catalytic activity while carrageenan and MNPs alone, do not have activity in the Michael addition.

This hybrid material is a unique chance to produce new compounds that have inorganic, organic and magnetic properties (Figure 3).

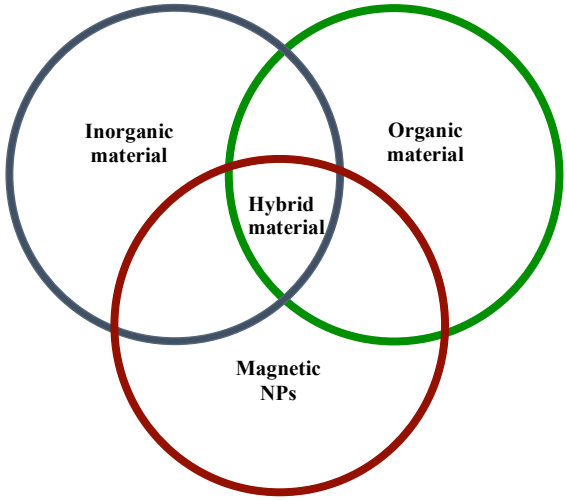

Figure 3. Combination of organic and inorganic materials and magnetic nanoparticles.

2.4. Carrageenan

Carrageenans are a family of sulphated polysaccharides, which are extracted from red seaweeds. The structure of carrageenan is made of repeating D-galactopyranose units as linear backbones which are linked together with α-1,3 and β-1,4 glycosidic linkages.[16]

[14] a) Mammeri, F.; Bourhis, E. L.; Rozes, L.; Sanchez, C. *J. Mater. Chem*, **2005**, *15*, 3787; b) Boucle, J.; Ravirajan, P.; Nelson, J. *J. Mater. Chem*. **2007**, *17*, 3141.
[15] Sanchez, C.; Julian, B.; Belleville, P.; Popall, M. *J. Mater. Chem.* **2005**, *15*, 3559.
[16] a) Piculell, L. (2006). Gelling carrageenans. In A. M. Stephen *et al.* (Ed.), Food polysaccharides and their applications, Second Edition (p. 239-287). New York: Marcel Dekker; b) Bourriot, S.; Gamier, C.; Doublier, J. L.

They have widespread applications in food industry, where carrageenan can be used as natural thickener, formulation stabilizer, or gelling agent, especially in dairy products.[17] In the non-food industry, carrageenan is used in cosmetics, pharmaceutical products, printing and textile formulations.[18]

In industry, carrageenans are divided into three industrially categories based on the number of sulphate groups in each repeating unit, namely λ-, ι-, or κ-carrageenan (Figure 4).

Kappa and iota carrageenan contain one and two sulphate groups, per monomeric unit respectively and a 3,6-anhydro ring, whereas lambda carrageenan contains three such sulphate groups.[19]

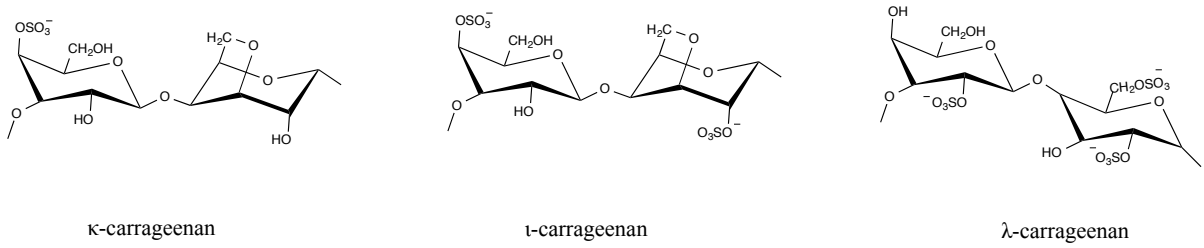

Figure 4. Schematic representation of the different repeating units of carrageenans, κ, ι and λ-carrageenan.

2.4.1. Application of Hybrid Carrageenan-Magnetic Nanoparticles

Among these three kinds, κ-carrageenan, is reported as an ecological compound because it is nontoxic, environmentally friendly, mucoadhesive, biodegradable and biocompatible. All of these significant features bring κ-carrageenan to the center of attention to be used for in vivo applications such as drug delivery.[20] Many efforts have been done in this area in the past decades, searching for an ideal method to transport sufficient dosage of medicine to the goal cells or tissues.[21] Indeed, researchers did a lot of efforts to achieve controlled and sustained release of medicines.[22] To this end, different systems with various types of polymers, a variety of functional

Carbohydr Polym. **1999**, *40*, 145.

[17] van de Velde, F.; Knutsen, S. H.; Usov, A. I.; Rollema, H. S.; Cerezo, A. S. *Trends Food. Sci. Technol*. **2002**, *13*, 73.

[18] a) Imeson, A. P. **2000**. Carrageenan. In: G. O. Phillips and P. A. Williams (Eds.), Handbook of Hydrocolloids. Woodhead Publishing Limited, Cambridge, England; b) De Ruiter, G. A.; Rudolph, B. *Trends Food. Sci. Technol.* **1997**, *8*, 389.

[19] a) Yuguchi, Y.; Thuy, T. T. T.; Urakawa, H.; Kajiwara, K. *Food Hydrocoll*. **2002**, *16*, 515; b) Doyle, J.; Giannouli, P.; Philp, K.; Morris, E. R. *Gums and Stabilizers in the Food Industry*, **2002**, 11, 158; c) Bixler, H. J. *Brit. Food J.* **1994**, *96*, 12.

[20] a) Daniel-da-Silva, A. L.; Ferreira, L.; Gil, A. M.; Trindade, T. *J. Colloid Interface Sci.* **2010**, *355*, 512; b) Leong, K. H.; Chung, L. Y.; Noordin, M. I.; Mohamad, K.; Nishikawa, M.; Onuki, Y.; Morishita, M.; Takayama, K. *Carbohydr. Polym.* **2011**, *83*, 1507.

[21] a) Chertok, B., David, A. E.; Yang, V. C. *J. Control. Release*. **2011**, *155*, 393; b) Pradhan, P.; Giri, J.; Rieken, F.; Koch, C.; Mykhaylyk, O.; Döblinger, M.; Banerjee, R.; Bahadur, D.; Plank, C. *J. Control. Release* **2010**, *142*, 108.

[22] Liu, X.; Kaminski, M. D.; Chen, H.; Torno, M.; Taylor, L. T.; Rosengart, A. J. *J. Control. Release* **2007**, *119*, 52.

groups or modified nanoparticles were investigated.[23] Among them, modified magnetic nanoparticles showed significant results based on their biocompatibility.[24] In the case of hybrid materials made from combination of magnetic nanoparticles and carrageenan, it is possible to take advantage of the magnetic properties of NPs to lead the materials inside of organs, thus using carrageenan as a biocarrier to lead medicines to the envisaged site, where they should act.

Herein, we will summarize some examples of combinations of magnetic nanoparticles and carrageenan described in the literature.

The first hybrid material we will highlight was prepared by dispersion of Fe_3O_4 nanoparticles in a κ-carrageenan aqueous solution.[25] Results showed that the new material swelled slightly faster than κ-carrageenan because the degree of osmotic swelling is in proportion with the amount of charge and concentration of nanoparticles. Afterwards, methylene blue (MB) was selected as a model for drug delivery due to its solubility in water and the results could be observed by the colour change. Further studies stated that the release kinetics of MB depend on the Fe_3O_4 nanoparticles loading and swelling factor.

In another interesting report, three different kinds of hydrogel material with κ-carrageenan were designed.[26] First κ-carrageenan hydrogel particles, p(CRN) were prepared based on the water-in-oil micro emulsion polymerization technique using divinyl sulfone (DVS) as chemical crosslinker in a sodium bis(2-ethylhexyl) sulfosuccinate (AOT) (Figure 5).

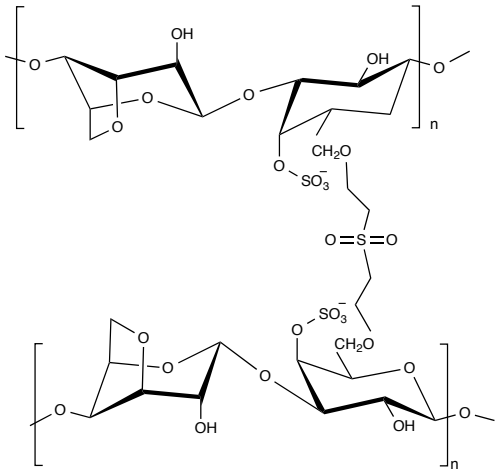

Figure 5. Crosslinking linear CRN polymers with DVS.

[23] a) Grenha, A.; Gomes, M. E.; Rodrigues, M.; Santo, V. E.; Mano, J. F.; Neves, N. M.; Reis, R. L. *J. Biomed. Mater. Res. A*, **2010**, *92A*, 1265; b) Satarkar, N. S.; Hilt, J. Z. *J. Control. Release* **2008**, *130*, 246.

[24] Mejías, R.; Costo, R.; Roca, A. G.; Arias, C. F.; Veintemillas-Verdaguer, S.; González-Carreño, T.; del Puerto Morales, M.; Serna, C. J.; Mañes, S.; Barber, D. F. *J. Control. Release* **2008**, *130*, 168.

[25] Daniel-da-Silva, A. L.; Moreira, J.; Neto, R.; Estrada, A. C.; Gil, A, M.; Trindade, T. *Carbohydr. Polym.* **2012**, *87*, 328.

[26] Sagbas, S.; Butun, S.; Sahiner, N. *Carbohydr. Polym*. **2012**, *87*, 2718.

Then, ferromagnetic materials were synthesized using magnetic nanoparticles and carrageenan (m-p(CRN)) to assemble the envisaged drug delivery system (Scheme 1). Another interesting idea involves the generation of a positive charge on the p(CRN) using a quaternization reaction with a 3-chloro-2-hydroxypropyl trimethyl ammonium chloride aqueous solution to produce q-p(CRN) (Scheme 2).

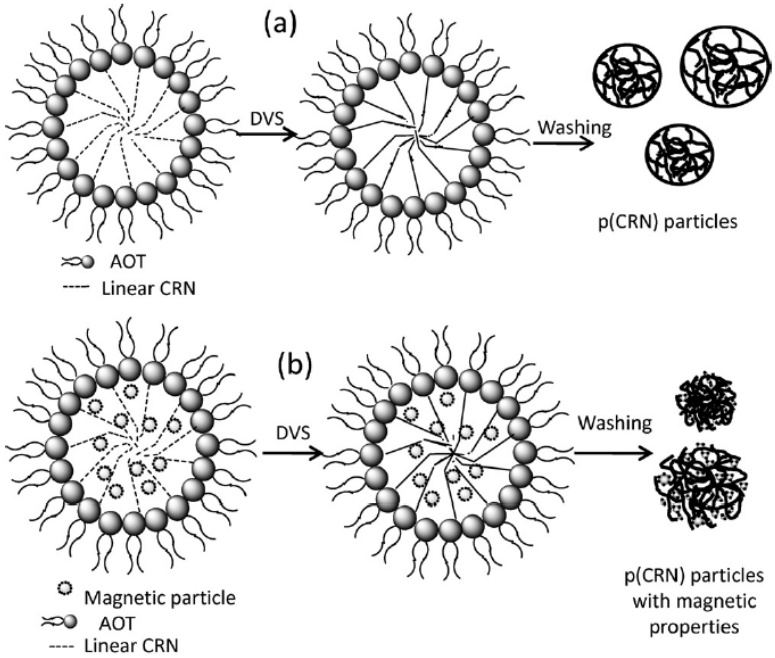

Scheme 1. Synthetic pathway for p(CRN) and m-p(CRN) particles in AOT reverse micelles. Picture taken from reference 26.

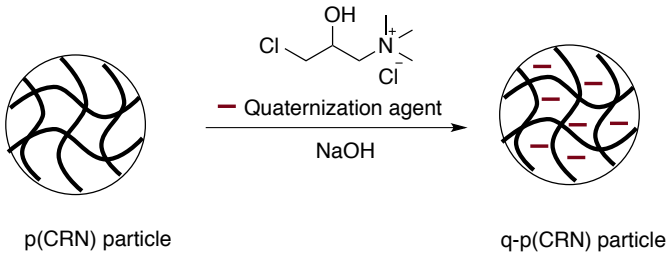

Scheme 2. p(CRN) Modified with ammonium group.

Afterwards, phenylephrine·HCl was selected as a medicine model to investigate a system for in vitro drug delivery. Results showed that loading the phenylephrine·HCl onto q-p(CRN) is more effective than two other particles and indeed q-p(CRN) is releasing the medicine at a faster rate due to the ammonium group.

Apart from drug delivery and biomedical applications, the behaviour of modified κ-carrageenan with magnetic nanoparticles for dye adsorption from aqueous solutions was studied.[27] This material is well suited for absorption of cationic dyes (such as methylene blue) due to electrostatic interactions between the sulfonate moieties of carrageenan and the positive charge in methylene blue.

2.5. Enamine Catalysis

The rapid development of aminocatalysis may be attributed to the conceptualization of the main activation modes: both the HOMO activation or enamine pathway and the LUMO activation or iminium ion pathway are the key concepts that revolutionized the field.

The basics of organocatalysis have been described in Chapter 1, so here we will focus on enamine catalysis, as it is closely related to this project.

The condensation between an aldehyde or ketone with an amine generates an imine or iminium ion that, after losing a proton, produces the enamine (Scheme 3).

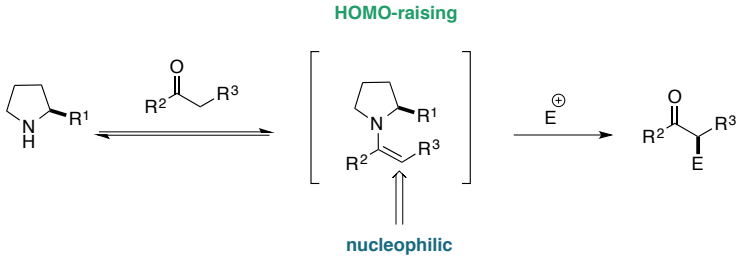

Scheme 3. Enamine activation mode.

The reversibility of this enamine formation has allowed to develop catalytic enantioselective protocols by using chiral amines in the absence of metal. Enamines as a nucleophile can react with an extensive variety of electrophiles, which can afford a lot of useful reactions in organic chemistry (Scheme 4).[28]

[27] Salgueiro, A. M.; Daniel-da-Silva, A. L.; Girão, A. V.; Pinheiro, P. C.; Trindade, T. *Chem. Eng. J.* **2013**, *229*, 276.
[28] Pihko, P. M.; Majander, I.; Erkkila, A. *Top. Curr. Chem.* **2010**, *291*, 29.

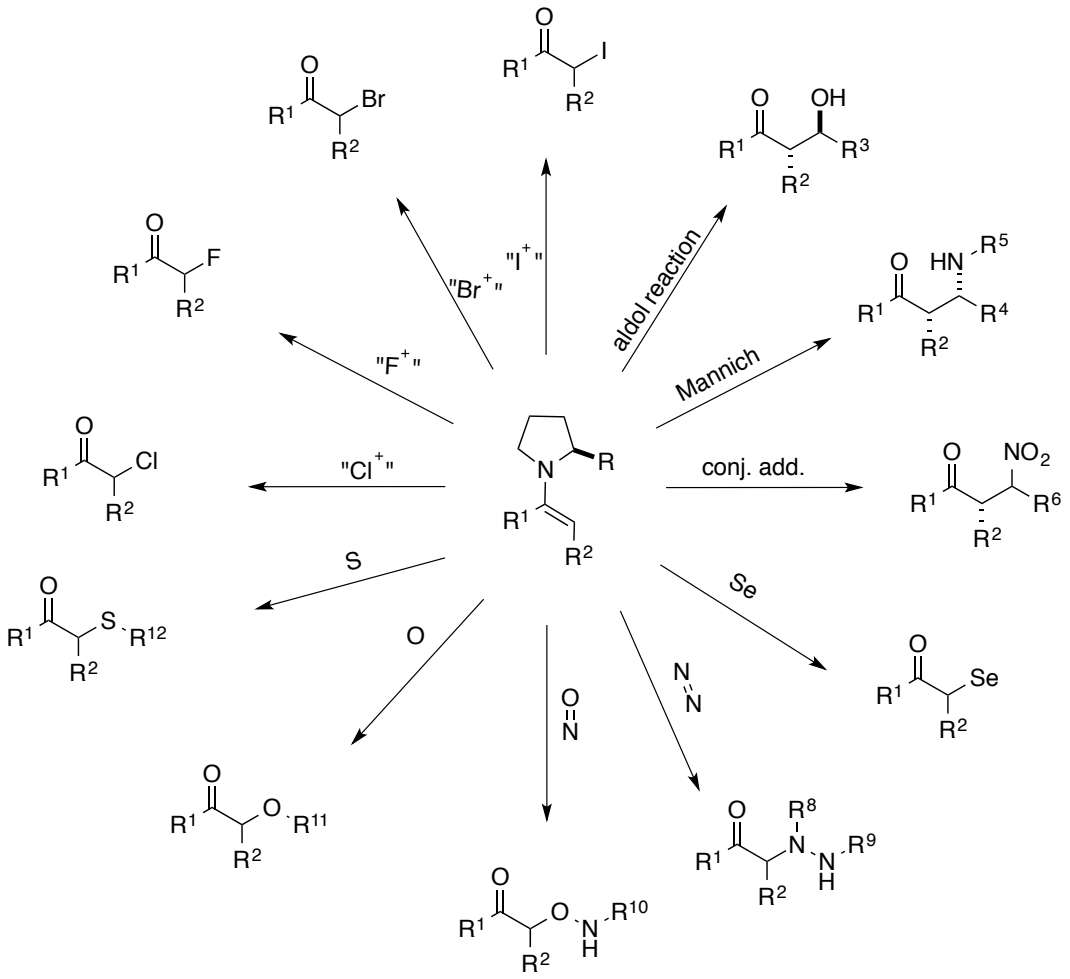

Scheme 4. A range of transformations can be promoted by enamine catalysis.

As it was mentioned in the first chapter, the initial idea of using proline as a catalyst was reported by the groups of Hajos and Parrish, and Eder, Sauer and Wiechert independently for the Robinson annulation to achieve Wieland-Miescher ketone (Scheme 5).[29]

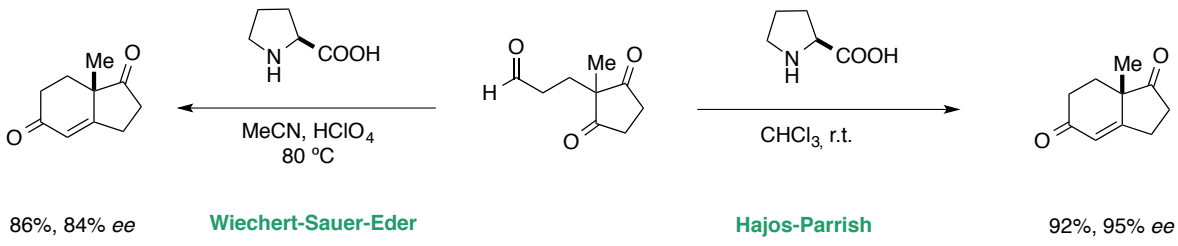

Scheme 5. Proline-catalyzed aldol reaction reported by Hajos, Parrish, Eder, Wiechert, and Sauer.

[29] (a) Hajos, Z. G.; Parrish, D. R. *J. Org. Chem*. **1974**, *39*, 1615; (b) Eder, U.; Sauer, G.; Wiechert, R. *Angew. Chem. Int. Ed*. **1971**, *10*, 496.

However, it took 30 years to realize the importance of enamine catalysis. In 2000, Barbas, Lerner and List highlighted it again in an intermolecular proline-catalyzed aldol reaction of acetone with aldehydes to reach the desired aldol products in up to 99% *ee* (Scheme 6)[30].

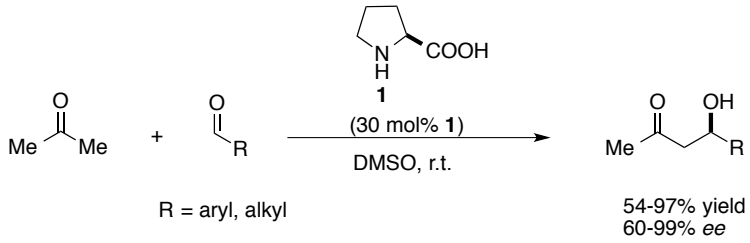

Scheme 6. Asymmetric aldol reaction catalyzed by proline.

In the mechanism they proposed for the reaction between proline and acetone, the sense of enantioinduction is explained by formation of a hydrogen bond between the carboxyl group and the aldehyde, reminiscent of the Zimmerman–Traxler type transition state[31] (intermediate 2, that is the enantiodiscriminating step). Finally, with a simple hydrolysis the desired aldol product is released, leaving proline ready for the next catalytic cycle.

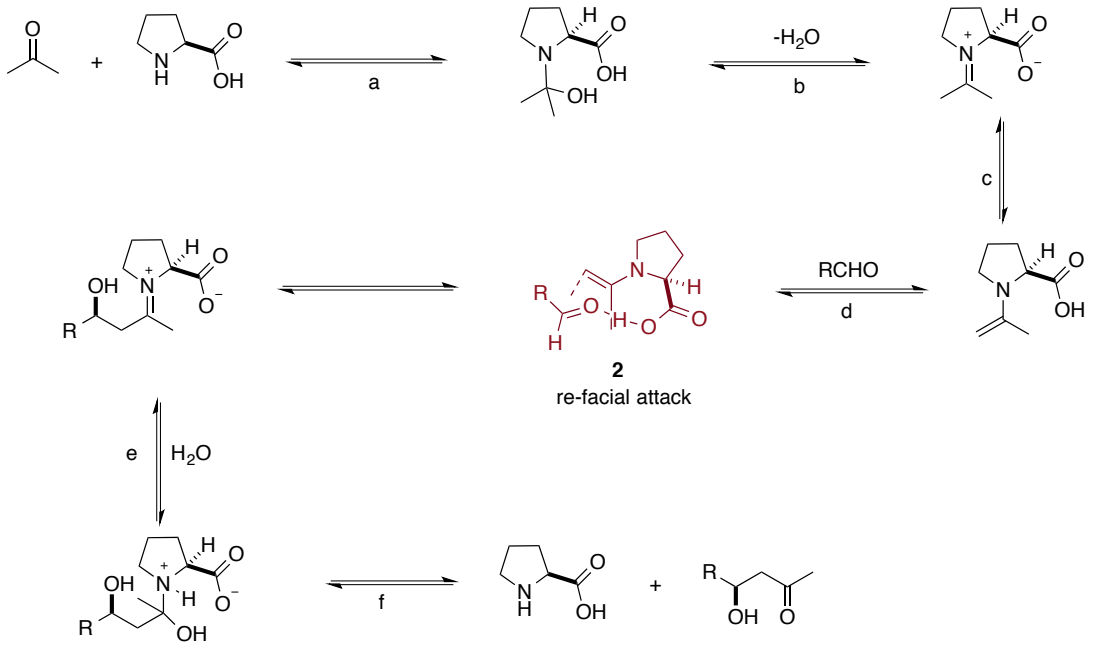

Scheme 7. Mechanism for proline catalyzed asymmetric aldol reaction.

[30] List, B.; Lerner, R. A.; Barbas III, C. F. *J. Am. Chem. Soc*. **2000**, *122*, 2395.
[31] Zimmerman, H. E.; Traxler, M. D. *J. Am. Chem. Soc*. **1957**, *79*, 1920.

In the same year, List reported the first direct, catalytic and asymmetric three-component Mannich reaction.[32] In this process, inexpensive proline was shown to catalyse the Mannich reaction between an aldehyde, *p*-anisidine and a ketone with high enantioselectivity (Scheme 8).

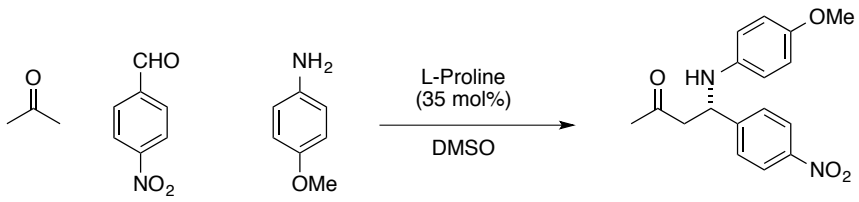

Scheme 8. Mannich reaction catalyzed by proline.

These preliminary studies unveiled the potential of enamine catalysis and motivated scientists to dedicate special attention to this concept.

In the search for other catalysts that could exploit this activation mode, the Jørgensen group developed a novel organocatalyst that was first applied in the enantioselective α-sulfenylation of aldehydes.[33]

Transforming L-proline into a range of diarylprolinol derivatives and protecting the tertiary alcohol with the trimethylsilyl (TMS) group, they could achieve a more efficient catalyst.

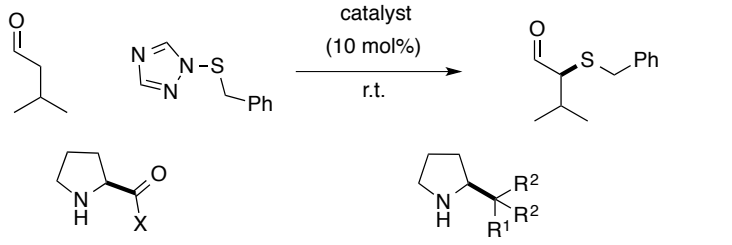

3 : X = NH_2
4 : X = OH

5 : R^1 = H R^2 = Ph
6 : R^1 = OH R^2 = Ph
7 : R^1 = OTMS R^2 = Ph
8 : R^1 = OTMS R^2 = 2-Napht
9 : R^1 = OTMS R^2 = 3,5-$(CH_3)_2$Ph
10 : R^1 = OTMS R^2 = 3,5-$(CF_3)_2$Ph

Scheme 9. Catalysts tested in the organocatalytic enantioselective sulfenylation of isovaleraldehyde.

The results for the α-sulfenylation reaction showed with L-proline is not effective catalyst for this reaction (only 16% yield, no ee). Also with unprotected α,α-diphenyl-L-prolinol no product was obtained.

[32] List, B. *J. Am. Chem. Soc*. **2000**, *122*, 9336.
[33] Marigo, M.; Wabnitz, T. C.; Fielenbach, D.; Jørgensen, K. A. *Angew. Chem. Int. Ed.* **2005**, *44,* 794.

Based on this observation, they proposed that the free hydroxyl group in α,α-diphenyl-L-prolinol and proline could form an unreactive hemiaminal species (**11**) (Scheme 10).

However, with the trimethylsilyl-protected catalyst good enantioselectivities as well as yields were obtained. The Jørgensen group further improved the catalyst through the modification of the aryl substituents in the catalyst structure. The best result was observed with the fluorinated (catalyst **10**) derivative which gave 90% yield and 98% *ee*.

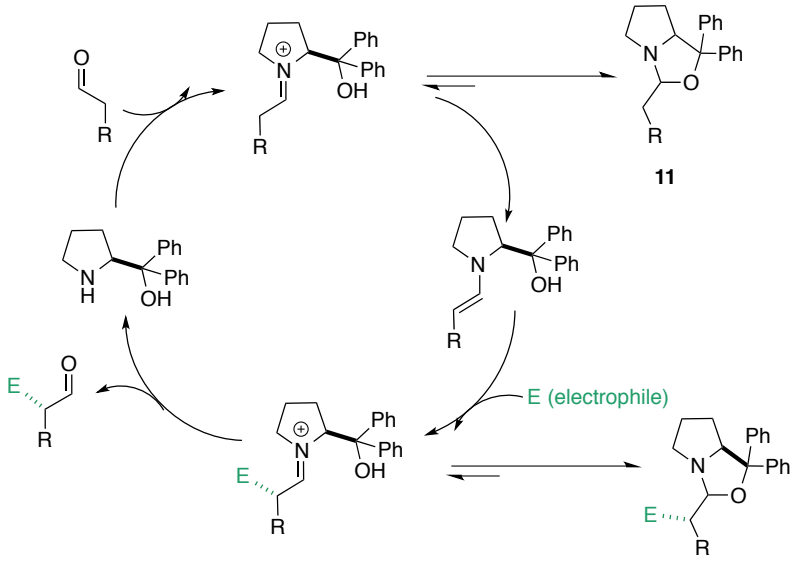

Scheme 10. Formation of hemiaminal species.

In the same year, the Hayashi group also developed TMS-protected diarylprolinol-derived catalysts for the Michael addition of aldehydes to nitroolefins.[34]

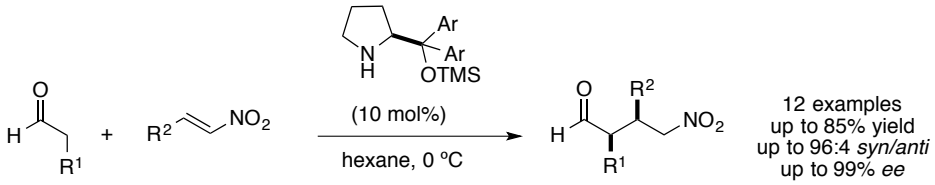

Scheme 11. First applications of the Jørgensen-Hayashi catalyst.

To account for the high enantioselectivity observed with diarylprolinol silyl ether derivatives, the reaction intermediates were extensively studied. The results showed the most stable conformer is the *E-anti* enamine intermediate because the steric interactions between the bulky substituents on the pyrrolidine catalyst and the enamine double bond could be minimized. In this conformer, excellent shielding of the *Si* face of the enamine was achieved, leaving the *Re* face exposed

[34] Hayashi, Y.; Gotoh, H.; Hayashi, T.; Shoji, M. *Angew. Chem. Int. Ed*. **2005**, *44*, 4212.

for the attacking electrophile.[35]

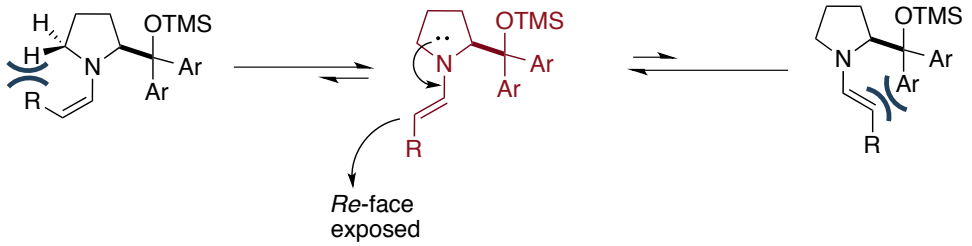

Scheme 12. Rationalization of the stereochemical induction.

In Scheme 13 we have summarized two common pathways for enamine catalysis. In pathway A, the electrophile interacts through hydrogen bonds or electrostatic interactions. This strategy facilitates *Re*-face attack to achieve *(R)*-product. In pathway B, one side of pyrrolidine catalyst is sterically hindered, so the electrophile approach take place by the *Si* face to give (*S*)-product.[36]

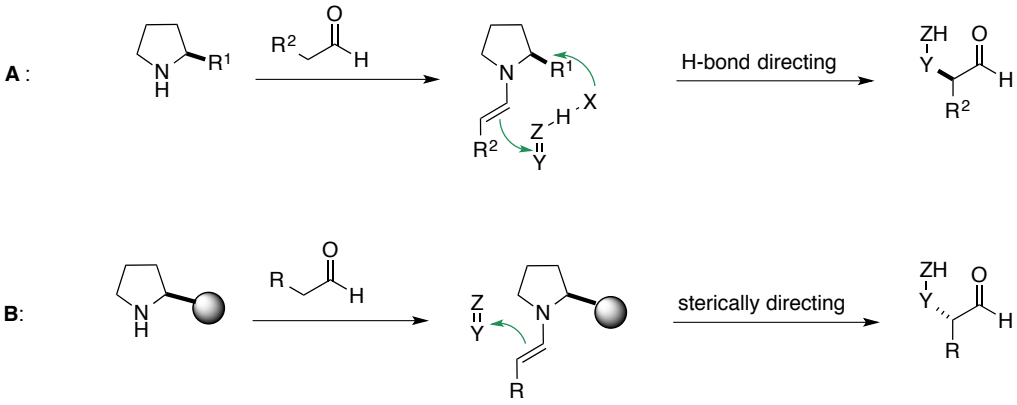

Scheme 13. Two different mechanisms for enamine catalysts.

Thanks to these efforts, enamine catalysis has given rise to a very broad range of asymmetric chemical transformations with aldehydes and ketones such as α-amination,[37] α-oxygenation,[38] α-halogenation,[39] α-selenylation,[40] intramolecular α-alkylation of aldehydes[41] and Michael addition

[35] a) Dinér, P.; Kjærsgaard, A.; Lie, M. A.; Jørgensen, K. A. *Chem. Eur. J.* **2008**, 14, 122; b) Seebach, D.; Beck, A. K.; Badine, D. M.; Limbach, M.; Eschenmoser, A.; Treasurywala, A. M.; Hobi, R.; Prikoszovich, W.; Linder, B.; *Helv. Chim. Acta* **2007**, *90*, 425. c) Grošelj, U.; Seebach, D.; Badine, D. M.; Schweizer, W. B.; Beck, A. K. *Helv. Chim. Acta* **2009** , *92* , 1225. d) Seebach, D.; Gilmour, R.; Grošelj, U.; Deniau, G.; Sparr, C.; Ebert, M.-O.; Beck, A. K.; McCusker, L. B.; Šišak, D.; Uchimaru, T. *Helv. Chim. Acta* **2010**, *93*, 603.

[36] a) Mukherjee, S.; Yang, J. W.; Hoffmann, S.; List, B. *Chem. Rev.* **2007**, *107*, 5471. b) Seebach, D.; Beck, A. K.; Badine, D. M.; Limbach, M.; Eschenmoser, A.; Treasurywala, A. M.; Hobi, R. *Helv. Chim. Acta* **2007**, *90*, 425.

[37] a) List, B. *J. Am. Chem. Soc.* **2002**, *124*, 5656.
b) Kumaragurubaran, N.; Juhl, K.; Zhuang, W.; Bøgevig, A.; Jørgensen, K. A. *J. Am. Chem. Soc.* **2002**, 124, 6254.

[38] Merino, P.; Tejero, T. *Angew. Chem. Int. Ed.* **2004**, *43*, 2995.

[39] b) Marigo, M.; Fielenbach, D.; Braunton, A.; Kjoersgaard, A.; Jøgensen, K. A. *Angew. Chem. Int. Ed.* **2005**, *44*, 3703. b) Bertelsen, S.; Halland, N.; Bachmann, S.; Marigo, M.; Braunton, A.; Jørgensen, K. A. *Chem. Commun.* **2005**, 4821. c) Brochu, M. P.; Brown, S. P.; MacMillan, D. W. C. *J. Am. Chem. Soc.* **2004**, 126, 4108.

reactions.[42]

α-Amination

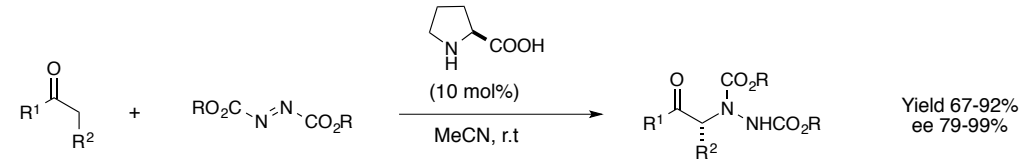

R^1, R^2 = Alkyl R = *t*-Bu, Bn, Et

α-Oxygenation

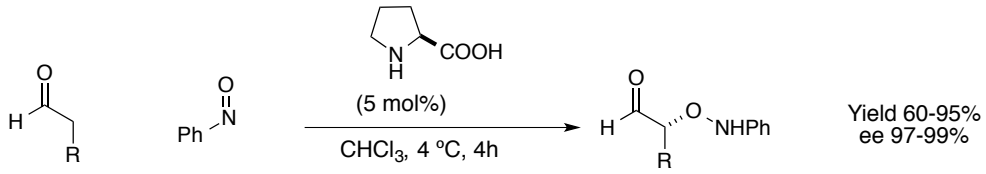

R = Alkyl

α-Halogenation

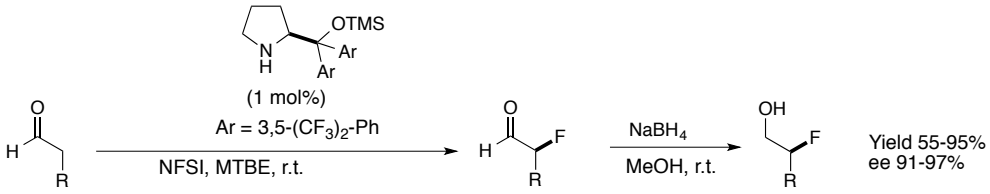

R = Alkyl

α-Selenylation

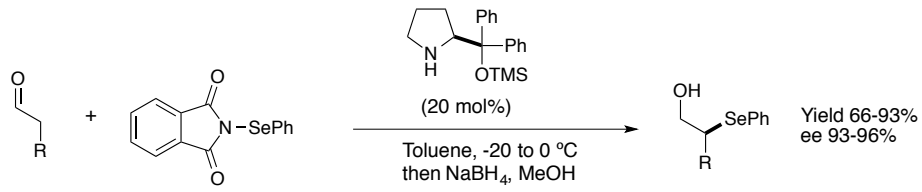

R = Alkyl

[40] a) Tiecco, M.; Carlone, A.; Sternativo, S.; Marini, F.; Bartoli, G.; Melchiorre, P. *Angew. Chem. Int. Ed*. **2007**, *46*, 6882. b) Sundén, H.; Rios, R.; Córdova, A. *Tetrahedron Lett*. **2007**, *48*, 7865.
[41] Vignola, N.; List, B.; *J. Am. Chem. Soc*. **2004**, *126*, 450.
[42] Wang, W.; Wang, J.; Li, H. *Angew. Chem. Int. Ed*. **2005**, *44*, 1369.

Intermolecular α-alkylation of aldehydes

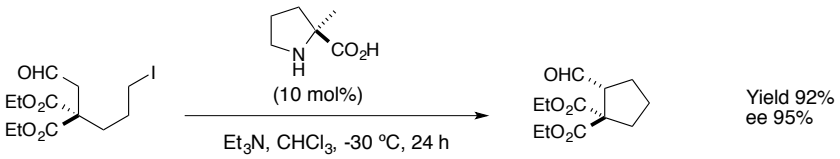

Michael addition reactions

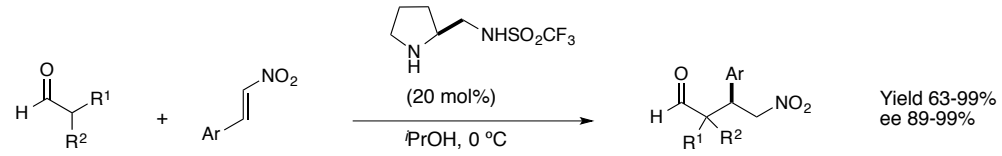

R^1, R^2 = Alkyl

Scheme 14. Some examples of enamine catalysis.

Yamamoto, Ley and Arvidsson developed another versatile catalyst[43] with the replacement of the carboxyl group in L-proline by the corresponding tetrazole. The most important advantage of this catalyst is better solubility than proline in common organic solvents. The catalyst has been applied in aldol reaction, synthesis of α-aminooxy carbonyl compounds and *N*-PMP-protected imino ethyl glyoxylate.

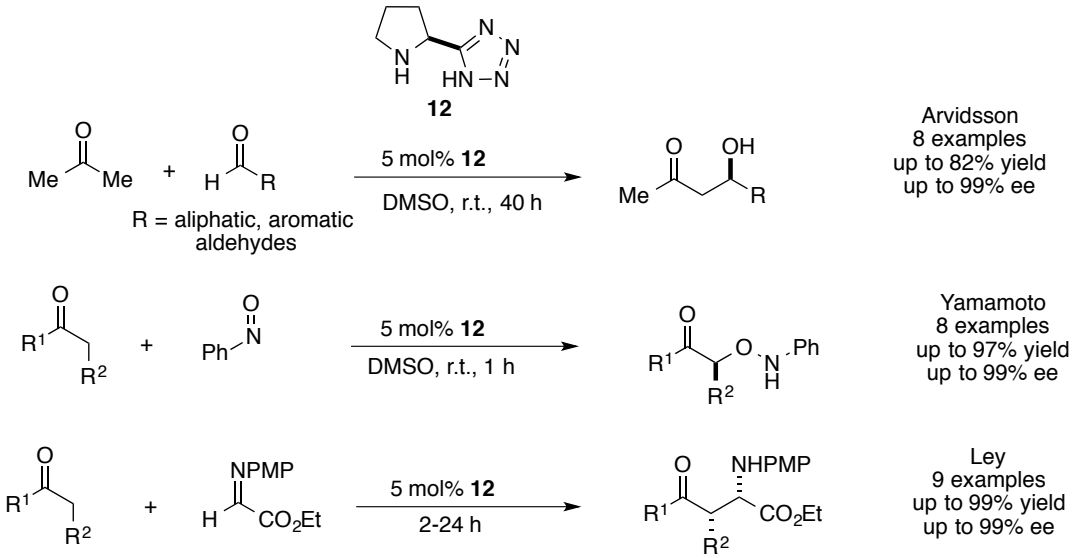

Scheme 15. Different reactions with the pyrrolidine tetrazole catalyst.

[43] a) Torii, H.; Nakadai, M.; Ishihara, K.; Saito, S.; Yamamoto, H. *Angew. Chem*. **2004**, *116*, 2017. *Angew. Chem. Int. Ed.* **2004**, *43*, 1983. b) Momiyama, N.; Torii, H.; Saito, S.; Yamamoto, H. *Proc. Natl. Acad. Sci. U.S.A.* **2004**, *101*, 5374. c) Cobb, A. J. A.; Shaw, D. M.; Ley, S. V.; *Synlett* **2004**, 558. d) Hartikka, A.; Arvidsson, P. I. *Tetrahedron: Asymmetry* **2004**, 15, 1831. e) A. Hartikka, A.; Arvidsson, P. I.; *Eur. J. Org. Chem*. **2005**, 4287.

2.6. Immobilized Proline Catalyst

Due to the efficiency of L-proline and the privileged Jørgensen-Hayashi catalyst, some authors have studied their immobilization onto a solid support. As discussed in Chapter 1, heterogeneous catalysts are more sustainable, environmentally friendly and easier to use in an industrial environment. Here we will briefly mention some examples about heterogenized L-proline and Jørgensen-Hayashi catalyst.

Ma *et al.* grafted 4-hydroxyproline to MNPs surrounded by a silica shell using triethoxysilylpropanecarbamate as a linker (scheme 16). The reported yield and enantioselectivity in the aldol reaction were between 24–96% and 6–99% respectively with 20 mol% catalyst.[44] Increased steric hindrance on the aldehyde resulted in a decrease in enantioselectivity, whereas with increasing carbon numbers onto the cyclic ketone, the yield dropped. The recyclability of the catalyst was tested for 4-nitrobenzaldehyde and cyclohexanone until five runs and no significant decrease in yield and *ee* was observed.

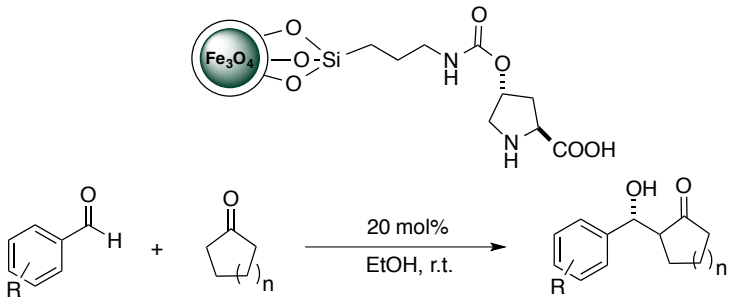

Scheme 16. Aldol reactions between aromatic aldehydes and ketones catalyzed by proline on MNPs.

In another application, the surface of MNPs was modified with *N*-[3-(triethoxysilyl)-propyl]-4,5-dihydroimidazole ionic liquid (IL) linker. Afterwards L-proline was immobilized on the surface with a covalent linkage. The advantage of using IL as linker is that it improves dispersibility of catalyst in water, making it more environmentally compatible.[45] The reaction between cyclohexanone and 2-nitrobenzaldehyde in water was catalyzed with 10 mol% of **13**, **14** and L-proline in water (scheme 17). Only in the case of catalyst **13,** good results were achieved (92% yield and 85% *ee*) which seems to indicate the importance of this linker. With catalyst **14** only 10% yield was recorded, whereas with L-proline no reactivity was observed.

Apart from compatibility of this catalyst, the polarity and ionic character make it a suitable catalyst for using in aqueous media in reactions which need to form stabilized enamine intermediates.

[44] Yang, H.; Li, S.; Wang, X.; Zhang, F.; Zhong, X.; Dong, Z.; Ma, J. *J. Mol. Catal. A: Chem.* **2012**, *363*, 404.
[45] Kong, Y.; Tan, R.; Zhaoa, L.; Yin, D. *Green Chem*. **2013**, *15*, 2422**.**

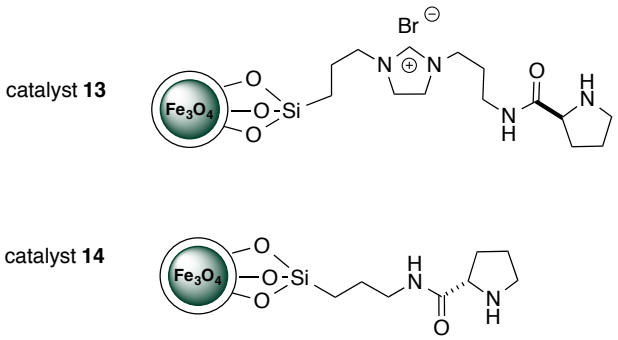

Scheme 17. Structure of proline-based catalysts 13 and 14.

In another study, Fe_3O_4 MNPs were functionalized with phosphates or acrylic acids to give rise to functional magnetic Fe_3O_4 nanoparticles **15** and **16**. Then, these were polymerized with acrylates and methacrylates and the resulting products were separated by magnetic decantation very easily.[46] These four catalysts were tested in the asymmetric aldol reaction of benzaldehyde with ketones. It seems that the addition of benzoic acid as cocatalyst is necessary as it accelerates the reaction. The catalysts exhibited very good enantioselectivity with a wide range of substrates, and they could be easily isolated using an external magnet and reused more than 10 times without losing their activity (Scheme 18).

[46] Yacob, Z.; Nan, A .; Liebscher, J. *Adv. Synth. Catal*. **2012**, *354*, 3259.

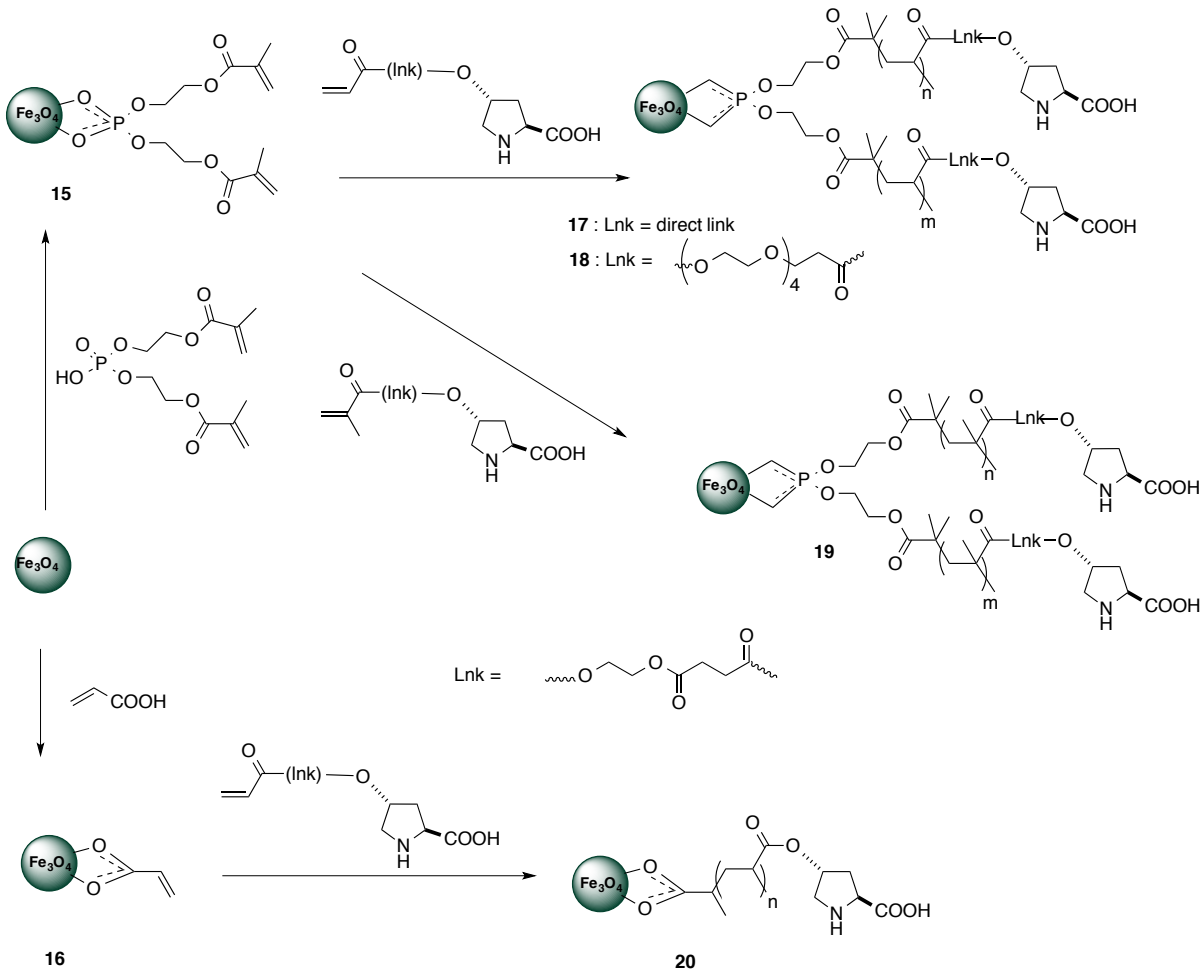

Scheme 18. Synthesis of magnetically modified proline polyacrylates.

Jørgensen–Hayashi catalysts also represent a good option for developing heterogeneous catalysts. Wang *et al.* supported (*S*)-diarylprolinol trimethylsilyl ether onto the surface of Fe_3O_4@SiO_2 to carry out Michael addition of several aldehydes to nitroalkenes.[47] The reported size of particle after anchoring catalyst was 190±10 nm and yield and *ee* were between 53–96% and 75–90% *ee* with 20 mol% of catalyst.

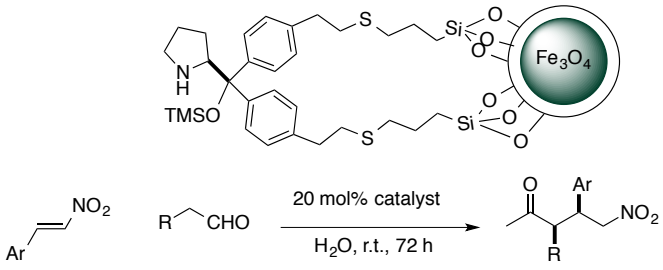

Scheme 19. Michael addition with (*S*)-α,α-diphenylprolinol trimethylsilyl ether supported onto MNPs.

[47] Wang, B. G.; Ma, B. C.; Wang, Q.; Wang, W. *Adv. Synth. Catal*. **2010**, *352*, 2923.

In our group, plenty of efforts have been devoted to develop supported aminocatalysts to perform different kinds of reactions. (*S*)-Diphenylprolinol trimethylsilyl ether was supported onto Merrifield resin via a CuAAC reaction. This catalyst was applied to the Michael addition of aldehydes to nitroolefins,[48] asymmetric addition of dialkyl malonates to α,β-unsaturated aldehydes or the Michael addition of nitromethane to α,β-unsaturated aldehydes (Scheme 20).[49]

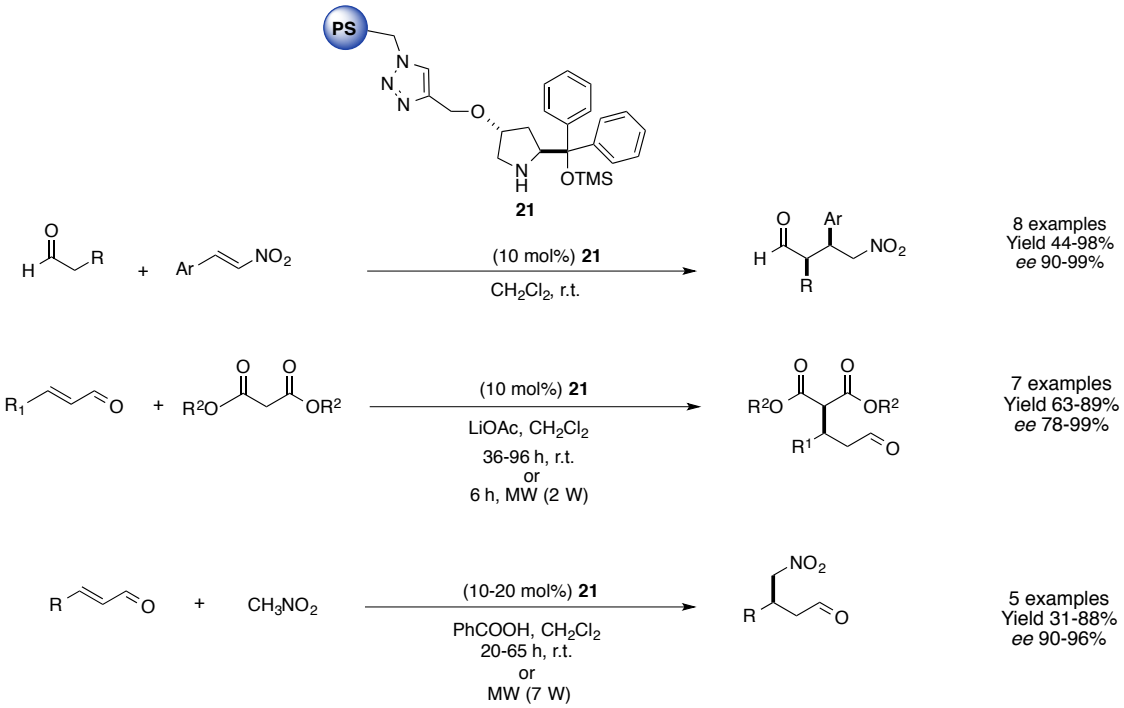

Scheme 20. (*S*)-Diphenylprolinol trimethylsilyl ether supported onto polystyrene: catalytic applications.

However this catalyst lost activity after prolonged recycling, probably due to silyl group cleavage. Indeed, after treatment with trimethylsilyl *N*,*N*-dimethylcarbamate to reprotect the hydroxy group, the catalyst could be used for 6 more runs with constant *ee* (Scheme 21).

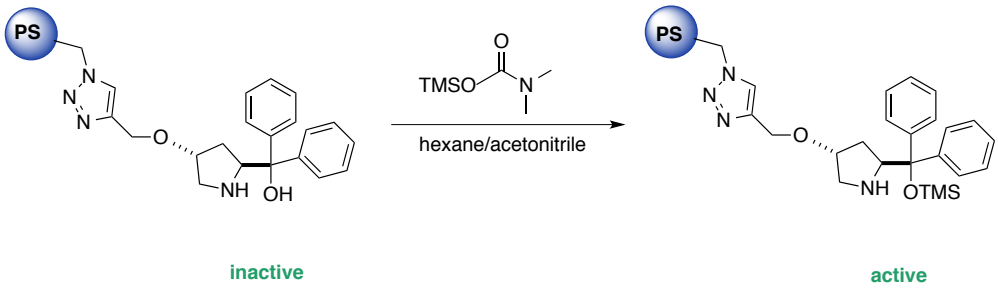

Scheme 21. Reactivation process for immobilized Jørgensen-Hayashi catalyst.

[48] Alza, E.; Pericàs, M. A. *Adv. Synth. Catal*. **2009**, *351*, 3051.
[49] Alza, E.; Sayalero, S.; Kasaplar, P.; Almaşi, D.; Pericàs, M. A. *Chem. Eur. J.* **2011**, *17*, 11585.

Concerned about the deprotection of the OH group, our group designed some experiments to develop a new catalyst that could be more robust.[50] Different groups such as TES (triethylsilyl), TBS (*tert*-butyldimethylsilyl) or TIPS (triisopropylsilyl) were examined instead of the TMS group.

Among all of these, the TBS seemed to be the more promising according to the results obtained (Scheme 22).

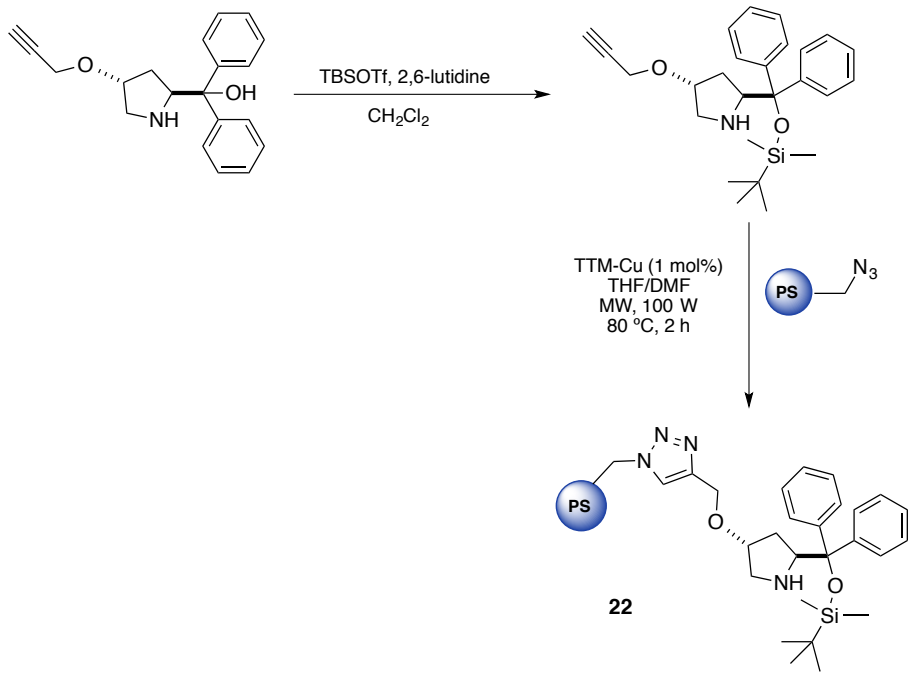

Scheme 22. Design and synthesis of a more robust catalyst with a TBS protecting group.

Catalyst **22**, featuring the TBS protecting group, was applied in the α-amination of aldehydes with high *ee* and yield (Scheme 23).

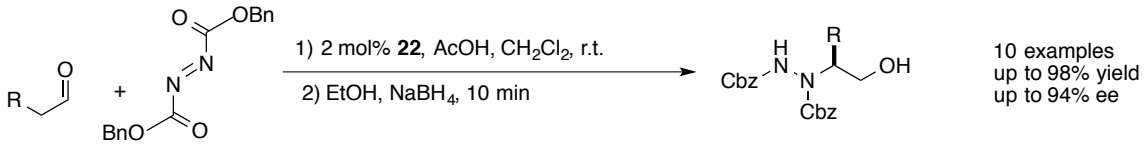

Scheme 23. α-Amination of aldehydes catalyzed by TBS protected catalyst.

In order to evaluate the robustness of this new design, the recyclability was checked for a mixture of propanal, AcOH and catalyst in CH_2Cl_2 with slow addition of DBAD to prevent byproduct formation. Under these conditions, the catalyst could be used for six runs with the constant *ee* and yield.

Use of MNPs to immobilize Jørgensen–Hayashi catalyst has also been studied in our group. To

[50] Fan, X.; Sayalero, S.; Pericás, M. A. *Adv. Synth. Catal*. **2012**, *354*, 2971 .

this end, the surfaces of uncoated MNPs were functionalized with 3-azidopropyl units and then a functionalized diarylprolinol was anchored to the support through copper-catalyzed alkyne–azide cycloaddition.[51] The size distribution for modified nanoparticles was between 4.8±0.8 nm and no agglomeration was observed in the TEM pictures. Michael addition of propanal to nitroolefins was used to evaluate the catalytic activity with only 10 mol% of catalyst. Furthermore, recyclability of catalyst was studied until four runs; although the *ee* did not have a significant change (97-92% *ee*), the yield dropped (89 to 57%), which can be attributed to hydrolysis of the silyl ether group (Scheme 24)

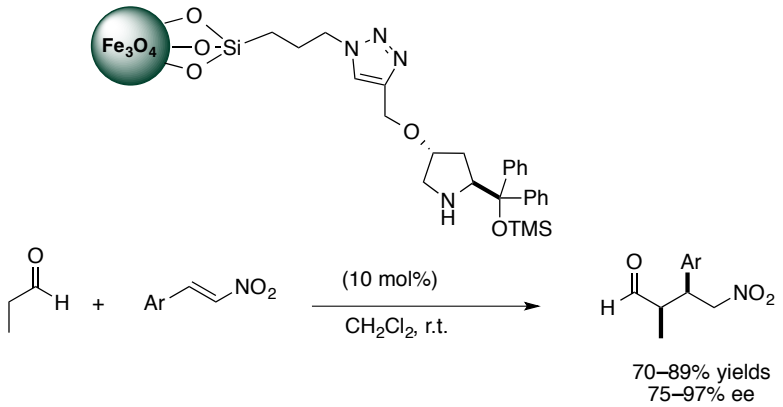

Scheme 24. Immobilization of Jørgensen–Hayashi catalysts for Michael addition.

2.7. Enamine-Catalyzed Asymmetric Michael Addition to Nitroalkenes

The addition of nucleophiles to the β position of α,β-unsaturated compounds is known as Michael addition reaction. It is an important process for carbon-carbon bond formation and it is widely used in organic synthesis.[52] After developing chiral organocatalysts, chemists started to extend the concept to asymmetric conjugate addition of aldehydes or ketones to different Michael acceptors.[53] List *et al.* pioneered the use of (*S*)-proline for enantioselective Michael addition of ketones to nitroolefins via an enamine pathway. Although they got 94% yield, the *ee* was not very promising, remaining as low as 23%.

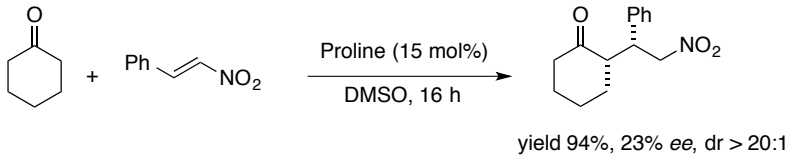

Scheme 25. First enantioselective Michael addition of ketones to nitroolefins catalyzed by (*S*)-proline.

[51] Riente, P.; Mendoza, C.; Pericás, M. A. *J. Mater. Chem*. **2011**, *21*, 7350.
[52] P. Perlmutter, Conjugate Addition Reactions in Organic Synthesis, Pergamon Press, Oxford, 1992.
[53] List, B.; Pojarliev, P.; Martin, H. J. *Org. Lett.* **2001**, *3*, 2423.

However, this reaction was later improved by using a variety of catalysts and different conditions that allowed achieving better results. In Scheme 26 we have summarized the pioneering studies concerning Michael addition with different pyrrolidine-based catalysts.[54]

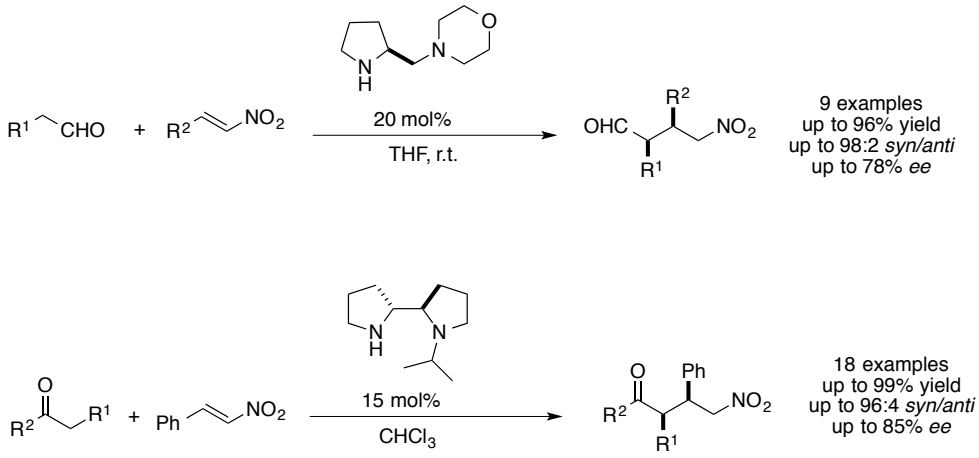

Scheme 26. Michael addition with different proline based catalysts.

H-bond directing pyrrolidine sulfonamide was not only used for α-aminooxylation,[55] Mannich,[56] α-sulfenylation[57] or α-selenylation reactions,[58] but also applied to Michael additions of aldehydes to nitroolefins.[59]

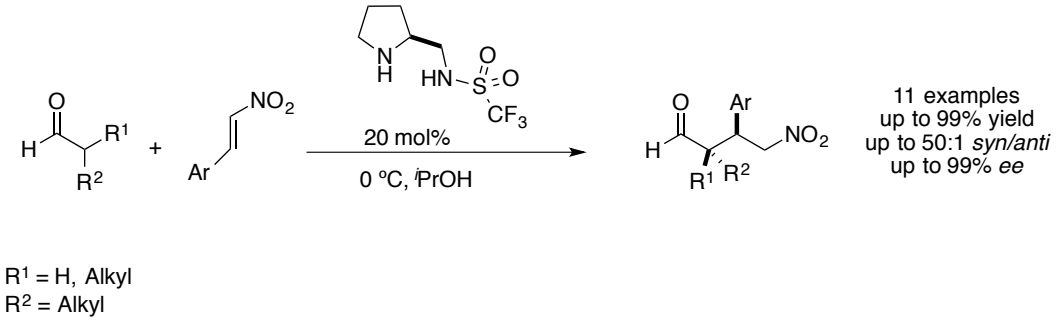

Scheme 27. Michael addition with pyrrolidine-sulfonamide catalyst.

Cheng *et al*. developed pyrrolidine–ionic liquid conjugates to catalyze Michael additions of ketones to nitroalkenes with excellent enantioselectivity and yield (Scheme 28). The ionic liquid moiety can act as phase tag to allow an easier recycling and also as an effective chiral induction

[54] a) Betancort, J. M.; Barbas III, C. F, *Org. Lett*. **2001**, *3*, 3737. b) Alexakis, A.; Andrey, O. *Org. Lett*. **2002**, *4*, 3611.
[55] Wang, W.; Wang, J.; Li, H.; Liao, L. *Tetrahedron Lett*. **2004**, *45*, 7235.
[56] Wang, W.; Wang, J.; Li, H. *Tetrahedron Lett*. **2004**, *45*, 7243.
[57] Wang, W.; Li, H.; Wang, J.; Liao, L. *Tetrahedron Lett*. **2004**, *45*, 8229.
[58] Wang, W.; Wang, J.; Li, H, *Org. Lett*. **2004**, 6, 2817.
[59] Wang, W.; Wang, J.; Li, H. *Angew. Chem. Int. Ed.* **2005**, *117*, 1393.

group to achieve high selectivity. [60]

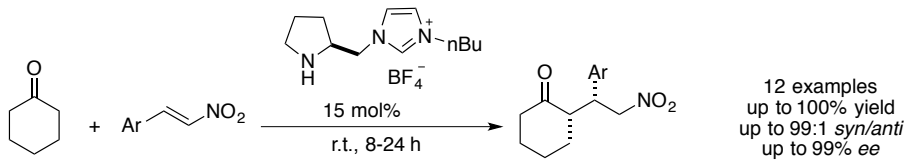

Scheme 28. Michael addition with pyrrolidine-ionic liquid.

Tang *et al*. applied a bifunctional catalyst based on pyrrolidine thiourea for Michael addition of cyclohexanone to aryl and alkyl nitroolefins (Scheme 29).[61] High stereoselectivities were achieved due to the ability of the thiourea moiety catalyst to coordinate to the nitro group.

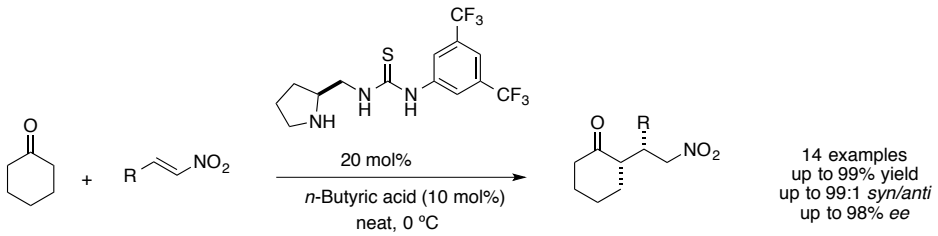

Scheme 29. Michael addition with bifunctional catalyst.

Our efforts to generate novel catalytic materials based on MNPs, polysaccharides and organocatalysts gave rise to one publication which is included hereafter.

[60] Luo, S.; Mi, X.; Zhang, L.; Liu, S.; Xu, H.; Cheng, J.-P. *Angew. Chem. Int. Ed.* **2006**, *45*, 3093.
[61] Cao, C. L.; Ye, M. C.; Sun, X. L.; Tang, Y. *Org. Lett*. **2006**, *8*, 2901.

2.8. Article

This research has been done in collaboration with Carmen A. Mak.

Tetrahedron 70 (2014) 6169–6173

Contents lists available at ScienceDirect

Tetrahedron

journal homepage: www.elsevier.com/locate/tet

Hybrid magnetic materials (Fe_3O_4–κ-carrageenan) as catalysts for the Michael addition of aldehydes to nitroalkenes

Carmen A. Mak [a,†,‡], Sara Ranjbar [a,†,‡], Paola Riente [a,†], Carles Rodríguez-Escrich [a,†], Miquel A. Pericàs [a,b,*,†]

[a] Institute of Chemical Research of Catalonia, Av. Països Catalans, 16, 43007 Tarragona, Spain
[b] Department de Química Orgànica, Universitat de Barcelona, c/ Martí i Franquès 1-11, 08028 Barcelona, Spain

ARTICLE INFO

Article history:
Received 18 March 2014
Received in revised form 11 June 2014
Accepted 16 June 2014
Available online 20 June 2014

Keywords:
Hybrid materials
Magnetic nanoparticles
κ-Carrageenan
Michael reaction
Click chemistry

ABSTRACT

Two hybrid magnetic materials have been prepared from κ-carrageenan and Fe_3O_4 nanoparticles and tested as catalysts for the Michael addition of aldehydes to nitroalkenes. Remarkably, the material prepared from unmodified κ-carrageenan showed catalytic activity in the reaction of choice, while the individual components were inactive. This points out to a synergistic effect between the MNPs and κ-carrageenan. The second catalyst, bearing a diphenylprolinol silyl ether moiety, was also shown to promote the reaction, giving rise to the corresponding adducts in excellent ees. After the reaction is complete, the catalysts can be conveniently retrieved by simple magnetic decantation.

1. Introduction

Organic–inorganic hybrid nanomaterials have generated increasing interest in recent years due to their optical and electrical properties and potential biomedical applications.[1] Particularly, nanoparticle-based hybrid materials are very promising systems for a wide range of biomedical applications, including drug delivery.[2]

κ-Carrageenan (**1**) is a natural sulfated polysaccharide extracted from different species of edible red seaweed, which is mainly used in the food industry as gelling agent. It is a commercially available material that possesses interesting properties, being nontoxic, mucoadhesive, biodegradable, and biocompatible. κ-Carrageenan has also been used as an immobilization support, mainly for biocatalysts in industrial processes.[3]

The combination of these polysaccharides with Fe_3O_4 magnetic nanoparticles (MNPs) as inorganic supports opens up the possibility of exploiting their properties in a synergistic manner, which constitutes an appealing approach to generate new materials for sustainable chemistry.[4] Indeed, precedents of such hybrid nanostructures have been described for various biomedical applications—mainly as drug delivery systems[5]—or as detoxification agents for the magnetically assisted removal of methylene blue from aqueous solutions.[6]

However, to the best of our knowledge, the use of polysaccharide-coated MNPs in catalysis has not been described. Herein, we report the synthesis of such materials and their application as either catalyst or support for a catalytically active species in the Michael addition of aldehydes to nitroolefins.

2. Results and discussion

Before assessing the catalytic ability of the hybrid material we started by establishing a reliable synthetic method that allowed the anchoring of carrageenan onto MNP (**2**) in two simple steps. First, the MNPs were generated by thermal decomposition of $Fe(acac)_3$ in the presence of oleylamine and oleic acid as surfactants, following a reported procedure.[7] The transmission electron microscopy (TEM) images show that the MNPs obtained are spherical, monodispersed, and small sized (4.8±0.9 nm; Fig. 1a).

The hybrid material was prepared in a very simple manner by mixing κ-carrageenan and the MNPs in the presence of glacial acetic acid and ultrapure water in DMF at 110 °C (Scheme 1). Interestingly, the attachment of the polysaccharide did not lead to any significant increase in the size of the MNPs (5.1±0.8 nm, Fig. 1b). The functionalization level of κ-carrageenan in the hybrid nanomaterial, determined by elemental analysis of sulfur, was found to be 0.80 mmol (S) g^{-1}. The progress of formation of **2** was

* Corresponding author. E-mail address: mapericas@iciq.es (M.A. Pericàs).
† Tel.: +34 977 920 243; fax: +34 977 920 244.
‡ These authors contributed equally to this paper.

http://dx.doi.org/10.1016/j.tet.2014.06.063
0040-4020/

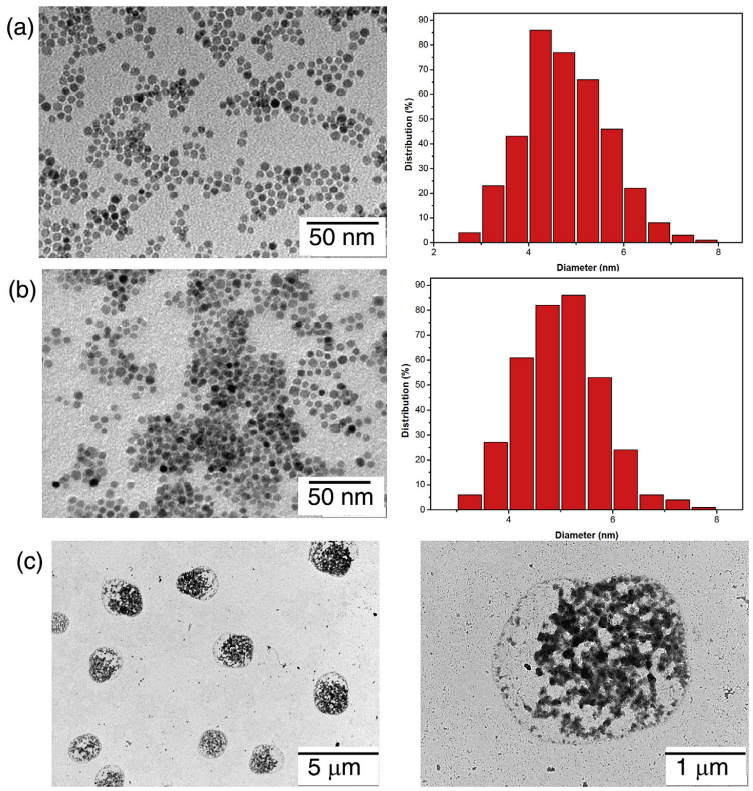

Fig. 1. (a) TEM micrography and size distribution plot for Fe_3O_4 MNPs; (b) TEM micrography and size distribution plot for the hybrid material **2**; (c) TEM micrographies for **5**.

easily followed by IR spectroscopy (Fig. 2) through the appearance of new bands at 845 cm^{-1} and 930 cm^{-1}, corresponding to the stretching vibrations of sulfate esters and 3,6-anhydro rings, respectively, present in κ-carrageenan.[8]

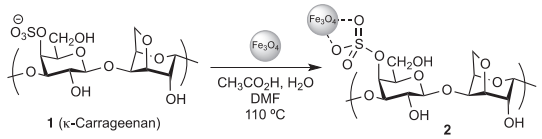

Scheme 1. Preparation of the hybrid material **2**.

Alternatively, and considering the previous experience in our group,[9] we envisaged the use of this kind of hybrid magnetic materials as mere supports for a chiral organocatalyst. The interest of this approach lies in the fact that it would be a water-dispersible magnetic material able to catalyze enantioselective organic reactions. To this end, the free hydroxy groups in the hybrid material **2** were transformed into chlorides via Appel reaction, and these were substituted with sodium azide to generate **3** (f=1.09 mmol g^{-1}) as a ready-to-click hybrid material. The incorporation of the azide group was confirmed by the appearance of a band around 2040 cm^{-1} in the IR spectra, corresponding to the stretching vibration of the azide group (Fig. 2). Finally, a diphenylprolinol derivative bearing a propargyl group (**4**) was chosen as the organocatalytic counterpart.[10] This was anchored onto **3** by means of copper-catalyzed azide–alkyne cycloaddition[11] (CuAAC), giving rise to **5** (f=0.61 mmol g^{-1}, Scheme 2). The progress of this CuAAC reaction could be easily monitored by IR, through the disappearance of the azide band and the appearance of new bands at 850, 959, and 996 cm^{-1}, attributed to the diphenylprolinol (Fig. 2).

With the two hybrid materials in hand, the stage was set to study their catalytic activity in the Michael addition of aldehydes to nitroolefins.[12] For this purpose, the reaction between propanaldehyde and β-nitrostyrene was chosen as a model reaction to optimize reaction conditions (Table 1).

As expected, in most cases the control reactions run with **2** did not give any reactivity, but under neat conditions we were surprised to see full conversion in less than 16 h.

In the vast majority of cases, the catalytic α-functionalization of aldehydes takes place via enamine activation. Thus, this result was rather unexpected, given the lack of amino groups in **2**. To gain insight into the mechanistic details of the reaction we decided to run blank reactions with only the MNPs, κ-carrageenan and a combination of both. Even more surprisingly, these reactions failed to give any product, so we treated the polysaccharide under the same conditions used for the preparation of **2**. Again, this proved inefficient to catalyze the reaction. Overall these results seem to indicate that the hybrid material exerts some kind of

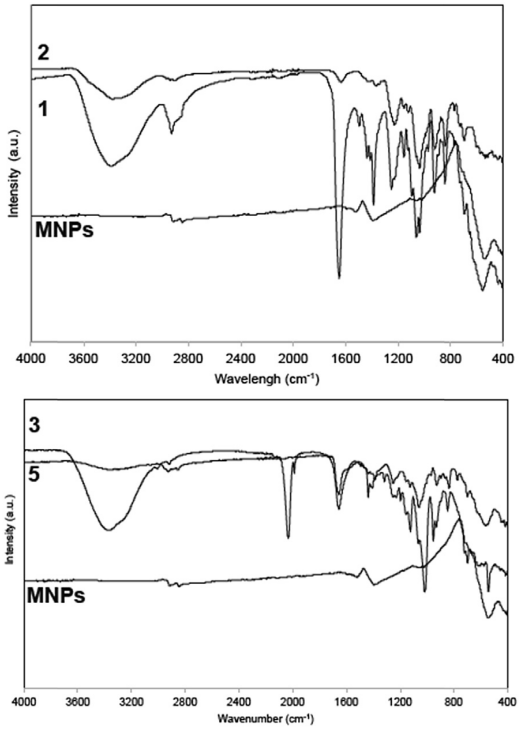

Fig. 2. IR spectrum of MNPs, κ-carrageenan (**1**), Fe_3O_4–κ-carrageenan (**2**), azide-functionalized magnetic material (**3**), and diphenylprolinol decorated material **5**.

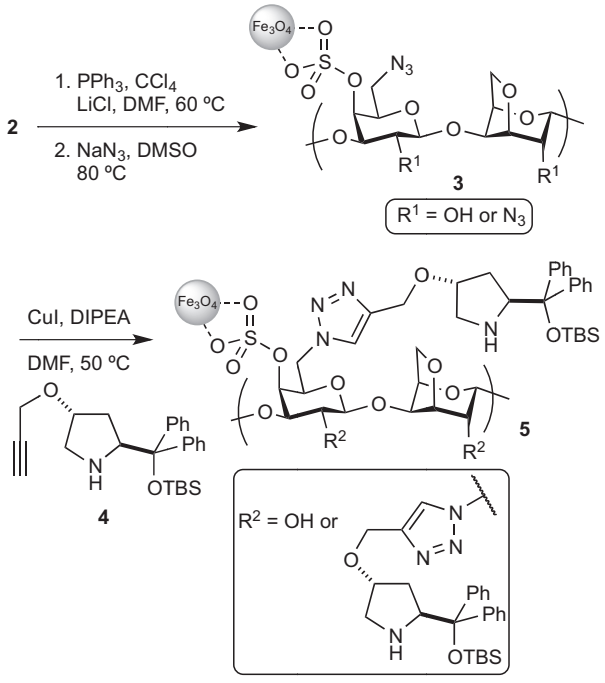

Scheme 2. Preparation of the hybrid material **5**.

Table 1
Solvent screening for **2**

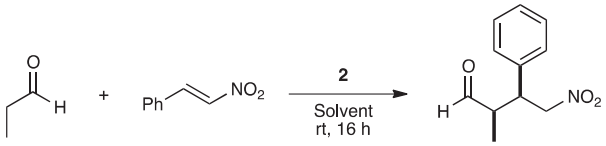

Entry[a]	Solvent	Conversion (%)
1	CH_2Cl_2	<5
2	Toluene	—
3	THF	—
4	Water	—
5	Ethyl acetate	<5
6	Neat	100[b]

[a] Nitroolefin (0.1 mmol), aldehyde (0.5 mmol), **2** (15 mol %) in solvent (0.5 mL) at room temperature.
[b] dr 87:13; 7% ee.

Table 2
Michael addition of aldehydes to β-nitrostyrene catalyzed by **2**[a]

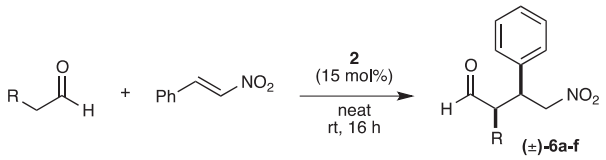

Entry	Product	*t* (h)	Conversion[b] (%)	Yield[c] (%)	*syn*/*anti*[b]
1	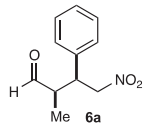 **6a**	15	>99	80	87:13
2	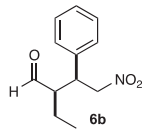 **6b**	25	>99	71	92:8
3	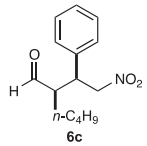 **6c**	48	>99	68	88:12
4	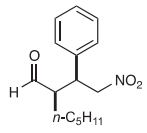 **6d**	28	>99	54	91:9
5	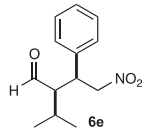 **6e**	48	>99	59	93:7
6	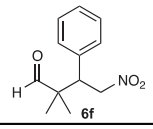 **6f**	48	0	—	—

[a] Nitroolefin (0.1 mmol), aldehyde (0.5 mmol), and **2** (15 mol %) at room temperature.
[b] Determined by ^1H NMR.
[c] Isolated yield after column chromatography.

synergistic effect, which is the ultimate responsible for the catalysis. At present, however, the exact mechanistic details remain unclear.

With the aim of establishing the generality of this reaction, several aldehydes were tested (Table 2). In most cases the corresponding Michael adducts **6** were obtained with good yields and diastereomeric ratios. The reaction seems to be tolerant to β-branched aldehydes (Table 2, entry 5), which is in contrast with what we reported for the case of polystyrene-supported diphenylprolinol silyl ethers.[13] However, α-branched aldehydes like isobutanal (Table 2, entry 6) did not give any product under the reaction conditions. It is also worth mentioning that, despite the fact that the polysaccharide provides a chiral environment for the reaction, no enantioselectivity was recorded for any of the substrates.

This lack of enantioselectivity prompted us to use an analogous hybrid magnetic material as a mere support for a chiral aminocatalyst. Thus, **5** was prepared as abovementioned and its catalytic activity was tested using the same benchmark reaction. To our delight, a set of Michael adducts was obtained in good yields and excellent ees (Table 3), which confirms the utility of these hybrid materials in enantioselective catalysis.

Table 3
Enantioselective Michael addition catalyzed by **5**[a]

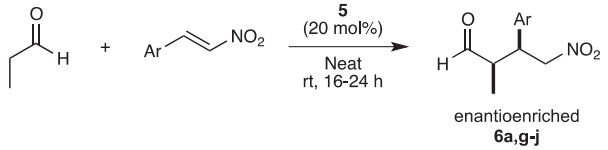

enantioenriched **6a,g-j**

Entry	Product (Ar)	Yield[b] (%)	*syn*/*anti*[c]	ee[d]
1	**6a** (Ph)	70	78:22	93
2	**6g** (*p*-MeC_6H_4)	58	90:10	91
3	**6h** (*p*-$(OMe)C_6H_4$)	83	89:11	86
4	**6i** (*p*-BrC_6H_4)	75	70:30	91
5	**6j** (*p*-ClC_6H_4)	57	79:21	90

[a] Nitroolefin (0.1 mmol), aldehyde (0.3 mL), and **5** (20 mol %) at room temperature.
[b] Isolated yield after column chromatography.
[c] Determined by ^1H NMR.
[d] Determined by HPLC.

3. Conclusions

The preparation of a magnetic, organic–inorganic hybrid material has been described. This can be used as a support for a chiral aminocatalyst but, strikingly, it also displays catalytic activity in the Michael addition of aldehydes to nitroolefins. Both materials can be easily separated from the reaction mixture by magnetic decantation. Attempts to recycle the magnetic materials **2** and **5** have proven fruitless so far. Studies to this end are currently underway.

4. Experimental section

4.1. General

Unless otherwise stated, all commercial reagents were directly used without any purification. All starting materials were commercially available of the best grade and were used without further purification. NMR spectra were registered in a Bruker Advance 400 Ultrashield spectrometer in $CDCl_3$ at room temperature, operating at 400 MHz or 500 MHz (^1H) and 100 MHz or 125 MHz (^{13}C). TMS was used as internal standard for ^1H NMR and $CDCl_3$ for ^{13}C NMR. FTIR measurements were carried out on a Bruker Optics FTIR Alpha spectrometer equipped with a DTGS detector. Ultrapure water was obtained from an SG Water Ultra Clear system that provides water with conductivity at 25 °C of 0.055 μS. Elemental analyses were performed at the MEDAC Ltd. Laboratories (Madrid, Spain). High performance liquid chromatography (HPLC) was performed on Agilent Technologies Chromatographs (Series 1100 and 1200), using Chiralpak columns fitted with guard column. TEM images were recorded using a JEOL JEM 1011 microscope equipped with a lanthanum hexaboride filament, operated at an acceleration voltage of 100 kV. The Michael adducts **6a**–**j** are known and their spectroscopic data matched with the reported in the literature.[14]

4.2. Preparation of 2

A suspension of 200 mg of κ-carrageenan (**1**) and 400 mg of MNPs in glacial acetic acid (60 μL), ultrapure water (80 μL), and DMF (15 mL) was stirred overnight at 110 °C. The resulting material was isolated by washing with EtOAc and centrifugation (×3) and finally dried under vacuum (f=0.80 mmol g^{-1}; see Fig. 2 for IR spectra).

4.3. Preparation of 5

Preparation of **3**.[15] The hybrid material **2** (600 mg), PPh_3 (1.00 g, 3.8 mmol), and LiCl (0.60 g, 14.2 mmol) were added to 20 mL DMF and stirred at room temperature for 3 h. Then, 4 mL of CCl_4 (41.3 mmol) were added dropwise and the mixture was stirred for 24 h at 60 °C. After this time, NaN_3 (1.00 g, 15.4 mmol) in 15 mL DMSO was added and it was heated for 36 h at 80 °C. The material was washed with EtOAc and dried (f=1.09 mmol g^{-1}; see Fig. 2 for IR spectra).

Preparation of **5**. The azide-functionalized hybrid material **3** (608 mg), (2*S*,4*R*)-4-(propargyloxy)diphenylprolinol *tert*-butyl-dimethyl silyl ether **4**[16] (400 mg, 0.95 mmol), CuI (30 mg, 0.16 mmol), and DIPEA (0.8 mL, 4.54 mmol) were mixed in 15 mL DMF and stirred for 48 h at 50 °C. The resulting material was isolated by washing with EtOAc and centrifugation (×3) and finally dried under vacuum (f=0.61 mmol g^{-1}; see Fig. 2 for IR spectra).

4.4. General procedure for the Michael reaction

The corresponding aldehyde (0.5 mmol for **2**, 0.3 mL for **5**), β-nitrostyrene (0.1 mmol), and catalyst (15 mol % of **2**, 20 mol % of **5**) were mixed and stirred at room temperature. The reaction was monitored by TLC until the total consumption of the nitroalkene was observed. Then, 2×1 mL of $CHCl_3$ were added, the catalyst was removed by magnetic decantation and the organic mixture was concentrated and purified by column chromatography on silica gel, eluting with hexanes/EtOAc, to give the desired Michael adduct.

Acknowledgements

This work was supported by the EU-ITN network Mag(net)icFun (PITN-GA-2012-290248), MINECO CTQ2012-38594-C02-01, and DEC grant 2009SGR623. C.R.-E. acknowledges AGAUR (Generalitat de Catalunya) for a Beatriu de Pinós B fellowship.

References and notes

1. For reviews, see: (a) Yuan, J.; Xu, Y.; Müller, A. H. E. *Chem. Soc. Rev.* **2011**, *40*, 640; (b) Lebeau, B.; Innocenzi, P. *Chem. Soc. Rev.* **2011**, *40*, 886; (c) Zheng, H.; Li, Y.; Liu, H.; Yin, X.; Li, Y. *Chem. Soc. Rev.* **2011**, *40*, 4506; (d) Mehdi, A.; Reye, C.; Corriu, R. *Chem. Soc. Rev.* **2011**, *40*, 563; (e) Ge, J.; Lei, J.; Zare, R. N. *Nat. Nanotechnol.* **2012**, *7*, 428.
2. For reviews, see: (a) Liu, T.-Y.; Hu, S.-H.; Liu, D.-M.; Chen, S.-Y.; Chen, I.-W. *Nano Today* **2009**, *4*, 52; (b) Zhou, L.; Yuan, J.; Wei, Y. *J. Mater. Chem.* **2011**, *21*, 2823 For selected examples; (c) Angelatos, A. S.; Katagiri, K.; Caruso, F. *Soft Matter* **2006**, *2*, 18; (d) Ruiz-Hernández, E.; Baeza, A.; Vallet-Regí, M. *ACS Nano* **2011**, 1259.

3. For reviews, see: (a) van de Velde, F.; Lourenço, N. D.; Pinheiro, H. M.; Bakker, M. *Adv. Synth. Catal.* **2002**, *344*, 815; (b) Campo, V. L.; Kawano, D. F.; da Silva, D. B., Jr.; Carvalho, I. *Carbohydr. Polym.* **2009**, *77*, 167; (c) Li, L.; Ni, R.; Shao, Y.; Mao, S. *Carbohydr. Polym.* **2014**, *103*, 1.
4. (a) Daniel-da-Silva, A. L.; Trindade, T.; Goodfellow, B. J.; Costa, B. F. O.; Correia, R. N.; Gil, A. M. *Biomacromolecules* **2007**, *8*, 2350; (b) Oya, K.; Tsuru, T.; Teramoto, Y.; Nishio, Y. *Polym. J.* **2013**, *45*, 824.
5. (a) Daniel-da-Silva, A. L.; Fateixa, S.; Guiomar, A. J.; Costa, B. F. O.; Silva, N. J. O.; Trindade, T.; Goodfellow, B. J.; Gil, A. M. *Nanotechnology* **2009**, *20*, 355602; (b) Dias, A. M. G. C.; Hussain, A.; Marcos, A. S.; Roque, A. C. A. *Biotechnol. Adv.* **2011**, *29*, 142.
6. Salgueiro, A. M.; Daniel-da-Silva, A. L.; Girão, A. V.; Pinheiro, P. C.; Trindade, T. *Chem. Eng. J.* **2013**, *229*, 276.
7. Riente, P.; Mendoza, C.; Pericàs, M. A. *J. Mater. Chem.* **2011**, *21*, 7350.
8. Pereira, L.; Sousa, A.; Coelho, H.; Amado, A. M.; Ribeiro-Claro, P. J. A. *Biomol. Eng.* **2003**, *20*, 223.
9. (a) Font, D.; Jimeno, C.; Pericàs, M. A. *Org. Lett.* **2006**, *8*, 4653; (b) Bastero, A.; Font, D.; Pericàs, M. A. *J. Org. Chem.* **2007**, *72*, 2460; (c) Alza, E.; Pericàs, M. A. *Adv. Synth. Catal.* **2009**, *351*, 3051; (d) Kasaplar, P.; Riente, P.; Hartmann, C.; Pericàs, M. A. *Adv. Synth. Catal.* **2012**, *354*, 2905; (e) Riente, P.; Yadav, J.; Pericàs, M. A. *Org. Lett.* **2012**, *14*, 3668; (f) Osorio-Planes, L.; Rodríguez-Escrich, C.; Pericàs, M. A. *Chem.—Eur. J.* **2014**, *20*, 2367.
10. For related catalytic materials bearing a diphenylprolinol anchored onto magnetic nanoparticles, see (a) Ref. 7; (b) Wang, B. G.; Ma, B. C.; Wang, Q.; Wang, W. *Adv. Synth. Catal.* **2010**, *352*, 2923; (c) Keller, M.; Perrier, A.; Lindhart, R.; Travers, L.; Wittman, S.; Caminade, A.-M.; Majoral, J.-P.; Reiser, O.; Ouali, A. *Adv. Synth. Catal.* **2013**, *355*, 1748.
11. Kolb, H. C.; Finn, M. G.; Sharpless, K. B. *Angew. Chem., Int. Ed.* **2001**, *40*, 2004.
12. For reviews, see: (a) Sulzer-Mossé, S.; Alexakis, A. *Chem. Commun.* **2007**, 3123; (b) Tsogoeva, S. B. *Eur. J. Org. Chem.* **2007**, 1701; (c) Almaşi, D.; Alonso, D. A.; Nájera, C. *Tetrahedron: Asymmetry* **2007**, *18*, 299; (d) Vicario, J. L.; Badía, D.; Carrillo, L. *Synthesis* **2007**, 2065; (e) Vicario, J. L.; Badía, D.; Carrillo, L.; Reyes, E. *Organocatalytic Enantioselective Conjugate Addition Reactions*; RSC: Cambridge, 2010.
13. Alza, E.; Sayalero, S.; Kasaplar, P.; Almaşi, D.; Pericàs, M. A. *Chem.—Eur. J.* **2011**, *17*, 11585.
14. Previously reported characterization data: (a) for the Michael adducts **6a**–**c** and **6e**, see: Betancort, J. M.; Barbas, C. F., III. *Org. Lett.* **2001**, *3*, 3737; (b) for **6d**, see: Wang, W.; Wang, J.; Li, H. *Angew. Chem., Int. Ed.* **2005**, *44*, 1369; (c) for **6g**, see: Wang, W.-H.; Wang, X.-B.; Kodama, K.; Hirose, T.; Zang, G.-Y. *Tetrahedron* **2010**, *66*, 4970; (d) for **6h**,**i**, see: Luo, R.-S.; Weng, J.; Ai, H.-B.; Lu, G.; Chan, A. S. C. *Adv. Synth. Catal.* **2009**, *351*, 2449; (e) for **6j**, including HPLC conditions, see: Ref. 10b; (f) for the HPLC conditions for **6a**,**g**–**i**, see Ref. 7.
15. Elchinger, P.-H.; Faugeras, P.-A.; Boëns, B.; Brouillette, F.; Montplaisir, D.; Zerrouki, R.; Lucas, R. *Polymer* **2011**, *3*, 1607 and references therein.
16. Fan, X.; Sayalero, S.; Pericàs, M. A. *Adv. Synth. Catal.* **2012**, *354*, 2971.

2.9. Summary and Outlook

An interesting hybrid material with the combination of an organocatalyst molecule, an inorganic material and magnetic nanoparticles was developed. The chiral organocatalyst could be used as a powerful tool for asymmetric synthesis. The organic support, here is k-carrageenan, which can be used as a versatile platform for carrying organocatalysts, whereas the magnetic nanoparticles can be used as an efficient tool for separating the organocatalyst from the reaction media.

The main interest in this project is the novelty of the hybrid material, as well as the easy preparation and separation of the catalyst based on the magnetic decantation.

We believe these materials have a lot of potential to work on and are still far from mature. In our research group, there are still ongoing projects that deal this material.

Polystyrene or Magnetic Nanoparticles as Support in Enantioselective Organocatalysis? A Case Study in Friedel–Crafts Chemistry

Table of Contents

3.1. Introduction to Iminium Ion Catalysis

Imines are the product of condensation of aldehydes or ketones with primary amines (Scheme 1). In 1864, Schiff was the first to identify this reaction, which is why in the old nomenclature imines are also called Schiff bases. Primary amine-derived imines show basic properties (pK_a ca. 7), and in acidic media they convert to iminium ions.[1]

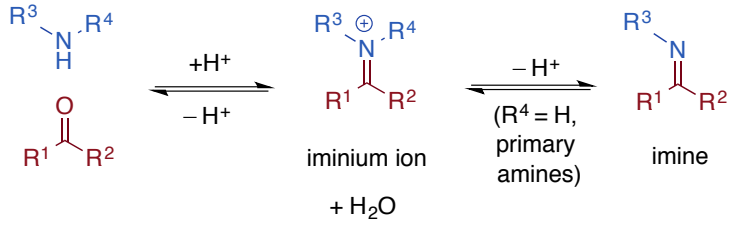

Scheme 1. Formation of iminium ions and imines.

The formation of iminium ion species is a reversible reaction. In the case of α,β-unsaturated aldehydes, the energy of the lowest-unoccupied molecular orbital (LUMO) is decreased with respect to the starting materials. This feature has given rise to a catalytic strategy known as iminium activation, which mimics Lewis acid activation of α,β-unsaturated carbonyl compounds regarding to equilibrium dynamics and π-orbital electronics (Scheme 2).[2]

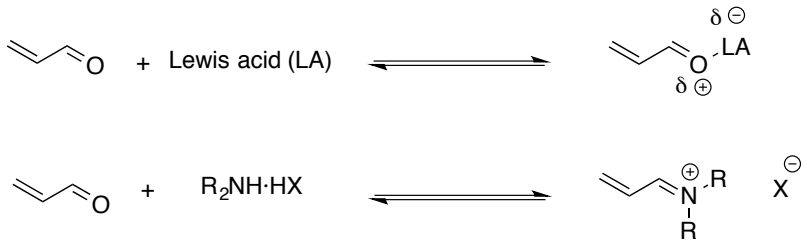

Scheme 2. Concept of iminium ion activation (LOMO lowering).

The first example of iminium ion activation mode was reported by MacMillan *et al.* at the beginning of the 21st century. This seminal example involved the first enantioselective Diels-Alder reaction of α,β-unsaturated aldehydes using an imidazolidinone catalyst which acts through a covalent intermediate.[3] Since then, imidazolidinone-based organocatalysts have evolved, mainly thanks to MacMillan *et al*., who expanded their scope and enhanced their catalytic activity and selectivity (Scheme 3).

[1] a) Layer, R. W. *Chem. Rev.* **1963**, *63*, 489; b) Schiff, H. *Liebigs Ann*. **1864**, *131*, 118.
[2] Ricci, A. *ISRN Organic Chemistry*. **2014**, 2014, 29.
[3] Ahrendt, K. A.; Borths, C. J.; MacMillan, D. W. C. *J. Am. Chem. Soc*. **2000**, *122*, 4243.

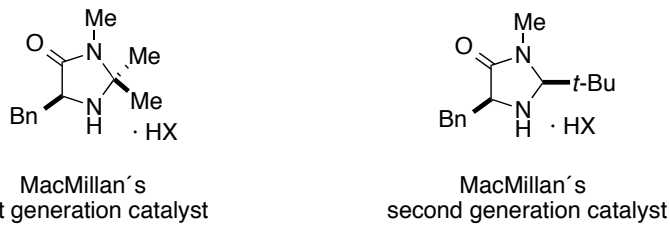

Scheme 3. MacMillan's chiral benzyl imidazolidinone organocatalysts.

3.2. First Generation MacMillan Catalyst

The first report involving iminium ion activation is the asymmetric Diels-Alder reaction of enals and dienes promoted by **1** (Scheme 4). The reaction afforded bicyclic products with moderate *exo-endo* selectivities but with good enantioselectivity (83-96% *ee*).[3]

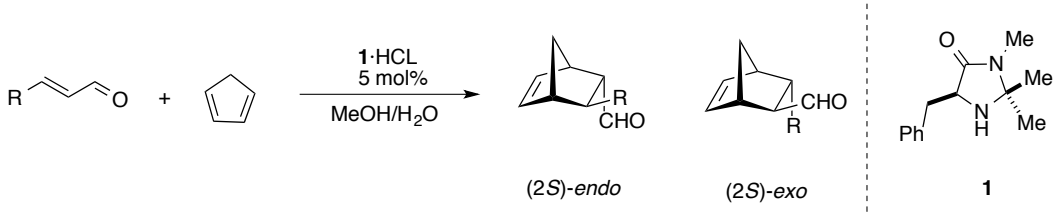

Scheme 4. Diels-Alder reaction with the first generation MacMillan catalyst.

After preliminary experimental findings, the mechanistic details were studied by computational methods. The results showed that the catalyst and the aldehyde condense to form an iminium ion in the *E* form to avoid repulsive interactions between the hydrogen atom in the α position and the gem-dimethyl substituents of the catalyst. This geometry leaves the *Re* face of the iminium intermediate exposed for addition of dienes, while the *Si* face is shielded by the benzene group (Scheme 5). This mechanistic study explains the high enantioselectivities observed with imidazolidinone-based catalysts.[4]

[4] a) Jen, W. S.; Wiener, J. J. M.; MacMillan, D. W. C. *J. Am. Chem. Soc.* **2000**, *122*, 9874; b) Holland, M. C.; Paul, S.; Schweizer, W. B.; Bergander, K.; Lichtenfeld, C. M.; Lakhdar, S.; Mayr, H.; Gilmour, R. *Angew. Chem. Int. Ed.* **2013**, *52*, 7967.

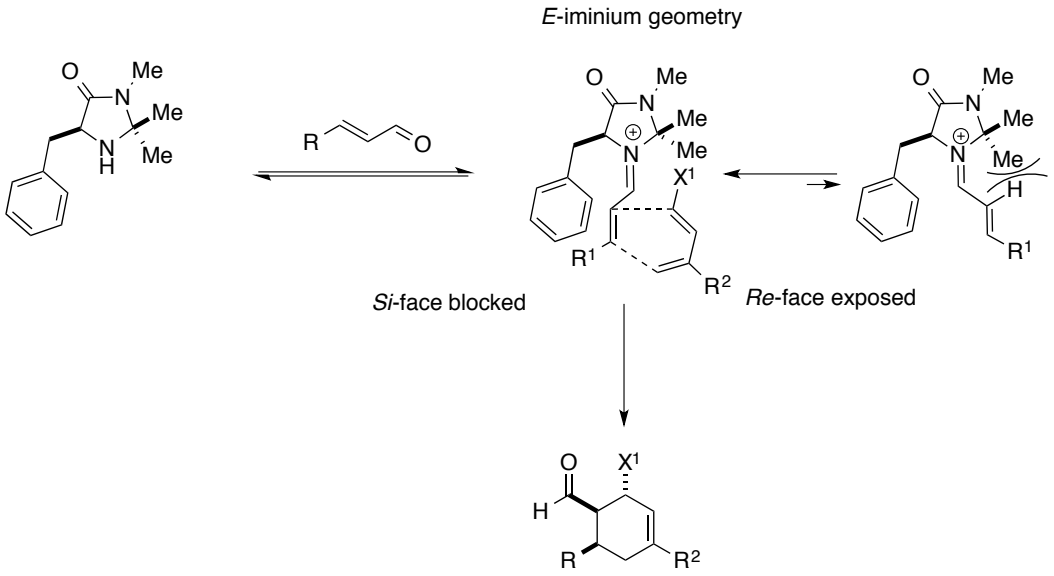

Scheme 5. Stereochemical model for the enantioselective Diels-Alder reaction.

The electrophilicity parameters (*E*) of some iminium ions were defined by kinetic measurements using secondary amines as nucleophiles and cinnamaldehyde.[5] The results confirmed that imidazolidinone-derived and diarylprolinol-derived iminium ions present higher electrophilicity than the common cyclic amine-derived iminium ions (Scheme 6). In conclusion, the first generation MacMillan organocatalyst turned out to be perfectly suited for the LUMO-lowering iminium ion activation mode using weak nucleophiles.

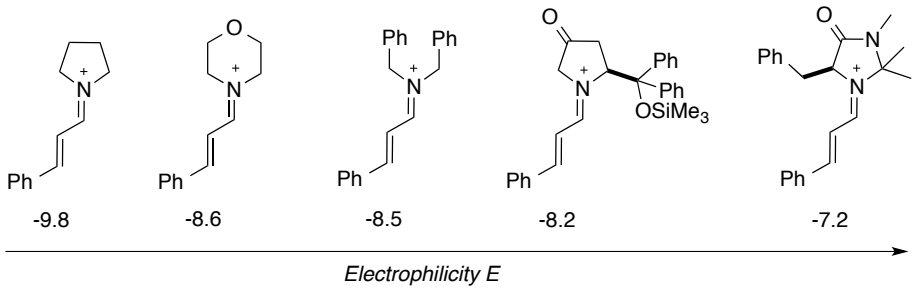

Scheme 6. Relative eletrophilicity *E* of selected iminium ions

3.2.1. Enantioselective Friedel-Crafts Reactions

One year later, MacMillan *et al*. applied the same catalyst to the Friedel-Crafts alkylation of pyrroles with α,β-unsaturated aldehydes (Scheme 7).[6]

[5] Lakhdar, S.; Tokuyasu, T.; Mayr, H. *Angew. Chem. Int. Ed*. **2008**, *47*, 8723.
[6] Paras, N. A.; MacMillan, D. W. C. *J. Am. Chem. Soc*. **2001**, *123*, 4370.

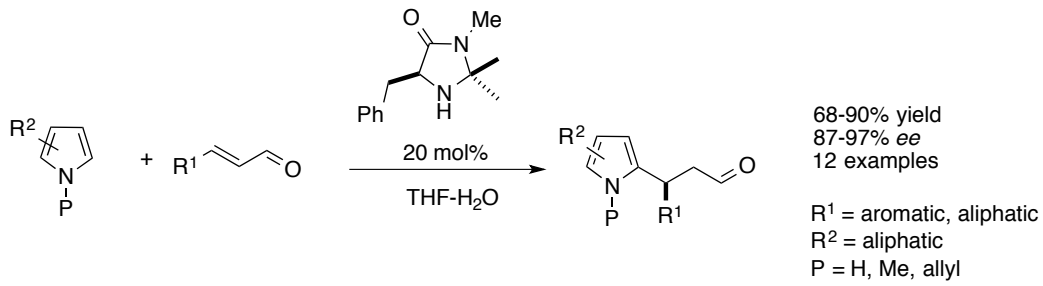

Scheme 7. Friedel-Crafts alkylation of pyrroles.

In this work, the results showed a pyrrole preference for pathway b (Scheme 8, 1,4-addition) because of the lower steric hindrance. This nucleophilic addition afforded the products with high enantiomeric excess.

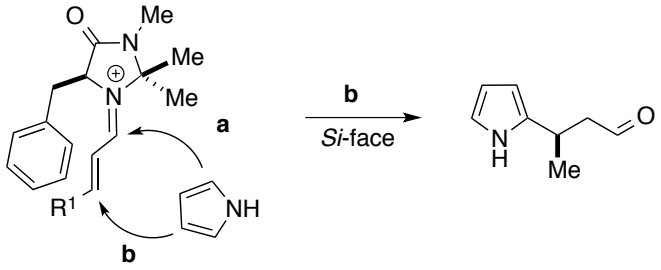

Scheme 8. Possible pathways for pyrrole addition.

A simplified mechanism of iminium ion activation is described in Scheme 9. The condensation between the first generation MacMillan catalyst and the α,β-unsaturated aldehyde generates an iminium ion intermediate which is in equilibrium between the *E* and *Z* form (**A**). Normally, the major product is in the *E* configuration to minimize the repulsive interaction between hydrogen and methyl groups (as explained in the Diels-Alder reaction mechanism).[7] Afterwards, the addition of the nucleophile to the β-carbon of the iminium ion produces the β-functionalized enamine (**B**). At the end, the hydrolysis of the enamine gives the β-functionalized aldehyde and releases the catalyst (**D**).

[7] a) Seebach, D.; Gilmour, R.; Grošelj, U.; Deniau, G.; Sparr, C.; Ebert, M. O.; Beck, A. K. *Helv. Chim. Acta* **2010**, *93*, 603. b) Nielsen, M.; Worgull, D.; Zweifel, T.; Gschwend, B.; Bertelsen, S.; Jørgensen, K. A. *Chem. Commun.* **2011**, *47*, 632.

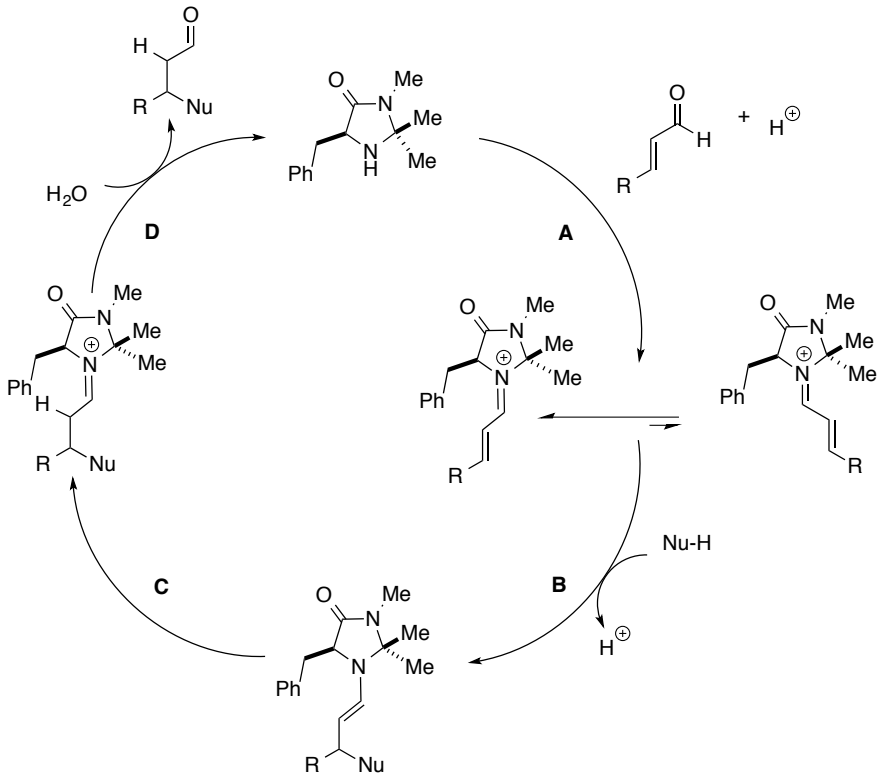

Scheme 9. Catalytic cycle for iminium ion activation mode.

In conclusion, in reactions mediated by the first generation Macmillan catalyst, the methyl group in the imidazolidinone controls the iminium geometry whereas the addition of the nucleophile is controlled by the benzyl group (Scheme 10).

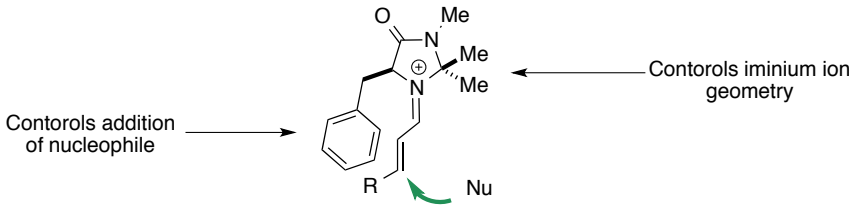

Scheme 10. Stereocontrolling elements of the first generation imidazolidinone organocatalyst.

3.3. Second Generation MacMillan Catalyst

With this success in pyrrole addition, the Friedel-Crafts reaction was developed for indoles. The reaction between (*E*)-crotonaldehyde and indole using this imidazolidinone catalyst generated a product with poor enantioselectivity (56% *ee*) and also the reaction was slow (83% yield after 48 h). A closer study based on theoretical calculations of the first generation MacMillan catalyst illustrated that there are two steps which are crucial in this reaction: formation of iminium ion and

carbon-carbon bond formation. In the first generation MacMillan organocatalyst there is an interaction between the nitrogen and the CH_3 group. In addition, there are some interactions between one of the methyl substituents and the phenyl ring of the benzyl group in indole. Due to these difficulties, the structure of first generation of MacMillan was evolved and a modified catalyst was designed. In the new catalyst structure, the position of nitrogen ione pair is away from steric hindrance and thus more exposed. As a result the formation of iminium ion will be faster and more convenient (Scheme 11).

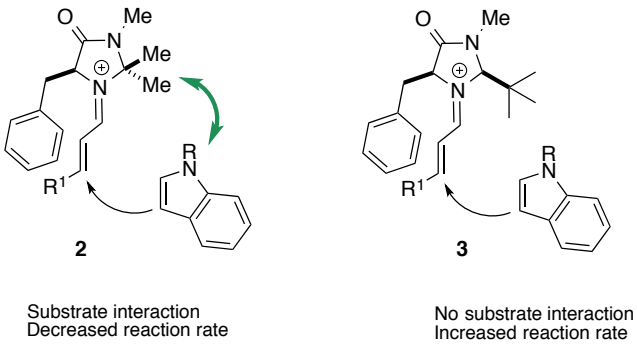

Scheme 11. Comparison between first and second generation MacMillan catalyst.

On these grounds, the second generation MacMillan organocatalyst was developed, where the gem-dimethyl group had been replaced by a *tert*-butyl substituent (moiety 3). This novel catalyst was successfully applied to the enantioselective Friedel-Crafts alkylation of indole. A range of aromatic and aliphatic unsaturated aldehydes with different indole substrates was applied to this reaction (Scheme 12).[8]

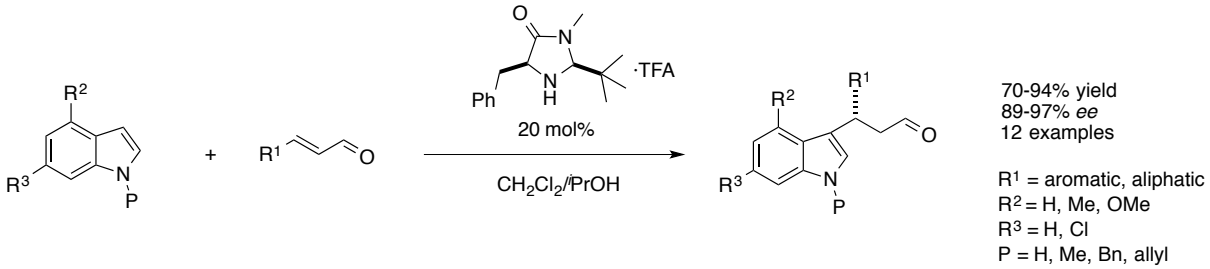

Scheme 12. Friedel-Crafts alkylation with second generation MacMillan catalyst.

In 2002, another imidazolidinone catalyst was developed for the asymmetric Diels-Alder reaction of conjugate ketones. This reaction was first tested with catalysts **4** and **5**. The yield was 20% and 27% respectively and the reaction proceeded without any enantioselectivity. However, introducing a (5-methyl) furyl group on the imidazolidinone (**6**, Scheme 13), the reaction between cyclopentadiene and different ketones afforded the desired products with good yields and

[8] Austin, J. F.;MacMillan, D. W. C. *J. Am. Chem. Soc*. **2002**, *124*, 1172.

selectivities (Scheme 14).[9]

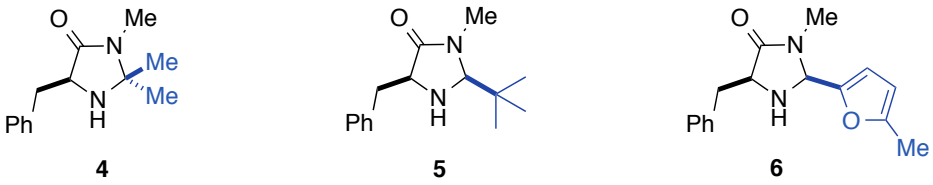

Scheme 13. Different kinds of imidazolidinone catalyst.

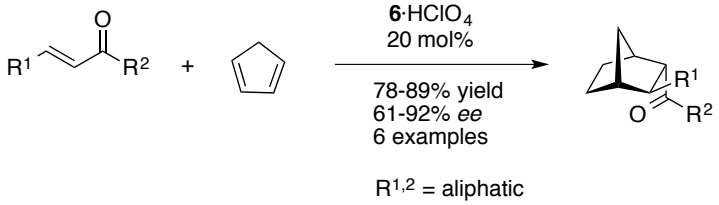

Scheme 14. Diels-Alder reaction with MacMillan catalyst 6.

This reaction was also tested for a variety of cyclic ketones. The results showed the enantioselectivity was good with larger rings because the diene in these cyclic systems had the *S-cis* conformation locked (Scheme 15).

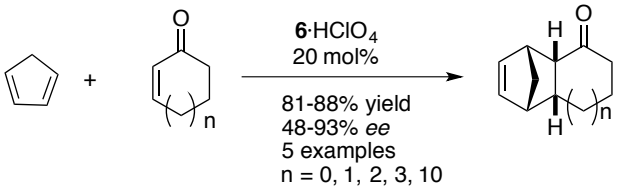

Scheme15. Diels-Alder cycloaddition between cyclic enones and cyclopentadiene catalyzed by **6**.

3.4. Other Catalytic Reactions with MacMillan Imidazolidinone

The iminium ion concept and MacMillan catalysts have been used in different reactions such as Mukaiyama Michael addition,[10] 1,3-dipolar cyclization,[4a] organocatalyzed transfer hydrogenation [11] or reductive Michael cyclization[12] (Scheme 16).

[9] Northrup, A. B.; MacMillan, D. W. C. *J. Am. Chem. Soc*. **2002**, 124, 2458.
[10] Brown, S. P.; Goodwin, N. C.; MacMillan, D. W. C. *J. Am. Chem. Soc.* **2003**, *125*, 1192.
[11] Ouellet, S. G.; Tuttle, J. B.; MacMillan, D. W. C. *J. Am. Chem. Soc*. **2005**, *127*, 32.
[12] Yang, J. W.; Hechavarria Fonseca, M. T.; List, B. *J. Am. Chem. Soc*. **2005**, *127*, 15036.

Mukaiyama-Michael addition

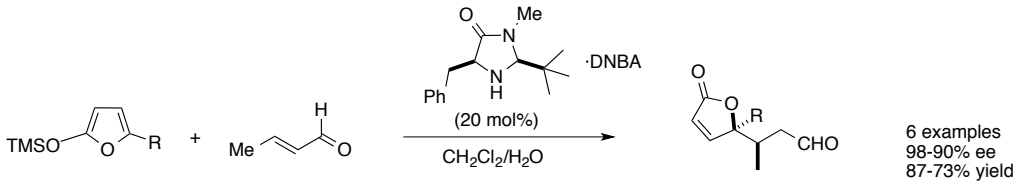

1,3-Dipolar cycloaddition

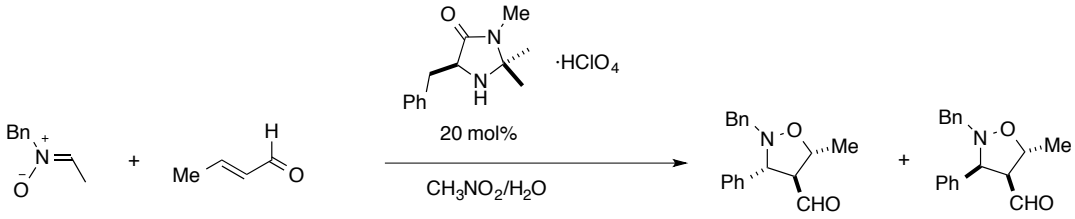

Organocatalyzed transfer hydrogenation

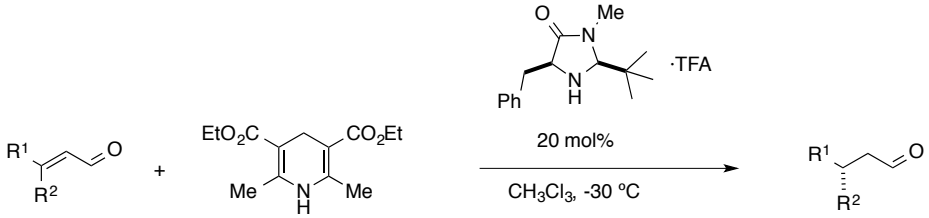

Reductive Michael cyclization

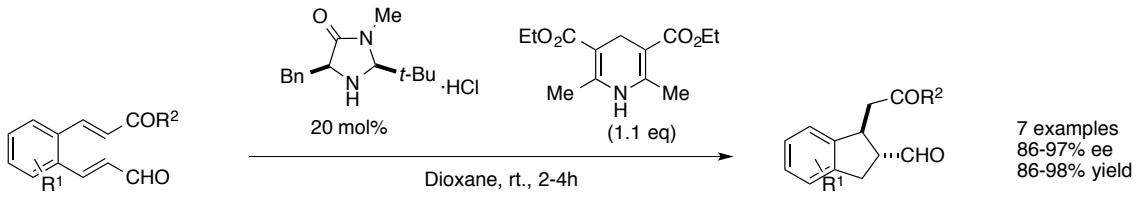

Scheme 16. Some examples of imidazolidinone-catalyzed reactions.

3.5. Immobilized Imidazolidinone Organocatalysts

Considering the efficient results obtained with homogeneous catalysts, several authors have studied their immobilization and recycling.

Imidazolidin-4-one was anchored on siliceous mesocellular foam (MCF) and polymer-coated MCF with different linker groups (Scheme 17). However, the silanol groups in MCF can interact with the catalyst and have an effect on its efficiency. To avoid this problem, silanol groups in

MCF are covered with polymer, so they do not interfere with the catalyst. These immobilized imidazolidinones have been applied to the Friedel–Crafts alkylation with yields similar to the homogeneous system. However, stereoselectivities depended on the surface of the support and the linker. Within siliceous mesocellular foam (MCF) strong interactions exist between silanol groups in the surface of the inorganic material and the catalyst; for this reason, a drop was observed in *ee*. In the case of polymer-coated catalysts *ee* was constant until the second run, so it was proposed that this catalyst is more efficient in recyclability.[13]

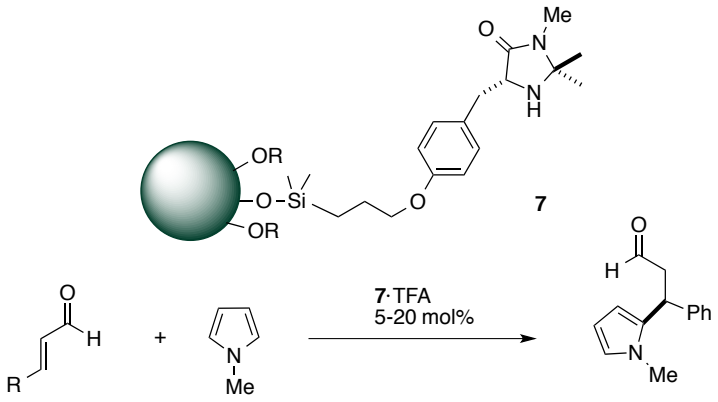

Scheme 17. Heterogenized first generation MacMillan catalyst for conjugate addition of pyrroles to enals.

The Wang group developed a method to take advantage of the activity of homogeneous and recyclability of heterogeneous catalyst at the same time. They developed an imidazolidinone-bridged chiral organosilica polymer, which could be dissolved in CH_3CN/H_2O and THF/H_2O. However it was insoluble in H_2O, CH_2Cl_2, or Et_2O, which enabled its recovery (Scheme 18). This catalyst was used for Diels-Alder reaction with excellent enatioselectivities.[14]

[13] Zhang, Y.; Zhao, L.; Lee, S. S.; Ying, J. Y. *Adv. Synth. Catal*. **2006**, *348*, 2027.
[14] Wang, C. A.; Zhang, Y.; Shi, J, Y.; Wang, W. *Chem. Asian J.* **2013**, *8*, 1110.

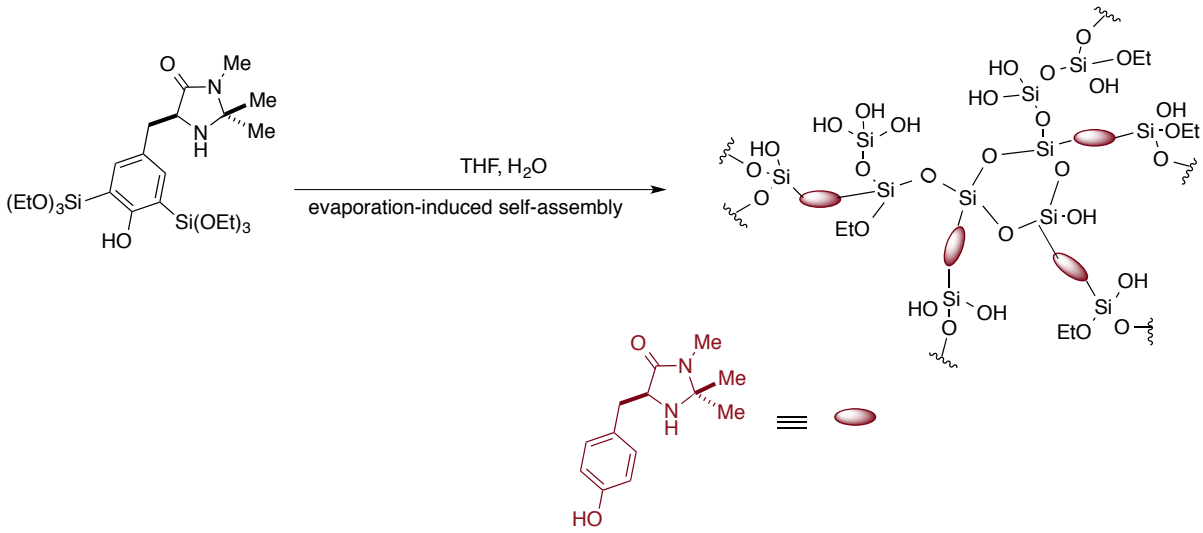

Scheme 18. A self-supported polymeric MacMillan catalyst.

In another work by Puglisi and Benaglia, four different imidazolidinone-based catalysts were synthesized.[15] All of them were tested in the Diels-Alder cycloaddition between cyclopentadiene and different aldehydes. Among them, catalyst **10** showed better results than its analogues. However, the recyclability, studied for the Diels-Alder reaction between cyclopentadiene and cinnamaldehyde, results showed the yield was decreasing from 91% to 63% and 41%. Enantiomeric excesses also decreased from 92% to 87% and 72% for the *endo* isomer in the second and third runs, respectively. The authors mention this limitation could be due to partial degradation of the imidazolidinone moiety and the silica network.

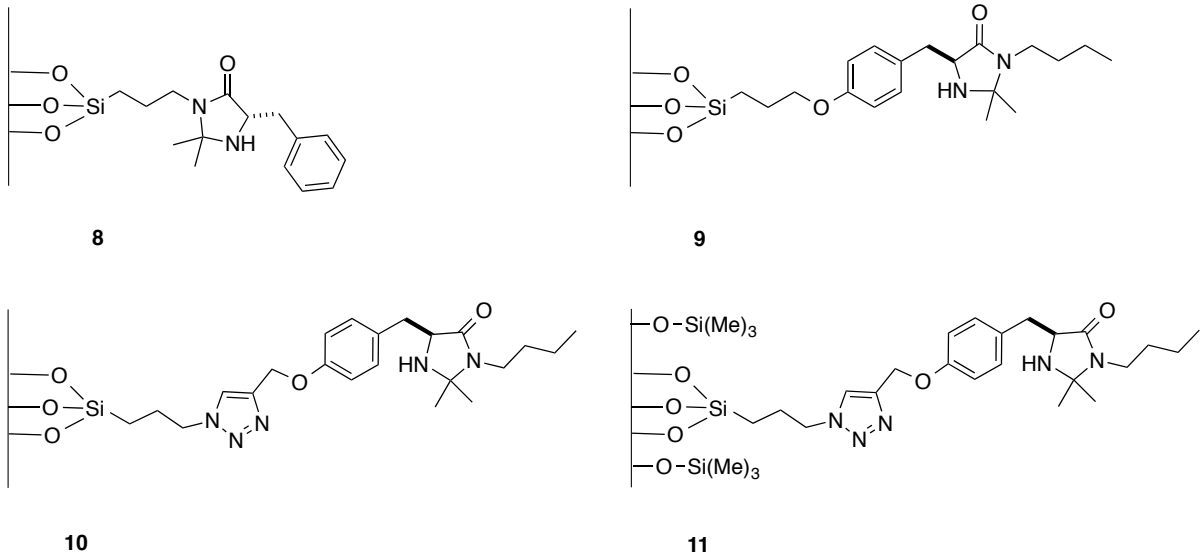

Scheme 19. Silica-supported imidazolidinones.

[15] Puglisi, A.; Benaglia, M.; Annunziata, R.; Chiroli, V.; Porta, R.; Gervasini, A. *J. Org. Chem*. **2013**, *78*, 11326.

In our group, the first generation MacMillan imidazolidin-4-one catalyst was immobilized onto a Merrifield resin as well as magnetic nanoparticles (Fe_3O_4) exploiting the copper-catalyzed alkyne azide cycloaddition (CuAAC) strategy. This immobilized catalyst was applied to the Friedel-Crafts reactions of *N*-substituted pyrroles with α,β-unsaturated aldehydes, the results being very satisfactory (Scheme 19). The study showed that, whereas PS-supported imidazolidinone gave better results, MNP-supported ones displayed better stability during the recycling process. In addition, the magnetic properties allowed a facile separation of the catalyst from the reaction media.[16]

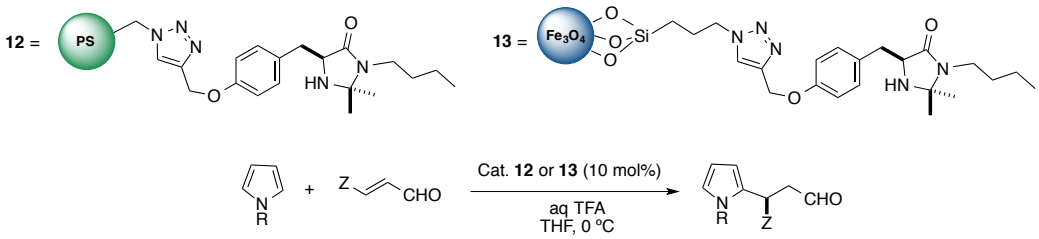

Scheme 19. Immobilization of first generation MacMillan organocatalyst on polystyrene and magnetic nanoparticles.

According to the abovementioned, we reasoned that an immobilized second generation MacMillan catalyst would give an interesting new range of reactions that were not available with **12** or **13**. This heterogenization study gave rise to the paper attached hereafter.

[16] Riente, P.; Yadav, J.; Pericàs, M. A. *Org. Lett*. **2012**, *14*, 2012.

3.6. Article

Organic LETTERS

Letter

pubs.acs.org/OrgLett

Polystyrene or Magnetic Nanoparticles as Support in Enantioselective Organocatalysis? A Case Study in Friedel–Crafts Chemistry

Sara Ranjbar,[†] Paola Riente,[†] Carles Rodríguez-Escrich,[†] Jagjit Yadav,[†,§] Kishore Ramineni,[†,⊥] and Miquel A. Pericàs*[,†,‡]

[†]Institute of Chemical Research of Catalonia (ICIQ), The Barcelona Institute of Science of Technology, Avda. Països Catalans, 16, 43007 Tarragona, Spain

[‡]Department de Química Orgànica, Universitat de Barcelona, 08080 Barcelona, Spain

Supporting Information

ABSTRACT: Heterogenized versions of the second-generation MacMillan imidazolidin-4-one are described for the first time. This versatile organocatalyst has been supported on 1% DVB Merrifield resin and Fe_3O_4 magnetic nanoparticles through a copper-catalyzed alkyne–azide cycloaddition (CuAAC) reaction. The resulting catalytic materials have been successfully applied to the asymmetric Friedel–Crafts alkylation of indoles with α,β-unsaturated aldehydes. While both catalytic systems can be easily recovered and admit repeated recycling, the polystyrene-based catalyst shows higher stability and provides better stereoselectivities.

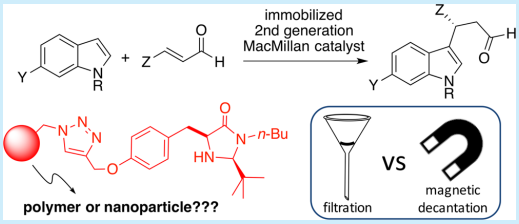

In the year 2000, MacMillan and co-workers introduced iminium ion catalysis as a new activation concept in a seminal paper that opened the organocatalysis field.[1] For this novel mode of activation, they developed a chiral secondary amine integrated in an imidazolidin-4-one framework (the first-generation MacMillan catalyst), whose efficiency was demonstrated in a variety of asymmetric processes involving enals.[1,2] Among them, the first highly enantioselective Friedel–Crafts (FC) alkylation of pyrroles with α,β-unsaturated aldehydes was developed.[2b] However, when the same strategy was attempted with less electron-rich heteroaromatics, such as indoles, poor results were achieved. Efforts directed to the solution of this problem led to the development of the so-called second-generation MacMillan catalyst, a more active and versatile imidazolidin-4-one featuring an additional stereocenter.[3] This type of organocatalyst has been successfully applied to a large variety of important transformations, including cycloadditions,[4] hydrogenations,[5] and conjugate additions.[6]

However, some drawbacks arise in connection with its preparation when compared to the facile synthesis of the first-generation imidazolidin-4-one. For instance, synthesis of the second-generation *cis*-imidazolidin-4-one (*cis*-**2**) requires condensation of the phenylalanine amide derivative (**1**) with an excess of pivalaldehyde using iron(III) chloride as the Lewis acid (Scheme 1). This transformation yields a mixture of diastereoisomers with the undesired *trans*-**2** as the major product. Given the manifold applications of this organocatalyst and the problems associated with its preparation, development of a modified

Scheme 1. Reported Synthesis of 2

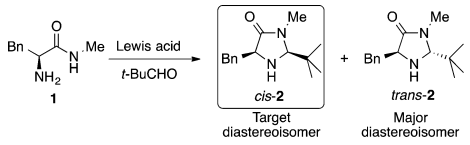

version that could allow for its easy recovery and multiple reuse becomes highly desirable.

Recycling of organocatalysts has been tackled from different perspectives.[7] Among them, covalent immobilization onto insoluble supports furnishes an excellent platform to simplify catalyst separation from the reaction medium. In fact, the heterogenization of the first-generation MacMillan catalyst onto a variety of solid supports such as organic polymers,[8] magnetic nanoparticles,[8d] and mesoporous materials[9] has been reported in the literature.

The use of a copper-catalyzed alkyne–azide cycloaddition reaction (CuAAC) as a tool to anchor different organocatalysts onto polymers[8d,10] and magnetic nanoparticles[8d,11] has been explored in detail, with excellent results in our laboratory. We envisioned that such a late-stage immobilization would be ideal to support the versatile second-generation MacMillan catalyst (the target *cis* diastereomer could be previously separated). This would only require a simple modification in the starting amino

Received: February 17, 2016
Published: March 24, 2016

DOI: 10.1021/acs.orglett.6b00462
Org. Lett. 2016, 18, 1602–1605

acid to provide an anchoring point remote from the catalyst active site.

We report the covalent immobilization of the second-generation imidazolidin-4-one organocatalyst onto 1% DVB Merrifield resin (PS) and iron oxide magnetic nanoparticles (MNPs) according to these principles and the use of the resulting recyclable catalysts in the enantioselective FC alkylation of indoles with α,β-unsaturated aldehydes. In contrast to what one might expect, the employed support has a significant effect not only on the recyclability of the catalyst but also on its enantioselectivity.

Monomeric species **5** was prepared as shown in Scheme 2. The sequence started with the amidation of the commercially

Scheme 2. (a) Synthesis of Second-Generation Imidazolidin-4-one Derivative 5 and (b) General Methodology To Prepare PS-Supported Imidazolidinone (Catalyst A) and MNPs-Supported Imidazolidinone (Catalyst B)

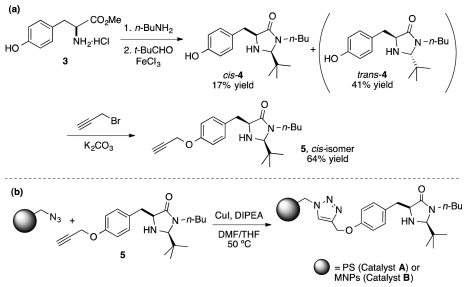

available L-tyrosine methyl ester hydrochloride (**3**). As mentioned above, the *para*-hydroxy substituent in the aryl group of this amino acid will be instrumental for the immobilization process. Next, condensation of the resulting amide with pivalaldehyde in the presence of $FeCl_3$ gave imidazolidin-4-one **4** as a 1:2.4 mixture of *cis*/*trans* diastereoisomers, with the desired *cis*-**4** being isolated in 17% yield after separation by column chromatography. Final propargylation led to the ready-to-anchor *cis*-imidazolidin-4-one **5** in 64% yield.

To prepare PS-supported second-generation imidazolidin-4-one (catalyst **A**), commercially available Merrifield resin (1% DVB, f = 0.6 mmol·g^{-1}) was converted to azidomethylpolystyrene by treatment with sodium azide, and the resulting PS-azide (f = 0.54 mmol·g^{-1}) was conjugated with **5**. To prepare catalyst **B**, Fe_3O_4 MNPs (5.7 ± 1.3 nm) prepared by thermal decomposition[12] were functionalized with azide groups by ligand exchange with 3-(azidopropyltriethoxy)silane to give 3-azidopropyl-MNPs (f = 0.72 mmol·g^{-1}). In both cases, imidazolidinone **5** was immobilized using a CuAAC reaction. Functionalization of both materials was followed by infrared spectroscopy (see Supporting Information). Also, the size distribution and morphology of the MNPs were monitored by transmission electron microscopy (TEM) after each step. This allowed us to rule out any agglomeration phenomena during the preparation of the immobilized catalyst (Figure 1; see Supporting Information for details).

Next, we investigated the activity of catalysts **A** and **B** on the enantioselective FC alkylation of indoles with α,β-unsaturated aldehydes.[13] The reaction between *N*-methylindole (**6a**) and cinnamaldehyde (**7a**) was chosen to optimize the reaction conditions. The effects of solvent and temperature were studied

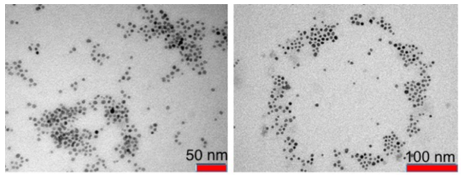

Figure 1. TEM images of MNPs before (left) and after (right) functionalization with **5**.

with polystyrene-based catalyst **A**. As shown in Table 1, good results were obtained when the reaction was carried out in

Table 1. Optimization of the Reaction Conditions for the FC Alkylation of Indoles with Enals Mediated by Catalyst A[a]

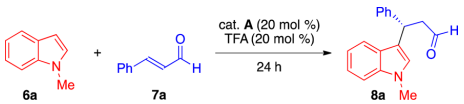

entry	temp (°C)	solvent	yield (%)[b]	ee (%)[c]
1	−20	CH_2Cl_2	64	60
2	−20	*i*-PrOH	–	–
3	−20	THF	51	59
4	−20	toluene	52	69
5	−20	CH_2Cl_2/*i*-PrOH[d]	71	84
6	rt	CH_2Cl_2/*i*-PrOH[d]	76	69
7	0	CH_2Cl_2/*i*-PrOH[d]	73	75

[a]Reaction conditions: *N*-methylindole (0.3 mmol), *trans*-cinnamaldehyde (0.9 mmol), catalyst **A** (20 mol %), TFA (0.5 M, 20 mol %), solvent (1 mL). [b]Isolated yield. [c]Enantioselectivity determined by chiral HPLC. [d]85:15 ratio.

CH_2Cl_2, tetrahydrofuran, or toluene (entries 1, 3, and 4). While no conversion was observed in isopropyl alcohol alone (entry 2), the best result was observed in a CH_2Cl_2/*i*-PrOH mixture at −20 °C (entry 5). Good yields and enantioselectivities of FC adduct **8a** were also recorded with the same solvent mixture at room temperature or at 0 °C (entries 6 and 7).

The asymmetric FC reaction was next studied with representative combinations of α,β-unsaturated aldehydes and indoles or *N*-methylindoles under the optimized reaction conditions, using catalysts **A** and **B** (Scheme 3). Both systems displayed good tolerance toward the reaction of β-alkyl- and β-aryl-substituted enals (Z = Pr, Et, Ph, 4-ClC_6H_4, 4-$NO_2C_6H_4$), with *N*-methylindole and indole giving the corresponding adducts with good yields and enantioselectivities. On the other hand, incorporation of a halogenated group on the C_6 position of the indole moiety had a deleterious effect on the activity and enantioselectivity of catalysts **A** and **B** (products **8g** and **8h**).

Comparison seems to favor the polystyrene-based catalyst **A** in all cases. Thus, this catalyst leads to higher enantioselectivities and similar or better yields in shorter reaction times (24 h) than MNP-based catalyst **B** (48 h). A tentative explanation to this behavior can be found on the differential efficiency of interphase mass transfer with both types of material. MNPs, despite their inherently high specific surface, do not normally exhibit perfect dispersibility in organic solvents.[14] The agglomerates formed in these conditions only allow for limited accessibility of the reagents to the catalytic sites, leading to TOFs well below its theoretical maximum. On the contrary, when polystyrene-based catalysts operate in reaction media that lead to perfect swelling

DOI: 10.1021/acs.orglett.6b00462
Org. Lett. 2016, 18, 1602−1605

Scheme 3. Substrate Scope for the FC Alkylation of Indoles[a]

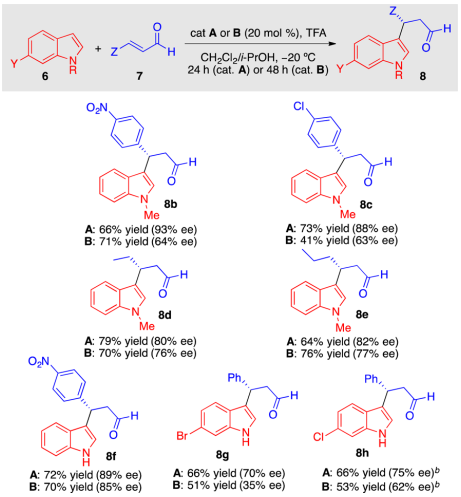

[a]Reaction conditions: indole or *N*-methylindole (0.3 mmol), enal (0.9 mmol), catalyst (20 mol %), TFA (0.5 M, 20 mol %), CH_2Cl_2/*i*-PrOH (1 mL, 85:15) at −20 °C. Isolated yields after column chromatography. Enantioselectivity determined by chiral HPLC. [b]At 0 °C.

(as is the case for catalyst **A** in dichloromethane), mass transfer limitations are effectively overcome, so that reaction rate can approach its theoretical maximum. As far as enantioselectivity is concerned, it is well-known that the surface of metal oxide nanoparticles is covered with a layer of hydroxy groups.[15] A complete capping of these groups during the functionalization of the nanoparticles is virtually impossible. These residual OH groups might interact with the organocatalyst and/or the substrates by hydrogen bonding or by protonation, thus entailing a decrease in the enantioselectivity of the process.[16] In this respect, it is worth noting that no background reaction was observed using nonfunctionalized MNPs (alone or in the presence of TFA).

As discussed above, the most important purpose of catalyst immobilization is to facilitate recycling and reuse. In the present case, the polystyrene-based catalyst **A** could be easily recovered by filtration, while catalyst **B** was separated by simple magnetic decantation. This being secured, the robustness of catalysts **A** and **B** upon reuse was studied. Reaction between *trans*-cinnamaldehyde and *N*-methylindole was selected as a model (Table 2). For each run, equimolar amounts of TFA were added to recondition the catalysts.

Following the protocol detailed in the Supporting Information, catalysts **A** and **B** could be reused for five consecutive runs. A slight decline in catalytic activity was observed in both cases as the recycling progressed. For enantioselectivity, the reactions involving the MNP-supported catalyst exhibited a slight but continuous decrease. With the PS-based catalyst **A**, in turn, the ee recorded in the fifth run was still fully comparable with the initial one.

Possible explanations for the lower stability of **B** under the recycling conditions could be the occurrence of reversible agglomeration phenomena in the reaction media that could lead to a decrease of the effective surface area of the MNPs or the sensitivity toward trifluoroacetic acid of the silicon−oxygen

Table 2. Recycling and Reuse Experiments for Catalysts A and B

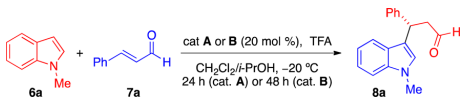

	A		B	
run	yield (%)	ee (%)	yield (%)	ee (%)
1	71	84	68	65
2	70	86	65	54
3	68	85	64	58
4	52	80	61	56
5	50	79	27	48

bonds involved in catalyst immobilization that could provoke a progressive decrease in functionalization.

In conclusion, we have developed an efficient way to support the second-generation MacMillan organocatalyst onto slightly cross-linked polystyrene (catalyst **A**) and iron oxide MNPs (catalyst **B**). The catalytic efficiency of these functional materials has been demonstrated in the enantioselective FC alkylation of indoles with α,β-unsaturated aldehydes. Both catalysts could be easily recovered and reused for five consecutive runs. When the suitability of both supports is critically assessed, the polystyrene-based catalyst proves to be much more active and selective than the magnetic iron oxide based one. It seems that the polymeric nature of the support in the PS-based catalyst might offer a beneficial microenvironment to the active sites, resulting in better reactivity and stereoselectivity compared to that of the iron oxide MNP-based catalyst. It is suggested that magnetic nanoparticles lacking excess hydroxy functionalization on their surfaces and that do not show a tendency to agglomerate, like cobalt nanoparticles coated with graphitic carbon,[17] could overcome this limitation.

■ ASSOCIATED CONTENT

Supporting Information

The Supporting Information is available free of charge on the ACS Publications website at DOI: 10.1021/acs.orglett.6b00462.

Experimental details, spectroscopic data of all compounds, and TEM images (PDF)

■ AUTHOR INFORMATION

Corresponding Author

*E-mail: mapericas@iciq.es.

Present Addresses

[§]Polymers & Functional Materials Division, CSIR-Indian Institute of Chemical Technology, Hyderabad, India 500007.
[⊥]Clean Energy Research Center, Korea Institute of Science and Technology, Hwarang-ro 14-gil, Seongbuk-gu, Seoul 02792.

Notes

The authors declare no competing financial interest.

■ ACKNOWLEDGMENTS

This work was funded by the EU-ITN network Mag(net)icFun (PITN-GA-2012-290248) and Institute of Chemical Research of Catalonia (ICIQ) Foundation. MINECO (Grant CTQ2012-38594-C02-01) and DEC Generalitat de Catalunya (Grant 2014SGR827) are gratefully acknowledged. We also thank

DOI: 10.1021/acs.orglett.6b00462
Org. Lett. 2016, 18, 1602−1605

MINECO for support through Severo Ochoa Excellence Accreditation 2014−2018 (SEV-2013- 0319).

REFERENCES

(1) Ahrendt, K. A.; Borths, C. J.; MacMillan, D. W. C. *J. Am. Chem. Soc.* **2000**, *122*, 4243.
(2) (a) Jen, W. S.; Wiener, J. J. M.; MacMillan, D. W. C. *J. Am. Chem. Soc.* **2000**, *122*, 9874. (b) Paras, N. A.; MacMillan, D. W. C. *J. Am. Chem. Soc.* **2001**, *123*, 4370.
(3) Austin, J. F.; MacMillan, D. W. C. *J. Am. Chem. Soc.* **2002**, *124*, 1172.
(4) (a) Northrup, A. B.; MacMillan, D. W. C. *J. Am. Chem. Soc.* **2002**, *124*, 2458. (b) Wilson, R. M.; Jen, W. S.; MacMillan, D. W. C. *J. Am. Chem. Soc.* **2005**, *127*, 11616.
(5) Ouellet, S. G.; Tuttle, J. B.; MacMillan, D. W. C. *J. Am. Chem. Soc.* **2005**, *127*, 32.
(6) (a) Paras, N. A.; MacMillan, D. W. C. *J. Am. Chem. Soc.* **2002**, *124*, 7894. (b) Brown, S. P.; Goodwin, N. C.; MacMillan, D. W. C. *J. Am. Chem. Soc.* **2003**, *125*, 1192.
(7) For reviews on solid-supported enantioselective organocatalysts, see: (a) Cozzi, F. *Adv. Synth. Catal.* **2006**, *348*, 1367. (b) Benaglia, M. *New J. Chem.* **2006**, *30*, 1525. (c) Gruttadauria, M.; Giacalone, F.; Noto, R. *Chem. Soc. Rev.* **2008**, *37*, 1666. (d) Kristensen, T. E.; Hansen, T. *Eur. J. Org. Chem.* **2010**, *2010*, 3179. (e) Mrówczyński, R.; Nan, A.; Liebscher, J. *RSC Adv.* **2014**, *4*, 5927. (f) Ferré, M.; Pleixats, R.; Man, M. W. C.; Cattöen, X. *Green Chem.* **2016**, *18*, 881. (g) Giacalone, F.; Gruttadauria, M. *ChemCatChem* **2016**, *8*, 664.
(8) For selected examples of polymer or MNP-supported first-generation MacMillan catalysts, see: (a) Selkälä, S. A.; Tois, J.; Pihko, P. M.; KosKinen, A. M. P. *Adv. Synth. Catal.* **2002**, *344*, 941. (b) Benaglia, M.; Celentano, G.; Cinquini, M.; Puglisi, A.; Cozzi, F. *Adv. Synth. Catal.* **2002**, *344*, 149. (c) Puglisi, A.; Benaglia, M.; Cinquini, M.; Cozzi, F.; Celentano, G. *Eur. J. Org. Chem.* **2004**, *2004*, 567. (d) Riente, P.; Yadav, J.; Pericàs, M. A. *Org. Lett.* **2012**, *14*, 3668. (e) Salvo, A. M. P.; Giacalone, F.; Noto, R.; Gruttadauria, M. *ChemPlusChem* **2014**, *79*, 857. (f) Pecchioli, T.; Muthyala, M. K.; Haag, R.; Christmann, M. *Beilstein J. Org. Chem.* **2015**, *11*, 730.
(9) For mesoporous material-supported first-generation MacMillan catalysts, see: (a) Zhang, Y.; Zhao, L.; Lee, S. S.; Ying, J. Y. *Adv. Synth. Catal.* **2006**, *348*, 2027. (b) Shi, J. Y.; Wang, C. A.; Li, Z. J.; Wang, Q.; Zhang, Y.; Wang, W. *Chem. - Eur. J.* **2011**, *17*, 6206. (c) Puglisi, A.; Benaglia, M.; Annunziata, R.; Chiroli, V.; Porta, R.; Gervasini, A. *J. Org. Chem.* **2013**, *78*, 11326.
(10) Kasaplar, P.; Rodríguez-Escrich, C.; Pericàs, M. A. *Org. Lett.* **2013**, *15*, 3498. (b) Fan, X.; Rodríguez-Escrich, C.; Sayalero, S.; Pericàs, M. A. *Chem. - Eur. J.* **2013**, *19*, 10814. (c) Henseler, A. H.; Ayats, C.; Pericàs, M. A. *Adv. Synth. Catal.* **2014**, *356*, 1795. (d) Ayats, C.; Henseler, A. H.; Dibello, E.; Pericàs, M. A. *ACS Catal.* **2014**, *4*, 3027. (e) Izquierdo, J.; Ayats, C.; Henseler, A. H.; Pericàs, M. A. *Org. Biomol. Chem.* **2015**, *13*, 4204.
(11) (a) Mak, C. A.; Ranjbar, S.; Riente, P.; Rodríguez-Escrich, C.; Pericàs, M. A. *Tetrahedron* **2014**, *70*, 6169. (b) Riente, P.; Mendoza, C.; Pericàs, M. A. *J. Mater. Chem.* **2011**, *21*, 7350.
(12) (a) Sun, S.; Zeng, H. *J. Am. Chem. Soc.* **2002**, *124*, 8204. (b) Sun, S.; Zeng, H.; Robinson, D. B.; Raoux, S.; Rice, P. M.; Wang, S. X.; Li, G. *J. Am. Chem. Soc.* **2004**, *126*, 273.
(13) For selected examples of enantioselective FC alkylation of indoles with α,β-unsaturated aldehydes, see: (a) King, H. D.; Meng, Z.; Denhart, D.; Mattson, R.; Kimura, R.; Wu, D.; Gao, Q.; Macor, J. E. *Org. Lett.* **2005**, *7*, 3437. (b) Shi, Z.-H; Sheng, H.; Yang, K.-F.; Jiang, J.-X; Lu, Y.; Xu, L.-W. *Eur. J. Org. Chem.* **2011**, *2011*, 66. (c) Liang, X.; Li, S.; Su, W. *Tetrahedron Lett.* **2012**, *53*, 289. For an example with an immobilized peptidic catalyst, see: (d) Akagawa, K.; Suzuki, R.; Kudo, K. *Adv. Synth. Catal.* **2012**, *354*, 1280.
(14) Kharisov, B. I.; Dias, H. V. R.; Kharissova, O. V.; Vázquez, A.; Peña, Y.; Gómez, I. *RSC Adv.* **2014**, *4*, 45354.
(15) McCafferty, E.; Wightman, J. P. *Surf. Interface Anal.* **1998**, *26*, 549.
(16) Gleeson, O.; Davies, G.-L.; Peschiulli, A.; Tekoriute, R.; Gun'ko, Y. K.; Connon, S. J. *Org. Biomol. Chem.* **2011**, *9*, 7929.
(17) (a) Kainz, Q. M.; Linhardt, R.; Grass, R. N.; Vilé, G.; Pérez-Ramírez, J.; Stark, W. J.; Reiser, O. *Adv. Funct. Mater.* **2014**, *24*, 2020. (b) Linhardt, R.; Kainz, Q. M.; Grass, R. N.; Stark, W. J.; Reiser, O. *RSC Adv.* **2014**, *4*, 8541. (c) Kainz, Q. M.; Zeltner, M.; Rossier, R.; Stark, W. J.; Reiser, O. *Chem. - Eur. J.* **2013**, *19*, 10038. (d) Kainz, Q. M.; Reiser, O. *Acc. Chem. Res.* **2014**, *47*, 667.

DOI: 10.1021/acs.orglett.6b00462
Org. Lett. 2016, 18, 1602−1605

3.7. Conclusions

This chapter describes the first immobilization of second-generation MacMillan imidazolidin-4-one onto magnetic nanoparticles and polystyrene. The organocatalyst was anchored onto both solid supports through a copper-catalyzed alkyne-azide cycloaddition (CuAAC) reaction. The resulting catalytic materials were applied to the asymmetric Friedel-Crafts alkylation of indoles with α,β-unsaturated aldehydes. With PS-catalyst the role of solvent and temperature was explored, afterwards with optimized condition, the asymmetric Friedel-Crafts alkylation of indoles with α,β-unsaturated aldehydes for both catalyst and the scope of the reaction were studied. To evaluate activity of catalyst for reusing, the recyclability of MNPs and polystyrene catalysts was investigate for five consecutive runs. In both catalysts a slight decline in catalytic activity was observed. In this study, the polystyrene-based catalyst showed higher stability and provided better stereoselectivities.

Supporting information

Polystyrene or Magnetic Nanoparticles as Support in Enantioselective Organocatalysis? A Case Study in Friedel-Crafts Chemistry

Sara Ranjbar,[a] Paola Riente,[a] Carles Rodríguez-Escrich,[a] Jagjit Yadav,[a] Kishore Ramineni,[a] Miquel A. Pericàs*[,a,b*]

[a] Institute of Chemical Research of Catalonia (ICIQ), The Barcelona Institute of Science of Technology, Av-da. Països Catalans, 16. 43007 Tarragona (Spain)

[b] Departament de Química Orgànica, Universitat de Barcelona. 08080 Barcelona (Spain)

Table of contents

1. General

Unless otherwise stated, all starting materials were commercially available and were used without further purification. Flash chromatography was carried out using flash grade silica gel (SDS Chromatogel 60 ACC, 40-60 µm). NMR spectra were recorded at 23 ºC on a Bruker Advance 300, 400 or Bruker Advance 500 Ultrashield apparatus for ^{1}H NMR and 75, 100 and 126 MHz for ^{13}C NMR using $CDCl_3$ as solvent (unless otherwise stated) and TMS as internal standard. Chemical shifts (δ) are reported in ppm referred to TMS and coupling constants (*J*) in Hz. High-resolution mass spectra (HRMS) were recorded on a Waters GCT gas chromatograph coupled time-of-flight mass spectrometer (GC/MS-TOF) with electron ionization (EI). ATR spectra were recorded on Bruker Optics FTIR Alpha spectrometer equipped with a DTGS detector. Elemental analyses (C; H; N) were performed in LECO CHNS 932 microanalyses at the Universidad Complutense de Madrid, Spain. Racemic standard products were prepared using 5-benzyl-2-(*tert*-butyl)-3-butylimidazolidin-4-one as catalyst in order to establish chiral HPLC conditions. Specific optical rotation measurements were carried out on a Jasco P-1030 model polarimeter equipped with a PMT detector using the Sodium line at 589 nm. TEM images were recorded using JEOL JEM 1011 microscope equipped with lanthanum hexaboride filament, operated at an acceleration voltage of 100 kV, at Microscopy Units, Universitat Rovira i Virgili, Tarragona, Spain. A drop of the magnetic nanoparticles suspension was added to a holey-carbon coated 200 mesh copper grid allowing the solvent to evaporate before being introduced into the microscope. All products that are known were characterized by comparison of their physical and spectroscopic properties with those described in the literature.

2. Synthesis of (2*S*,5*S*)-2-(*tert*-butyl)-3-butyl-5-(4-(prop-2-yn-1-yloxy)benzyl)imidazo-lidin-4-one (5)

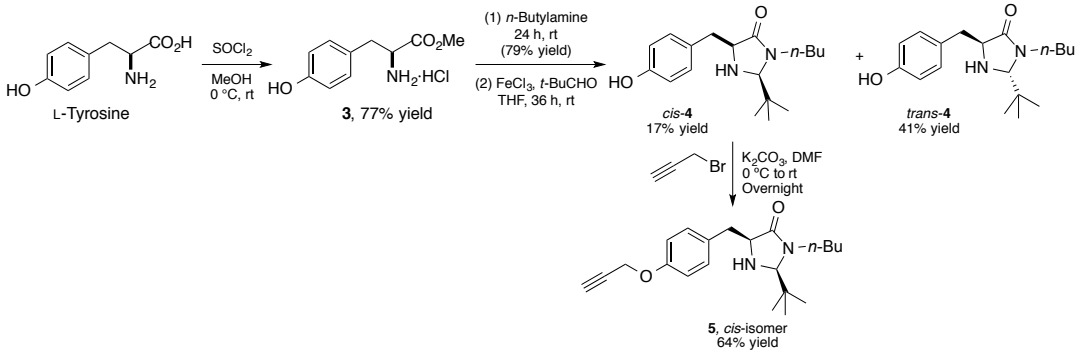

2.1. (*S*)-Tyrosine methyl ester hydrochloride (3).[1]

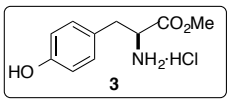

A solution of (*S*)-Tyrosine (50.0 g, 276.2 mmol) in dry methanol (500 mL) under argon atmosphere was cooled to 0 °C and thionyl chloride (50.8 mL, 699 mmol) was added dropwise through an addition funnel. After the addition was complete, the cooling bath was removed and stirring was continued at room temperature overnight. The reaction mixture was concentrated under vacuum and the solid residue was stirred with acetone (2 x 250 mL) for one hour. Then it was concentrated in vacuum, and the process was repeated (dissolve in acetone, stir for 1 h and evaporate). The solid was filtered off and washed with acetone (3 x 100 mL). The separated solid was dried under vacuum to afford (*S*)-tyrosine methyl ester hydrochloride (**3**) as a white solid (52.3 g, 77% yield).

^{1}H NMR (300 MHz, d_6-DMSO): δ 9.45 (br s, 1H), 8.54 (br s, 3H), 7.00 (d, *J* = 8.2 Hz, 2H), 6.71 (d, 2H, *J* = 8.2), 4.20–4.12 (br t, *J* = 6.44 Hz, 1H), 3.66 (s, 3H), 3.05 (dd, *J* = 14.2, 5.9 Hz, 1H), 2.98 (dd, *J* = 14.2, 7.0 Hz, 1H). **^{13}C NMR** (75 MHz, d_6-DMSO): δ 169.5, 156.7, 130.4 (×2), 124.4, 115.5 (×2), 53.5, 52.6, 35.2.

2.2. (2*S*,5*S*)-2-(*tert*-Butyl)-3-butyl-5-(4-hydroxybenzyl)imidazolidin-4-one (*cis*-4).

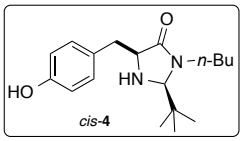

(*S*)-Tyrosine methyl ester hydrochloride (**3**) (18 g, 77.7 mmol) was treated with *n*-butylamine (60 mL, 608 mmol) and the resulting mixture was stirred at room temperature for 24 hours. The excess *n*-butylamine was removed by concentration in vacuo, washing with THF and concentrating again several times until the *N*-butyl amide product was obtained as a white solid. This was dried under vacuum overnight (17.5 g, 79% yield) and the product was directly used for the next step without further purification.

[1] Riente, P.; Yadav, J.; Pericàs, M. A. *Org. Lett*. **2012**, *14*, 3668.

The crude (*S*)-2-amino-*N*-butyl-3-(4-hydroxyphenyl)propanamide (3.6 g, 13.0 mmol), 5 g of activated 4 Å MS and anhydrous $FeCl_3$ (0.5 g, 2.6 mmol) were suspended in dry THF (30 mL) under argon atmosphere. Then, pivalaldehyde (1.8 mL, 14.3 mmol) was added and the reaction mixture was stirred at room temperature for 36 hours. After the starting material was consumed, 20 mL of H_2O were added. Then, the reaction mixture was filtered off and the solid residue was washed with CH_2Cl_2 (3 × 100 ml). The filtrate was transferred to a 500 mL extraction funnel and the aqueous layer was separated. The organic phase was washed with 50 mL of H_2O and it was dried over $MgSO_4$. The solvent was evaporated under reduced pressure and the residue was purified by silica gel chromatography (cyclohexane/EtOAc 60:40) to furnish *cis*-**4** as a yellow oil (670 mg, 17% yield).

^{1}H NMR (500 MHz, $CDCl_3$): δ 7.07 (d, *J* = 8.3 Hz, 2H), 6.72 (d, *J* = 8.3 Hz, 2H), 4.24 (d, *J* = 1.5 Hz, 1H), 3.78 (ddd, *J* = 7.0, 9.5, 14.0 Hz, 1H), 3.64 (ddd, *J* = 1.5, 4.3, 6.1 Hz, 1H), 2.99–3.12 (m, 2H), 2.92 (dd, *J* = 6.9, 14.0 Hz, 1H), 1.64–1.76 (br s, 1H), 1.53–1.63 (m, 1H), 1.43–1.50 (m, 1H), 1.21–1.35 (m, 2H), 0.92 (t, *J* = 7.4 Hz, 3H), 0.84 (s, 9H).

^{13}C NMR (126 MHz, $CDCl_3$): δ 175.8, 155.3, 130.7 (×2), 128.4, 115.7 (×2), 79.7, 59.4, 42.4, 36.6, 35.1, 29.0, 25.5 (×3), 20.0, 13.7.

HRMS (ESI+): calculated for $C_{18}H_{29}N_2O_2$ $[M+H]^+$: 305.2224, found 305.2214.

IR (ATR): ν 3288, 2965, 2931, 2893, 1665, 1614, 1594, 1515, 1445, 1365, 1310, 1239, 1171, 1108, 933, 894, 824, 722, 618, 528, 432 cm^{-1}.

2.3. (2*S*,5*R*)-2-(*tert*-Butyl)-3-butyl-5-(4-(prop-2-yn-1-yloxy)benzyl)imidazolidin-4-one (5).

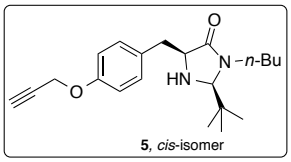

5, *cis*-isomer

(2*S*,5*S*)-2-(*tert*-Butyl)-3-butyl-5-(4-hydroxybenzyl)imidazoli-din-4-one (*cis*-**4**) (970 mg, 3.18 mmol) was added to a suspension of K_2CO_3 (1.3 g, 9.5 mmol) and propargyl bromide (80% w/w solution in toluene, 3.8 mmol, 0.6 mL) in dry DMF (20 mL) at 0 °C under argon atmosphere. The resulting mixture was stirred at room temperature overnight. After complete consumption of the starting material, 50 mL of sat. aq. NH_4Cl were added to the reaction mixture. Then, 100 mL of EtOAc were added and the mixture was stirred for 30 minutes. The organic layer was separated and the aqueous layer was again extracted with ethyl acetate (50 mL). The combined organic layers dried over Na_2SO_4. The solvent was evaporated under reduced pressure and the residue was purified by silica gel chromatography (cyclohexane/EtOAc 60:40) to obtain **5** as yellow oil (890 mg, 2.6 mmol, 82% yield).

^{1}H NMR (500 MHz, $CDCl_3$): δ 7.18 (d, *J* = 8.6 Hz, 2H), 6.90 (d, *J* = 8.6 Hz, 2H), 4.65 (d, *J* = 2.4 Hz, 2H), 4.21 (d, *J* = 1.5 Hz, 1H), 3.78 (ddd, *J* = 7.1, 9.6, 14.0 Hz, 1H), 3.64 (ddd, *J* = 1.5, 4.0, 7.4 Hz, 1H), 3.00–3.12 (m, 2H), 2.89 (dd, *J* = 7.4, 14.0 Hz, 1H), 2.48 (t, *J* = 2.4 Hz, 1H), 1.66–1.78 (br s, 1H), 1.52–1.63 (m, 1H), 1.40–1.51 (m, 1H), 1.25–1.34 (m, 2H), 0.93 (t, *J* = 7.4 Hz, 3H), 0.84 (s, 9H).

^{13}C NMR (126 MHz, $CDCl_3$): δ 175.3, 156.4, 131.0, 130.6 (×2), 115.1 (×2), 79.6, 78.7, 75.3, 59.4, 55.9, 42.3, 37.2, 35.3, 29.0, 25.5 (×3), 20.1, 13.7.

HRMS (ESI+): calculated for $C_{21}H_{31}N_2O_2$ $[M+H]^+$: 343.2380 found 343.2379.

IR (ATR): ν 3307, 2965. 2931, 2861, 1687, 1610, 1580, 1510, 1476, 1433, 1392, 1339, 1307, 1295, 1233, 1179, 1120, 1029, 963, 935, 896, 824, 804, 788, 734, 662, 635, 617, 585, 557, 521, 497, 428 cm^{-1}.

3. Synthesis of the polystyrene-based catalyst (catalyst A)

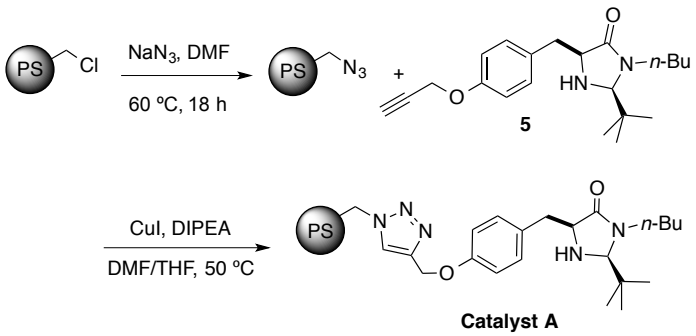

3.1. Preparation of azidomethylpolystyrene

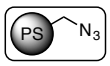

To a suspension of Merrifield resin (100-200 mesh, Novabiochem, $f \approx 0.5$ mmol g^{-1}, 4.0 g, 2 mmol) in dry DMF (40 mL) was added sodium azide (1.3 g, 20 mmol). The mixture was shaken (orbital shaker) at 60 °C overnight, cooled to room temperature and filtered. The resin was washed successively with 100 mL volumes of H_2O, a 1:1 mixture of H_2O/MeOH, MeOH, a 1:1 mixture of THF/MeOH, THF, and DCM, and dried under vacuum at 40 °C for 48 h. The functionalization was calculated on the basis of nitrogen elemental analysis. Found (%): N: 2.27, H: 7.47, C: 89.74; $f = 0.54$ mmol·g^{-1}.

IR (ATR): ν 3024, 2919, 2844, 2096, 1597, 1492, 1451, 1068, 1026, 905, 841, 745, 699, 540 cm^{-1}.

3.2. Supporting the alkyne-functionalized imidazolidin-4-one through click chemistry (catalyst A).

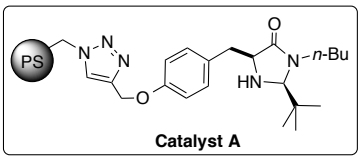

To a suspension of azidomethylpolystyrene ($f \approx 0.48$ mmol g^{-1}, 600 mg, 0.32 mmol) in a mixture of 10 mL of dry THF/DMF (1:1) was added (2*S*,5*S*)-2-(*tert*-butyl)-3-butyl-5-(4-(prop-2-yn-1-yloxy)benzyl)imidazolidin-4-one (**5**) (0.13 g, 0.39 mmol) DIPEA (0.75 mL, 4.2 mmol) and CuI (12.4 mg, 0.06 mmol). The mixture was shaken (orbital shaker) at 40 °C for 15 h. The completion of the reaction was judged by the absence of the characteristic azide peak in the IR (around 2100 cm^{-1}). Then, the reaction mixture was allowed to cool to room temperature, filtered and the solid was washed with 500 mL of H_2O and 500 mL MeOH. In order to remove the remaining CuI, the resin was taken in a 100-mL round bottom flask and 30 mL of THF and 1 mL of ethylenediamine were added. The mixture was shaken (orbital shaker) at room temperature for 20 min and then it was filtered off and washed with 50 mL of THF and 50 mL of MeOH. These steps were repeated for two more times. Finally, the solid was washed with 500 mL volumes of H_2O, a 1:1 mixture of H_2O/MeOH, MeOH, a 1:1 mixture of THF/MeOH, THF, and DCM and dried under vacuum at 40 °C. The functionalization was calculated on the basis of nitrogen elemental analysis. Found (%): N 3.39, H 7.57, C 84.96; $f = 0.48$ mmol g^{-1}.

IR (ATR): ν 3304, 2965, 2927, 2860, 1685, 1609, 1576, 1505, 1434, 1392, 1342, 1228, 1173, 1115, 1026, 897, 825, 737, 616, 578, 514 cm^{-1}.

NOTE: different batches of catalyst **A** gave varying functionalization levels. The exact functionalization of the catalyst used in each example will be indicated in the experimental procedure.

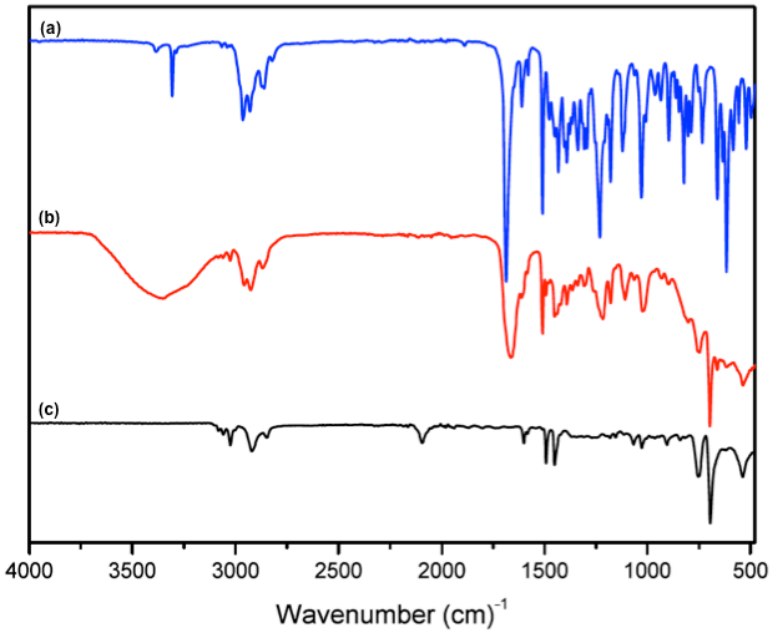

IR spectrum of (a) second generation imidazolidin-4-one derivative (**5**), (b) second generation imidazolidin-4-one derivative supported onto PS (catalyst **A**) and (c) azide-functionalized PS (PS-N_3).

4. Synthesis of magnetic nanoparticles-based catalyst (catalyst B)

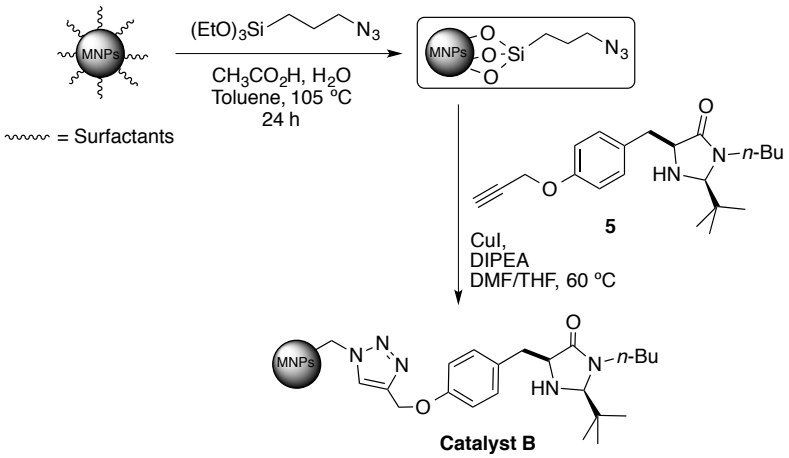

4.1. Synthesis of azido functionalized magnetic nanoparticles[1,2]

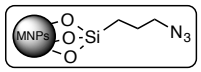

To a suspension of as-prepared MNPs[2] (5.7±1.3 nm, 1.2 g) in degassed dry toluene (20 mL), under argon, was added 3-(azidopropyl)triethoxysilane[3] (1.0 g, 4.04 mmol), glacial acetic acid (108 µL, 1.9 mmol) and ultrapure water (136 µL, 7.6 mmol). The reaction mixture was stirred at 105 °C for 24 h and then cooled to room temperature. The resultant MNPs were collected using an external magnetic field (neodymium magnet), washed several times with methanol, hexane, acetone and dried under vacuum overnight at 40 °C. The functionalization was calculated on the basis of nitrogen elemental analysis. Found (%): N 3.03, H 1.36, C 6.97, S 0.05; f = 0.72 mmol g^{-1}.

IR (ATR): ν 2924, 2851, 2093, 1703, 1524, 1425, 1360, 1214, 1026 cm^{-1}.

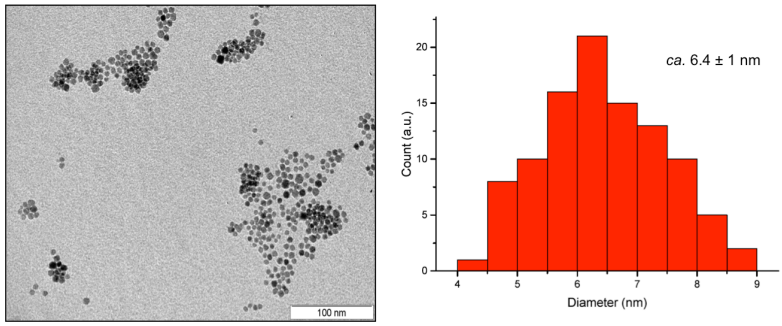

Micrograph (left) and size distribution (right) of azide-functionalized MNPs obtained by TEM. The sizes were determined for 101 azide-functionalized MNPs selected at random.

[2] Riente, P.; Mendoza, C.; Pericàs, M. A. *J. Mater. Chem*. **2011**, *21*, 7350.
[3] Zhang, Q.; Su, H.; Luo, J.; Wei, Y. *Catal. Sci. Technol*. **2013**, *3*, 235.

4.2. Supporting the alkyne-functionalized imidazolidin-4-one onto MNPs through CuAAC (catalyst B)

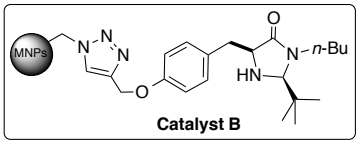

Catalyst B

To a solution of ((2*S*,5*S*)-2-(*tert*-butyl)-3-butyl-5-(4-(prop-2-yn-1-yloxy)benzyl)imidazolidin-4-one (**5**) (192 mg, 0.56 mmol) in dry DMF/THF (1:1), (40 ml) was added azide-functionalized MNPs (*f* = 0.72 mmol g^{-1}, 694 mg, 0.50 mmol), CuI (16 mg, 0.084 mmol) and DIPEA (0.7 mL, 5.46 mmol), under argon. The mixture was stirred at 50 °C for 48 h. The reaction was monitored by IR (ATR) until the disappearance of the azide band at *ca*. 2100 cm^{-1}. The functionalized MNPs were removed using an external magnetic field (neodymium magnet), washed several times with methanol and acetone and dried under vacuum overnight at 40 °C. The functionalization was calculated on the basis of nitrogen elemental analysis. Found (%): N 3.53, H 2.35, C 16.32, S 0.04; *f* = 0.50 mmol g^{-1}.

IR (ATR): ν 1006, 1110, 1173, 1236, 1311, 1420, 1505, 1596, 1665, 2859, 2919 cm^{-1}.

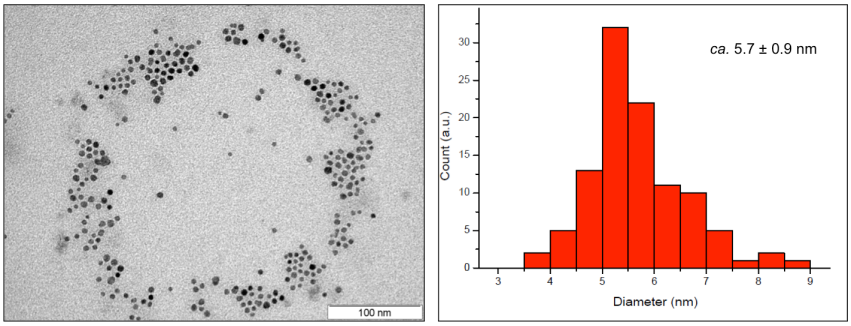

Micrograph (left) and size distribution (right), obtained by TEM, for alkyne-functionalized imidazolidin-4-one onto MNPs. The sizes were determined for 104 functionalized MNPs selected at random.

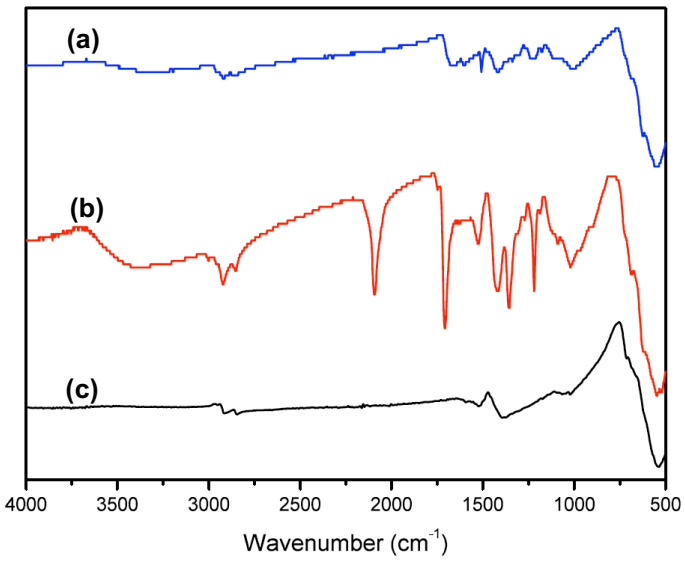

IR spectrum of (a) second generation imidazolidin-4-one derivative supported onto MNPs, (b) azide-functionalized MNPs and (c) MNPs.

S9

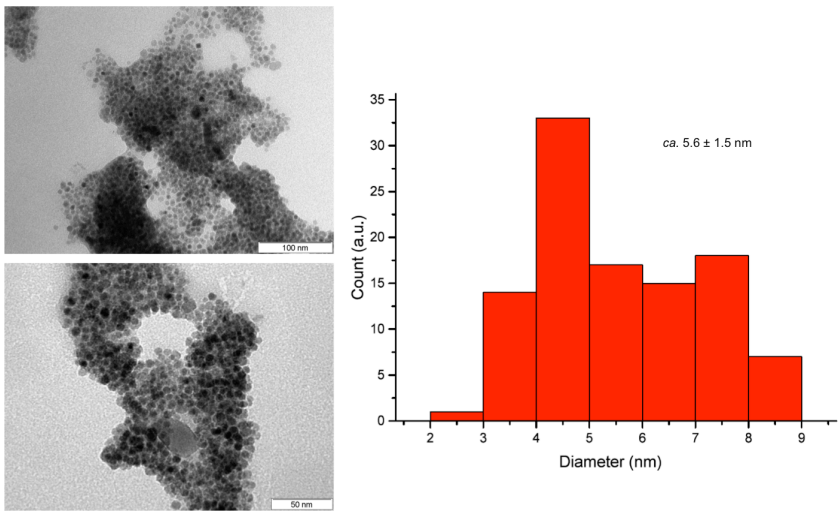

Micrographs (left) and size distribution (right), obtained by TEM, for alkyne-functionalized imidazolidin-4-one onto MNPs after the fifth run. The sizes were determined for 106 functionalized MNPs selected at random.

5. General experimental procedures

5.1. General procedure for the Friedel-Crafts alkylation of indoles with α,β-unsaturated aldehydes

A vial with a magnetic stir bar containing catalyst **A** or **B** (20 mol%) was charged with 1 mL of a CH_2Cl_2/isopropanol mixture (85:15) and pure TFA (1.54 µl, 20 mol%) and was stirred for 10 minutes at room temperature under nitrogen. Then the vial was placed in a bath at the indicated temperature and the solution was stirred for a further 10 minutes. After that, the α,β-unsaturated aldehyde (3 equiv.) was added and it was stirred for 5 minutes before the indole substrate (1 equiv.) was added. The reaction was monitored by TLC until the indole was consumed. The MNPs-supported catalyst was removed by magnetic decantation whereas the polystyrene supported one was removed by filtration. The catalytic materials were washed several times with CH_2Cl_2. After that, water was added to the liquid mixture obtained, in both cases, and the organic phase was extracted three times with CH_2Cl_2 and washed with brine. After concentration the crude reaction was purified by silica gel chromatography (cyclohexane/EtOAc mixture).

5.2. General procedure for recycling experiments

A suspension of the catalyst **A** or **B** (20 mol%) in 1 mL of a CH_2Cl_2/isopropanol mixture (85: 15) and pure TFA (1.54 µl, 20 mol%) and was stirred for 10 minutes at room temperature under nitrogen. Then, the vial was placed in a bath at the indicated temperature and the solution was stirred for a further 10 minutes. After that, the α,β-unsaturated aldehyde (3 equiv.) was added and it was stirred 5 minutes before the indole substrate (1 equiv.) was added. The reaction was monitored by TLC until the indole was consumed. The MNP-supported catalyst was removed by magnetic decantation whereas the polystyrene-supported one was removed by filtration. Both catalysts were washed several times with EtOAc before the next portion of reactants was added.

6. Characterization data for the Friedel-Crafts alkylation products

(*S*)-3-(1-Methyl-1*H*-indol-3-yl)-3-phenylpropanal (8a)[4]

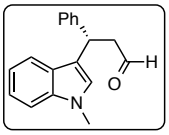

Prepared according to the general procedure from *trans*-cinnamaldehyde (103 µL, 0.90 mmol), 1-methyl-1*H*-indole (39 µL, 0.30 mmol), TFA (4.60 µL, 0.06 mmol), catalyst **A** (*f* = 0.48 mmol/g, 125 mg, 20 mol%, 0.06 mmol) in CH_2Cl_2 (2.55 mL) and isopropanol (0.45 mL) at −20 °C for 24 h. The title compound was isolated after silica gel chromatography (cyclohexane/EtOAc 95:5 to 70:30) in 71% yield (56.8 mg, 0.21 mmol) and 84% ee.

^{1}H NMR (500 MHz, $CDCl_3$): δ 9.78 (t, *J* = 1.8, 2.7 Hz, 1H), 7.39 (dt, *J* = 0.9, 8.1 Hz, 1H), 7.21–7.35 (m, 5H), 7.14–7.22 (m, 2H), 7.02 (ddd, *J* = 1.0, 6.9, 8.0 Hz, 1H), 6.8 (d, *J* = 0.9 Hz, 1H), 4.7 (t, *J* = 7.7 Hz, 1H), 3.74 (s, 3H), 3.19 (ddd, *J* = 2.7, 8.3, 16.5 Hz, 1H), 3.08 (ddd, *J* = 1.8, 7.2, 16.5 Hz, 1H).

^{13}C NMR (126 MHz, $CDCl_3$): δ 202.1, 143.7, 137.5, 128.8 (×2), 127.8 (×2), 127.0, 126.7, 126.5, 122.1, 119.5, 119.2, 116.8, 109.4, 50.0, 37.4, 32.9.

HPLC (after reduction to the corresponding alcohol with $NaBH_4$ in MeOH): Chiralcel AS-H column (hexane/*i*-PrOH 90:10, flow rate 1.0 ml/min, 254 nm); t_r = 11.8 min (minor), t_r = 14.3 min (major).

(*S*)-3-(1-Methyl-1*H*-indol-3-yl)-3-(4-nitrophenyl)propanal (8b).

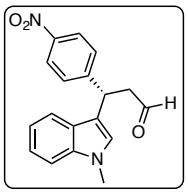

Prepared according to the general procedure from 4-nitrocinnamaldehyde (163 ml, 0.9 mmol), 1-methyl-1H-indole (39 µL, 0.30 mmol), TFA (4.6 µL, 0.06 mmol) and catalyst **A** (*f* = 0.44 mmol/g, 136 mg, 0.06 mmol) in CH_2Cl_2 (2.55 mL) and isopropanol (0.45 mL) at −20 °C for 24 h The title compound was isolated after silica gel chromatography (cyclohexane/EtOAc 95:5 to 70:30) in 66% yield (60.7 mg, 0.21 mmol) and 93% ee.

^{1}H NMR (500 MHz, $CDCl_3$): δ 9.78 (dd, *J* = 1.4, 2.2 Hz, 1H), 8.12–8.15 (m, 2H), 7.5–7.6 (m, 2H), 7.30 (ddt, *J* = 1.0, 2.2, 8.5 Hz, 2H), 7.22 (ddd, *J* = 1.1, 6.7, 8.3 Hz, 1H), 7.03 (ddd, *J* = 1.0, 7.0, 8.0 Hz, 1H), 6.90 (d, *J* = 0.8 Hz, 1H), 4.98 (t, *J* = 7.6 Hz, 1H), 3.78 (s, 3H), 3.28 (ddd, *J* = 2.2, 8.0, 17.0 Hz, 1H), 3.15 (ddd, *J* = 1.4, 7.2, 17.0 Hz, 1H).

^{13}C NMR (126 MHz, $CDCl_3$): δ 200.2, 151.4, 146.7, 137.4, 128.6 (×2), 126.4 (×2), 123.9 (×2), 122.3, 119.4, 119.0, 115.1, 109.6, 49.6, 37.0, 33.0.

IR (ATR): 3055, 2931, 2825, 2727, 1719, 1595, 1512, 1473, 1341, 1244, 1156, 1109, 1079, 1047, 1012, 907, 857, 825, 739, 700, 553, 427 cm^{-1}.

[4] Austin, J. F.; MacMillan, D. W. C. *J. Am. Chem. Soc*. **2002**, *124*, 1172.

HRMS (ESI+): calculated for $C_{18}H_{16}N_2NaO_3$ $[M+Na]^+$: 331.1053, found 331.1055.

$[\alpha]_D$ = +27.8 (*c* 0.79, CH_2Cl_2).

HPLC (after reduction to the corresponding alcohol with $NaBH_4$ in MeOH): Chiralcel AD-H column (hexane/*i*-PrOH 90:10, flow rate 1.0 ml/min, 210 nm); t_r = 27.6 min (minor), t_r = 37.6 min (major).

(*S*)-3-(4-Chlorophenyl)-3-(1-methyl-1*H*-indol-3-yl)propanal (8c).

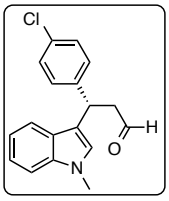

Prepared according to the general procedure from 4-chlorocinnamaldehyde (156 mg, 0.9 mmol), 1-methyl-1H-indole (40 µL, 0.30 mmol), TFA (4.6 µL, 0.06 mmol) and catalyst **A** (*f* = 0.44 mmol/g, 136 mg, 20 mol%, 0.06 mmol) in CH_2Cl_2 (2.55 mL) and isopropanol (0.45 mL) at −20 °C for 24 h The title compound was isolated after silica gel chromatography (cyclohexane/EtOAc 95:5 to 70:30) in 73% yield (64.7 mg, 0.21 mmol) and 88% ee.

^{1}H NMR (500 MHz, $CDCl_3$): δ 9.76 (dd, *J* = 1.7, 2.6 Hz, 1H), 7.33–7.40 (m, 1H), 7.30 (dt, *J* = 1.0, 8.3 Hz, 1H), 7.19–7.28 (m, 5H), 7.05 (ddt, *J* = 1.1, 7.0, 8.1 Hz, 1H), 6.87 (d, *J* = 1.1, 1H), 4.86 (t, *J* = 7.6 Hz, 1H), 3.77 (s, 3H), 3.21 (ddd, *J* = 2.6, 8.1, 16.7 Hz, 1H), 3.08 (ddd, *J* = 1.7, 7.3, 16.7 Hz, 1H).

^{13}C NMR (126 MHz, $CDCl_3$): δ 201.3, 142.1, 137.4, 132.2, 129.0 (×2), 128.7 (×2), 126.6, 126.4, 122.1, 119.3, 119.3, 116.1, 109.4, 49.8, 36.6, 32.8.

IR (ATR): 3055, 2930, 2276, 1720, 1613, 1489, 1471, 1373, 1329, 1244, 1155, 1090, 1013, 906, 816, 727, 648, 427 cm^{-1}.

HRMS (ESI+): Calculated for $C_{18}H_{16}ClNNaO$ $[M+Na]^+$: 320.0813, found 320.0806

HPLC (after reduction to the corresponding alcohol with $NaBH_4$ in MeOH): Chiralcel AS-H column (hexane/*i*-PrOH 95:5, flow rate 1.0 ml/min, 215 nm); t_r = 31.3 (minor), t_r = 47.5 min (major).

$[\alpha]_D$ = +12.8 (*c* 0.48, $CHCl_3$)

(*R*)-3-(1-Methyl-1*H*-indol-3-yl)-pentanal (8d).

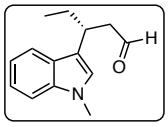

Prepared according to the general procedure from *trans*-2-pentenal (31 µL, 0.30 mmol), 1-methyl-1H-indole (13 µL, 0.1 mmol), TFA (1.50 µL, 0.02 mmol) and catalyst **A** (*f* = 0.39 mmol/g, 51 mg, 20 mol%, 0.02 mmol) in CH_2Cl_2 (0.85 mL) and isopropanol (0.15 mL) at −20 °C for 24 h. The title compound was isolated after silica gel chromatography (cyclohexane/EtOAc 95:5 to 70:30) in 79% yield (17.1 mg, 0.079 mmol) and 80 % ee.

^{1}H NMR (500 MHz, $CDCl_3$): δ 9.69 (t, *J* = 2.4 Hz, 1H), 7.63 (d, *J* = 8.0 Hz, 1H), 7.29–7.31 (m, 1 H), 7.23 (ddd, *J* = 1.1, 7.0, 8.1 Hz, 1H), 7.10–7.13 (m, 1 H), 6.84 (s, 1H), 3.75 (s, 3H), 3.41–3.47 (m, 1H), 2.83 (ddd, *J* = 2.4, 8.1, 16.0, 1H), 2.78 (ddd, *J* = 2.4, 6.3, 16.0, 1H), 1.74–1.88 (m, 2H), 0.90 (t, *J* = 7.4, 3H).

^{13}C NMR (126 MHz, $CDCl_3$): δ 203.2, 137.4, 127.1, 126.2, 121.8, 119.3, 118.9, 116.9, 109.5, 49.3, 33.2, 32.8, 29.0, 12.1.

IR (ATR): ν 3051, 2960, 2928, 2873, 2245, 1719, 1612, 1467, 1423, 1373, 1326, 1130, 1012, 908, 732, 647, 427 cm^{-1}.

HRMS (ESI+): calculated for $C_{14}H_{17}NNaO$ $[M+Na]^+$: 238.1202 found 238.1192.

$[\alpha]_D$ = −19.45 (*c* 0.63, CH_2Cl_2).

HPLC (after reduction to the corresponding alcohol with $NaBH_4$ in MeOH): Chiralcel AS-H column (hexane/*i*-PrOH 90:10, flow rate 1.0 ml/min, 230 nm); t_r = 12.4 min (minor), t_r = 16.0 min (major).

(*R*)-3-(1-Methyl-1*H*-indol-3-yl)-hexanal (8e)[4]

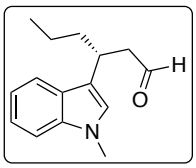

Prepared according to the general procedure from *trans*-2-hexenal (109 µL, 0.9 mmol), 1-methyl-1H-indole (39 µL, 0.30 mmol), TFA (4.6 µL, 0.06 mmol) and catalyst **A** (*f* = 0.44 mmol/g, 136 mg, 0.06 mmol) in CH_2Cl_2 (2.55 mL) and isopropanol (0.45 mL) at −20 °C for 24 h. The title compound was isolated after silica gel chromatography (cyclohexane/EtOAc 95:5 to 70:30), in 64% yield (44.40 mg, 0.19 mmol) and 82% ee.

^{1}H NMR (500 MHz, $CDCl_3$): δ 9.68 (t, *J* = 2.8 Hz, 1H), 7.63 (dt, *J* = 0.9, 8.0 Hz, 1H), 7.29 (dt, *J* = 1.0, 8.2 Hz, 1H), 7.23 (ddd, *J* = 1.1, 7.0, 8.1 Hz, 1H), 7.11 (ddd, *J* = 1.1, 7.0, 8.0 Hz, 1H), 6.83 (s, 1H), 3.74 (s, 3H), 3.48–3.54 (m, 1H), 2.82 (ddd, *J* = 2.8, 8.2, 16.2 Hz, 1H), 2.76 (ddd, *J* = 2.8, 7.0, 16.2 Hz, 1H), 1.76–1.84 (m, 1H), 1.66-1.74 (m, 1H), 1.27-1.34 (m, 2H), 0.88 (t, *J* = 7.3 Hz, 3H).

^{13}C NMR (126 MHz, $CDCl_3$): δ 203.3, 137.5, 127.2, 126.2, 121.9, 119.4, 119.0, 117.3, 109.6, 49.9, 38.6, 32.9, 31.5, 20.9, 14.3.

IR (ATR): ν 2954, 2928, 2870, 2720, 1720, 1613, 1547, 1466, 1423, 1374, 1326, 1243, 1132, 1047, 1013, 804, 736, 559, 427 cm^{-1}.

HRMS (ESI+): calculated for $C_{15}H_{19}NaNO$ $[M+Na]^+$: 252.1359 found 252.1362.

HPLC (after reduction to the corresponding alcohol with $NaBH_4$ in MeOH): Chiracel AS-H column (hexane/i-PrOH 90:10, flow rate 1.0 ml/min, 216 nm); S isomer tr = 17.2 min (minor), R isomer tr = 24.8 min (major), 82% ee.

$[\alpha]^D$ = –65.0 (*c* 0.86, CH_2Cl_2).

(*S*)-3-(1-Methyl-1*H*-indol-3-yl)-nitrocinnamaldehyde (8f).

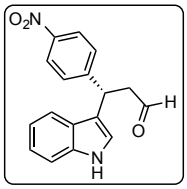

Prepared according to the general procedure from 4-nitrocinnamaldehyde (18.0 mg, 0.1 mmol), indole (14.2 mg, 0.12 mmol), TFA (1.5 µL, 0.02 mmol) and catalyst **A** (*f* = 0.25 mmol/g, 80 mg, 0.02 mmol) in CH_2Cl_2 (0.85 mL) and isopropanol (0.15 mL) at –20 °C for 24 h. The title compound was isolated after silica gel chromatography (cyclohexane/EtOAc 95:5 to 70:30) in 72% yield (21.4 mg, 0.072 mmol) and 89% ee.

^{1}H NMR (500 MHz, $CDCl_3$): δ 9.71 (dd, *J* = 1.4, 2.2 Hz, 1H), 8.12–8.18 (m, 3H), 7.46–7.49 (m, 2H), 7.37 (dt, *J* = 0.9, 8.2 Hz, 1H), 7.31 (dd, *J* = 1.0, 8.0 Hz, 1H), 7.19 (ddd, *J* = 1.1, 7.1, 8.2 Hz, 1H), 7.08 (dd, *J* = 1.0, 2.5 Hz,

1H), 7.04 (ddd, *J* = 1.0, 7.1, 8.0 Hz, 1H), 4.99 (t, *J* = 7.6 Hz, 1H), 3.30 (ddd, *J* = 2.2, 7.8, 17.1 Hz, 1H), 3.16 (ddd, *J* = 1.4, 7.3, 17.1 Hz, 1H).

^{13}C NMR (126 MHz, $CDCl_3$): δ 200.2, 151.2, 146.7, 136.6, 128.6 (×2), 126.0, 123.9 (×2), 122.8, 121.7, 119.9, 118.9, 116.7, 111.4, 49.3, 36.8.

IR (ATR): 3411, 2929, 2852, 2252, 1719, 1664, 1596, 1514, 1458, 1417, 1343, 1180, 1107, 1013, 906, 856, 729, 648, 582, 425, 317 cm^{-1}.

HRMS (ESI+): calculated for $C_{17}H_{13}N_2O_3$ $[M]^-$: 293.0932 found 293.0936.

$[\alpha]_D$ = +35.9 (*c* 1.00, CH_2Cl_2).

HPLC (after reduction to the corresponding alcohol with $NaBH_4$ in MeOH): Chiralcel AD-H column (hexane/*i*-PrOH 85:15, flow rate 1.0 ml/min, 254 nm); t_r = 26.6 (minor), t_r = 34.1 min (major).

(*S*)-3-(1*H*-Indol-3-yl-6-bromo)-3-phenyl-propanal (8g).

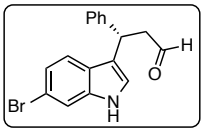

Prepared according to the general procedure from cinnamaldehyde (38 µL, 0.3 mmol), 6-bromoindole (20.4 mg, 0.30 mmol), TFA (1.5 µL, 0.02 mmol) and catalyst **A** (*f* = 0.44 mmol/g, 136 mg, 20 mol%, 0.06 mmol) in CH_2Cl_2 (2.55 mL) and isopropanol (0.45 mL) at 0 °C for 24 h. The title compound was isolated after silica gel chromatography (cyclohexane/EtOAc 95:5 to 70:30) in 66% yield (21.6 mg, 0.066 mmol) and 70% ee.

^{1}H NMR (500 MHz, $CDCl_3$): δ 9.76 (dd, *J* = 1.8, 2.6 Hz, 1H), 8.03 (s, 1H), 7.49 (d, *J* = 1.7 Hz, 1H), 7.26–7.30 (m, 4H), 7.18–7.22 (m, 2H), 7.11 (dd, *J* = 1.7, 8.5 Hz, 1H), 7.01 (dd, *J* = 0.9, 2.5 Hz, 1H), 4.82 (dd, *J* = 7.1, 8.1 Hz, 1H), 3.18 (ddd, *J* = 2.6, 8.1, 16.5 Hz, 1H), 3.10 (ddd, *J* = 1.8, 7.1, 16.5 Hz, 1H).

^{13}C NMR (126 MHz, $CDCl_3$): δ 201.4, 143.0, 137.4, 128.7 (×2), 127.6 (×2), 126.8, 125.4, 122.9, 122.1, 120.6, 118.5, 116.0, 114.1, 49.8, 37.0.

IR (ATR): 3063, 3028, 2927, 2855, 2249, 1711, 1601, 1480, 1452, 1177, 1052, 906, 845, 802, 729, 700, 648, 423 cm^{-1}.

HRMS (ESI−): calculated for $C_{17}H_{13}BrNO$ $[M-H]^-$: 326.0186 found 326.0178.

$[\alpha]_D$ = +67.6 (*c* 0.89, CH_2Cl_2).

HPLC (after reduction to the corresponding alcohol with $NaBH_4$ in MeOH): Chiralcel IC column (hexane/*i*-PrOH 95:5, flow rate 1.0 ml/min, 254 nm); t_r = 25.3 (major), t_r = 37.0 min (minor).

(*S*)-3-(1*H*-indol-3-yl-6-chloro)-3-phenyl-propanal (8h).

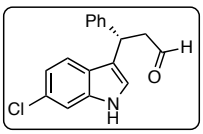

Prepared according to the general procedure from cinnamaldehyde (113 µL, 0.9 mmol), 6-chloroindole (46 µL, 0.30 mmol), TFA (4.6 µL, 0.06 mmol) and catalyst **A** (*f* = 0.44 mmol/g, 136 mg, 20 mol%, 0.06 mmol) in CH_2Cl_2 (2.55 mL) and isopropanol (0.45 mL) at 0 °C for 24 h. The title compound was isolated after silica gel chromatography (cyclohexane/EtOAc 95:5 to 70:30) in 66% yield (56 mg, 0.20 mmol) and 75% ee.

^{1}H NMR (500 MHz, $CDCl_3$): δ 9.75 (dd, *J* = 1.8, 2.7 Hz, 1H), 8.05 (br s, 1H), 7.31 (d, *J* = 1.8 Hz, 1H), 7.17-7.29 (m, 6H), 7.00 (dd, *J* = 1.0, 2.5 Hz, 1H), 6.96 (dd, *J* = 1.8, 8.5 Hz, 1H), 4.81 (ddd, *J* = 1.0, 7.1, 8.2 Hz, 1H), 3.17 (ddd, *J* = 2.7, 8.2, 16.6 Hz, 1H), 3.08 (ddd, *J* = 1.8, 7.1, 16.6 Hz, 1H).

^{13}C NMR (126 MHz, $CDCl_3$): δ 201.5, 143.1, 136.9, 128.7 (×2), 128.4, 127.6 (×2), 126.8, 125.1, 122.2, 120.3, 120.2, 118.4, 111.1, 49.8, 37.1

IR (ATR): 2982, 2929, 1721, 1603, 1544, 1433, 1373, 1241, 1043, 907, 846, 802, 751, 701, 634, 606, 426 cm^{-1}.

HRMS (ESI−): calculated for $C_{17}H_{13}ClNO$ $[M-H]^-$: 282.0691 found 282.0686.

$[\alpha]_D$ = +63.9 (*c* 0.74, CH_2Cl_2).

HPLC (after reduction to the corresponding alcohol with $NaBH_4$ in MeOH): Chiralcel AS-H column (hexane/*i*-PrOH 85:15, flow rate 1.0 ml/min, 254 nm); t_r = 20.1 (minor), t_r = 29.8 min (major).

7. ^{1}H and ^{13}C NMR Spectra

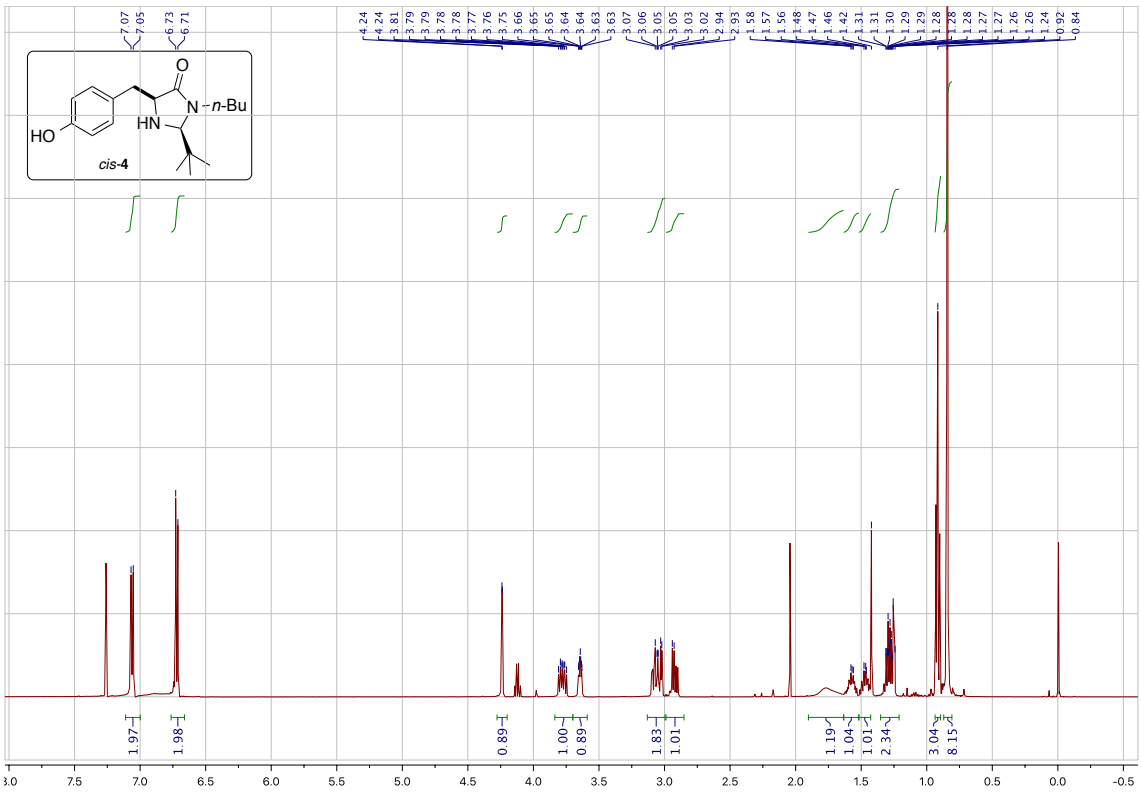

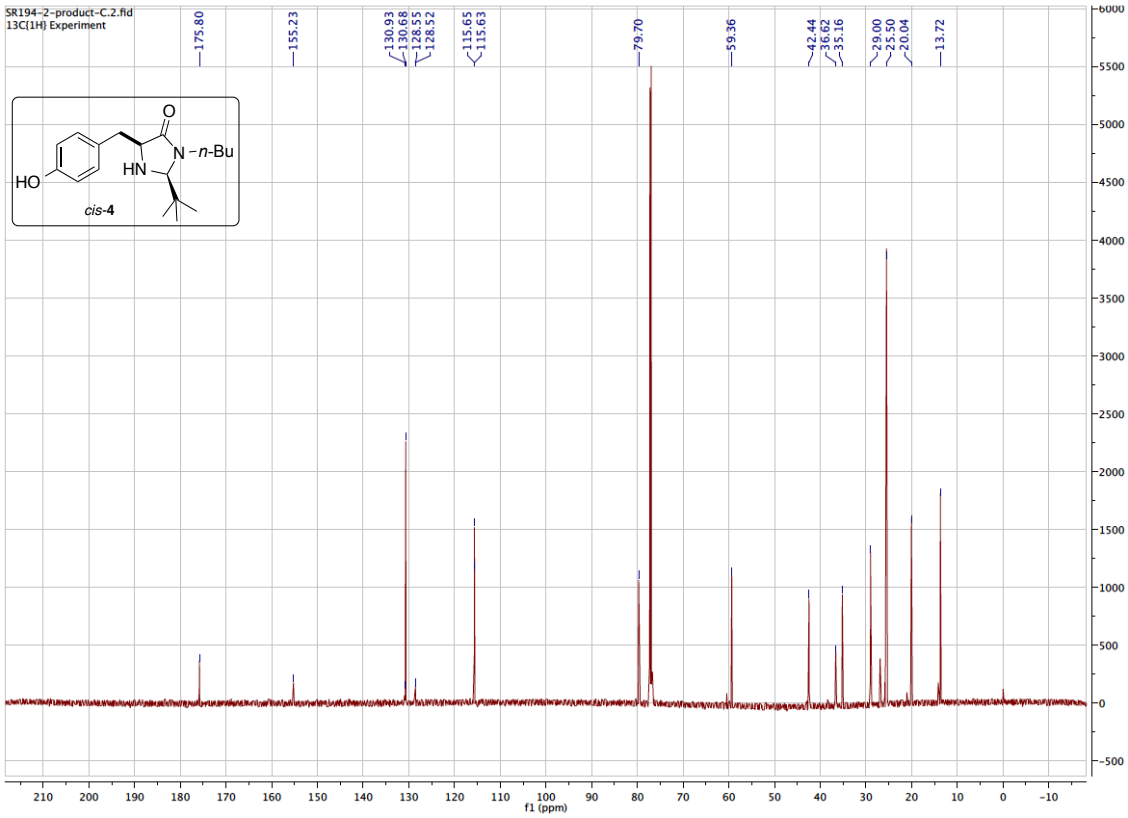

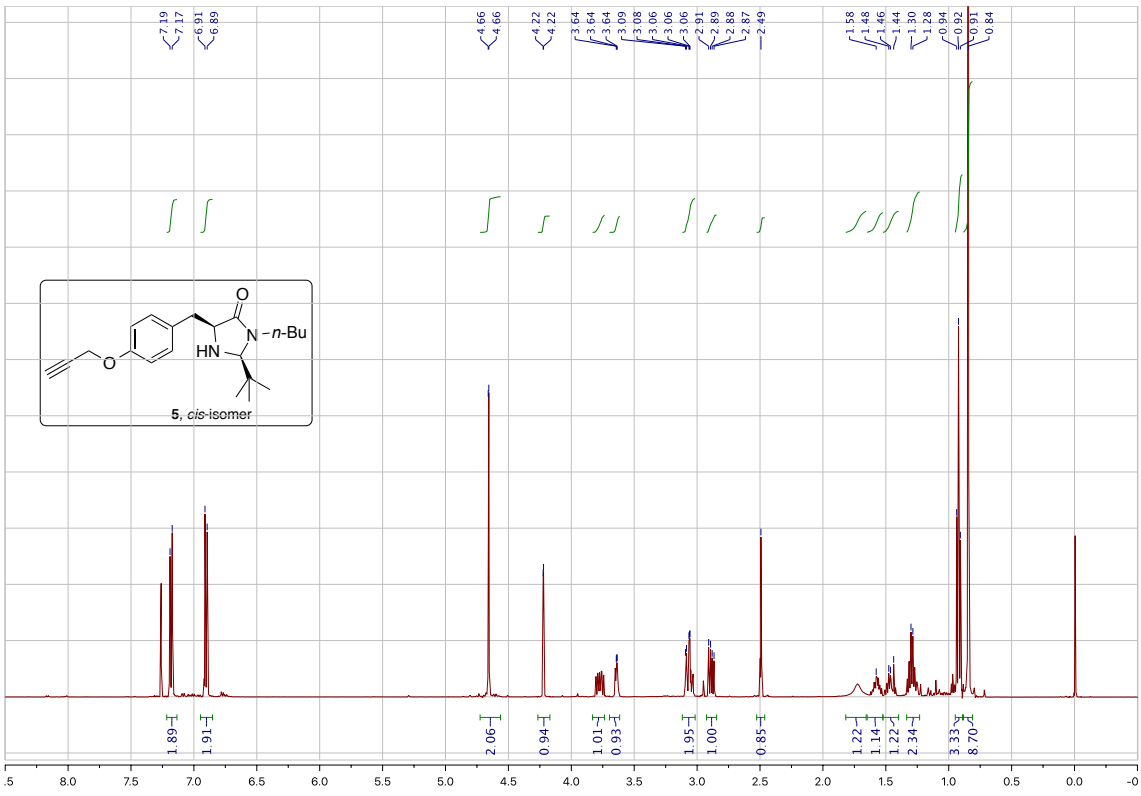
7.19
7.17
6.91
6.89
4.66
4.66
4.22
4.22
3.64
3.64
3.64
3.09
3.08
3.06
3.06
3.06
2.91
2.89
2.88
2.87
2.49
1.58
1.48
1.46
1.44
1.30
1.28
0.94
0.92
0.91
0.84
1.89
1.91
2.06
0.94
1.01
0.93
1.95
1.00
0.85
1.22
1.14
1.22
2.34
3.33
8.70
O
N –n-Bu
HN
O
5, cis-isomer

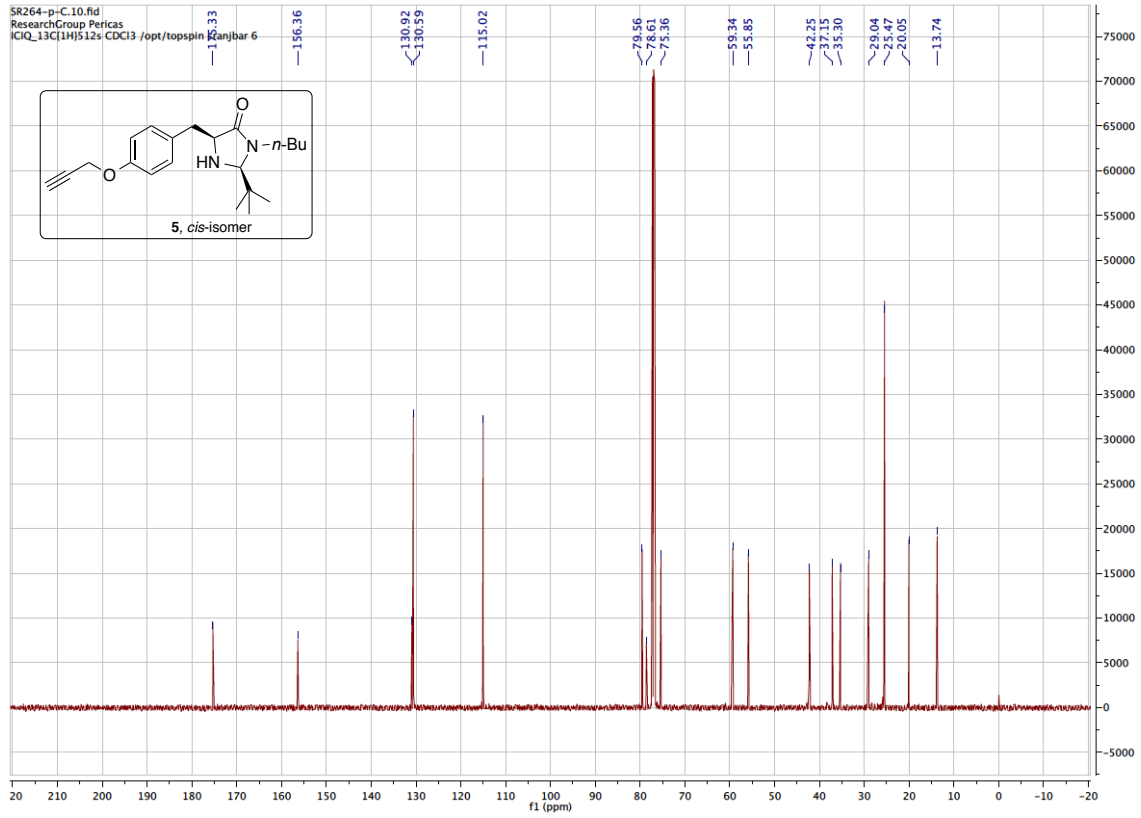
SR264-p+C.10.fid
ResearchGroup Pericas
ICIQ_13C{1H}512s CDCl3 /opt/topspin Zanjbar 6
173.33
156.36
130.92
130.59
115.02
79.56
78.61
75.36
59.34
55.85
42.25
37.15
35.30
29.04
25.47
20.05
13.74
O
N –n-Bu
HN
O
5, cis-isomer
f1 (ppm)

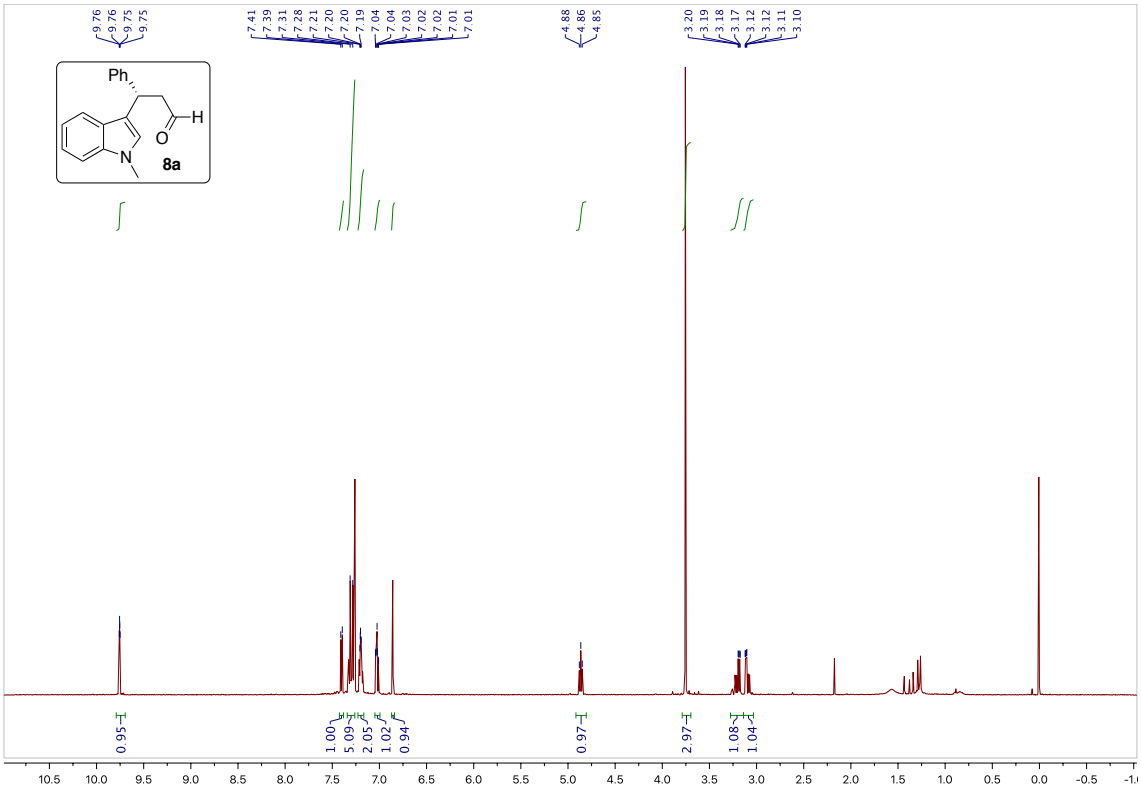
9.76
9.76
9.75
9.75
7.41
7.39
7.31
7.28
7.21
7.20
7.20
7.19
7.04
7.04
7.03
7.02
7.02
7.01
7.01
4.88
4.86
4.85
3.20
3.19
3.18
3.17
3.12
3.12
3.11
3.10
Ph
H
O
N
8a
0.95
1.00
5.09
2.05
1.02
0.94
0.97
2.97
1.08
1.04

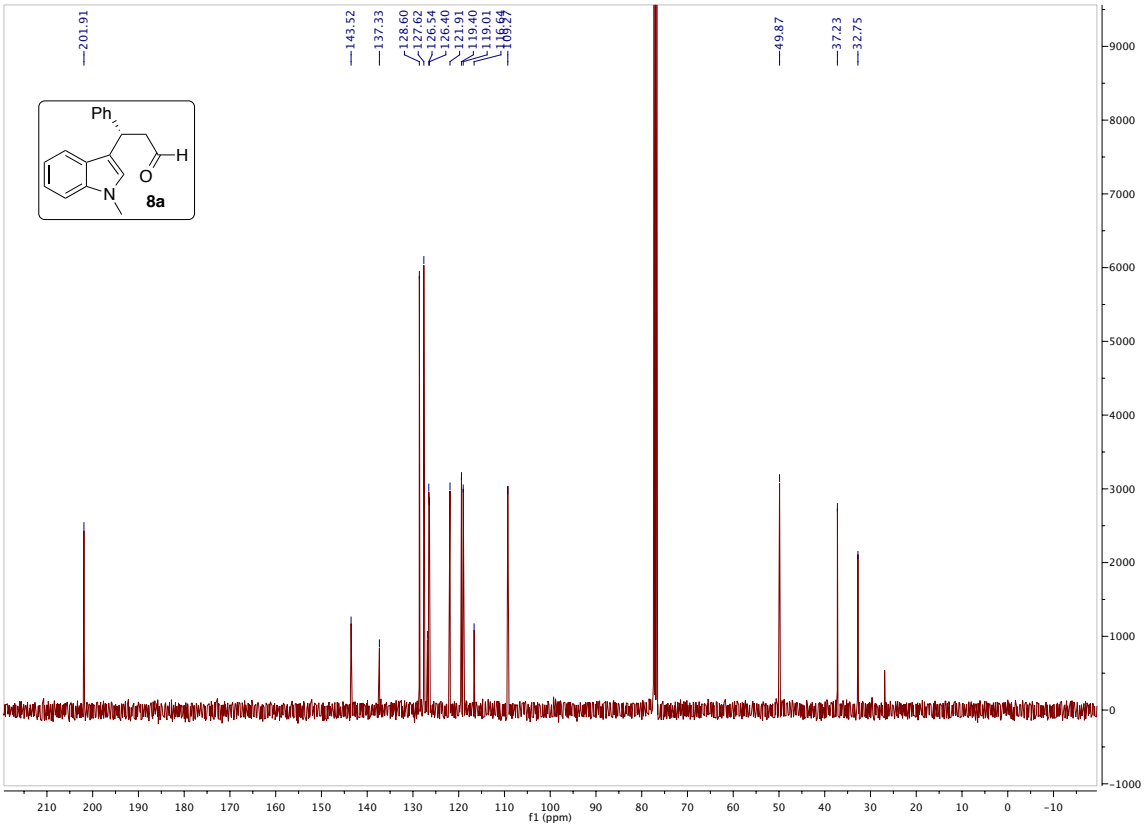
201.91
143.52
137.33
128.60
127.62
126.54
126.40
121.91
119.40
119.01
49.87
37.23
32.75
Ph
H
O
N
8a
f1 (ppm)

S19

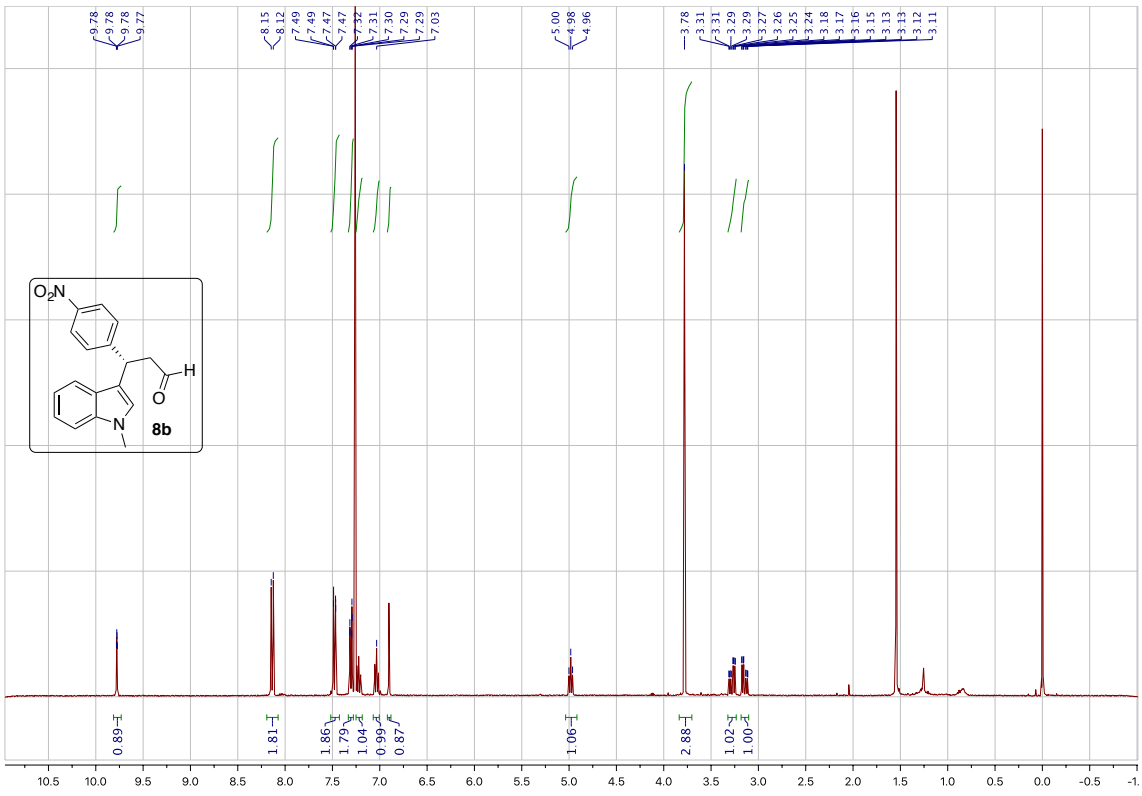
9.78
9.78
9.78
9.77
8.15
8.12
7.49
7.49
7.47
7.47
7.32
7.31
7.30
7.29
7.29
7.03
5.00
4.98
4.96
3.78
3.31
3.31
3.29
3.29
3.27
3.26
3.25
3.24
3.18
3.17
3.16
3.15
3.13
3.13
3.12
3.11
O2N
H
O
N
8b
0.89
1.81
1.86
1.79
1.04
0.99
0.87
1.06
2.88
1.02
1.00
10.5
10.0
9.5
9.0
8.5
8.0
7.5
7.0
6.5
6.0
5.5
5.0
4.5
4.0
3.5
3.0
2.5
2.0
1.5
1.0
0.5
0.0
-0.5

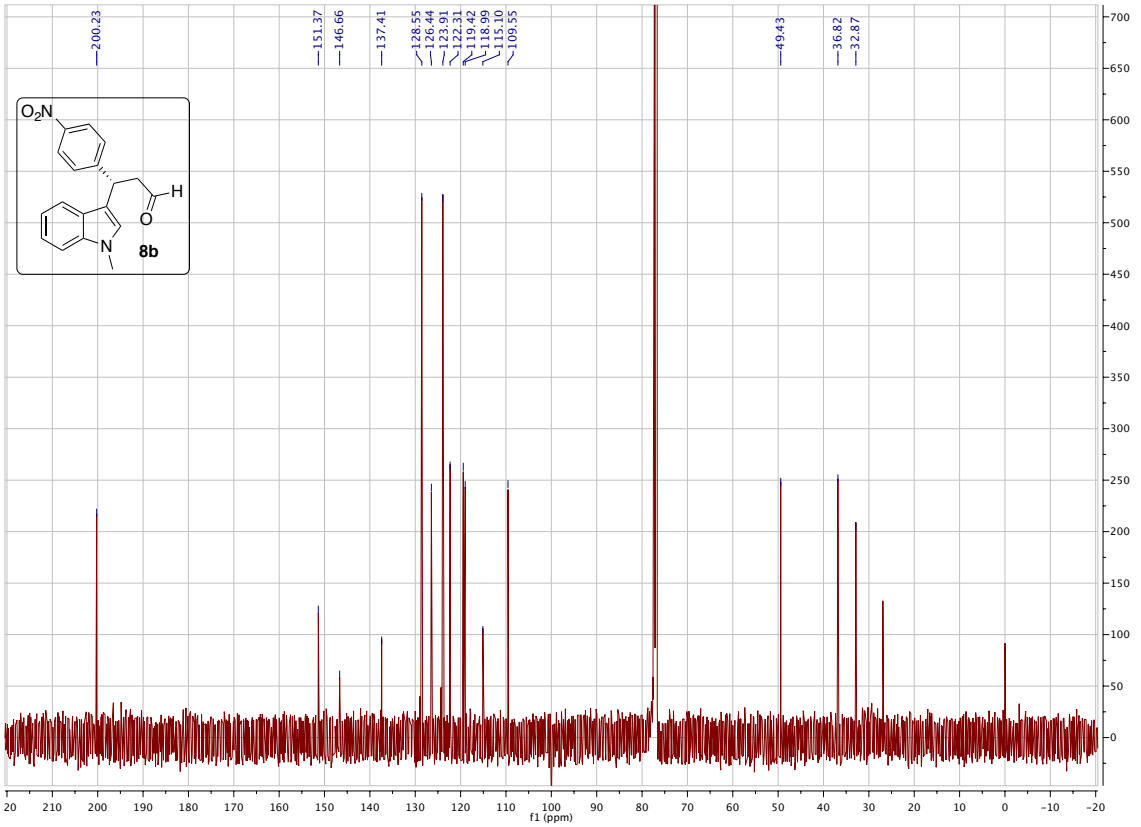
200.23
151.37
146.66
137.41
128.55
126.44
123.91
122.31
119.42
118.99
115.10
109.55
49.43
36.82
32.87
O2N
H
O
N
8b
700
650
600
550
500
450
400
350
300
250
200
150
100
50
0
20
210
200
190
180
170
160
150
140
130
120
110
100
90
80
70
60
50
40
30
20
10
0
-10
-20
f1 (ppm)

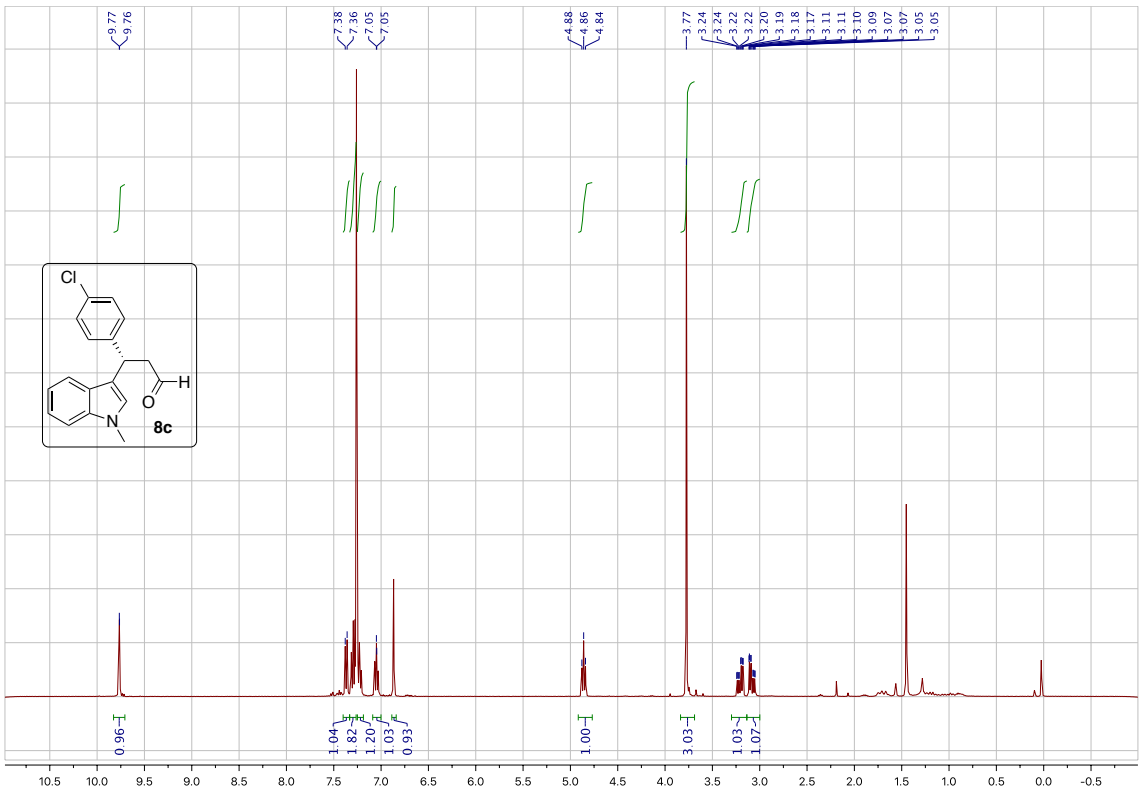
9.77
9.76
7.38
7.36
7.05
7.05
4.88
4.86
4.84
3.77
3.24
3.22
3.20
3.19
3.18
3.17
3.11
3.10
3.09
3.07
3.05
Cl
H
O
N
8c
0.96
1.04
1.82
1.20
1.03
0.93
1.00
3.03
1.03
1.07

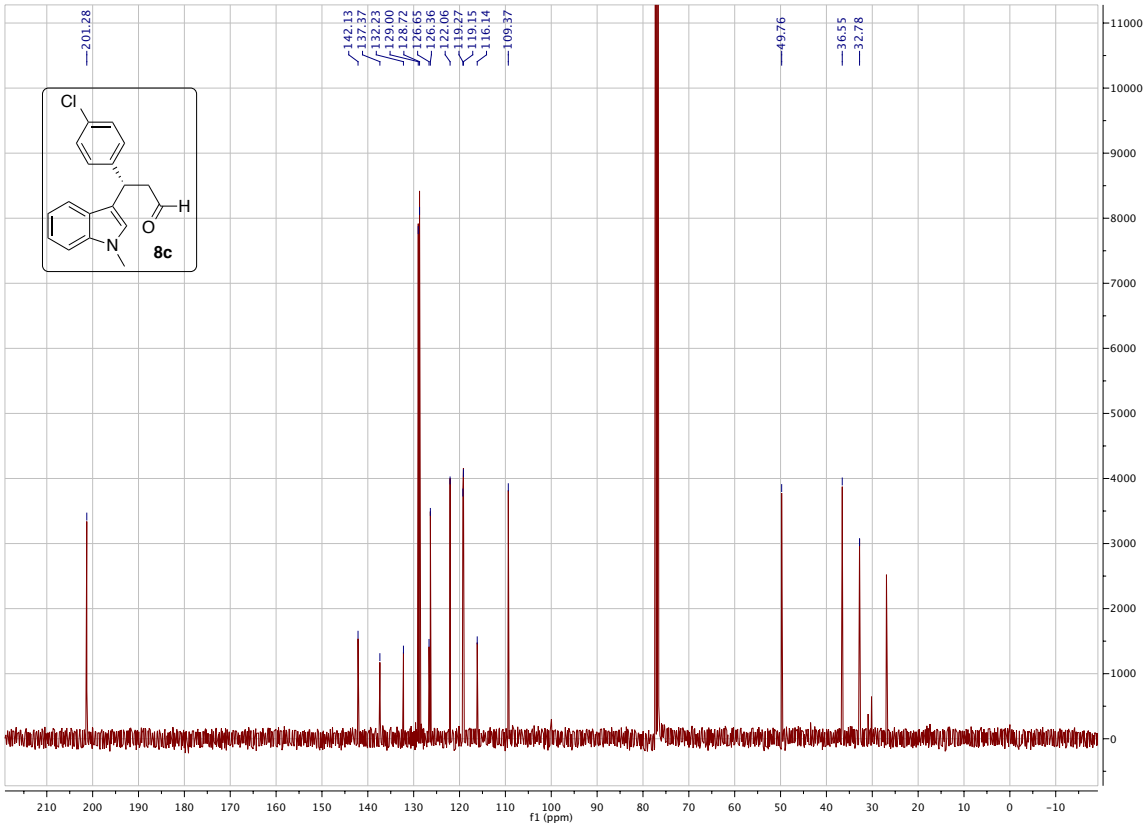
201.28
142.13
137.37
132.23
129.00
128.72
126.65
126.36
122.06
119.27
119.15
116.14
109.37
49.76
36.55
32.78
Cl
H
O
N
8c
f1 (ppm)

S21

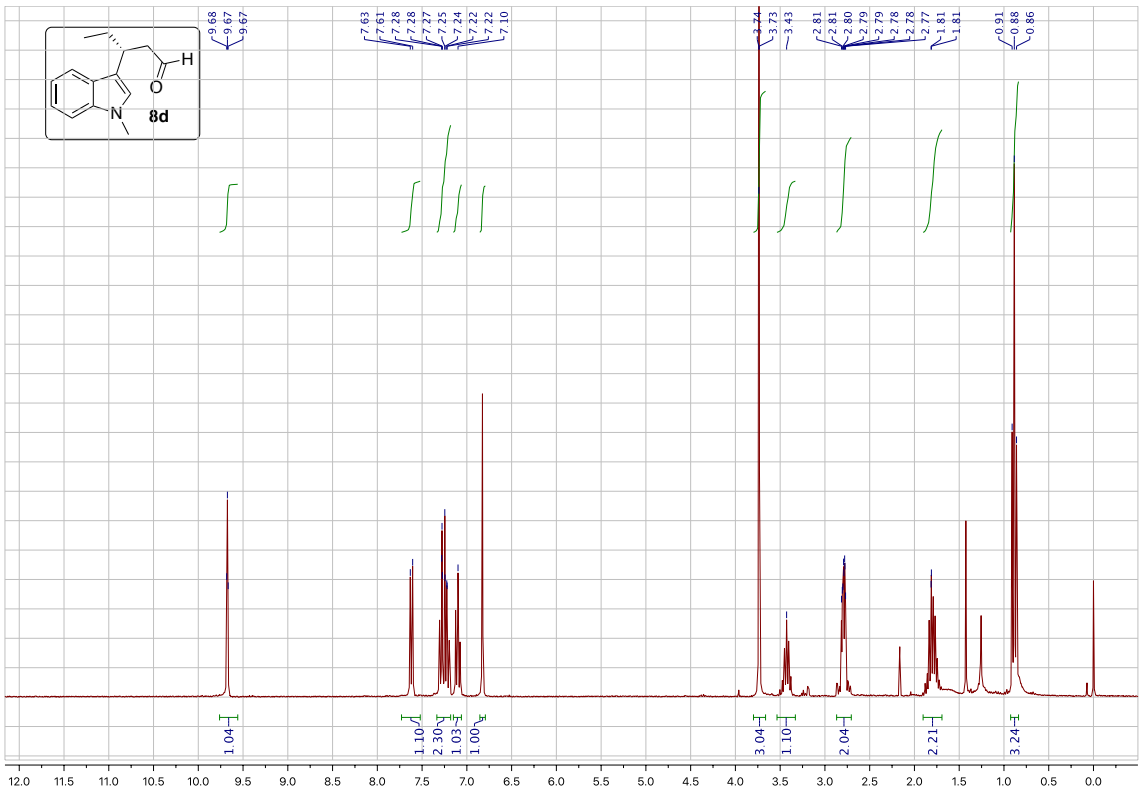
9.68
9.67
9.67
7.63
7.61
7.28
7.28
7.27
7.25
7.24
7.22
7.22
7.10
3.74
3.73
3.43
2.81
2.81
2.80
2.79
2.79
2.78
2.78
2.77
1.81
1.81
0.91
0.88
0.86
1.04
1.10
2.30
1.03
1.00
3.04
1.10
2.04
2.21
3.24
8d

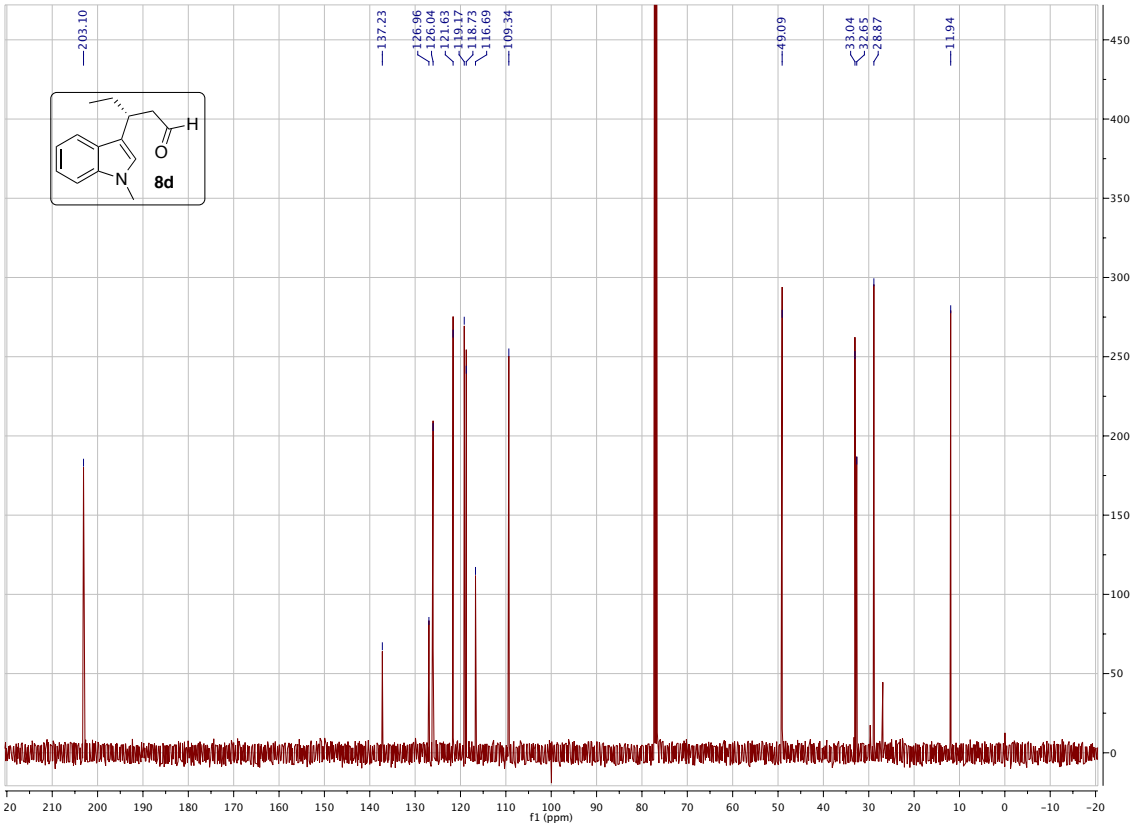
203.10
137.23
126.96
126.04
121.63
119.17
118.73
116.69
109.34
49.09
33.04
32.65
28.87
11.94
8d
f1 (ppm)

S22

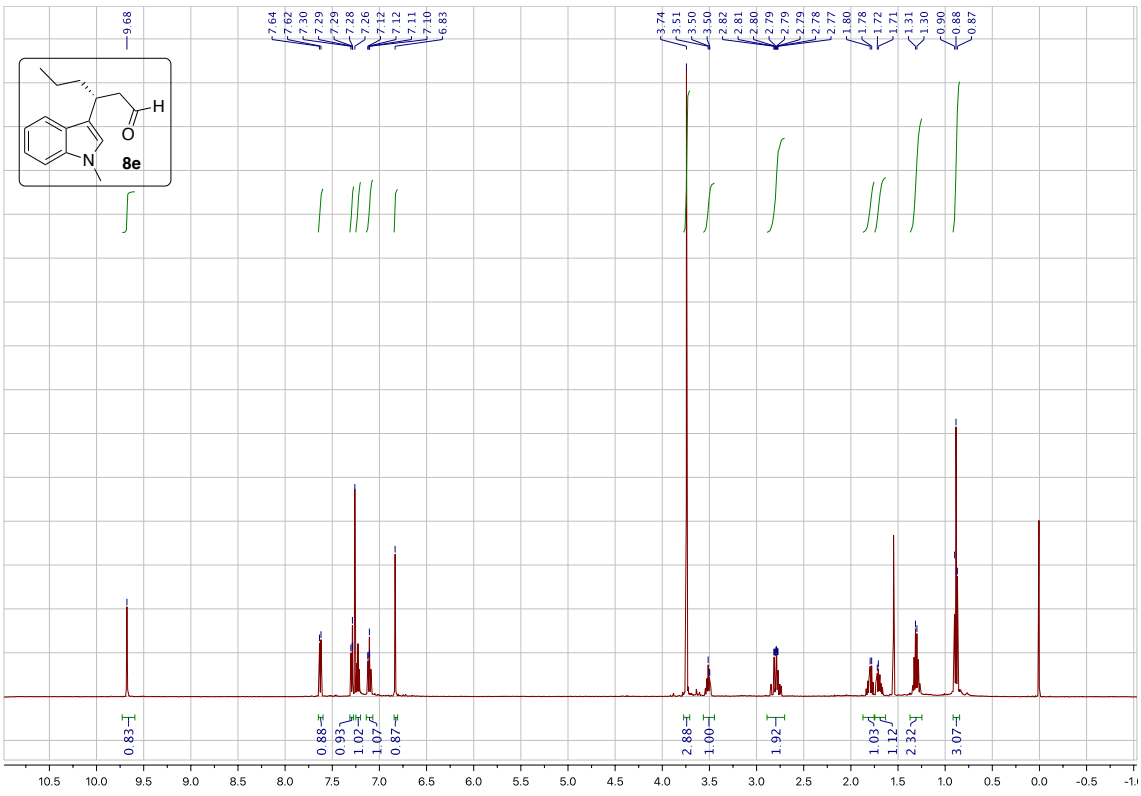
9.68
7.64
7.62
7.30
7.29
7.29
7.28
7.26
7.12
7.12
7.11
7.10
6.83
3.74
3.51
3.50
3.50
2.82
2.81
2.80
2.79
2.79
2.79
2.78
2.77
1.80
1.78
1.72
1.71
1.31
1.30
0.90
0.88
0.87
H
O
N
8e
0.83
0.88
0.93
1.02
1.07
0.87
2.88
1.00
1.92
1.03
1.12
2.32
3.07

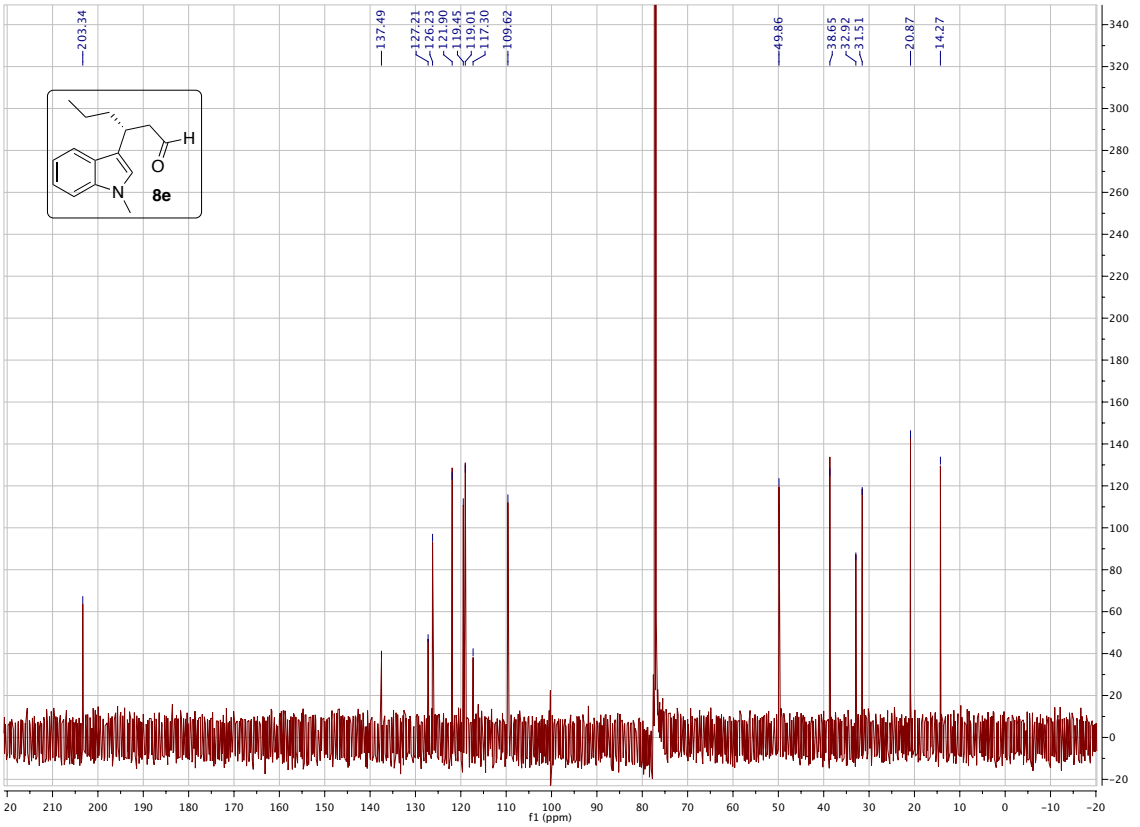
203.34
137.49
127.21
126.23
121.90
119.45
119.01
117.30
109.62
49.86
38.65
32.92
31.51
20.87
14.27
H
O
N
8e
f1 (ppm)

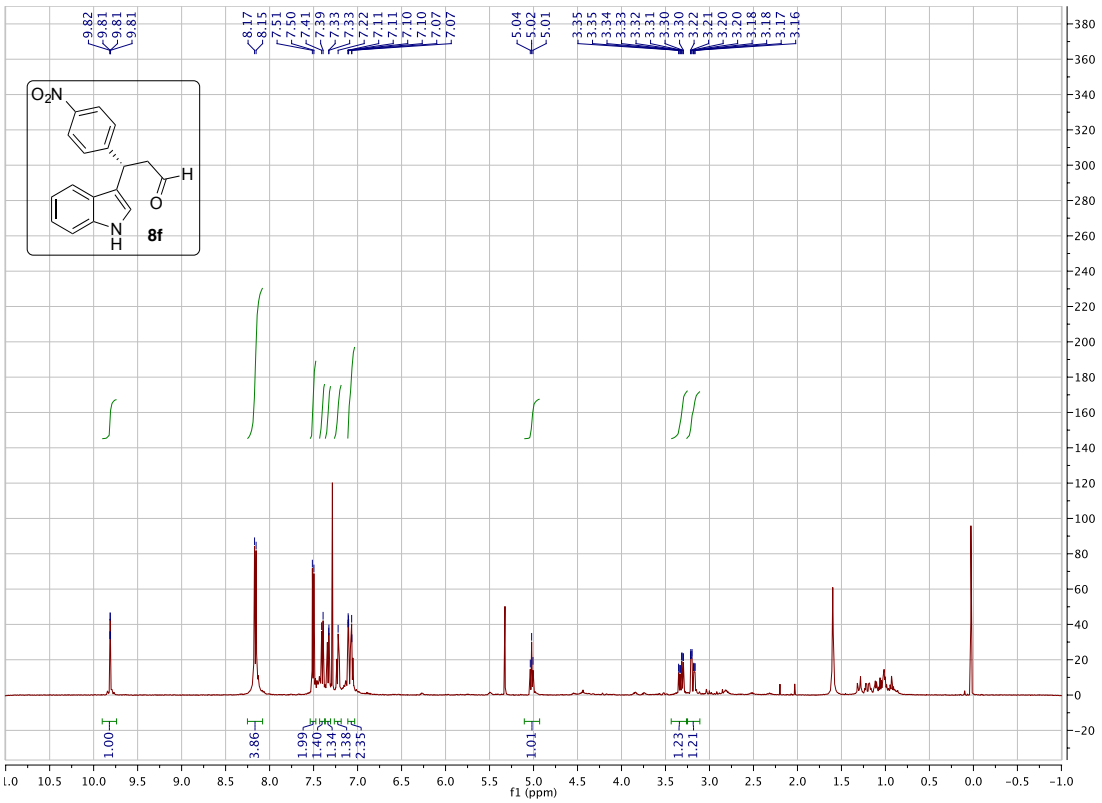
9.82
9.81
9.81
9.81
8.17
8.15
7.51
7.50
7.41
7.39
7.33
7.33
7.22
7.11
7.11
7.10
7.10
7.07
7.07
5.04
5.02
5.01
3.35
3.35
3.34
3.33
3.32
3.31
3.30
3.30
3.22
3.21
3.20
3.20
3.18
3.18
3.17
3.16
O2N
H
O
N
H
8f
1.00
3.86
1.99
1.40
1.34
1.38
2.35
1.01
1.23
1.21
f1 (ppm)

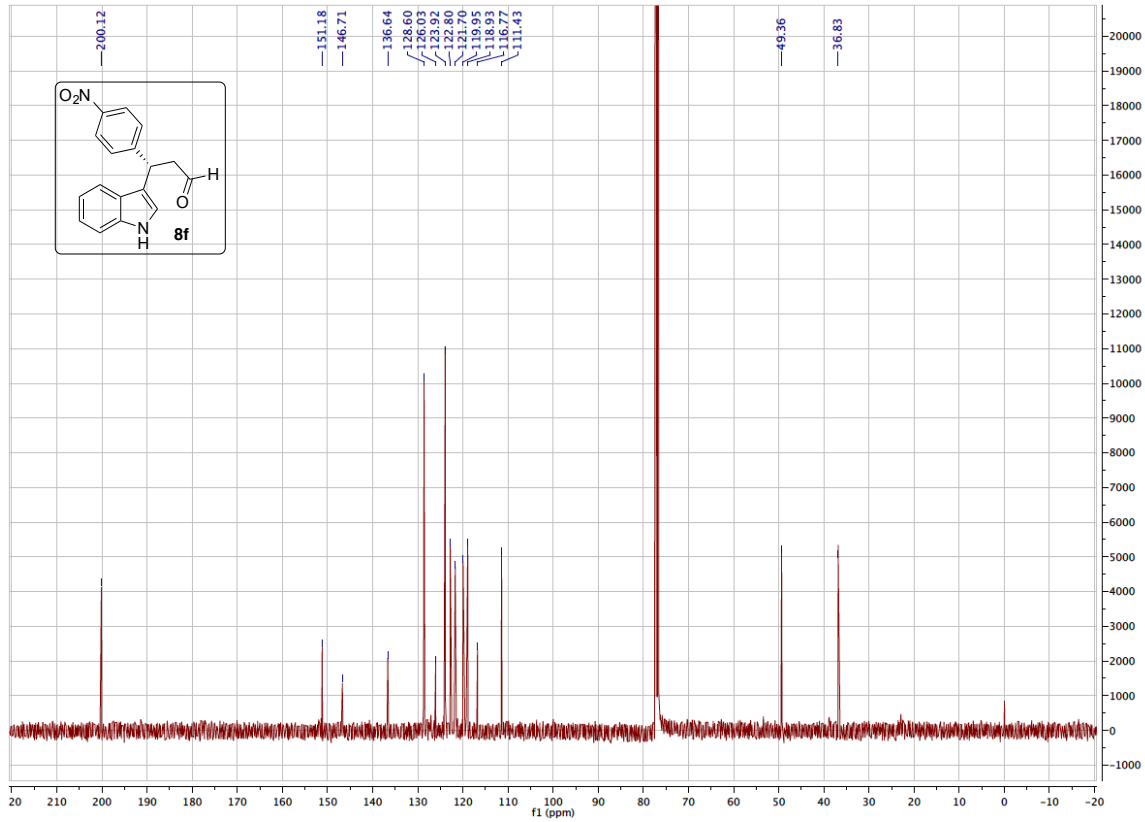
200.12
151.18
146.71
136.64
128.60
126.03
123.92
122.80
121.70
119.95
118.93
116.77
111.43
49.36
36.83
O2N
H
O
N
H
8f
f1 (ppm)

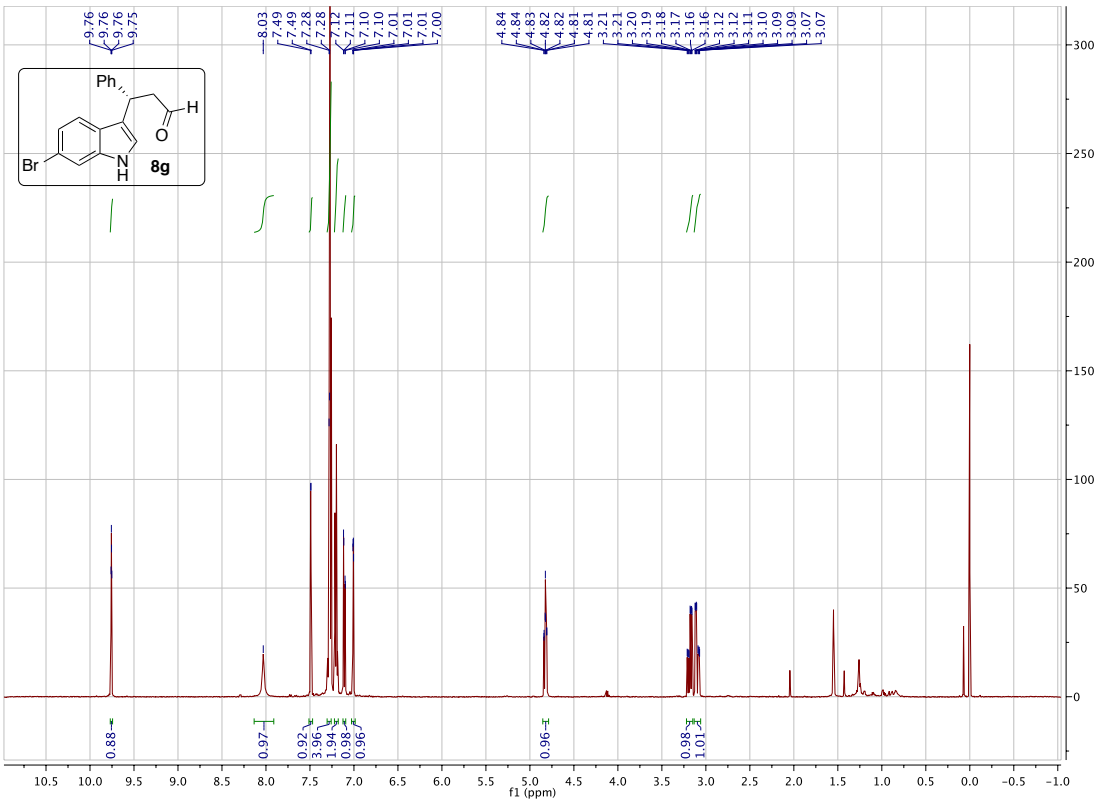

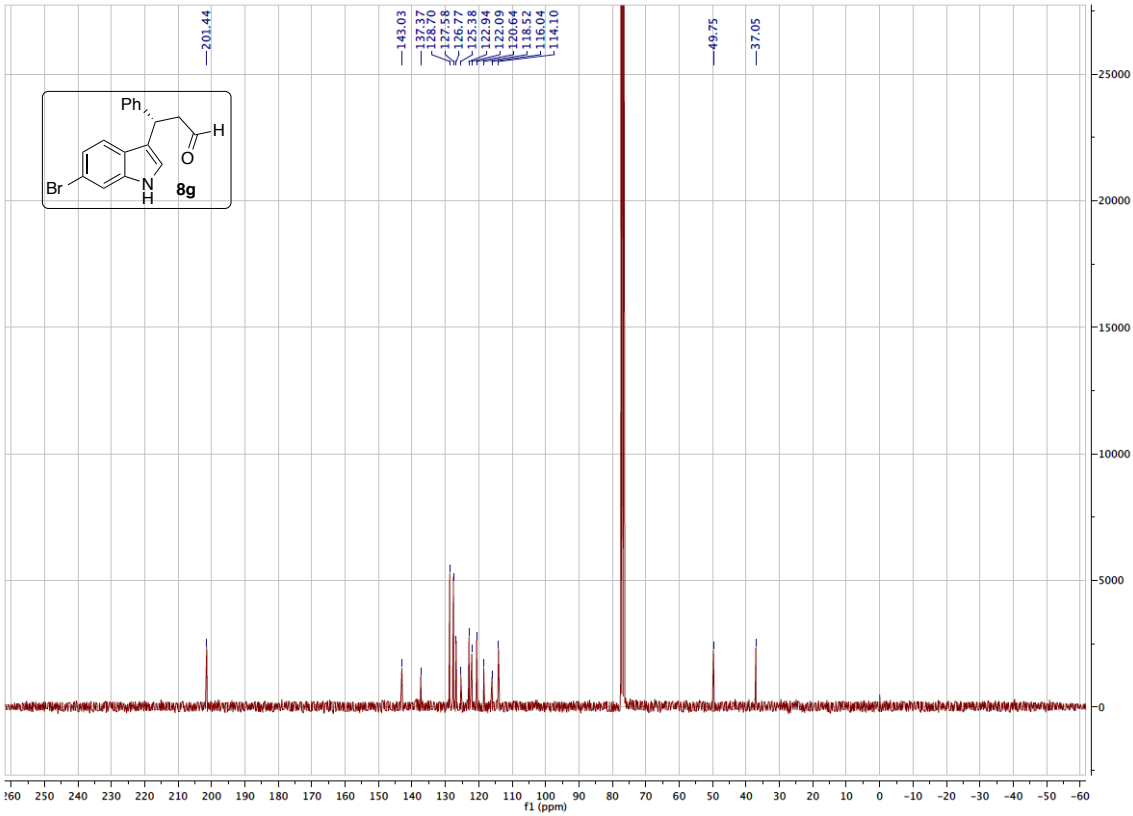

S25

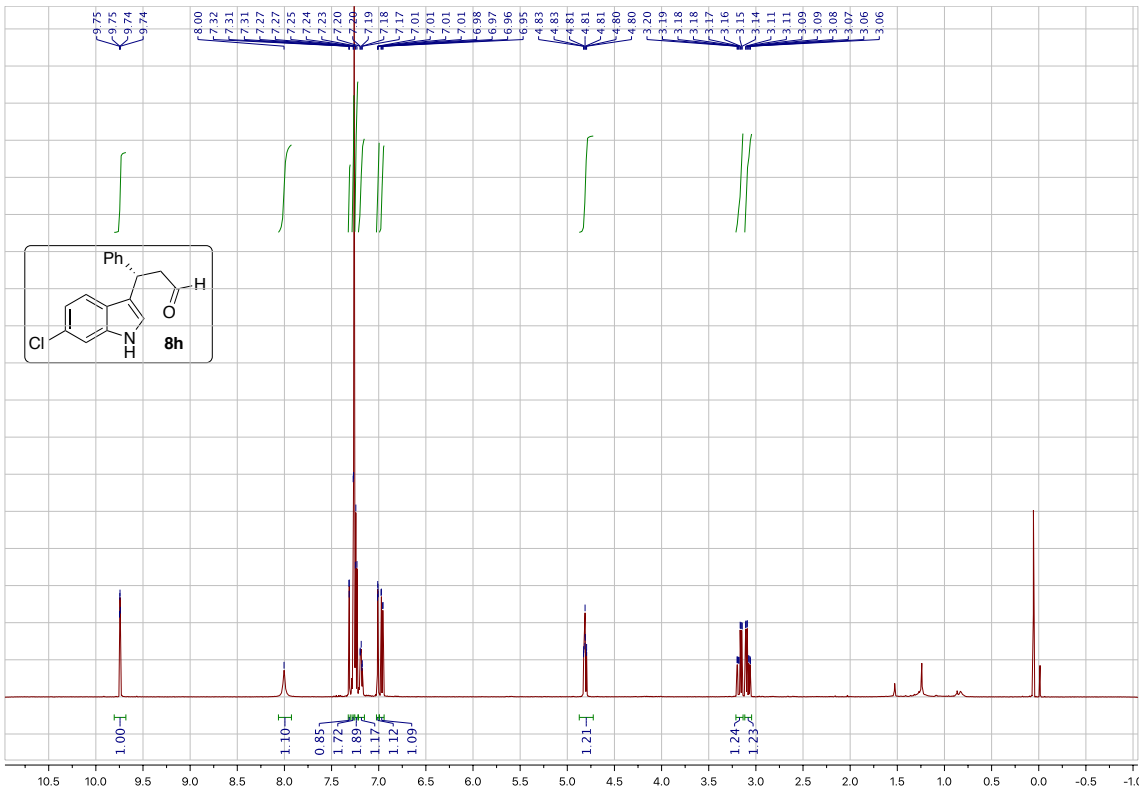
Ph
H
O
Cl
N
H
8h

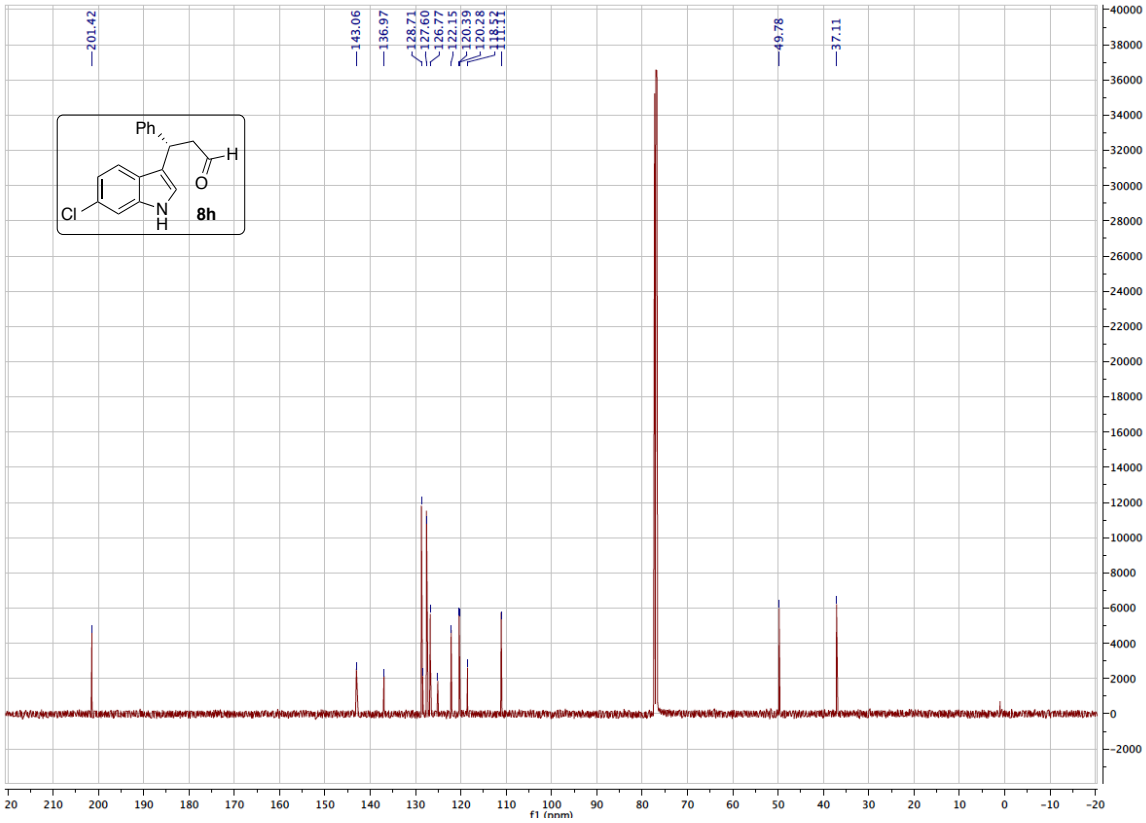
Ph
H
O
Cl
N
H
8h

8. HPLC chromatograms

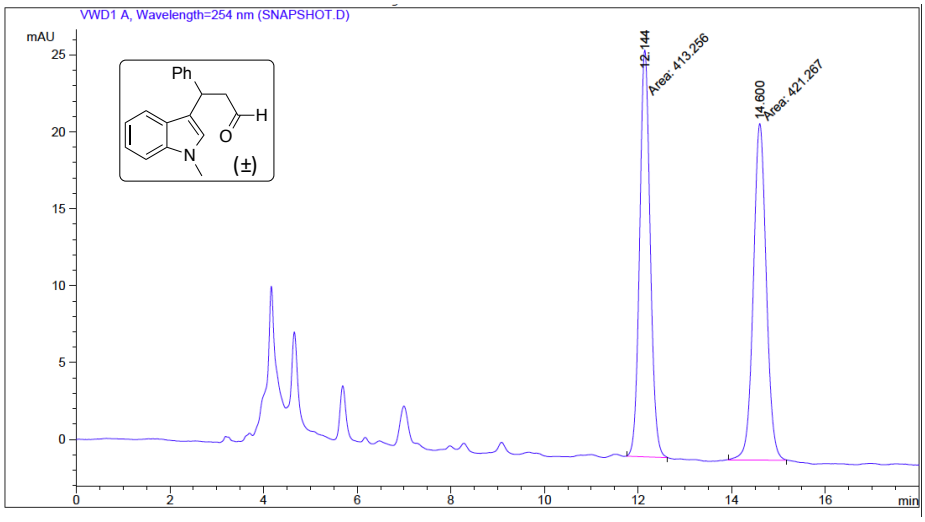

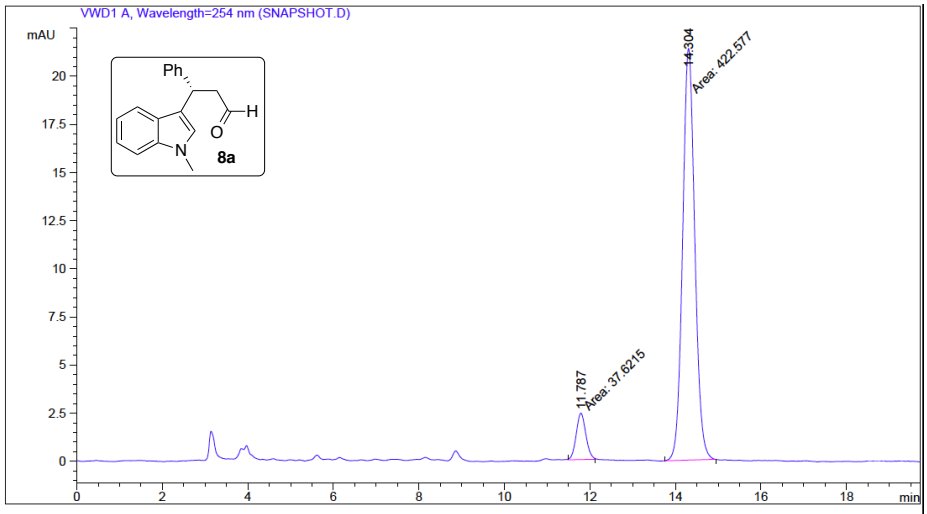


```
=====================================================================
                    Area Percent Report
=====================================================================

Sorted By             :      Signal
Multiplier:                   :      1.0000
Dilution:                     :      1.0000
Use Multiplier & Dilution Factor with ISTDs


Signal 1: VWD1 A, Wavelength=254 nm

Peak RetTime Type  Width     Area      Height     Area
  #   [min]        [min]  mAU   *s    [mAU   ]      %
----|-------|----|-------|----------|----------|--------|
   1  11.787 MM    0.2603   37.62149    2.40863   8.1751
   2  14.304 MM    0.3293  422.57675   21.38775  91.8249
```

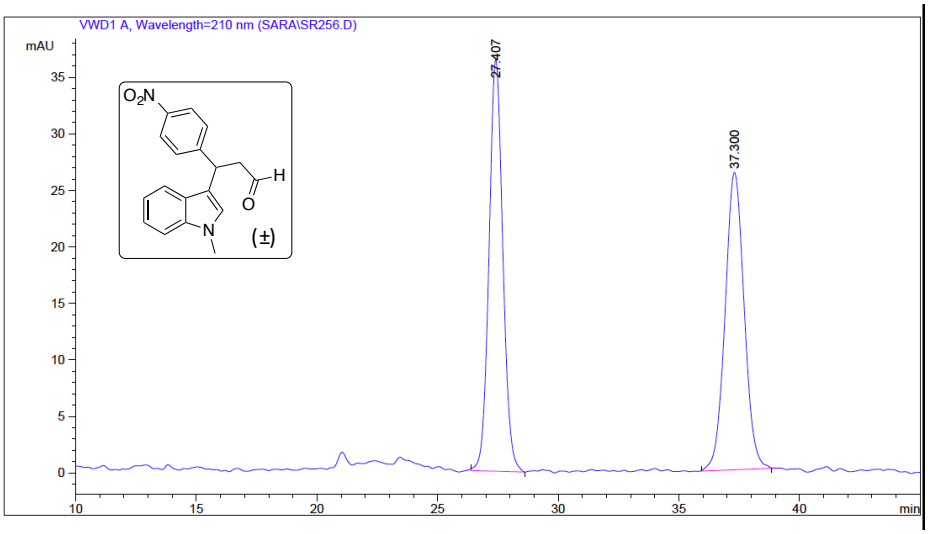

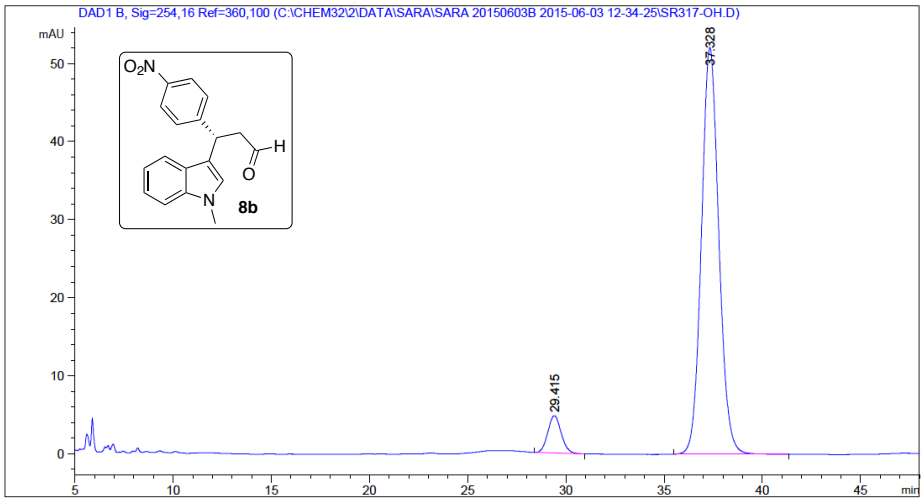


```
=====================================================================
                    Area Percent Report
=====================================================================

Sorted By             :      Signal
Multiplier            :      1.0000
Dilution              :      1.0000
Use Multiplier & Dilution Factor with ISTDs


Signal 1: DAD1 B, Sig=254,16 Ref=360,100

Peak RetTime Type  Width     Area      Height     Area
  #   [min]        [min]   [mAU*s]     [mAU]       %
----|-------|----|-------|----------|----------|--------|
   1  29.415 BB    0.6943  226.70984    4.77196   6.5936
   2  37.328 BB    0.9389 3211.62427   52.12182  93.4064
```

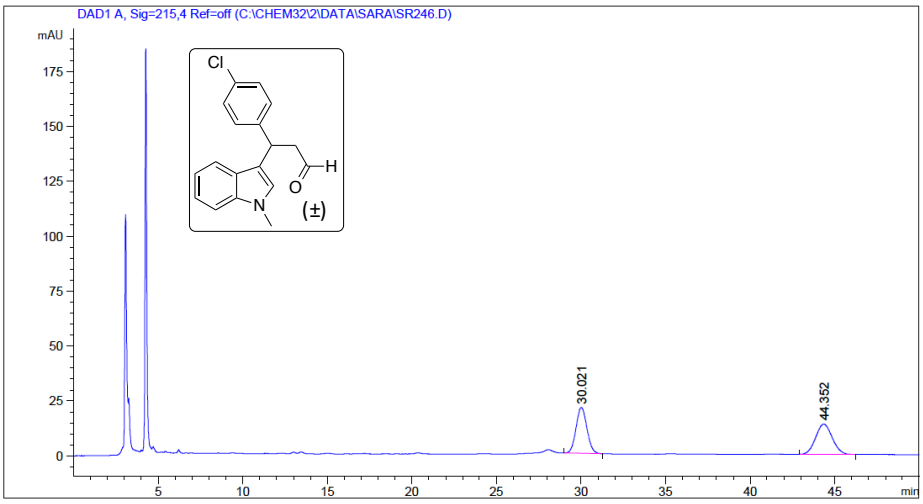

Additional Info : Peak(s) manually integrated

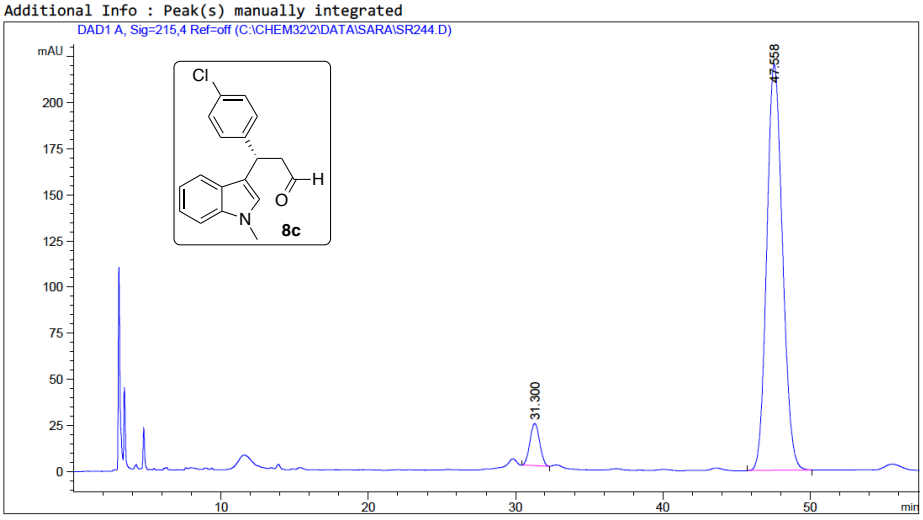


```
=====================================================================
                      Area Percent Report
=====================================================================

Sorted By             :      Signal
Multiplier            :      1.0000
Dilution              :      1.0000
Use Multiplier & Dilution Factor with ISTDs


Signal 1: DAD1 A, Sig=215,4 Ref=off

Peak RetTime Type  Width     Area      Height     Area
  #   [min]        [min]   [mAU*s]     [mAU]       %
----|-------|----|-------|----------|----------|--------|
   1  31.300 BB    0.7147 1052.93994   22.97398   6.0485
   2  47.558 BB    1.1489 1.63553e4   220.10159  93.9515
```

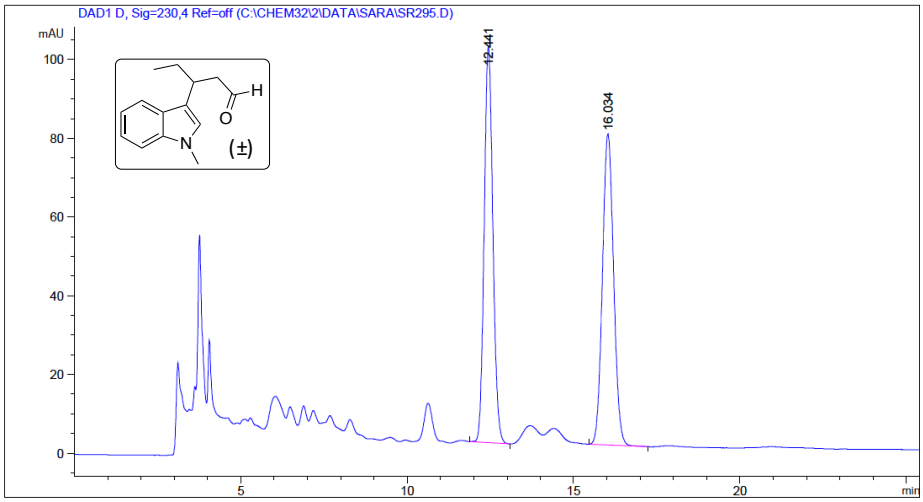

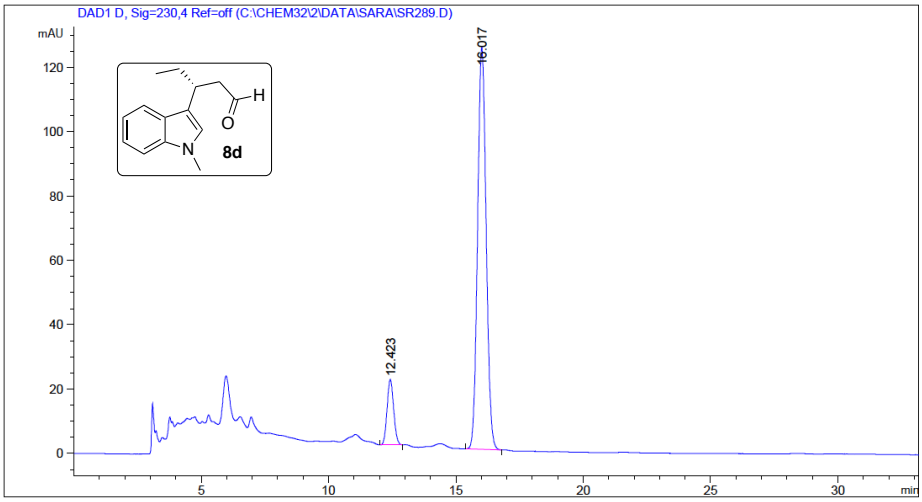


```
=====================================================================
                      Area Percent Report
=====================================================================

Sorted By             :      Signal
Multiplier            :      1.0000
Dilution              :      1.0000
Use Multiplier & Dilution Factor with ISTDs


Signal 1: DAD1 D, Sig=230,4 Ref=off

Peak RetTime Type  Width     Area      Height     Area
  #   [min]        [min]   [mAU*s]     [mAU]       %
----|-------|----|-------|----------|----------|--------|
   1  12.423 BB    0.2814  365.55396   20.37032  11.1205
   2  16.017 BB    0.3647 2921.64307  124.97135  88.8795
```

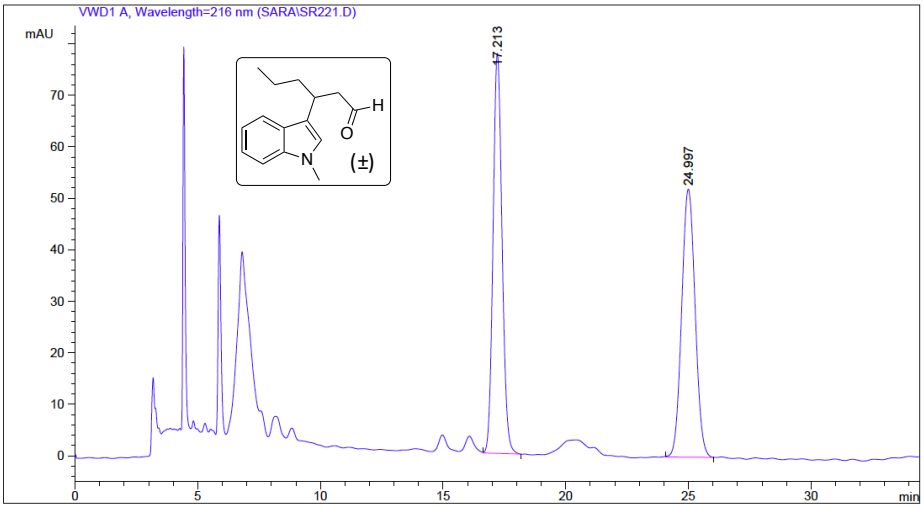

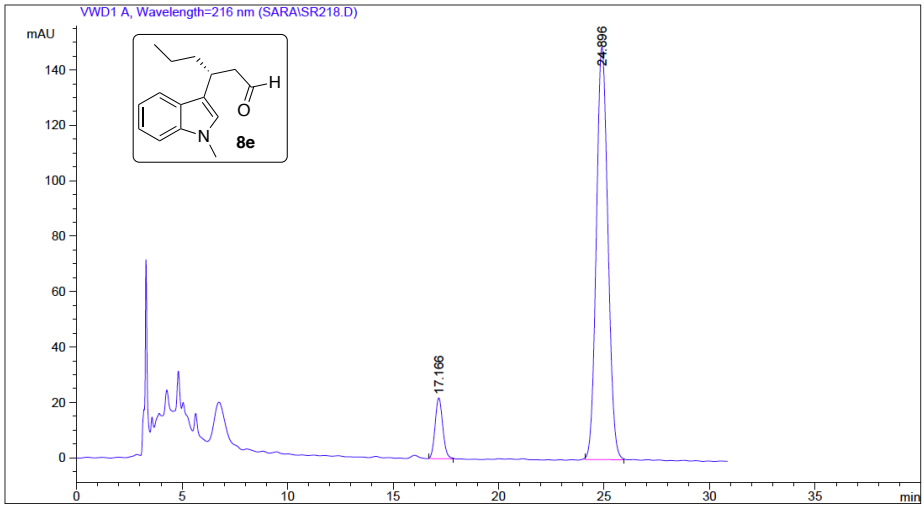


```
=====================================================================
                        Area Percent Report
=====================================================================

Sorted By             :      Signal
Multiplier:                   :      1.0000
Dilution:                     :      1.0000
Use Multiplier & Dilution Factor with ISTDs


Signal 1: VWD1 A, Wavelength=216 nm

Peak RetTime Type  Width     Area      Height     Area
  #   [min]        [min]  mAU   *s    [mAU   ]      %
----|-------|----|-------|----------|----------|--------|
   1  17.166 BB    0.3880  551.59302   21.93672   8.8649
   2  24.896 BB    0.5958 5670.59473  148.86369  91.1351
```

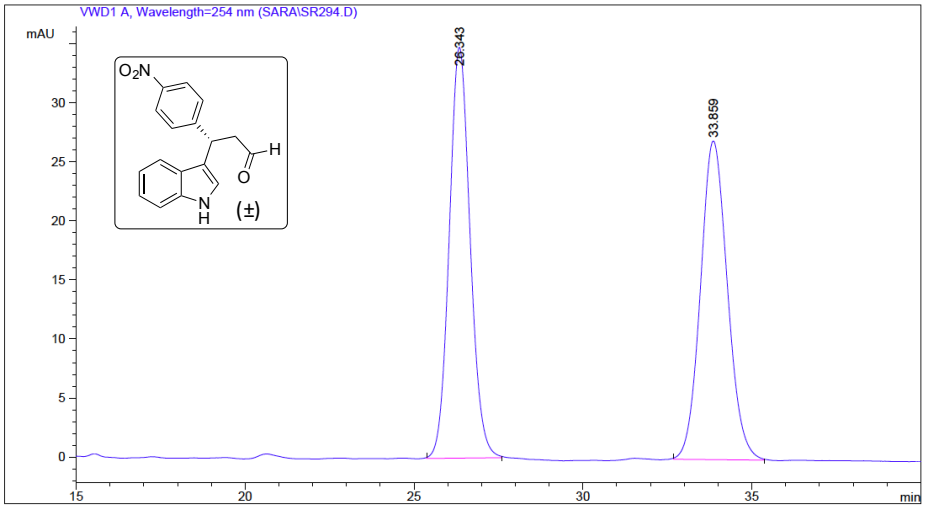

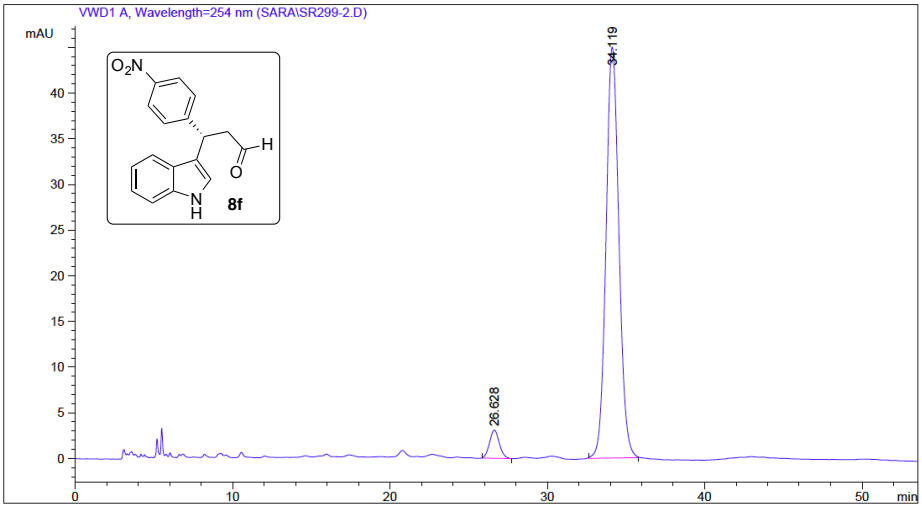


```
=====================================================================
                        Area Percent Report
=====================================================================

Sorted By             :      Signal
Multiplier:                   :      1.0000
Dilution:                     :      1.0000
Use Multiplier & Dilution Factor with ISTDs


Signal 1: VWD1 A, Wavelength=254 nm

Peak RetTime Type  Width     Area      Height     Area
  #   [min]        [min]  mAU   *s    [mAU   ]      %
----|-------|----|-------|----------|----------|--------|
   1  26.628 BB    0.6605  133.27730    3.08946   4.9461
   2  34.119 BB    0.8798 2561.34180   44.97915  95.0539
```

S32

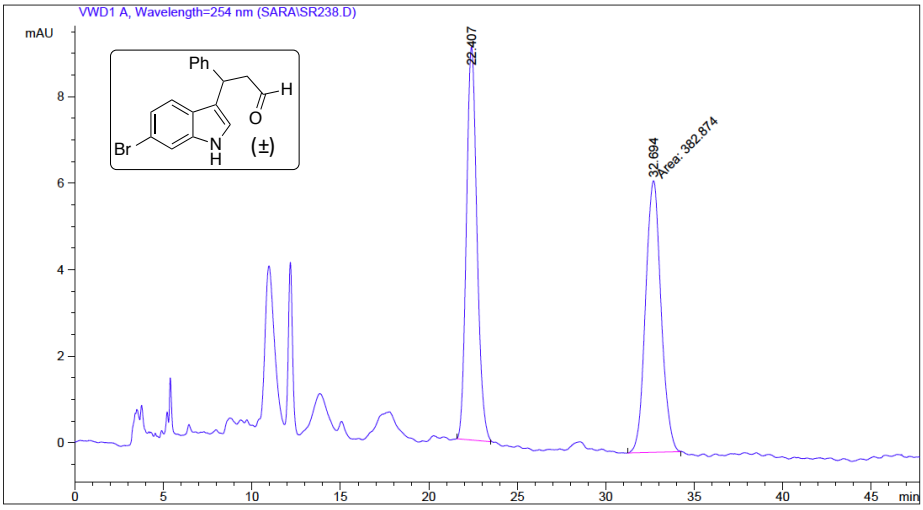

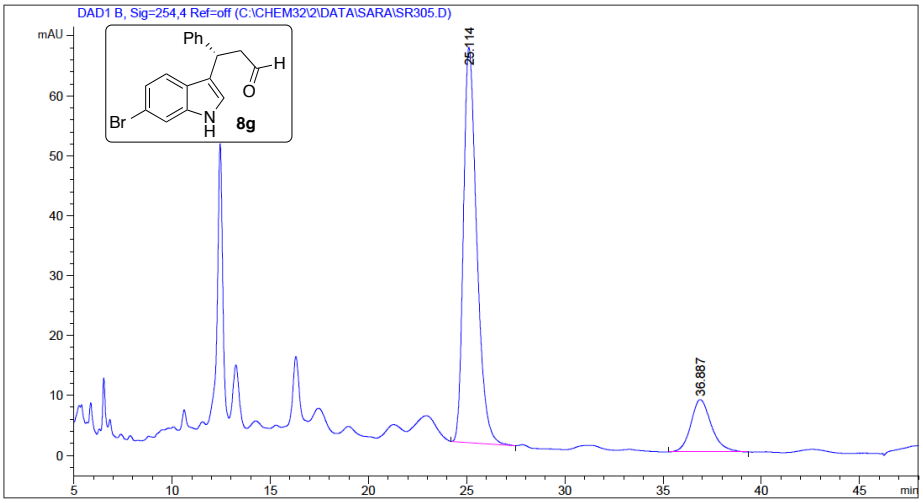


```
=====================================================================
                      Area Percent Report
=====================================================================

Sorted By             :      Signal
Multiplier            :      1.0000
Dilution              :      1.0000
Use Multiplier & Dilution Factor with ISTDs


Signal 1: DAD1 B, Sig=254,4 Ref=off

Peak RetTime Type  Width     Area      Height     Area
  #   [min]        [min]   [mAU*s]     [mAU]       %
----|-------|----|-------|----------|----------|--------|
   1  25.114 BB    0.7179 3109.41870   65.96893  82.9604
   2  36.887 BB    0.9013  638.65759    8.75280  17.0396
```

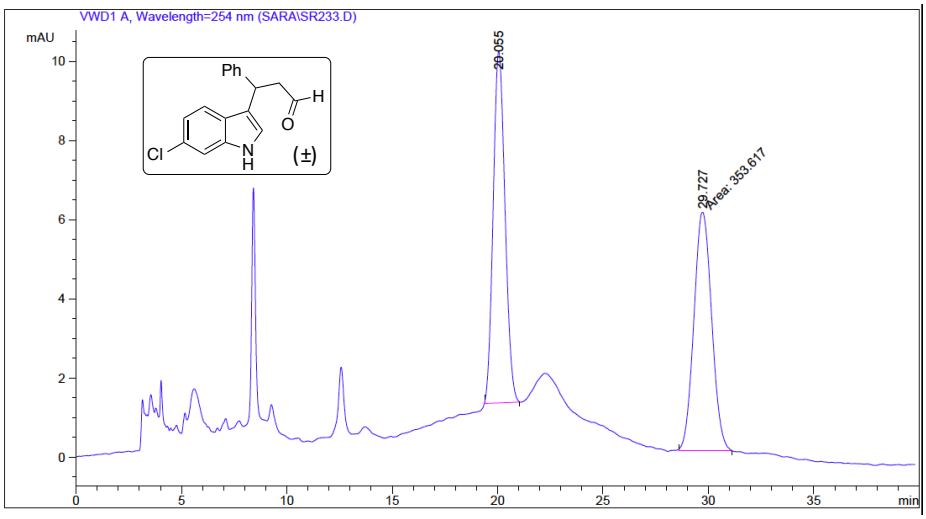

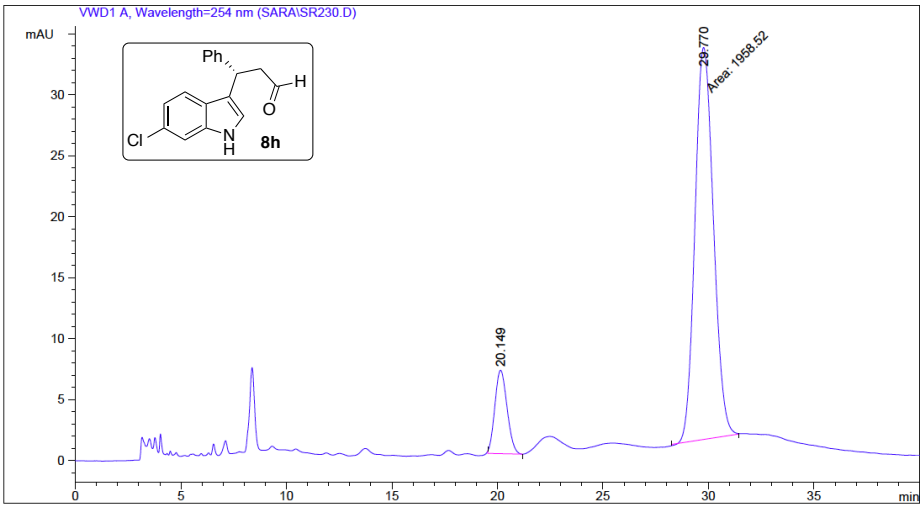


```
=====================================================================
                        Area Percent Report
=====================================================================

Sorted By             :      Signal
Multiplier:                   :      1.0000
Dilution:                     :      1.0000
Use Multiplier & Dilution Factor with ISTDs


Signal 1: VWD1 A, Wavelength=254 nm

Peak RetTime Type  Width     Area      Height     Area
  #   [min]        [min]  mAU   *s    [mAU   ]      %
----|-------|----|-------|----------|----------|--------|
   1  20.149 BB    0.6276  275.11053    6.84572  12.3167
   2  29.770 MM    1.0144 1958.52124   32.17886  87.6833
```

Chapter IV

Microporous Organic Polymers Encapsulated with Metal Nanoparticles and Co/C Nanobeads

Table of Contents

4.1. Introduction

This chapter deals with the research carried out in the laboratory of Prof. Reiser in Regensburg (Germany) between July 2015-March 2016.

Here, another hybrid material was synthesized based on the microporous aryl polymer networks encapsulated with palladium nanoparticles and carbon-coated cobalt (Co/C) nanoparticles. Afterwards, this catalyst was applied in the Suzuki cross-coupling and hydrogenation reactions. Herein, we will summarize the results achieved in these transformations.

4.1.1. Importance of Pd Nanoparticles (Pd NPs) in Catalysis

The importance of nanomaterials, a breakthrough of modern science, was mentioned in Chapter one. The novel techniques associated with them have enabled to form nanodimensional materials (in the 1-100 nm size domain) from bulky ones.

It is of interest to develop new catalysts that are environmentally benign and effective and one possible solution is using nanoparticles. Application of nanoparticles as catalysts is increasing because of their high surface-to-volume ratio and high activity of surface atoms compared to bulk catalysts, which allows achieving high turnover numbers. Due to this high activity, no ligands are required to prepare the catalyst. Indeed, using nanoparticles as catalysts could allow decreasing the amount of metal loaded in organic reactions, which is an important point in green chemistry.[1]

In this field, one of the most successful NPs in catalysis is palladium derived ones, which have been broadly used in oxidations,[2] carbon-carbon bond forming cross-coupling reactions (Suzuki, Heck, Stille and Sonogashira reactions)[3], hydrogenations[4] and electrochemical reactions in fuel cells.[5] In addition, palladium showed promising capacity in hydrogen absorption[6] and palladium nanoparticle thin films have been applied as microsensors for hydrogen detection.[7]

---

[1] Linhardt, R.; Kainz, Q. M.; Grass, R. N.; Stark, W. J.; Reiser, O. *RSC Adv*. **2014,** *4*, 8541.

[2] a) Dimitratos, N.; Porta, F.; Prati, L. *Appl. Catal. A: Gen*. **2005**, *291*, 210; b) Hou, Z.; Theyssen, N.; Brinkmann, A.; Leitner, W. *Angew. Chem. Int. Ed*. **2005**, *44*, 1346.

[3] a) Beller, M.; Fischer, H.; Kühlein, K.; Reisinger, C.-P.; Herrmann, W. A.; *J. Organomet. Chem.* **1996**, *520*, 257; b) Narayanan, R.; El-Sayed, M. A. *J. Catal*. **2005**, *234*, 348; c) Stille, J. K.; Tanaka, M. *J. Am. Chem. Soc*. **1987**, *109*, 3785; d) Negishi, E.; Anastasia, L. *Chem. Rev*. **2003**, *103*, 1979; e) Miyaura, N.; Suzuki, A. *J. Chem. Soc. Chem. Commun.* **1979**, 866.

[4] a) Semagina, N.; Renken, A.; Kiwi-Minsker, L. *J. Phys. Chem.* C. **2007**, *111*, 13933; b) Wilson, O. M.; Knecht, M. R.; Garcia-Martinez, J. C.; Crooks, R. M. *J. Am. Chem. Soc*. **2006**, *128*, 4510.

[5] Cheong, S.; Watt, J. D.; Tilley, R. D. *Nanoscale* **2010**, *2*, 2045.

[6] Adams, B. D.; Chen, A. *Mater. Today* **2011**, *14*, 282.

[7] Jeon, K. J.; Lee, J. M.; Lee, E.; Lee, W, *Nanotechnology* **2009**, *20*, 135502.

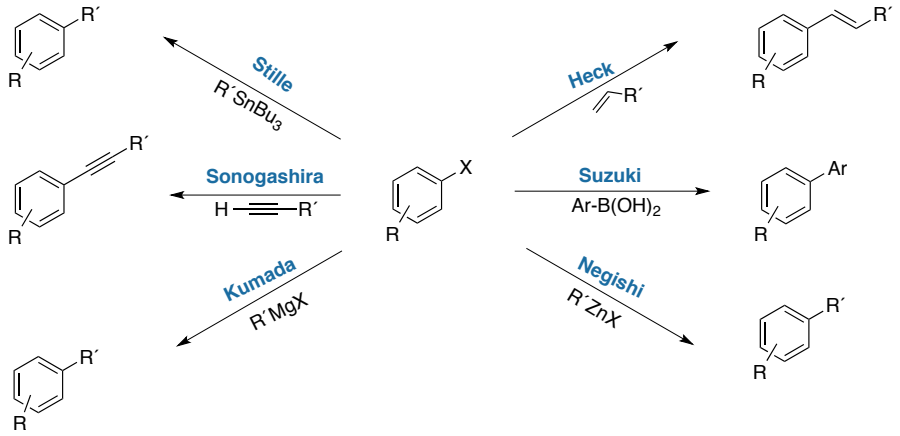

Scheme 1. Most representative Pd-catalyzed carbon-carbon bond-forming cross-coupling reactions (where X = Cl, Br, or I).

In this chapter we will briefly summarize the literature concerning the application of Pd NPs in Suzuki cross-coupling and hydrogenation and then we will describe our results in these two reactions.

4.1.2. Suzuki Cross-Coupling and Application of Pd NPs as Catalysts

The Suzuki cross-coupling reaction is a powerful method for the synthesis of C-C bonds. Normally it is used for the synthesis of biphenyls and styrenes and the reaction happens between a boronic acid and an aryl halide in the presence of palladium catalyst and base (Scheme 2).[8]

Besides applications in synthesis,[9] its use has become popular even in biology,[10] synthesis of polymers, agrochemicals and advanced materials.[11] The mild reaction conditions required and the commercial availability of the starting materials make the reaction very attractive.

Owing to the importance of these reactions, Suzuki received the 2010 Nobel Prize in Chemistry, along with Richard F. Heck and Ei-ichi Negishi for their contribution to palladium catalyzed cross-couplings in organic synthesis.

[8] a) Vaccaro, A. L.; Lanari, D. Marrocchi, A.; Strappaveccia, G. *Green Chem*. **2014**, *16*, 3680; b) Miyaura, N.; Yamada, K.; Suzuki, A. *Tetrahedron Lett.* **1979**, *20*, 3437.
[9] Soloway, A. H.; Tjarks, W.; Barnum, B. A.; Rong, F.-G.; Barth, R. F.; Codogni, I. M.; Wilson, J. G. *Chem. Rev.* **1998**, *98*, 1515.
[10] Suzuki, A, *J. Organomet. Chem*. **1999**, *576*, 147.
[11] a) Metal-Catalyzed Cross-Coupling Reactions, 2nd Ed. de Meijere, A., Diederich, F., Eds.; Wiley-VCH: Weinheim, 2004; b) Torborg, C.; Beller, *M. Adv. Synth. Catal*. **2009**, *351*, 3027.

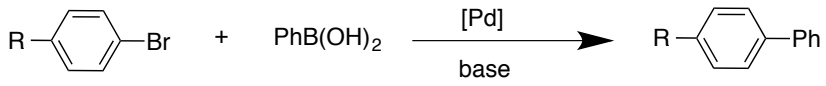

Scheme 2. Suzuki cross-coupling.

Pd(0) or Pd(II) derivatives associated with suitable phosphine-based ligands have been traditionally used for the Suzuki cross-coupling. Figure 1 shows some examples of phosphine ligands that have been employed in this transformation.[12]

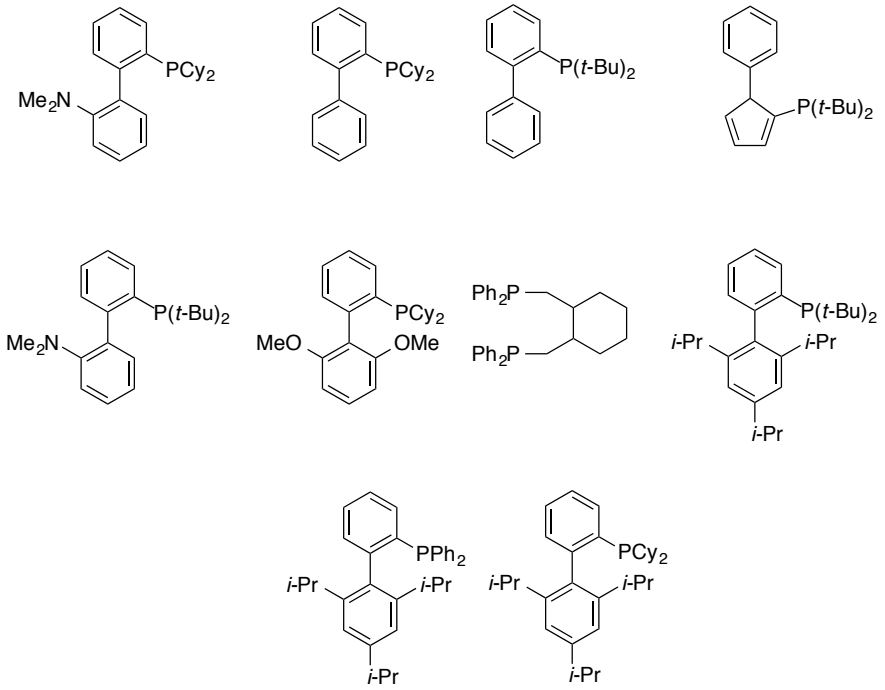

Figure 1. A variety of monodentate and bidentate ligands have been used in conjunction with palladium.

Whereas Pd complexes show excellent catalytic activity, this reaction has some drawbacks such as air sensitivity of these ligands or cost of the palladium complexes.[13] Alternatively, one can think of running phosphine-free Suzuki reactions, using for instance carbene complexes coordinated with palladium. The activity of the catalyst is then affected by the substituents of the carbene ligands. However, preparing larger analogues of these systems can involve a lot of steps.[14]

[12] Phan, N. T. S.; Van Der Sluys, M.; Jones, C. W. *Adv. Synth. Catal.* **2006**, *348*, 609.
[13] a) Navarro, O.; Kaur, H.; Mahjoor, P.; Nolan, S. P. *J. Org. Chem*. **2004**, *69*, 3173; b) Marion, N.; Nolan, S. P. *Acc. Chem. Res*. **2008**, *41*, 1440; c) Li, J. H.; Liu, W. J. *Org. Lett*. **2004**, *6*, 2809; d) Costa, D. P.; Nobre, S. M. *Tetrahedron Lett*. **2013**, *54*, 4582.
[14] a) Li, L.; Zhao, S.; Joshi-Pangu, A.; Diane. M.; Biscoe, M. R. *J. Am. Chem. Soc*. **2014**, *136*, 14027; b) Peh, G.-R.; Kantchev, E. A. B.; Er, J.-C.; Ying, J. Y. *Chem. Eur. J*. **2010**, *14*, 4010; c) Li, S.; Lin, Y.; Cao, J.; Zhang, S. *J. Org. Chem*. **2007**, *72*, 4067; d) Rahimi, A.; Schmidt, A.; *Synlett* **2010**, 1327; e) Bermejo, A.; Ros, A.; Fernández, R.; Lassaletta, J. M. *J. Am. Chem. Soc*. **2008**, *130*, 15798.

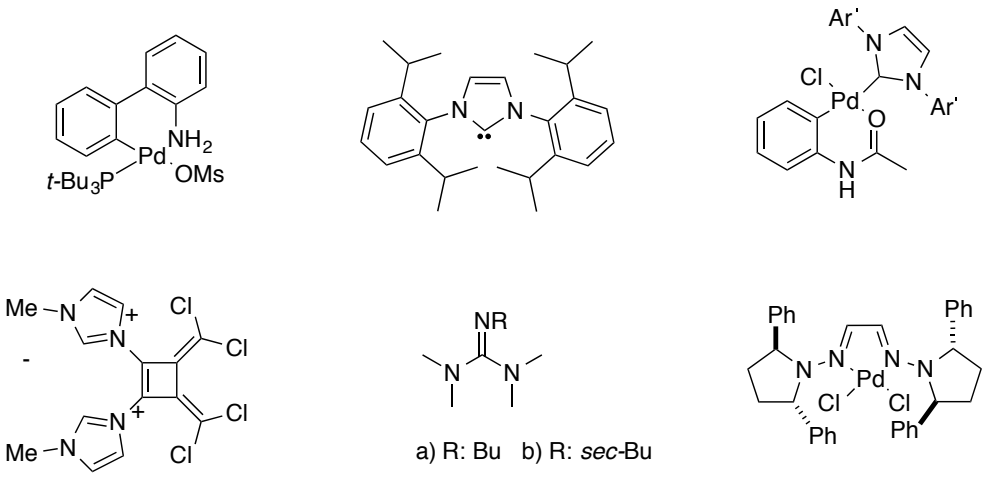

Figure 2. Phosphine-free palladium complexes and ligands.

In this respect, development of Pd NPs in cross-coupling reactions[15] can be advantageous due to their cost effectiveness, allowing ligand free synthesis, simplifying workup procedures and separation final products. However, in most cases the synthesis of Pd NPs requires special conditions like high temperature, stabilizer or sonication.[16] Therefore, preparing Pd NPs under mild conditions is an interesting goal on its own.

In general, homogeneous catalysts are more active and present higher activity and selectivity than heterogeneous ones because of their solubility in the reaction media and uniformity at the molecular level. However, in large scale it is technically difficult and expensive to separate catalysts from the reaction media.[17] In contrast, heterogeneous catalysts provide many advantages that cannot be exploited with homogeneous species such as easy separation from the reaction mixture, recyclability and the possibility to use them in continuous flow processes.[18]

Besides aggregation, the main issue of metal nanoparticles is leaching. This term refers to the process by which the active metal species goes to the liquid phase, causing irreversible deactivation.[19] In pharmaceutical substances there is a strict limit to the amount of heavy metal they can contain.[20] Thus, to improve the greenness of chemical processes, it is important to develop a catalyst which minimizes the leaching of metals.

[15] a) Perez-Lorenzo, M. *J. Phys. Chem. Lett*. **2012**, *3*, 167; b) Das, S. K.; Parandhaman, T.; Pentela, N.; Maidul Islam, A. K. M.; Mandal, A. B.; Mukherjee, M. *J. Phys. Chem. C*. **2014**, *118*, 24623.
[16] a) Baruwati, B.; Guin, D.; Manorama, S. V. *Org. Lett*. **2007**, *9*, 5377; b) Xuan, S.; Zhou, Y.; Xu, H.; Jiang, W.; Leung, K. C.; Gong, X. *J. Mater. Chem*. **2011**, *21*, 1539; c) Li, Z.; Liu, J.; Huang, Z.; Yang, Y.; Xia, C.; Li, F. *ACS Catal*. **2013**, *3*, 839.
[17] Budarin, V. L.; Shuttleworth, P. S.; Clark, J. H.; Luque, R. *Curr. Org. Synth.* **2010**, *7*, 614.
[18] a) Zielinska, A.; Skulski, L. *Tetrahedron Lett*. **2004**, *45*, 1087; b) Scott, R. W. J.; Wilson, O. M.; Crooks, R. M. *J. Phys. Chem. B* **2005**, *109*, 692; c) Huang, W.; Kuhn, J. N.; Tsung, C.-K.; Zhang, Y.; Habas, S. E.; Yang, P.; Somorjai, G. A. *Nano Lett*. **2008**, *8*, 2027.
[19] Keav, S.; Barbier, J.; Duprez, D.; *Catal. Sci. Technol.* **2011**, *1*, 342.
[20] Garrett, C. E.; Prasad, K. *Adv. Synth. Catal*. **2004**, *346*, 889.

To solve these issues, metal nanoparticles can be stabilized on solid supports such as zeolites,[21] silica,[22] ionic liquid and ionic polymer,[23] carbon,[24] carbon nanotubes[25] and carbon-coated nanoparticles.[26]

In this regard, we will mention some examples of application of catalytic Pd NPs in Suzuki cross-coupling.

Khinast *et al*. investigated Pd leaching in Pd/C catalyzed Suzuki coupling. They realized oxidative addition of aryl bromides is the main reason behind Pd leaching. Indeed the oxidative addition of aryl borates is another step which causes the Pd leaching.[27]

El-Sayed *et al*. have studied Suzuki cross-coupling reaction regarding to the concentration and the size of Pd nanoparticles. In their initial publication, palladium nanoparticles were stabilized by poly(*N*-vinyl-2-pyrrolidone) (PVP).[28] The Suzuki coupling of aryl iodides with phenylboronic acid in aqueous media was studied to evaluate their catalytic activity. Fluorescence intensity of the biphenyl product was followed during the reaction and the initial reaction rate was found to depend linearly on the concentration of Pd catalyst.

In the second paper by the same authors, PVP-stabilized Pd NPs with different sizes were prepared and evaluated in the Suzuki reaction between phenyl boronic acid and iodobenzene.[29] The study of the initial rate of the reaction showed the activity of the catalyst decreased when the size of nanoparticle increased with one exception for smallest nanoparticles (activity of the catalyst: Pd (3.9 nm) > Pd (3.0 nm) ≈ Pd (5.2 nm) > Pd (6.6 nm)). As expected, when the particles size decreases, the surface area increases, consequently improving the activity of catalyst. In the case of the smallest nanoparticles, catalyst poisoning could be taking place.

[21] a) Yang, H.; Wang, Y.; Qin, Y.; Chong, Y.; Yang, Q.; Li, G.; Zhang, L.; Li. W. *Green Chem.* **2011**, *13*, 1352; b) Yang, H.; Han, X.; Ma, Z.; Wang, R.; Liu, J.; Ji, X. *Green Chem*. **2010**, *12*, 441; c) Yang, H.; Han, X.; Li, G.; Wang, Y. *Green Chem*. **2009**, *11*, 1184.

[22] a) Kume, Y.; Qiao, K.; Tomida, D.; Yokoyama, C. *Catal. Commun*. **2008**, *9*, 369; b) Karimi, B.; Elhamifar, D.; Clark, J. H.; Hunt, A. J. *Org. Biomol. Chem*. **2011**, *9*, 7420; c) Gruttadauria, M.; Liotta, L. F.; Salvo, A. M. P.; Giacalone, F.; La Parola, V.; Aprile, C.; Noto, R. *Adv. Synth. Catal*. **2011**, *353*, 2119.

[23] a) Zhao, D.; Fei, Z.; Ang, W. H.; Dyson, P. J. *Small* **2006**, 2, 879; b) Yang, X.; Fei, Z.; Zhao, D.; Ang, W. H.; Li, Y.; Dyson, P. J. *Inorg. Chem*. **2008**, *47*, 3292; c) Zeng, Y.; Wang, Y.; Xu, Y.; Song, Y.; Jiang, J.; Jin, Z. *Catal. Lett*. **2013**, *143*, 200; d) Zhu, W.; Yu, Y.; Yang, H.; Hua, L.; Qiao, Y.; Zhao, X.; Hou, Z. *Chem. Eur. J*. **2013**, *19*, 2059.

[24] Yang, J.; Tan, X.; Wang, Y.; Wang, X. *J. Porous Mater*. **2013**, *20*, 501.

[25] Chun, Y. S.; Shin, J. Y.; Song, C. E.; S.-G. Lee, *Chem. Commun*. **2008**, *8*, 942.

[26] Kainz, Q. M.; Linhardt, R.; Grass, R. N.; G, Vilé.; Pérez-Ramírez, J.; Stark, W. J.; Reiser, O. *Adv. Funct. Mater*. **2014**, *24*, 2020.

[27] Chen, J-S.; Vasiliev, A. N.; Panarello, A. P.; Khinast, J. G. *Appl. Cat. A: General* **2007**, 325, 76.

[28] Li, Y.; Hong, X. M.; Collard, D. M.; El-Sayed, M. A. *Org. Lett*. **2000**, *2*, 2385.

[29] Li, Y.; Boone, E.; El-Sayed, M. A. *Langmuir* **2002**, *18*, 4921**.**

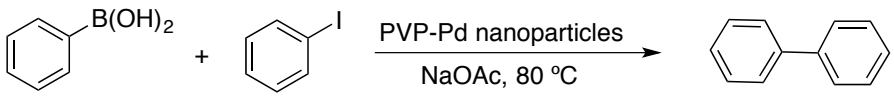

Scheme 3. Suzuki reaction of phenylboronic acid and iodobenzene.

Another efficient catalyst for Suzuki cross-coupling was developed by Diao *et al.*[30] First, magnetic Fe_3O_4@C (MFC) composites were prepared by carbonization of glucose in the presence of Fe_3O_4 nanoparticles. Then Pd nanoparticles were immobilized onto the Fe_3O_4@C composites. (Scheme 4). This catalyst was tested for the Suzuki reaction of aryl halides and phenylboronic acid. From a practical point of view, the catalyst was recovered with an external magnet and reused again until 5 runs without loss of activity. After the fifth cycle, they report 0.2% in Pd loss according to ICP measurements.

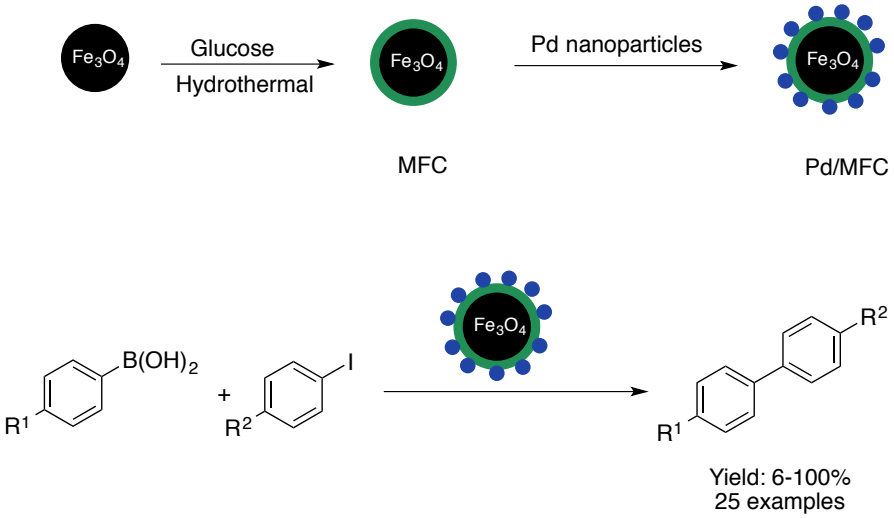

Scheme 4. Synthesis and application of the Pd/MFC catalyst in the Suzuki coupling reaction.

In a different approach, Fe_3O_4 nanoparticles were functionalized with dopamine (DA), then Pd^{II} and Pd^0 were stabilized on Fe_3O_4/DA based on the metal adsorption and reduction procedure (Scheme 5).[31] According to the authors the covalent bond between Pd and amine group in dopamine on the surface of Fe_3O_4 nanoparticles avoids Pd leaching. Indeed, dopamine increases the dispersibility of NPs in aromatic solvents. These two catalysts were applied in Suzuki reaction to compare their activity. As an outcome, the catalyst with Pd^{II} showed better results than its Pd^0 counterpart. Agglomeration of Pd^0 was considered a possible explanation for the decrease in activity.

[30] Zhu, M.; Diao, G. *J. Phys. Chem. C.* **2011**, *115*, 24743.
[31] Long, Y.; Liang, K.; Niu, J.; Tong, X.; Yuan, B.; Ma, J. *New J. Chem*. **2015**, *39*, 2988.

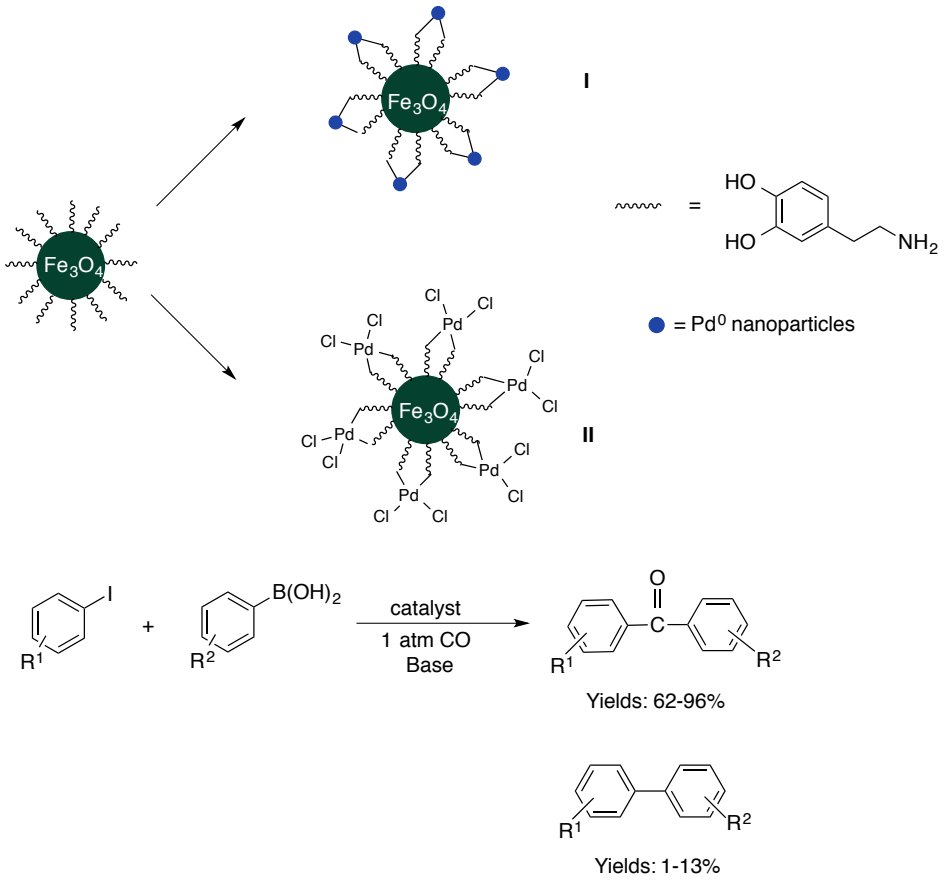

Scheme 5. Synthesis of Fe_3O_4/DA-Pd^{II} and Fe_3O_4/DA-Pd^0 catalysts and application in the Suzuki carbonylative cross-coupling reaction.

Li *et al.* prepared Fe@Pd core-shell nanoparticles on activated carbon as a versatile catalyst for the Suzuki cross-coupling reaction.[32] They synthesized the catalyst by a two step process: first formation of Fe NPs on activated carbon, followed by formation of Pd NPs by adding $PdCl_2$ to Fe/C containing solution and using outer-layer of the Fe core to reduce Pd^{2+} to Pd^0. The catalyst was used for Suzuki-Miyaura coupling of aryl halides with phenylboronic acid (13 examples, 20-100% yield). Also the catalyst was reused for 5 times without a significant decrease in the activity.

4.1.3. Catalytic Hydrogenation

The reduction of unsaturated compounds is a crucial step in the synthesis of many organic molecules. This transformation is thus very important in total synthesis, industrial production and pharmaceutical applications (Scheme 6).[33] For instance, it could be mentioned that 25% of all chemicals produced in industry contain a catalytic hydrogenation in at least one step.[34]

[32] Tang, W.; Li, J.; Jin, X.; Sun, J.; Huang, J.; Li, R. *Catal. Commun.* **2014**, *43*, 75.
[33] Tran, A. T.; Huynh, V. A.; Friz, E. M.; Whitney, S. K.; Cordes, D. B. *Tetrahedron Lett.* **2009**, *50*, 1817.
[34] Vilé, G.; Albani, D.; Almora-Barrios, N.; López, N.; Pérez-Ramírez, J. *ChemCatChem* **2016**, *8*, 21.

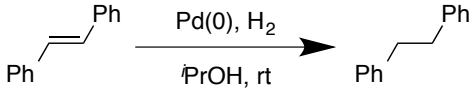

Scheme 6. Catalytic hydrogenation.

Lately, different magnetically recoverable metal nanocatalysts have been investigated for the hydrogenation of alkynes. Fe-based nanocatalysts perform well, albeit they have low selectivity for the alkene product.[35]

Pd nanoparticles supported on MNPs modified with ionic liquids showed high activity and selectivity for the (*Z*)-alkene in the hydrogenation of diphenylacetylene under harsh conditions.[36] Scott *et al.* stabilized Pd NPs with tetraalkylphosphonium halide ionic-liquid (IL) solvents and applied them in the hydrogenation of olefinic alcohols, aromatic nitro compounds, α,β-unsaturated carbonyls and alkynes. The Pd NPs showed good activity but in the case of cinnamaldehyde they had low selectivity for the alkene.[37] Later, investigation in catalytic hydrogenation moved towards the application of another support such as C, polymer or Co/C nanobeads (NBs) to make the catalyst more efficient.

Wai *et al*. used carbon nanotubes as a support for Pd nanoparticles.[38] They deposited Pd nanoparticles onto the surface of multiwall carbon nanotubes (MWCNT) by hydrogen reduction of Pd(II)-β-diketone precursor. The resulting catalyst was applied in the hydrogenation of *trans*-stilbene in liquid CO_2. 1,2-Diphenylethane was achieved as product with 96% conversion after 10 minutes.

Wang *et al.* synthesized two different 1,2,3-triazolyl-containing porous organic polymers. In one case the synthesis was based on the click reaction (CPP-C), and the other one on the Yamamoto coupling reaction (CPP-Y).[39] Ultrafine palladium nanoparticles were immobilized inside the pores using $Pd(OAc)_2$ solution and the reduction with a stream of H_2 /N_2. Both of them have a good catalytic activity in hydrogenation of olefins, however they showed different behavior in recyclability. *n*-Hexane was used for recyclability test and Pd@CPP-C reached 87% yield in second run and 64% in the fourth one. However, for Pd@CPP-Y the catalyst did not have a significant decrease in activity until the seventh run. After the evaluation of TEM images for both catalysts, some agglomeration was observed. In the case of Pd@CPP-Y, the catalyst showed more prevention against agglomeration because of higher surface area and larger pore

[35] a) Rangheard, C.; Fernandez, C. de Julian.; Phua, P.-H.; Hoorn, J.; Lefort, L.; de Vries, J. G. *Dalton Trans*. **2010**, *39*, 8464; b) Stein, M.; Wieland, J.; Steurer, P.; Tölle, F.; Mülhaupt, R.; Breit, B. *Adv. Synth. Catal*. **2011**, *353*, 523.
[36] Abu-Reziq, R.; Wang, D.; Post, M.; Alper, H. *Adv. Synth. Catal*. **2007**, *349*, 2145.
[37] Banerjee, A.; Theron, R.; Scott, R. W. J. *ChemSusChem*. **2012**, *5*, 109.
[38] Ye, X, R.; Linb, Y.; Wai, C. M. *Chem. Commun*. **2003**, 642.
[39] Li, L.; Zhao, H.; Wang, R. *ACS Catal*. **2015**, *5*, 948.

volume.

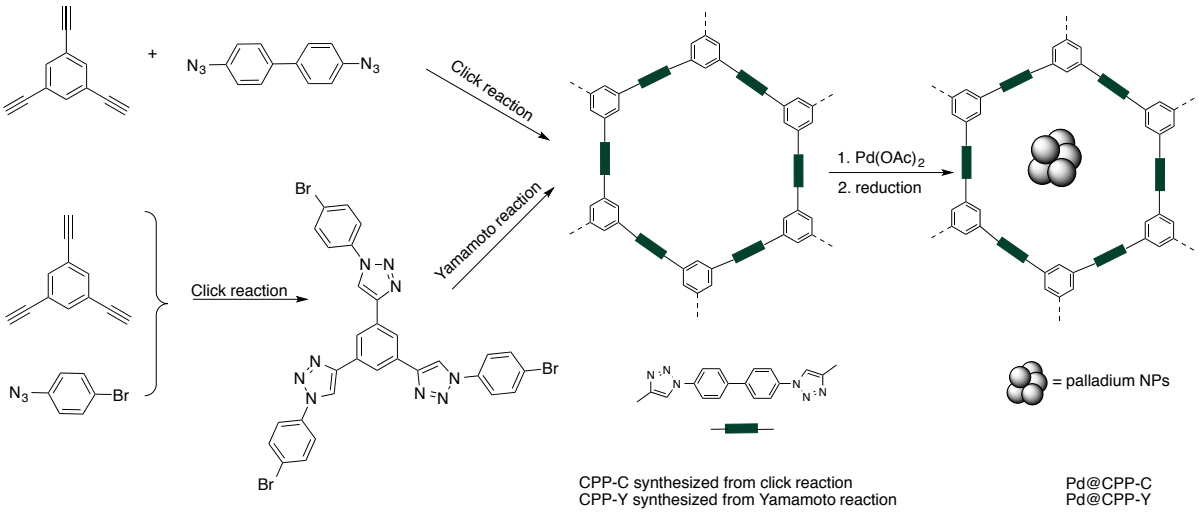

Scheme 7. Synthesis of Pd@CPP-C and Pd@CPP-Y.

In the group of Prof. Reiser, Pd nanoparticles have been immobilized on the surface of Co/C nanobeads using $Pd_2(dba)_3 \cdot CHCl_3$ by microwave irradiation (Scheme 8). The resulting catalyst was used in the hydrogenation of alkenes. Results showed that the catalyst is more efficient than Pd/C or Pd@CNT. It is worth highlighting that the catalyst could be prepared very easily from commercially available Co/C nanoparticles and $Pd_2(dba)_3 \cdot CHCl_3$. Indeed, the catalyst separation was simplified using magnetic decantation.[26]

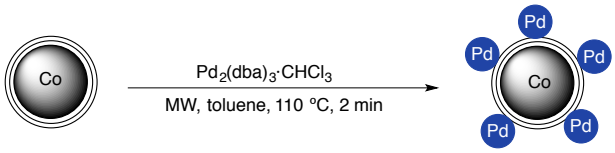

Scheme 8. Synthesis of Pd@Co/C nanocomposites.

4.1.4. Microporous Organic Polymers

Microporous organic polymers (MOPs) are a new category of porous material, which consists of C, H, N, and O with nanoscale porosity.[40] They have special advantages like large surface area, low skeletal density and high chemical stability,[41] which make them useful in light harvesting,[42] gas separation, storage[43] and catalysis.[44]At the end of the 1990s, Davankov resins[45] were

[40] Jiang, X.; Zhao, W.; Wang, W.; Zhang, F.; Zhuang, X.; Han, S.; Feng, X. *Polym. Chem*. **2015**, *6*, 6351.
[41] Li, B.; Gong, R.; Wang, W.; Huang, X.; Zhang, W.; Li, H.; Hu, C.; Tan, B. *Macromolecules* **2011**, *44*, 2410.
[42] Sun, L.; Liang, Z.; Yu, J .; Xu, R. *Polym. Chem*. **2013**, *4*, 1932.
[43] a) Dawson, R.; Stockel, E.; Holst, J. R.; Adams, D. J.; Cooper, A. I. *Energy Environ. Sci*. **2011**, *4*, 4239; b) Song, W. C.; Xu, X. K.; Chen, Q.; Zhuang, Z. Z.; Bu, X. H. *Polym. Chem*. **2013**, *4*, 4690.
[44] a) Kaur, P.; Hupp, J. T.; Nguyen, S. T. *ACS Catal*. **2011**, *1*, 819; b) Zhang, Y.; Riduan, S. N. *Chem. Soc. Rev*.

developed based on hypercrosslinking of linear polystyrene via Friedel-Crafts alkylation (Scheme 9). These materials contain mostly small pores, the production of hydrogen halide as byproduct being their main disadvantage. [46]

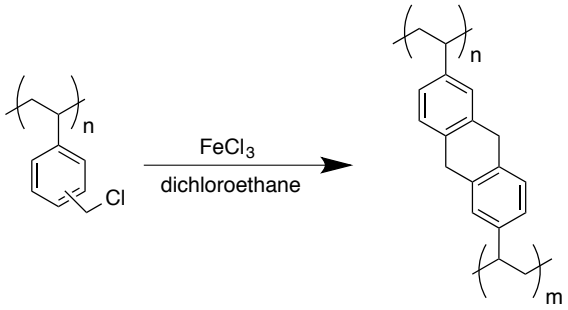

Scheme 9. Synthesis of hypercrosslinked styrenic polymer from poly-(vinylbenzyl chloride) gel-type resin precursor.

Afterwards, different kinds of MOPs have been investigated such as porous aromatic frameworks[47] (PAFs), produced by various cross-coupling reactions of aromatic compounds, polymers of intrinsic microporosity[48] (PIMs) with a dioxane unit or covalent triazine-based frameworks[49] (CTFs). With the synthesis of these polymers, the authors attempted to prepare more environmentally friendly materials with potential in catalysis or gas storage.

Tan *et al.* have developed an efficient strategy to synthesize MOPs,[41] based on simple one-step Friedel-Crafts reactions using a low cost cross-linker with ordinary aromatic compounds and the only byproduct is methanol (scheme 10).

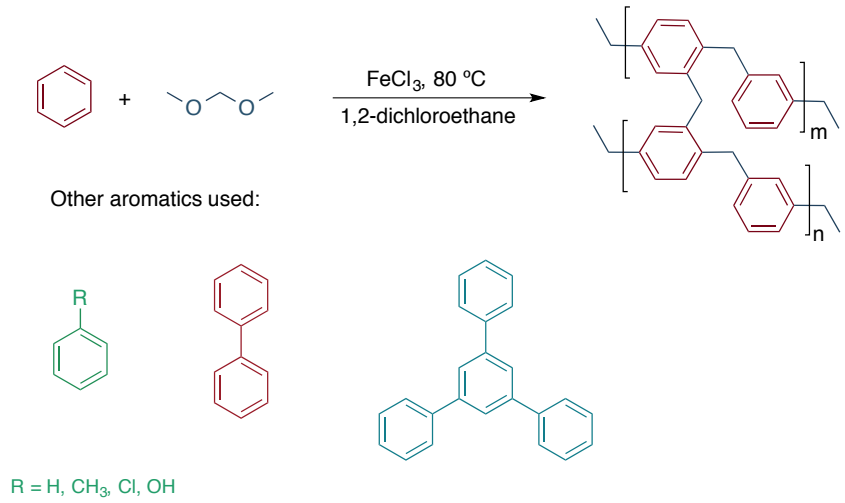

Scheme 10. Synthesis of microporous organic polymer.

2012, *41*, 2083.
[45] Davankov, V. A.; Rogozhin, S. V.; Tsyurupa, M. P. 3,729,457, **1971**.
[46] Lee, J-Y.; Wood, C. D.; Bradshaw, D.; Rosseinsky, M. J.; Cooper, A. I. *Chem. Commun*. **2006**, 2670.
[47] Ben, T.; Ren, H.; Ma, S.; Cao, D.; Lan, J.; Jing, X.; Wang, W.; Xu, J.; Deng, F.; Simmons, J.; Qiu, S.; Zhu, G. *Angew. Chem. Int. Ed*. **2009**, *48*, 9457.
[48] McKeown, N. B.; Gahnem, B.; Msayib, K. J.; Budd, P. M.; Tattershall, C. E.; Mahmood, K.; Tan, S.; Book, D.; Langmi, H. W.; Walton, A. *Angew. Chem. Int. Ed.* **2006**, *118,* 1836.
[49] a) Kuhn, P.; Thomas, A.; Antonietti, M. *Macromolecules* **2009**, *42*, 319; b) Zhu, X.; Tian, C.; Mahurin, S. M.; Chai, S.-H.; Wang, C.; Brown, S.; Veith, G. M.; Luo, H.; Liu, H.; Dai, S. *J. Am. Chem. Soc*. **2012**, *134*, 10478.

4.1.5. Aim of the Project

The main advantage of using magnetic nanoparticles as support is that the recovery of Pd NPs can be simply done by magnetic decantation. However, the catalytic activity of this material is compromised by the agglomeration of Pd NPs in the surface of the carbon-coated NPs.

Therefore, the merging of porous materials and NP technology has been an impressive area of interdisciplinary research.[50] Porous materials with high surface area afford a confined limited space for formation of NPs. In this way, they prevent NPs from agglomeration and their channels can assist mass transfer for an efficient catalysis.[51]

In this project, a new hybrid material will be presented based on the Co/C nanobeads, polymer and Pd nanoparticles.

To this aim, microporous aryl polymer networks with encapsulated palladium nanoparticles catalysts and commercially available Co/C nanobeads are synthesized through a low cost and facile strategy, resulting in a hybrid material that kills three birds with one stone: (1) forming a highly porous and hydrophobic environment for organic synthesis using toluene as building block; (2) stabilizing Pd catalysts in front of aggregation and/or leaching via their confinement within chemically stable polymers; (3) allowing efficient recyclability thanks to their magnetic properties.

Even if a large number of research studies on hydrogenation and Suzuki coupling reactions have been conducted, there is still a lot of interest to identify Pd catalysts that are cost effective, reusable and recoverable.

Present investigations are mainly focused on the development of an efficient way to synthesize microporous polymers which encapsulate Co/C and Pd nanoparticles.

4.2. Preparation of the Catalytic Material

In 2007, Stark *et al*. reported the preparation of novel ferromagnetic carbon-coated cobalt nanobeads (denoted as Co/C NBs), which are synthesized via reducing flame-spray pyrolysis on large scale.[52] These particles have been successfully used in a variety of applications such as purification of blood,[53] extraction of vitamins and contaminants from aqueous solutions[54] or

[50] Gascon, J.; Aktay, U.; Hernandezalonso, M.; Vanklink, G.; Kapteijn, F. *J. Catal*. **2009**, *261*, 75.

[51] a) Cárdenas-Lizana, F.; Berguerand, C.; Yuranov, I.; Kiwi-Minsker, L. *J. Catal*. **2013**, *301*, 103; b) Li, X.-H.; Antonietti, M. *Chem. Soc. Rev*. **2013**, *42*, 6593.

[52] Grass, R. N.; Athanassiou, E. K.; Stark, W. J. *Angew. Chem. Int. Ed.* **2007**, *46*, 4909.

[53] a) Herrmann, I. K.; Urner, M.; Koehler, F. M.; Hasler, M.; Roth-Z'Graggen, B.; Grass, R. N.; Ziegler, U.; Beck-Schimmer, B.; Stark, W. J. *Small* **2010**, *6*, 1388; b) Herrmann, I. K.; Bernabei, R. E.; Urner, M.; Grass, R. N.; Beck-Schimmer, B.; Stark, W. J. *Nephr. Dial. Transpl.* **2011**, *26*, 2948.

[54] a) Rossier, M.; Koehler, F. M.; Athanassiou, E. K.; Grass, R. N.; Aeschlimann, B.; Günther, D.; Stark, W. J. *J. Mater. Chem*. **2009**, *19*, 8239; b) Rossier, M.; Schaetz, A.; Athanassiou, E. K.; Grass, R. N.; Stark, W. J. *Chem. Eng. J.* **2011**, *175*, 244; c) Fuhrer, R.; Herrmann, I. K.; Athanassiou, E. K.; Grass, R. N.; Stark, W. J. *Langmuir* **2011**, *27*, 1924; d) Rossier, M.; Schreier, M.; Krebs, U.; Aeschlimann, B.; Fuhrer, R.; Zeltner, M.; Grass, R. N.; Günther, D.;

mercury extraction from water,[55] as well as catalytic applications.[56] Co/C NBs have several graphene layers which protect metal core from oxidation (Figure 3). These particles can be functionalized with different linkers using diazonium chemistry.

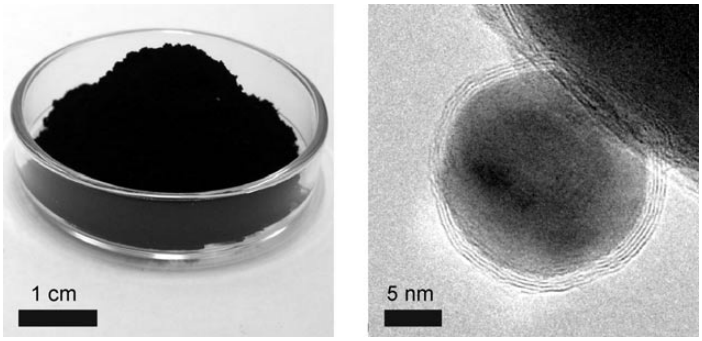

Figure 3. Carbon-coated NPs and TEM pictures. Picture taken from reference 52.

4.2.1 Synthesis of Aromatic Microporous Polymers Encapsulated with Co/C Nanobeads and Pd(0) Nanoparticles

In order to prepare highly magnetic MOPs of polymer-Pd-Co/C composites, the surface of Co/C nanobeads is covalently functionalized with phenylmethane by thermal decomposition of the diazonium salt derived from 4-aminotoluene. This strategy introduces phenyl moieties on the surface of **1** as a starting point for growing a bakelite type polymer on the nanoparticle graphene layer.

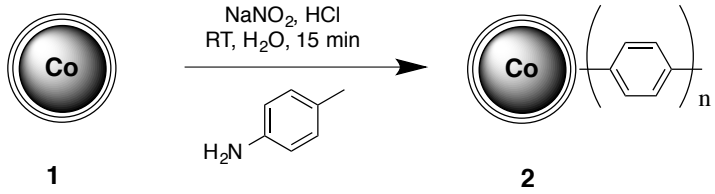

Scheme 11. Grafting of the diazonium salt of 4-aminotoluene onto carbon-coated cobalt particles.

Thus, the functionalized nanoparticles **2** are used as a substrate to knit aromatic toluene building blocks into microporous polymers **3**, employing formaldehyde dimethyl acetal (FDA) as an external cross-linker.

Stark, W. J. *Sep. Purif. Technol.* **2012**, *96*, 68; e) Kainz, Q. M.; Späth, A.; Weiss, S.; Michl, T. D.; Schätz, A.; Stark, W. J.; König, B.; Reiser. O. *ChemistryOpen* **2012**, *1*, 125.

[55] Fernandes, S.; Eichenseer, C. M.; Kreitmeier, P.; Rewitzer, J.; Zlateski, V.; Grass, R. N.; Stark, W. J.; Reiser, O. *RSC Adv.* **2015**, *5*, 46430.

[56] Schätz, A.; Grass, R. N.; Stark, W. J.; Reiser, O. *Chem. Eur. J.* **2008**, *14*, 8262.

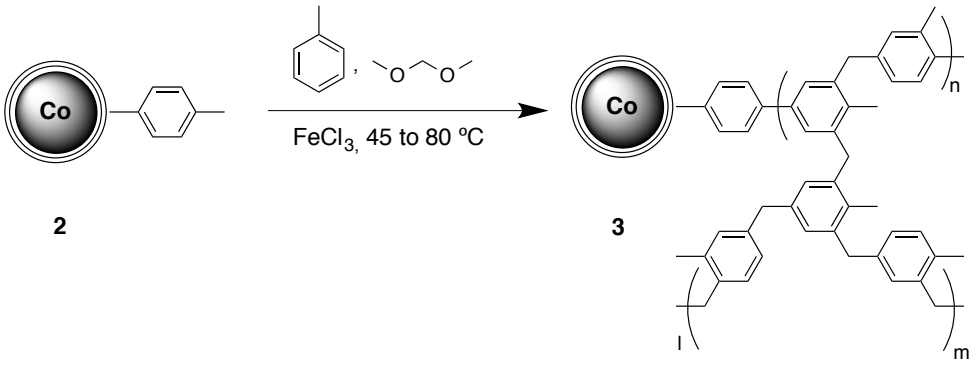

2 3

Scheme 12. Synthesis of Co/C MOP.

Owing to the super hydrophobic nature of the resulting aromatic polymer, catalyst precursors such as $Pd_2(dba)_3 \cdot CHCl_3$ in toluene solution can be swallowed into the polymer network. Pd nanoparticles were synthesized inside the pores of the polymer using microwave irradiation in 2 minutes.

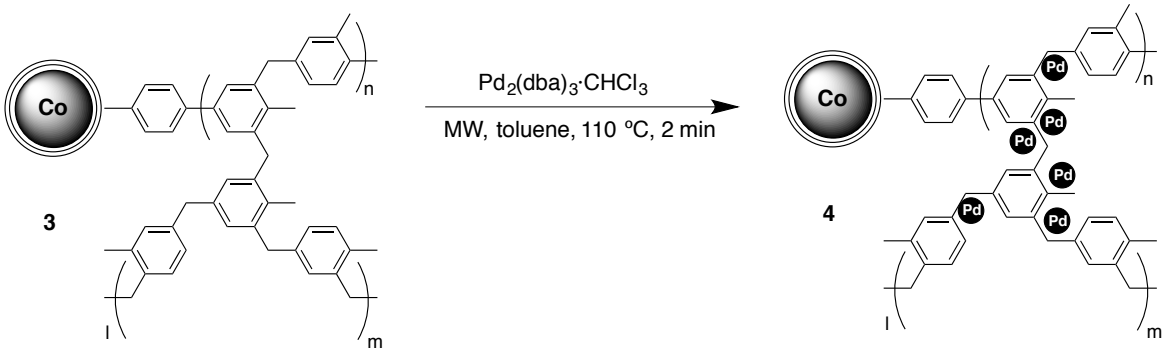

3 4

Scheme 13. Microwave-synthesis of Pd@Co/C MOP.

4.2.2. Characterization of the Hybrid Materials

Judging from transmission electron microscopy (TEM) images, it is observed that carbon-coated cobalt nanoparticles and Pd nanoparticles are surrounded with polymer; however, there is no agglomeration of Pd nanoparticles (Figure 4).

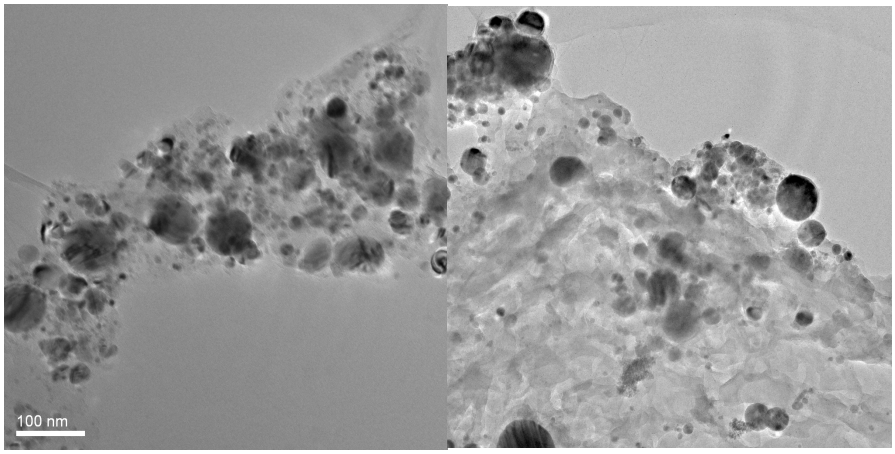

Figure 4. TEM Images of catalyst **4**.

Energy Dispersive X-Ray Analysis (EDX) in Figure 5 confirmed the presence of Co and Pd as expected.

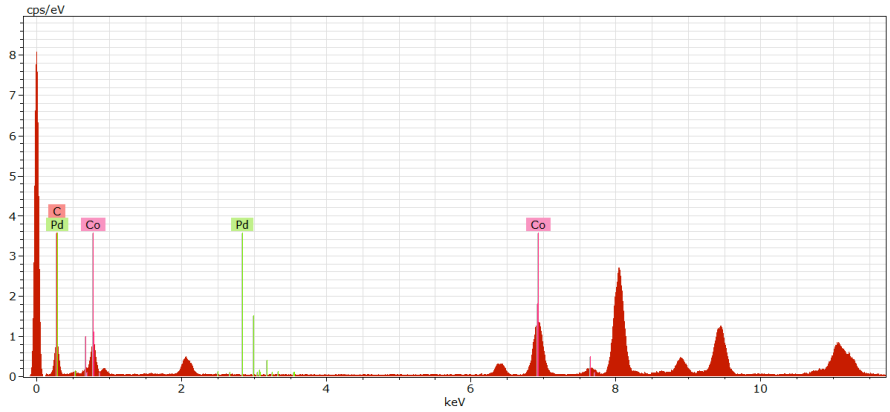

Figure 5. EDX analysis of catalyst 4.

In addition this hybrid material was characterized with thermal gravimetric analysis (TGA). It is mainly noticeable that the polymer is stable until 200 °C and cobalt carbon-coated nanoparticles are stable until 500 °C (Figure 6). This will be useful considering the conditions that will be used later for hydrogenation and Suzuki cross-coupling reaction.

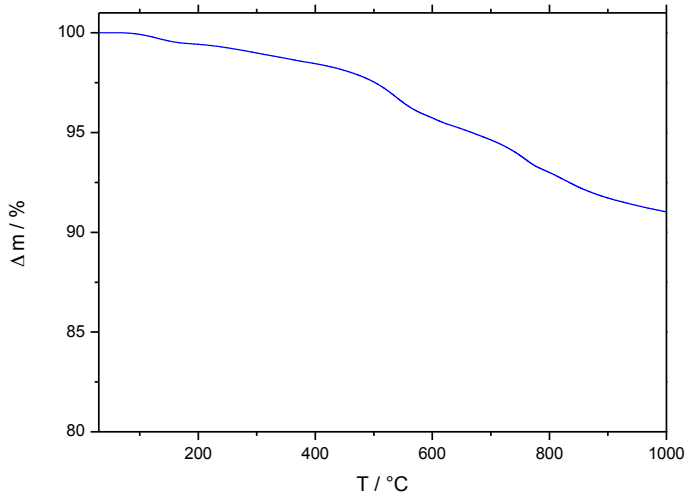

Figure 6. TGA weight loss curves for hybrid material **4**.

The hybrid material is also separated in a few seconds with an external magnet. Thus, the polymerization does not have any negative effect on magnetization.

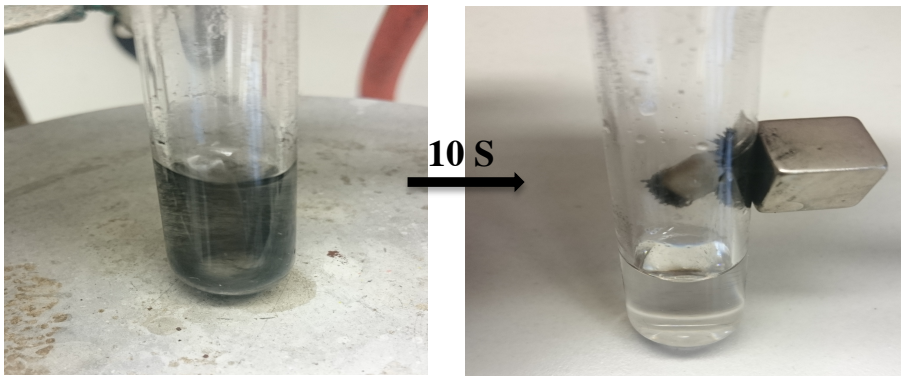

Figure 7. Separation of hybrid material with an external magnet.

4.3. Application of Pd@Co/C MOP in the Hydrogenation of *trans*-Stilbene

The hybrid material **4** was tested in the hydrogenation of alkenes to evaluate its catalytic activity (Figure 8). First, some screening was carried out to select the appropriate solvent. *trans*-Stilbene was selected as a substrate and it was hydrogenated with 0.1 mol% of catalyst.

In a polar solvent like MeOH, the hybrid material did not have a good dispersibility; the results showed the conversion in ^{i}PrOH is better than in some apolar solvents like $CHCl_3$ and toluene.

Figure 8. Hydrogenation system for stilbene.

Table 1. Hydrogenation of *trans*-stilbene using Pd@Co/C MOP with different solvents.

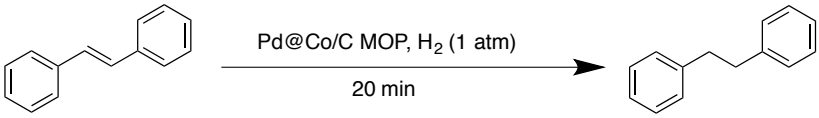

entry	solvent	conversion [%][a)]
1	MeOH	3
2	toluene	12
3	$CHCl_3$	2
4	DCM	14
5	^{i}PrOH	38

trans-Stilbene (0.2 mmol) in 4 ml solvent was hydrogenated by 0.2 µmol Pd cat. (0.1 mol% Pd) adding dodecane as internal standard [a)] Conversion determined by GC analysis using internal standard.

Afterwards, a series of experiments were performed to determine the optimal reaction time and catalyst loading (Table 2). After 60 min with 0.2 mol% catalyst full conversions were achieved. For the sake of comparison, a background reaction was studied without using any Pd catalyst and no conversion was observed.

Table 2. Hydrogenation of *trans*-stilbene using Pd@Co/C MOP at different times and catalyst loadings.

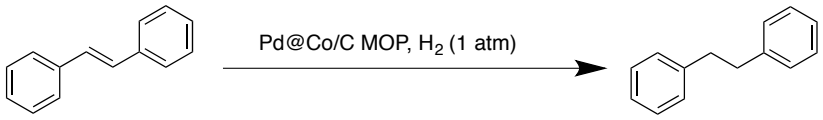

entry	Pd [mol%]	time [min]	conversion [%][a)]
1	0.1	20	38
2	0.1	40	59
3	0.1	80	>99
4	0.2	40	69
6	0.2	60	>99

trans-Stilbene (0.2 mmol) in 4 ml solvent was hydrogenated by Pd cat. adding dodecane as internal standard [a)] Conversion determined by GC analysis using internal standard.

4.3.1. Evaluation of the Hydrogenation Substrate Scope

In order to evaluate the catalytic activity of this hybrid material with other substrates, various olefins and a nitro compound were hydrogenated under the same conditions.

Phenylacetylene (Table 3, entries 2, 3) reacted in shorter times because of the effect of the aromatic ring. The reaction can be stopped at the alkene or brought to ethylbenzene with full conversion in 50 minutes.

Benzalacetone (Table 3, entry 4) was hydrogenated at slower rate than stilbene, probably due to the presence of a conjugated ketone that stabilizes the system.

In the case of 1-methylcyclohexene (Table 3, entry 6) hydrogenation is more difficult than with other substrates because of the donor alkyl group.

Table 3. Hydrogenation of olefins and a nitroarene compound by Pd@Co/C MOP

entry	substrate	product	t [min]	conversion [%][a)]
1	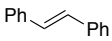	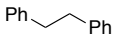	100	100
2	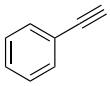	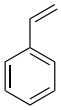	10	100
3	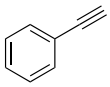	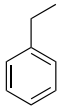	50	100
4	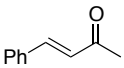	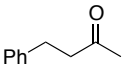	150	100
5	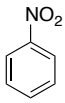	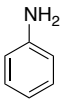	150	100
6			150	48
7	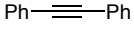	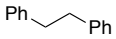	20	100

Substrates (0.2 mmol) were hydrogenated with 0.2 mol% Pd@Co/C MOP in 4 mL ^{i}PrOH.
[a)]Conversion determined by GC analysis using internal standard.

4.3.2. Recycling and Leaching Tests in the Hydrogenation

After examining the activity of the catalyst for different substrates, the most important aspect for a heterogeneous catalyst is the recyclability, which is crucial for practical applications.

In order to check this parameter, the hydrogenation experiment was done in a large scale with 0.2 mol% catalyst. All reactions were checked after 100 min and also evaluated to establish the time required to reach full conversion.

The separation was done with an external magnet which was placed next to the reaction flask for a few seconds, then the product solution was transferred to another flask and the catalyst was used for the next run. Clearly, this method is much more convenient than separation of other classic support such as SiO_2, zeolites or CNTs due to easy magnetic separation.

Table 4. Recyclability for hydrogenation of *trans*-stilbene by Pd@Co/C MOP

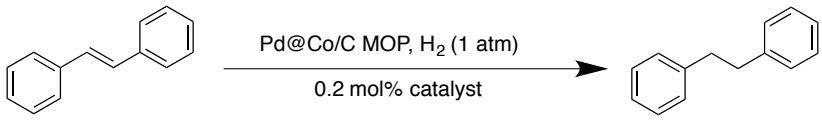

run	conversion after 100 min [%][a]	TOF [h^{-1}]	time to full conversion [min]	Pd leaching [ppm][b]	Co leaching [ppm][b]
1	100	300	100	11	18
2	100	300	100	9	26
3	74	223	220	18	25
4	53	160	260	15	36
5	53	160	340	13	33
6	28	83	400	20	33

Repetitive hydrogenation of *trans*-stilbene (0.5 mmol) using 0.2 mol% Pd-catalyst. [a)] Conversion determined by GC analysis using internal standard. [b)] Determined by ICP measurement.

4.4. Suzuki Cross-Coupling with Pd@Co/C MOP

In a first attempt to classify the catalytic activity, the new hybrid material was tested for Suzuki coupling between iodobenzene and phenylboronic acid. It was observed that increasing the catalyst loading, the yield increased to reach 89%.

Table 5. Suzuki cross-coupling with different catalyst loadings.

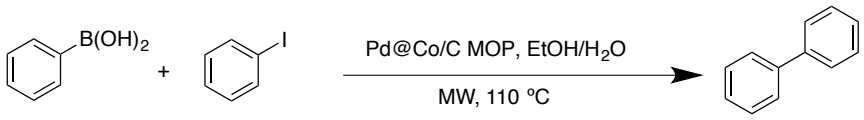

entry	Pd [mol%]	t [h]	yield [%][a)]
1	0.3	3	65
2	0.5	3	89

K_3PO_4 0.25 mmol, iodobenzene 0.1 mmol, phenylboronic acid 0.15 mmol. [a)] Determined by ^1H NMR analysis using an internal standard.

With 4-methoxy-substituted halogenated benzenes the reaction was faster because of the electron donating effect of methoxy group which facilitates the oxidative addition step. In the case of 4-iodoanisole the reaction is faster than with 4-bromoanisole as expected.

Table 6. Suzuki cross-coupling with different 4-methoxy haloarenes.

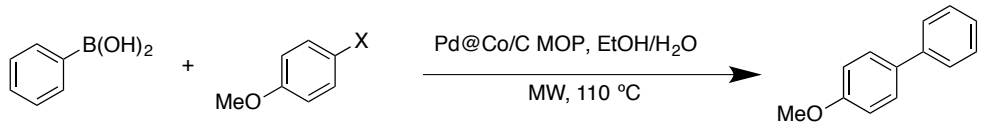

entry	X	Pd [mol%]	t [min]	Yield [%][a)]
1	I	0.5	10	93
2	Br	0.5	120	54

K_3PO_4 0.25 mmol, 4-methoxy haloarene 0.1 mmol, phenylboronic acid 0.15mmol. [a)] Determined by ^1H NMR analysis using an internal standard ($CHBr_3$).

The well established lower reactivity of bromide is due to the stronger C-Br bond (bond dissociation energies for Ph-X: Br: 81 kcal mol^{-1}; I: 65 kcal mol^{-1}) which is reflected in slower oxidative addition.

To evaluate the recyclability of the new hybrid material for Suzuki cross-coupling reaction, the reaction between 4-iodoanisole and phenylboronic acid was chosen as a model. For the first five runs, the reaction had a constant yield around 90%; however in the sixth run, the yield dropped to 77%.

Table 7. Recyclability for Suzuki cross-coupling.

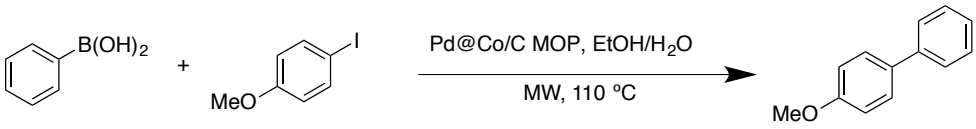

Run	TOF [h^{-1}]	Yield[%][a]	Pd leaching [ppm][b]	Co leaching [ppm][b]
1	1116	93	35	12
2	1092	91	23	83
3	1032	89	19	9
4	1032	89	13	2
5	1125	90	17	124
6	963	77	15	20

Catalyst 0.5 mol%, K_3PO_4 0.75 mmol, 4-iodoanisole 0.3 mmol, phenylboronic acid 0.45 mmol [a)] determined by ^1H NMR analysis using an internal standard. [b)] Determined by ICP measurement.

Due to the interest in applying Suzuki cross-couplings in the pharmaceutical industry, minimizing the amount of Pd in the product is getting more important. Further research focused then on the preparation of different supports to decrease the amount of Pd leaching. Thus, we decided to undertake the study of the influence of the polymer structure in the amount of Pd leaching.

4.5. Synthesis of Microporous Organic Polymers with Phenol and Aniline

The study focused on one main aspect: preparing an efficient polymer which minimized the Pd leaching. In particular, we wanted to study what would happen if we introduced a heteroatom, such as O or N in the structure of the polymer.

Therefore, this time, after synthesizing material **2**, aniline was used instead of toluene, which gave rise to polymer **5**. (15.65 C%, 1.12 N%, 0.69 H% determined by elemental analysis).

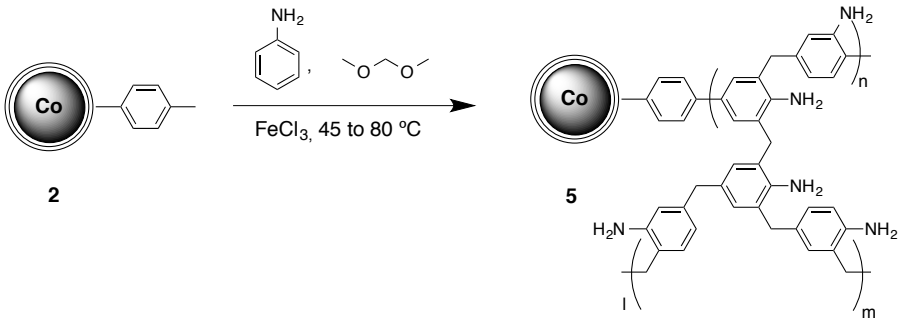

Scheme 14. Synthesis of the hybrid material with aniline.

The next step consisted in synthesizing Pd nanoparticles using microwave irradiation (15.42 C%, 1.08 N%, 0.75 H% determined by elemental analysis, 0.48 wt% Pd determined by ICP). The results obtained by elemental analysis for materials **5** and **6**, seemed to indicate that the polymer had formed around the particles.

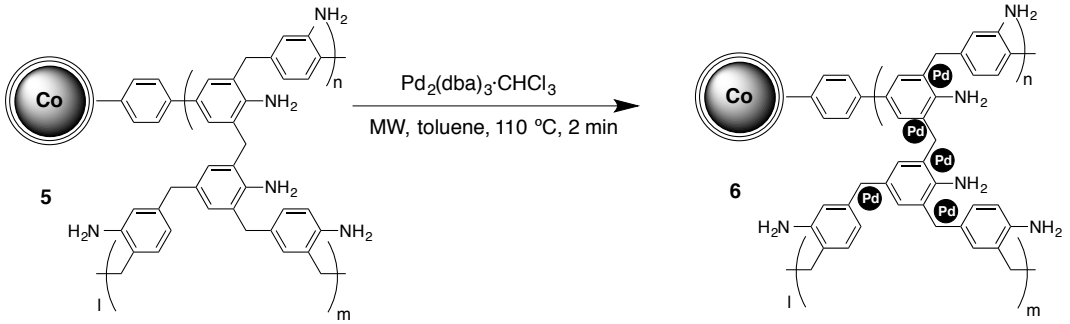

Scheme 15. Synthesis of PdNPs inside the pores of catalyst **6**.

In TEM and EDX images, polymer, Pd and Co NPs were observed. Indeed, it looks like the polymer could work as a network to prevent Pd NPs from agglomerating (Figure 9).

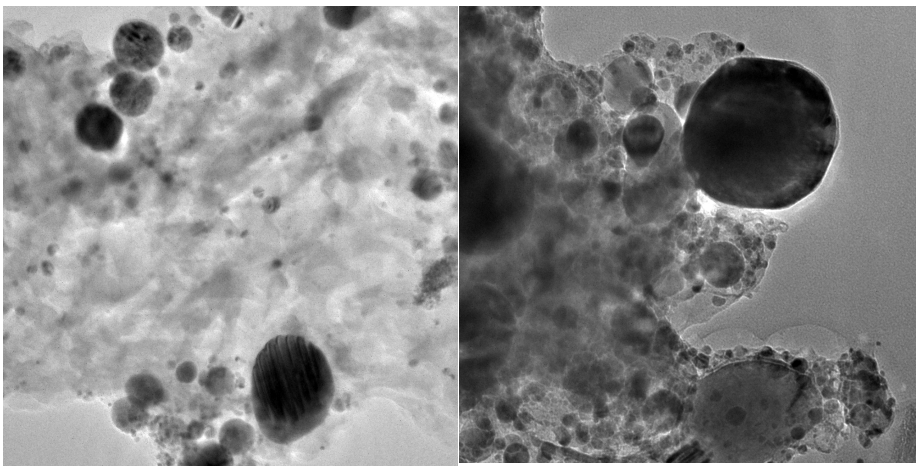

Figure 9. TEM analysis of catalyst **6**.

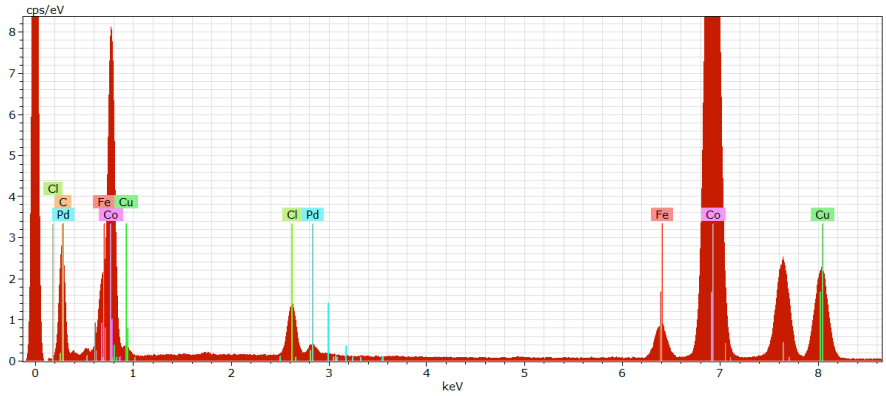

Figure 10. EDX image catalyst **6**.

With the new material synthesized (i.e. aniline@MOPs), we decided to study its behavior in catalytic applications. To this end, the Suzuki coupling between 4-iodoanisole and phenylboronic acid was chosen as a model reaction. In order to gain some preliminary information on the recyclibility of the catalyst, we decided to run two consecutive runs of this reaction (Table 8).

Table 8. Suzuki cross-coupling with catalyst **6**.

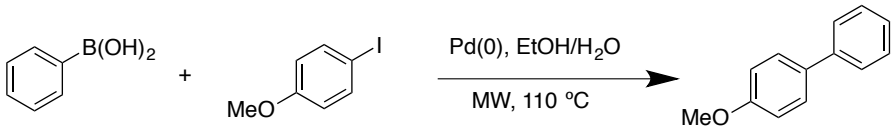

entry	Yield [%][a]	Pd leaching [ppm][b]	Co Leaching [ppm][b]
1	91	29	10
2	90	35	15

Catalyst (0.5 mol%), K_3PO_4 (0.25 mmol), 4-iodoanisole (0.1 mmol), phenylboronic acid (0.15 mmol). [a] Determined by ^1H NMR analysis using an internal standard ($CHBr_3$). [b] Determined by ICP measurement.

No significant change was observed in the amount of leaching. Therefore, we decided to prepare the analogous material derived from phenol, which would introduce more electronegative oxygen atoms in the polymer backbone. Using the strategy previuosly described, polymer **7** was obtained (16.72 C%, 0≈N%, 0.69 %H determined by elemental analysis).

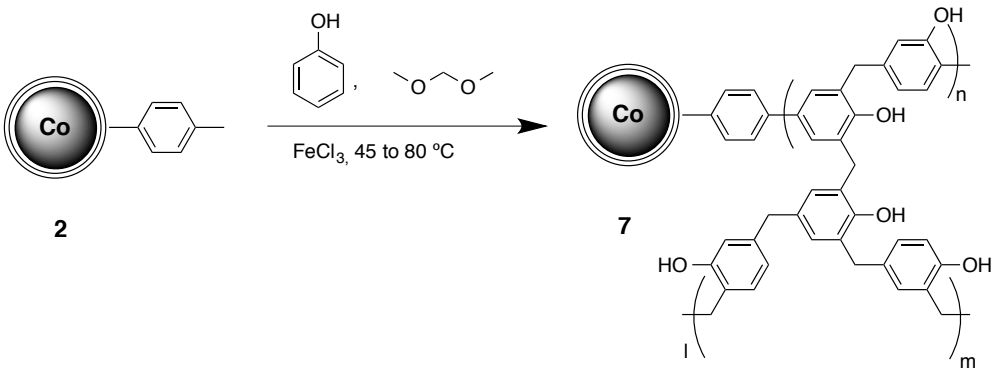

2 7

Scheme 16. Synthesis of phenol@MOPs.

Afterwards, using the same procedure, Pd NPs were synthesized inside the pores of phenol@MOPs **7** to generate the catalytic material **8** (16.21 C%, 0≈N%, 0.68 H% determine by elemental analysis).

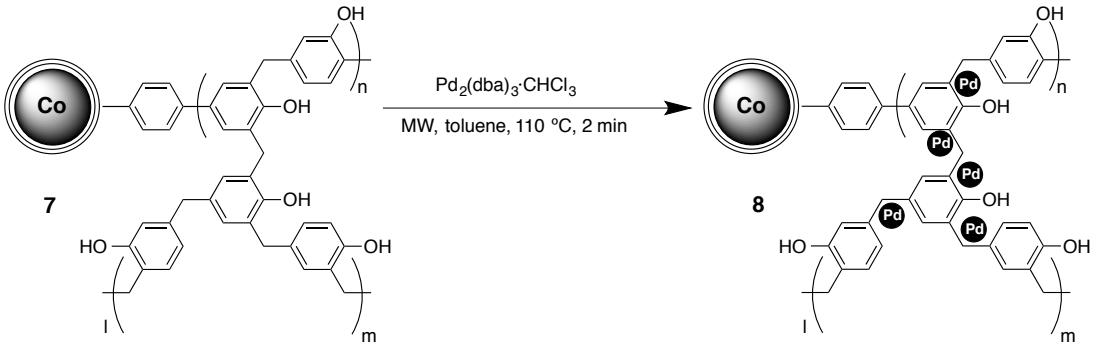

7 8

Scheme 17. Synthesis of PdNPs inside the pores of phenol@MOPs.

Elemental analysis was used to determine the extent of polymer formation (16.21 C%, 0≈N%, 0.68 H% determined by elemental analysis, 0.47 wt% Pd determined by ICP). Moreover, in TEM images the polymer layer around the Co/C NPs and Pd NPs could be detected.

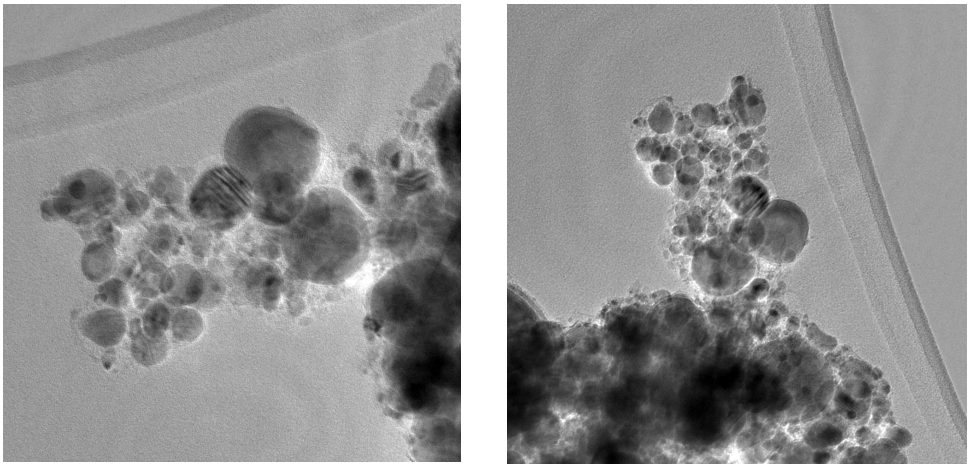

Figure 11. TEM images of catalyst **8**.

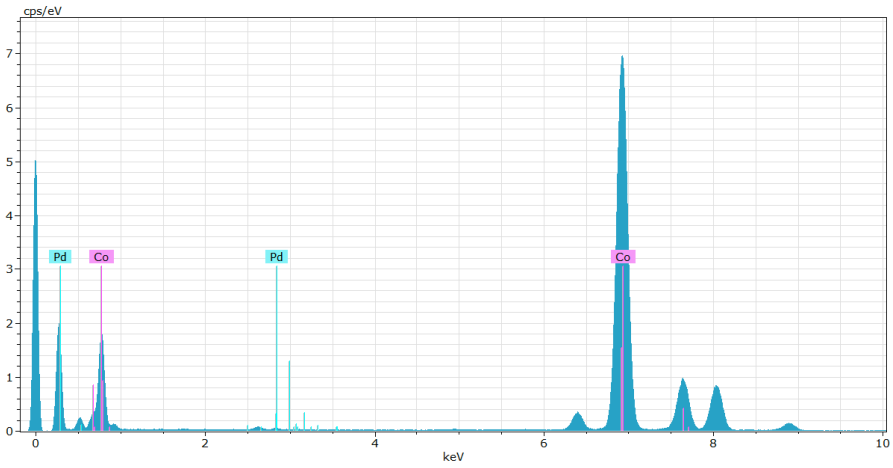

Figure 12. EDX analysis of catalyst **8**.

The reaction of 4-iodoanisole and phenylboronic acid was tested with the new hybrid material **8** under the previously reported conditions. The reaction yield was as good as in the previous cases, but no significant change was observed in terms of Pd leaching (Table 9).

Table 9. Suzuki cross-coupling with catalyst **8**.

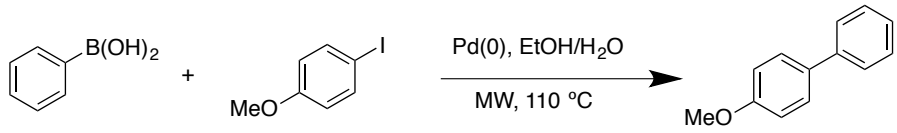

entry	Yield [%][a]	Leaching Pd [ppm][b]	Leaching Co [ppm][b]
1	93	35	9
2	91	29	16

Catalyst (0.5 mol%), K_3PO_4 (0.25 mmol), 4-iodoanisole (0.1 mmol), phenylboronic acid (0.15 mmol). [a] Determined by ^1H NMR analysis using $CHBr_3$ as the internal standard. [b] Determined by ICP measurement.

4.6. Summary and Outlook

This research project, which was started in Regensburg, is not finished. We think that this microporous polymer developed in Germany has a lot of potential for future work. We have tested toluene, phenol and aniline in the structure of polymer but we could not completely suppress Pd leaching. Thus, we will substitute toluene for imidazole substrate and study the same reactions and Pd leaching. We would also like to replace Pd with other metal nanoparticles like Ni, Ru and Fe and characterize these new polymers.

4.7. Experimental Section

Materials and Methods

Carbon-Coated Cobalt Nanobeads (1): (Co/C NBs, 20.5 m^2/g, mean particle size ≈ 25 nm) were obtained from Turbobeads Llc, Switzerland. Before use, they were washed five times for 24 h in a concentrated HCl (Merck, puriss) / deionized water (Millipore) mixture (1:1). Acid residues were removed by washing with millipore water (×5) and the particles were dried under vacuume.

Magnetic nanobeads were dispersed using an ultrasound bath (Sonorex RK 255 H-R, Bandelin) and recovered with the aid of a neodymium based magnet (side length 12 mm). They were characterized by transmission electron microscopy (CM30 ST-Philips, LaB6 cathode, operated at 300 kV point resolution ≈ 4 Å), and inductively coupled plasma optical emission spectrometry (Spectro Analytical Instruments ICP Modula EOP, λ = 340 nm).

^{1}H NMR (300 MHz) spectra were recorded on a Bruker AC 300 spectrometer with $CHCl_3$ (7.26 ppm) as a standard. Gas chromatography was performed on a Fisons Instruments GC8000 equipped with a capillary (30 m×250 μm×0.25 μm) and flame ionization detector.

Phenylmethanol Functionalized Carbon-Coated Cobalt Nanobeads (2): The as-prepared carbon-coated cobalt nanobeads 1 (0.1 g, 4.71 wt% C) were suspended in H_2O (5 mL) by the use of an ultrasonic bath (Sonorex RK 255 H-R, Bandelin). 4-Aminotoluene was transformed in the corresponding diazonium salt in situ by adding a cooled solution of sodium nitrite (2.3 mmol, 0.16 g in 12 mL H_2O) to a mixture of the 4-aminotoluene (1.5 mmol, 0.160 g), HCl (0.6 mL, concentrated) and H_2O (20 mL) in an ice bath. After addition of the carbon-coated nanobeads, the reaction mixture was sonicated for 30 min. The nanobeads were recovered from the reaction mixture with the aid of a neodymium based magnet (N48, W-12-N, Webcraft GmbH, side length 12 mm) and washed with water (3×5 mL) and acetone (6×5 mL). Each washing step consisted of suspending the particles in the solvent, ultrasonication (5 min) and retrieving the particles from the solvent by the aid of the magnet. After the last washing step and drying in vacuume 0.131 g of **2** were obtained (5.30 wt% C, 0.1 wt% H).

General Procedure for the Aromatic Microporous Polymers Encapsulated with Co/C Nanobeads: $FeCl_3$ (anhydrous, 0.163 g, 1 mmol) was added to a solution of **2** (0.1 g), aromatic compound (0.5 mmol) and Formaldehyde dimethyl acetal (FDA) (88 μL, 1 mmol) in 3 mL DCE and put in the ultrasonic bath for 10 minutes. Afterwards, the resulting mixture was stirred at room temperature to ensure good mixing, and then it was stirred at 45 °C for 5 h to form original network. After that it was heated at 80 °C for 19 h to complete the reaction. The resulting

precipitate was separated by an external magnet, washed three times with ethanol, then washed with methanol in a Soxhlet for 24 h, and finally dried under reduced pressure at 60 °C for 24 h.
3 was prepared according to the general procedure from methylbenzene (53 μL, 0.5 mmol), 168 mg of product was obtained (15.88 wt% C, 0.84 wt% H).
5 was prepared according to the general procedure from aniline (44 μL, 0.5 mmol), 157 mg of product was obtained (15.65 C%, 1.12 N%, 0.69 %H determined by elemental analysis).
7 was prepared according to the general procedure from phenol (48 mg, 0.5 mmol) 171 mg of product was obtained (16.72 C%, 0≈N%, 0.69 %H determine byelemental analysis).
Aromatic Microporous Polymers Encapsulated with Co/C Nanobeads and Pd(0) Nanoparticles (4) (0.43 wt% Pd): 1 ml toluene solution containing 2 mg $Pd_2(dba)_3 \cdot CHCl_3$ (0.0019 mmol) was added onto 5 ml toluene, and 0.1 g of **3** was added to the mixture. The solution was transferred to a microwave vial under nitrogen atmosphere. The reaction mixture was sonicated in an ultrasonic bath for 10 min and then heated in a microwave reactor to 110 °C for 2 min. The magnetic catalyst was recovered by an external magnet, the solution decanted, and the particles washed with DCM in a Soxhlet for 5 h to remove the Pd species adsorbed on the outer surface of **3**. After drying under vacuum a Pd loading of 0.43 wt% was determined by ICP-AES. (16.67 wt% C, 0.94 wt% H)

General Procedures for Hydrogenation

Pd@Co/C nanoparticles 4 (0.1 mol% Pd, 0.2μmol), substrate (0.2 mmol) and ^{i}PrOH (5 mL) were introduced in a schlenk tube. Dodecane (0.2 mmol) was added as internal standard and the slurry was sonicated in an ultrasonic bath for 10 min. The tube was evaporated and flushed with H_2 several times followed by vigorous stirring under 1 atm H_2 (balloon). The progress of the reaction was monitored by GC separating the magnetic material by an external magnet before sampling.

Catalyst Recycle and Reusing in the Hydrogenation

The reaction was performed under the conditions described above, employing *trans*-stilbene as substrate. Each time, the catalyst was isolated from the reaction mixture at the end of the reaction by an external magnet, washed with EtOAC, and then dried at 40 °C under vacuum. The dried catalyst was then reused in the next run.
The liquid pahse in each cycle was filtered using a HPLC filter. After collecting all the liquids of six cycles, ICP-AES measurements were done to determine the Pd contamination in the final product for each of the six performed cycles

General Procedure for the Suzuki Coupling

A Suspension of Pd@Co/C nanoparticles 4 (0.5 mol% Pd, 0.5μmol), K_3PO_4 (0.75 mmol), 4-iodoanisole (0.3 mmol), phenylboronic acid (0.45 mmol) in 12 ml ethanol and water (ratio 1:1) was prepared in a microwave vial. The reaction mixture was sonicated in an ultrasonic bath for 10 min and then heated in a microwave reactor to 120 °C for 10 min. The catalyst was recovered by a magnet and the solution was washed 3 times with DCM. Then, 0.28 mmol $CHBr_3$ (25 μL) were added to the product as internal standard and the conversion was determined by ^1H NMR.

Catalyst Recycling and Reuse for Suzuki Cross-Coupling

The reaction was performed under the conditiones described above, employing 4-iodoanisole as substrate. Each time, the catalyst was isolated from the reaction mixture at the end of the reaction by an external magnet, washed with DCM, and then dried at 40 °C under vacuum. The dried catalyst was then reused in the next run.

The liquid phase in each cycle was dried under vacuum and stored in a vial after filtration using a HPLC filter. After collecting all the liquids of six cycles, ICP-AES measurement was performed to determine the total Pd leaching during six cycles.

GC conditions:

Aniline: 3 min at 50 °C, 16 °C/min to 250; Retention time: ethylbenzene (5.90 min), aniline (8.04 min), nitrobenzol (9.98 min).

Methylcyclohexane: 3 min at 50 °C, 10 °C/min to 200 °C. methylcyclohexane (3.26 min), methylcyclohexene (4.10 min), Dodecane (12.52 min).

1,2-Diphenylethane: 3 min at 140 °C, 16 °C/min, to 300 °C, dodecane (3.76 min), bibenzyl (6.97 min), *trans*-stilbene (8.65 min).

4-Phenylbutan-2-one: 1min at 80 °C, 20 °C/ min to 220 °C; retention time: dodecane (5.69 min), 4-phenylbutan-2-one (5.84 min), (*E*)-4-phenylbut-3-en-2-one (6.72 min).

Styrene: 1 min at 50 °C, 1 °C/min to 75 °C (0 min), 20 °C/min to 250 °C; ethylbenzene (7.16 min), ethynylbenzene (7.68 min), styrene (8.45 min), dodecane (29.86 min).

Ethylbenzene: 1 min at 50 °C, 1 °C/min to 75 °C (0 min), 20 °C/min to 250 °C; ethylbenzene (7.16 min), ethynylbenzene (7.68 min), styrene (8.45 min), dodecane (29.86 min).

Conclusion

This thesis focuses on the application of magnetic nanoparticles (MNPs) in different catalytic reactions. In this research the main goal is to develop different catalysts based on MNPs and study the advantages and limitations of these catalytic materials.

In the first project, two new hybrid materials based on carrageenan and MNPs were developed. First, the MNPs were synthesized using thermal decomposition of $Fe(acac)_3$ in the presence of oleylamine and oleic acid as surfactants. Afterwards, the first hybrid material was prepared by mixing κ-carrageenan and the MNPs in the presence of glacial acetic acid and ultrapure water in DMF at 110 ºC. This catalyst was tested in the Michael addition of aldehydes to nitroalkenes; five examples were reported with different aldehyde substrates with yields in the range 54-80% and diastereoselectivities between 87:13 and 93:7. Interestingly, the individual components were inactive in the same reaction.

As for the second hybrid material, it involved modification to introduce an organocatalyst in order to apply in an enantioselective reaction. First, the free hydroxy groups in the hybrid material were substituted by an azide group, then an analog of the Jørgensen-Hayashi catalyst was anchored to the hybrid material using a copper-catalyzed azide-alkyne cycloaddition (CuAAC) strategy. This catalyst was also applied in the Michael addition and good yields and excellent *ee*'s were achieved (5 examples, yield: 57-83%, 86-93% *ee*)

In the second project, an analog of the second generation MacMillan catalyst was immobilized onto Fe_3O_4 NPs and polystyrene through a copper-catalyzed alkyne-azide cycloaddition reaction (CuAAC). The resulting catalytic materials were applied to the asymmetric Friedel-Crafts alkylation of indoles with α,β-unsaturated aldehydes. With the MNPs based catalyst yields and *ee* were between 41-76%, 35-85% and in the case of polystyrene derivative yields and *ee* are found to be between 64-79% and 70-93% respectively.

Then, the recyclability of MNPs and polystyrene catalysts was studied for five consecutive runs. In both catalysts a slight decline in catalytic activity was observed. Concerning the enantioselectivity, the results with the PS-based catalyst were more constant in these five runs. As a general conclusion of this study, the polystyrene-based catalyst showed higher stability and provided better stereoselectivities.

In the last project, another kind of hybrid material was synthesized based on microporous organic polymers (MOPs) encapsulated with Pd nanoparticles and Co/C nanobeads. Recently, microporous organic polymers (MOPs) have attracted particular attention due to their unique properties such as large surface area, low skeletal density, and high chemical stability. In this respect, metal catalysts loaded on MOPs have been studied for several heterogeneous catalytic reactions. For the preparation of polymer-Pd-Co/C composites, the surface of Co/C nanobeads is covalently functionalized with phenylmethane by thermal decomposition of the diazonium salt derived from 4-aminotoluene. This allows introducing phenyl moieties on the surface of Co/C nanobeads as a starting point for growing a bakelite type polymer on the nanoparticle graphene layer. Afterwards, using toluene, aniline and phenol as building blocks, microporous polymers were formed with employing formaldehyde dimethyl acetal (FDA) as an external cross-linker. In the last step, Pd NPs were formed by microwave irradiation inside the pores of the polymer using $Pd_2dba_3 \cdot CHCl_3$ as the Pd source. These catalysts were applied in hydrogenation and Suzuki cross-coupling reactions to evaluate the catalytic ability of the new hybrid material. Despite giving from good to moderate yields, these materials suffer from leaching of Pd, so further research is required.

In conclusion, in this thesis we have tried to develop new catalysts based on magnetic nanoparticles. In the first two chapters, MNPs were modified with an organocatalyst as powerful tools to promise asymmetric reactions. The first study involved the use of k-carregenan as a versatile platform to carry the organocatalyst while magnetic nanoparticles were used as an efficient tool for separating the material. In the second project, MNPs and polystyrene were modified with the second generation MacMillan catalyst using CuAAC strategy as a versatile method to functionalize particles. In this case, both catalysts could be separated from the reaction media easily, albeit polystyrene showed better results.

In the last project, new hybrid materials have been developed using micropours polymer and Co/C nanobeads. Research is still ongoing to develop a method that can minimize the amount of Pd leaching from the catalyst.